



UNIVERSITY OF  
LIVERPOOL

**Receptance-based frequency and eigenstructure  
assignment through structural modification and  
active control**

Thesis submitted in accordance with the requirements of the University of  
Liverpool for the degree of Doctor in Philosophy

By

Shike Zhang

November 2021



## Abstract

Vibration control is very important in engineering and in daily life. The aim of vibration control is to properly design the vibration responses of the structure, ensure the safety of machines or building, guarantee the quality of products or improve the comfortable feeling of the workers. Although people wish to tackle vibration problems in design stages, it is usually not the primary concern or is quite difficult and sometimes impossible due to unexpected vibration sources or manufacturing errors. Therefore, the control of vibration often occurs at project completion stage by modifying the dynamic behaviour of existing systems with structural modification or active control.

A vibrating system can be described using system eigenvalues and eigenvectors. By changing the system eigenvalues and/or eigenvectors, one can influence the dynamic behaviour of a system so that it can vibrate in a desirable way and avoid some vibration-induced problems, such as possibly failure caused by resonance or human body damage due to large vibration responses.

Among a variety of structural modification or active control methods, receptance-based methods are very convenient and efficient in practice because the receptance method, which directly uses the measured frequency response functions, can avoid the requirement of knowledge on system matrices ( $\mathbf{M}$ ,  $\mathbf{C}$  and  $\mathbf{K}$ ) and to a large extent modal truncation error. This research project investigates the application of the receptance-based structure modification and in active control, and dealing with some challenges of them.

Firstly, the receptance-based structure modification method is improved to a frequency assignment method for assembled structures. In some assembled structures, the substructures are difficult or not allowed to be modified which leaves only the links between substructures are modifiable. Those links are usually much simpler than the substructures. The dynamic behaviour of an assembled structure can be affected by the links so it is useful to optimize the properties of these links such that the assembled

structure can have desired dynamic behaviour. Only the receptances at the connection points of each substructure and the FE models of these simple links are needed.

Then the proposed frequency assignment method is validated on a laboratory test structure. This structure is composed of two substructures and six simple links. It is very important to obtain sufficient and good quality receptances when applying the receptance-based structural modification method, especially the rotational related receptances which can account for 75% of a full receptance matrix. In this study, the rotational receptances are obtained with the aid of an auxiliary structure and two angular accelerometers. The experimental results show the assembled structure can have desired natural frequencies by optimizing the geometry properties of the links.

Moreover, the partial eigenstructure assignment is studied and two receptance-based partial eigenstructure methods are put forward. Firstly, in the case that the force distribution matrix  $\mathbf{B}$  is predefined, a hybrid control method is proposed to overcome the limitation of the existing active control method that cannot assign a general desired eigenvector. A suitable passive modification is used to enlarge the set of eigenvectors which are assignable. Numerical examples show the hybrid control method can lead to the desired eigenvectors or their better approximations than a sole active control method.

The other method is a receptance-based active control method in the case that the force distribution matrix  $\mathbf{B}$  is not predefined. By leaving some elements in the force distribution matrix  $\mathbf{B}$  unknown and to be determined later, this method allows more freedoms to design the eigenvectors and it can also avoid the requirement of knowledge on the open-loop eigenvectors. Although the open-loop eigenvectors can be partly measured, it may take more efforts and the accuracy is not guaranteed. Therefore, the new method is more useful in some practical problems. This method is believed to be the first attempt to achieve partial eigenstructure assignment with only receptance.



## **Acknowledgements**

First and most importantly, I want to give my most sincere thanks to my supervisor, Professor Huajiang Ouyang, for his invaluable help throughout my PhD time. He is a serious scholar and is very responsible for his work and students. I gain a lot from him, not only the professional knowledge, but also the attitude to the work and research. What I learned from him will benefit me all my life. Without his kind offer and encouragement, I would not have the opportunity to pursue a PhD degree. It will be my honour to be his student forever and I will learn from him all the time.

Second, I would also show my appreciation to the support of University of Liverpool in a form of scholarship. I will try my best to return this favour to the University and society in the future. Moreover, I wish to thank my friends and colleagues in Liverpool, especially for people in Dynamics and Control Group at the University of Liverpool, such as Ningyu Liu, Yiqiang Fu and Huai Zhao. I have spent a wonderful time in this beautiful and diverse university. It will be my life-long memory.

Finally, I gratefully acknowledge the supports of my family and my girlfriend for the past four years. Their unconditional love is always my biggest motivation to move forward in my life.

# Table of Contents

<b>Abstract</b> .....	<b>I</b>
<b>Acknowledgements</b> .....	<b>III</b>
<b>Table of Contents</b> .....	<b>IV</b>
<b>List of Figures</b> .....	<b>IX</b>
<b>List of Tables</b> .....	<b>XII</b>
<b>Nomenclature</b> .....	<b>XIV</b>
<b>Chapter 1 Introduction</b> .....	<b>1</b>
1.1 Background .....	1
1.2 Motivations.....	2
1.3 Aim and objectives .....	3
1.4 Original contributions.....	4
1.5 Outline of the thesis.....	5
<b>Chapter 2 Literature review</b> .....	<b>8</b>
2.1 Basic knowledge.....	9
2.1.1 The concept of receptance.....	9
2.1.2 Structural modification and active control targets .....	11
2.2 Structural modification.....	12
2.2.1 Forward problem.....	14
2.2.2 Inverse problem.....	15
2.3 Active control .....	19
2.3.1 Pole/eigenvalue assignment .....	21
2.3.2 Eigenstructure assignment .....	23
2.3.3 Partial eigenvalue assignment.....	25
2.3.4 Partial eigenstructure assignment.....	27

2.4	Receptance measurement .....	28
2.4.1	Rotational receptance estimation .....	28
2.4.2	Modal analysis methods .....	30
2.4.3	Simple assessment of measured data .....	32
2.5	Conclusion .....	32
<b>Chapter 3 Receptance-based frequency assignment for assembled structures</b>		
<b>.....</b>		<b>34</b>
3.1	Introduction .....	35
3.2	Receptance-based structural modification theory .....	36
3.2.1	Introductory theory .....	36
3.2.2	Receptance-based structural modification method .....	37
3.2.3	Numerical Example .....	40
3.3	Receptance-based frequency assignment for assembled structures .....	43
3.4	Numerical examples .....	49
3.4.1	Discrete structure with one link .....	49
3.4.2	Continuous structure with multiple continuous links .....	52
3.5	Discussion .....	56
3.6	Conclusions .....	57
<b>Chapter 4 Experimental work on frequency assignment of an assembled structure</b>		
<b>.....</b>		<b>58</b>
4.1	Introduction .....	58
4.2	The tested assembled structure .....	59
4.3	Rotational receptance estimation .....	62
4.4	Finite element models .....	66
4.4.1	Material properties .....	67
4.4.2	The auxiliary structure .....	68
4.4.3	Links .....	72
4.5	Experimental results .....	76

4.5.1	Assembled structure .....	77
4.5.2	Substructure S .....	83
4.5.3	Substructure B .....	92
4.6	Frequency assignment .....	100
4.6.1	Assignment of one natural frequency .....	101
4.6.2	Assignment of two natural frequencies .....	102
4.7	Conclusions .....	104
<b>Chapter 5 Receptance-based partial eigenstructure assignment using hybrid control.....</b>		<b>106</b>
5.1	Introduction .....	108
5.2	Receptance-based partial eigenvalue assignment.....	109
5.2.1	Problem description .....	109
5.2.2	Receptance-based partial eigenvalue assignment method .....	110
5.2.3	Numerical examples .....	113
5.3	Receptance-based partial eigenstructure assignment by active control ...	116
5.3.1	Existence of solutions for partial eigenstructure assignment with state feedback control .....	116
5.3.2	Numerical Example.....	118
5.4	Receptance-based partial eigenstructure assignment with hybrid control	123
5.4.1	Passive modification .....	123
5.4.2	Eigenvector projection .....	126
5.4.3	Active control.....	127
5.5	Numerical examples .....	128
5.5.1	Undamped systems .....	128
5.5.2	Damped systems .....	132
5.5.3	Cantilever beam .....	134
5.6	Equivalent active control.....	137
5.7	Discussions .....	138

5.8	Conclusions .....	141
<b>Chapter 6 Receptance-based partial eigenstructure assignment with state feedback control .....</b>		
<b>143</b>		
6.1	Introduction .....	143
6.2	The effect of eigenvectors of open-loop systems on spill-over problem ..	144
6.2.1	The requirement of eigenvectors of open-loop systems .....	144
6.2.2	The effect of open-loop eigenvectors on spill-over problem.....	145
6.3	Receptance-based partial eigenstructure assignment method .....	147
6.3.1	Method derivation .....	149
6.3.2	Unchanged eigenvalues.....	153
6.3.3	The procedure and requirements.....	154
6.4	Systems with inaccessible degrees of freedom .....	155
6.5	A 4-DoF damped system.....	156
6.5.1	Assign two modes and keep the other modes unchanged .....	157
6.5.2	Assign two modes and keep the other eigenvalues unchanged.....	158
6.5.3	Assign two modes and keep one mode .....	159
6.6	An undamped 10-DoF system with inaccessible DoFs.....	161
6.7	Robustness analysis .....	163
6.7.1	Receptance matrices with several contaminated elements.....	164
6.7.2	Receptance matrices with one pair of contaminated eigenvalues.....	165
6.7.3	Fully contaminated receptance matrices .....	166
6.8	Conclusions .....	167
<b>Chapter 7 Conclusions and future work.....</b>		
<b>169</b>		
7.1	Conclusions .....	169
7.2	Future work .....	171
<b>Appendix A .....</b>		
<b>173</b>		
<b>Appendix B .....</b>		
<b>175</b>		

**References ..... 178**

## List of Figures

Fig. 1.1 The structural flowchart of the thesis .....	6
Fig. 3.1 A 3-DoF system .....	40
Fig. 3.2 Original (black dash line) and modified (red line) receptances $h_{11}$ : assignment of the natural frequency at 300 rad/s.....	42
Fig. 3.3 Original (black dash line) and modified (red line) receptances $h_{11}$ : assignment of the natural frequency at 300 rad/s and a zero at 400 rad/s.....	42
Fig. 3.4 Original (black dash line) and modified (red line) receptances $h_{11}$ : assignment of the natural frequencies at 300 rad/s and 750 rad/s.....	43
Fig. 3.5 Substructure A and B connected by links C and D .....	44
Fig. 3.6 Internal forces at the interfaces DoFs .....	44
Fig. 3.7 Substructure A and B coupled through link C.....	50
Fig. 3.8 FRF $h_{12}$ of the assembled structure with a natural frequency at $30\pi$ rad/s	51
Fig. 3.9 FRF $h_{12}$ of the assembled structure with a natural frequency at 15 Hz and a zero at 20 Hz. ....	52
Fig. 3.10 Finite element model of frames A and B and links .....	53
Fig. 3.11 The profile of the links .....	53
Fig. 3.12 FRF $h_{38,44}$ with one assigned frequency .....	54
Fig. 3.13 FRF $h_{38,44}$ with two assigned frequencies .....	55
Fig. 4.1 A schematic diagram of a floating raft system .....	59
Fig. 4.2 A floating raft system (This picture was taken with the kind permission of the national key laboratory of ship vibration and noise).....	60
Fig. 4.3 The designed test structure. ....	61
Fig. 4.4 Two Substructures (left: Substructure S, right: Substructure B) .....	61
Fig. 4.5 The links between two substructures .....	61
Fig. 4.6 Coupling of an auxiliary structure .....	63
Fig. 4.7 The auxiliary structure used in this experiment.....	64
Fig. 4.8 The small plate and sensor locations .....	67
Fig. 4.9 The FE model of the small plate.....	68
Fig. 4.10 Receptance $h_{1z3z}$ .....	68
Fig. 4.11 The auxiliary structure .....	69

Fig. 4.12 The mounting of this auxiliary structure.....	70
Fig. 4.13 The FE model of the auxiliary structure .....	70
Fig. 4.14 The first mode shape of this auxiliary structure .....	71
Fig. 4.15 Receptances of the auxiliary structure .....	72
Fig. 4.16 Schematic diagram of the link and the real links.....	73
Fig. 4.17 The first mode shape of a vertical link (free-free condition).....	73
Fig. 4.18 Modal test on the link .....	74
Fig. 4.19 Receptance $h_{31}$ of a vertical link .....	75
Fig. 4.20 The measurement set-up used in this work.....	77
Fig. 4.21 The test rig and measured locations.....	78
Fig. 4.22 Sensor locations .....	79
Fig. 4.23 Measured receptances of the assembled structure .....	81
Fig. 4.24 Mode shapes of the assembled structure .....	82
Fig. 4.25 Installation of substructure S .....	83
Fig. 4.26 Locations of sensors (red squares) and coordinate system on substructure S .....	84
Fig. 4.27 A group of translational receptances .....	86
Fig. 4.28 Coherence coefficients.....	87
Fig. 4.29 Receptances reciprocity of substructure S .....	88
Fig. 4.30 The geometrical symmetry property of substructure S.....	89
Fig. 4.31 The measurement of rotational receptances.....	89
Fig. 4.32 Rotational receptances of substructure S .....	90
Fig. 4.33 Mode shapes of substructure S .....	91
Fig. 4.34 Substructure B under free-free condition .....	92
Fig. 4.35 Sensor locations and coordinate system .....	93
Fig. 4.36 Part of measured translation receptances of substructure B .....	95
Fig. 4.37 Rigid body mode.....	96
Fig. 4.38 Receptances reciprocity of substructure B .....	97
Fig. 4.39 The geometrical symmetry property of substructure B .....	97
Fig. 4.40 Some rotational receptances of substructure B.....	98
Fig. 4.41 The comparison of measured receptances using two approaches.....	99
Fig. 4.42 The first 5 mode shapes of substructure B.....	100
Fig. 4.43 The objective function values versus thickness $t$ .....	102
Fig. 4.44 The objective function values in terms of thickness $t$ and breadth $w$ .....	103



Fig. 4.45 The first 3 mode shapes of the assembled structure .....	104
Fig. 5.1 FRF $h_{11}$ .....	114
Fig. 5.2 Eigenvector projection .....	118
Fig. 5.3 A 5-dof system.....	118
Fig. 5.4 The purpose of passive modification .....	127
Fig. 5.5 A cantilever beam with two spring-mass modifications.....	134
Fig. 5.6 The first mode shape of the cantilever beam .....	135
Fig. 5.7 A 20-DoF system.....	139
Fig. 5.8 Comparison of the performances with different number of actuators .....	140
Fig. 5.9 The effects of the number of masses under-actuated.....	141
Fig. 6.1 A 4-DoF system.....	146
Fig. 6.2 A10-DoF lumped mass system.....	161
Fig. 6.3 Eigenvalues of the closed-loop system (with a few contaminated elements in receptance matrices).....	165
Fig. 6.4 Eigenvalue spread (with contaminated receptance matrices $\mathbf{H}(\mu_{3,4})$ ).....	166
Fig. 6.5 Eigenvalues spread (all receptance matrices are contaminated).....	167

## List of Tables

Table 2.1 Relationship among the three models .....	13
Table 3.1 Substructures' parameters .....	50
Table 3.2 Natural frequencies of substructure A and B .....	50
Table 3.3 Natural frequencies of the assembled structure (a desired frequency 15 Hz) .....	51
Table 3.4 Natural frequencies of the assembled structure (a desired frequency at 15 Hz and a zero at 20 Hz) .....	52
Table 3.5 Cross-sectional areas of frames A and B .....	53
Table 3.6 First 5 natural frequencies of assembled structure with one assigned frequency at 34.99 Hz .....	54
Table 3.7 First 5 natural frequencies of assembled structure with two assigned frequencies at 35.40 Hz and 100.00 Hz .....	55
Table 3.8 First 5 natural frequencies of assembled structure with two assigned frequencies at 34.99 Hz and 101.31 Hz .....	56
Table 4.1 Important dimensions of the test small plate .....	67
Table 4.2 Some important dimensions of links.....	73
Table 4.3 Natural frequencies of the assembled structure .....	82
Table 4.4 First six natural frequencies of substructure S (Experiment).....	91
Table 4.5 First six natural frequencies of substructure S (Finite element model) .....	91
Table 4.6 The first 5 natural frequencies of substructure B.....	100
Table 4.7 Natural frequencies of the assembled structure (FE model) .....	103
Table 5.1 Eigenvalues and eigenvectors of the controlled system.....	115
Table 5.2 System parameters .....	118
Table 5.3 Eigenstructure of the open-loop system.....	119
Table 5.4 Desired eigenpairs.....	119
Table 5.5 Natural frequencies and eigenvectors of the closed-loop system .....	120
Table 5.6 Performance assessment for single input .....	120
Table 5.7 The qualities of obtained eigenvectors with different vector <b>b</b> .....	121
Table 5.8 Performance assessment for multiple inputs.....	122
Table 5.9 Structural modifications .....	129

Table 5.10 Eigenpair assignment comparison .....	130
Table 5.11 Spill-over assessment.....	130
Table 5.12 Structural modifications .....	131
Table 5.13 Eigenpair assignment comparison .....	131
Table 5.14 Spill-over assessment.....	131
Table 5.15 Damped frequencies and damping ratios .....	132
Table 5.16 Desired eigenpairs.....	132
Table 5.17 Structural modifications .....	133
Table 5.18 Eigenvalues of the cantilever beam (Before and after controlled).....	134
Table 5.19 Desired eigenvector and obtained eigenvector .....	135
Table 5.20 The parameters of passive modifications.....	136
Table 5.21 Spill-over assessments .....	136
Table 5.22 Desired eigenvector for the twenty-degree of freedom system .....	139
Table 6.1 Eigenstructure of the open-loop system.....	146
Table 6.2 Method comparison.....	155
Table 6.3 Desired eigenvalues and eigenvectors .....	157
Table 6.4 The desired eigenvectors and eigenvalues .....	158
Table 6.5 The desired eigenvalues and eigenvectors .....	159
Table 6.6 Eigenvalues and eigenvectors of the closed-loop system .....	160
Table 6.7 System parameters .....	161
Table 6.8 Natural frequencies of the open-loop system and the closed-loop system .....	162
Table 6.9 Eigenvectors corresponding to the first three modes .....	163
Table 6.10 Contaminated elements in each receptance matrix .....	164

## Nomenclature

<b>A</b>	System matrix
<b>B</b>	Control force distribution matrix
<b>C</b>	Damping matrix
<b>F</b>	Velocity feedback control gain matrix
<b>G</b>	Displacement feedback control gain matrix
<b>H</b>	Receptance matrix
$\hat{H}$	Modified receptance matrix
<b>K</b>	Stiffness matrix
$\Delta K$	Stiffness modification matrix
<b>M</b>	Mass matrix
$\Delta M$	Mass modification matrix
<b>Z</b>	Dynamic stiffness matrix
$\Delta Z$	Dynamic stiffness of modification
<b>b</b>	Single input control force distribution vector
<b>f</b>	Vector of forces
<b>v</b>	Eigenvector of original system or open-loop system
<b>w</b>	Closed-loop eigenvectors
<b>x</b>	Displacement in physical coordinate
<b>y</b>	Output vector
$h_{ij}$	the element of receptance matrix on the $i$ th row and $j$ th column

$\omega$	Frequency in rad/sec
$f$	Frequency in Hz
$\lambda_k$	open-loop eigenvalues
$\mu$	Closed-loop eigenvalue
$n$	Number of degrees of freedom
$n_b$	Number of actuators
$n_d$	Number of desired frequencies
$\mathbb{C}$	The set of complex numbers
$\mathcal{R}$	The set of real numbers
$\Gamma$	Physical constraints on passive modification

# Chapter 1

## Introduction

### 1.1 Background

With the rapid development of modern technology, noise and vibration requirements are becoming increasingly important in many fields, such as civil engineering, car sector, aircraft industry and so on. Although in some cases vibration can be useful and desirable (e.g., ultrasonic vibrations, vibration conveyers, impactors and musical Instruments), in most cases it is undesirable or even detrimental. Abnormal vibration will influence the durability and reliability of machinery systems or structures and may cause serious problems. For example, vibration due to the engine may cause discomfort to passengers in vehicles. Earthquake is also a disaster caused by vibration. Excessive vibration on an aircraft may lead to a fatigue failure which potentially cause the aircraft crash resulting in injuries or fatalities. A famous engineering disaster in history was the Tacoma Narrows Bridge disaster in 1940 which collapsed due to the resonance.

Although engineers acknowledge the importance of vibration control, it is usually not a primary concern in the design process. In addition, some designed structures may not behave as expected due to manufacturing errors or variations of operating conditions. So, many vibration studies are carried out only after systems are manufactured or built. In these cases, vibration problems are usually addressed using passive modification, active control or passive-active combined hybrid control.

Structural modification is an effective methodology of passive vibration control. It is a procedure aimed at determining values of physical parameters of a structure to achieve desirable dynamic characteristics (usually modal properties such as natural frequencies and modal shapes) or certain dynamic performance (such as the need to avoid resonance or creation of a node on the system at a certain frequency). A design modification can be as simple as a point mass or spring on a cantilever beam. It can

also be as complicated as adding a subsystem, like a vibration absorber or a magneto-rheological fluid damper, on a vibrating structure. Among a variety of structural modification methods, receptance-based structural modification method is very powerful because the information required can be directly obtained from experiments and thus can largely overcome the incompleteness of the modal representation of complicated systems and avoid the need for accurate physical models [1].

Although passive modification is convenient, stable and cheaper and usually more appealing, there are some situations that passive modification cannot achieve the desired dynamic behaviour due to physical limitations and mathematical difficulties. In contrast, active control can significantly overcome the limitations of passive modification and in theory, any desired forces can be achieved with active control. Active control has also been widely used to change the dynamic behaviour of original structures by relocating the eigenvalues of an open-loop system from their original values to desired locations in the complex eigenvalue plane or by shaping the eigenvectors of the closed-loop system to force the structure to vibrate in a more desirable way. Mottershead et al. [2] took advantage of the receptance method and developed this method into active control. Much work has been done on this topic and has been validated by experiments [3, 4].

With passive modification or active control, if care is not taken, the system may have some new undesired eigenvalues or become unstable, which could lead to more vibrations in the system. This phenomenon is called spill-over and the methods to suppress the spill-over problem are named partial assignment methods. Partial eigenvalue assignment is to change undesired eigenvalues to suitable values while keeping the other eigenvalues unchanged. Researchers have developed many partial eigenvalue assignment methods with passive modification or active control. In this thesis, some open problems in partial assignment are investigated.

## **1.2 Motivations**

Nowadays, ships are often required to be lighter and faster. With lighter structures, higher structural vibration and louder noise will be produced. Especially for those fast patrol boats which have powerful propulsion engines installed in a small space, the vibration and noise can become unbearable. Suitable vibration control methods are

needed to reduce the vibration caused by different kinds of machines. Most of machines on a ship are complex and it is difficult to construct their accurate mathematical models or finite element models. With the great advantage of the receptance method, one can modify the dynamic behaviour of structures without the mathematical models or big negative effects from modal truncation errors by adopting receptance method.

Very often, machines or structures are assembled together or installed on a ship through links such as isolators or specially designed metal components. Those machines are usually from different manufacturers and not allowed to be modified. Properly designing the properties of links between machines and the ship hull will be a very efficient way to reduce vibrations. This kind of problems forms a frequency assignment problem of assembled structures with unmodifiable substructures. Both theoretical and experimental work on this problem will be studied in this thesis to provide a solution for vibration control on a ship.

Active control has also been widely used in vibration control. Although the receptance method has been applied to solve eigenvalue assignment problem, a general eigenvector is still not guaranteed to be assignable by the existing receptance-based active control, especially for partial assignment problem. It is necessary to explore a receptance-based partial eigenstructure assignment method to expand the receptance method and provide efficient solutions.

### **1.3 Aim and objectives**

The aim of this research project is to establish receptance-based structural modification methods which can provide effective solutions to reduce vibration for assembled structures. Active control and passive modifications are also combined to deliver better control performance and to make partial eigenstructure assignment. To achieve the aim, some objectives are established, which are

(1) To build a receptance-based frequency assignment method for assembled structures. Assembled structures are composed of several unmodifiable substructures and a number of simple links. It is expected to assign frequencies for an assembled structure by optimizing the properties of the links with receptances at connection points.



(2) To design a laboratory test rig that can be used to validate the proposed frequency assignment method and carry out experiments on the designed structure. High quality receptances are needed to achieve frequency assignment. In particular, a rotational receptance is usually difficult to estimate in practice. Rotational receptance estimation methods are studied and implemented on the test structure. Modal analysis techniques are also very important to in the experimental work.

(3) To overcome the limitation of the existing receptance-based active control that a general eigenvector usually cannot be assigned. A possible solution is to resort to passive modification to enlarge the set of eigenvectors that can be assigned. It is needed to investigate how to determine required passive modifications and how to minimize the differences between desired eigenvectors and obtained eigenvectors. It should be mentioned that the force distribution matrix  $\mathbf{B}$  is assumed to be predefined.

(4) To avoid the requirement of open-loop eigenvectors in receptance-based active control method for partial assignment. The eigenvector, compared with eigenvalues, is prone to pollution of measurement uncertainties. Certain modes, especially higher modes, are difficult or even not able to be excited with an impact hammer or a single shaker. It will save efforts and avoid the inaccuracy from the polluted eigenvectors if the open-loop eigenvectors are not needed. Without knowing the open-loop eigenvectors, it is difficult to keep the eigenvectors corresponding to invariant eigenvalues unchanged with only receptances. If the shapes of the relevant eigenvectors be different, the requirement of knowledge on open-loop eigenvectors might be avoided.

## **1.4 Original contributions**

The original contributions of this thesis are summarised in the following:

1. Receptance-based frequency assignment for assembled structures: A receptance-based frequency assignment method for assembled structures is put forward. This method is able to assign several frequencies of an assembled structure by optimizing the properties of the links between substructures. Only the receptances at the connection points must be measured. This method is useful when modifications of substructures are not allowed or difficult to implement and is efficient when there are several substructures and multiple links.

2. Experimental application on an assembled structure: The proposed frequency assignment method for assembled structures is validated on a real structure. This test structure is composed of two substructures and six simple links. Only the receptances at connection points are measured. Moreover, the rotational receptances are estimated using an auxiliary structure and two angular accelerometers. Natural frequencies can be successfully assigned to the assembled structure by optimizing the dimensions of the cross sections of the links.

3. Receptance-based partial eigenstructure assignment using hybrid control: This method is the first one that can achieve partial eigenstructure assignment of a second-order system with a hybrid control method. A proper passive modification is used to widen the set of eigenvectors that are assignable. The required structural modifications, which are usually mass and stiffness modifications or spring-mass oscillators, are determined by solving an optimization problem.

4. Receptance-based partial eigenstructure assignment with state feedback control: The existing receptance-based active control methods need the eigenvectors of the open-loop system. However, the efforts to get accurate eigenvectors are usually big. To avoid the requirement of knowledge on eigenvectors of the open-loop system, a new receptance-based partial eigenstructure assignment method by multiple-input active control is proposed in this work. Some elements of the force distribution matrix  $\mathbf{B}$  may be left as unknowns at the start and then determined so as to achieve eigenstructure assignment. This method is believed to be the first attempt to achieve partial eigenstructure assignment with only receptance.

## 1.5 Outline of the thesis

There are seven chapters in this thesis and the original contributions in this thesis are mainly presented in chapter 3 to 6. Fig. 1.1 shows the overall structure of this thesis and the outline of each chapter is given as follows:

**Chapter 1** introduces the motivations, the objectives of this research and the outline of this thesis. The research work in this thesis is motivated by a common engineering problem on a ship and some problems of the existing receptance-based active control method.

**Chapter 2** shows a comprehensive literature review on the structural modification, active control and receptance measurement. Structural modification is divided into forward approaches and inverse approaches. The active control methods are reviewed from four aspects regarding their purposes. The difficulties in receptance measurement and some simple assessments of measured data are presented in the end.

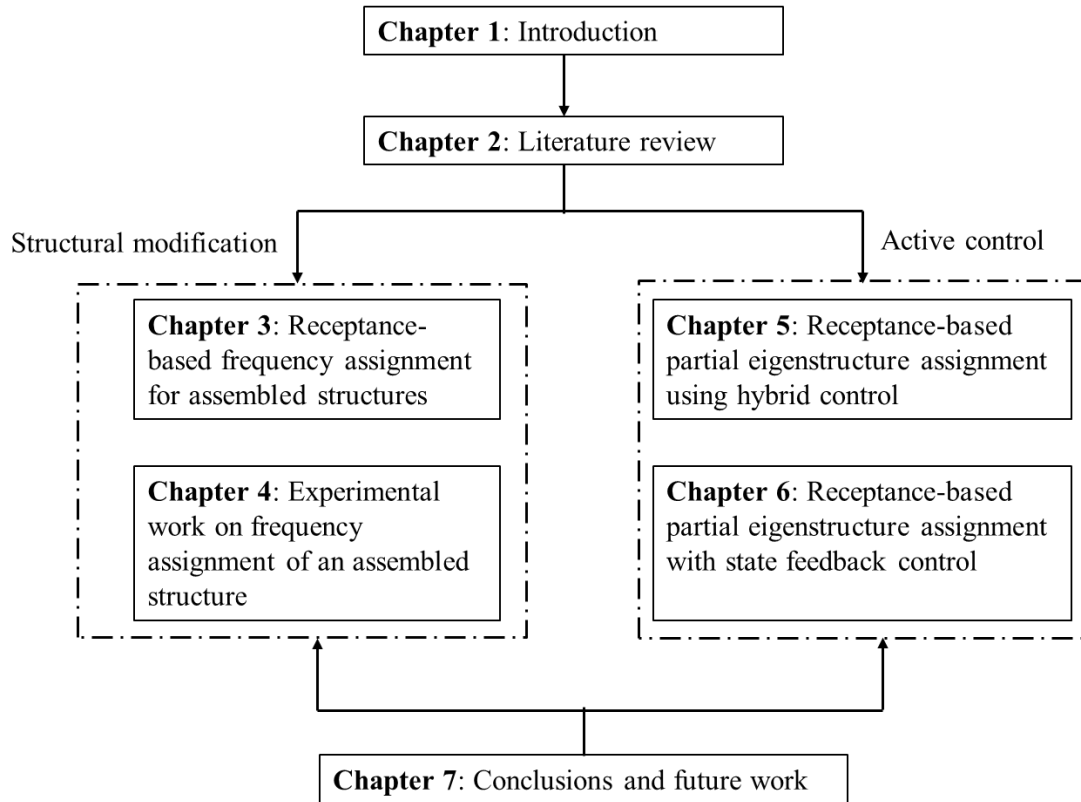


Fig. 1.1 The structural flowchart of the thesis

**Chapter 3** proposes a frequency assignment method for assembled structures with receptance. This method achieves the frequency assignment by optimizing the properties of links between substructures. It is very useful when substructures are not allowed or difficult to be modified. Also, modifying links is usually much easier and cheaper than modifying substructures.

**Chapter 4** demonstrates an experimental work on an assembled structure. The receptances at connection points on each substructure are measured. Moreover, rotational receptances are obtained with the aid of an auxiliary structure and two angular sensors. Experimental results show the proposed method in chapter 3 is able to achieve frequency assignment for assembled structures by designing the links.

**Chapter 5** derives a receptance-based partial eigenstructure assignment method with hybrid control. To overcome the limitation of the existing receptance-based active control on the assignment of a general eigenvector, passive modification is adopted to enlarge the assignable set of closed-loop eigenvectors.

**Chapter 6** develops a receptance-based partial eigenstructure assignment method through state feedback control. Unlike the existing receptance-based active control method, this method can avoid the using of open-loop eigenvectors.

**Chapter 7** makes a brief summary of this PhD project and gives some thoughts for the future work.

## **Chapter 2**

### **Literature review**

There has been a vast amount of literature which aims to modify or assign the dynamic properties of a vibrating system. The most important work in this topic is how to determine the required modifications or control inputs and what kind of information is needed in order to this. This chapter presents a detailed review of the state-of-the-art literature on this subject in three aspects: structural modification, active control, and receptance measurement. For structural modification, there are mainly two kinds of approaches: forward analysis and inverse analysis. The structural modification methods for assembled structures are introduced in particular. For active control, the papers are generally classified into four groups, pole/eigenvalue assignment, eigenstructure assignment, partial eigenvalue assignment and partial eigenstructure assignment. In addition, several hybrid control methods, which use both passive modification and active control, are also discussed in this subsection. Due to the limitations of passive modification, there are only a few papers which can address the partial eigenvalue/eigenstructure assignment with passive modification. Therefore, structural modification methods are not classified into the above groups. Then, for receptance measurement, the difficulties in receptance measurement are also discussed. Some modal analysis methods and some methods that can assess the quality of measured data are included. The structural modification and active control methods reviewed in this chapter are mainly about the linear vibrating systems, while they can be extended to nonlinear vibrating system by using some linearization methods, for example, the methods introduced in [5, 6]

## 2.1 Basic knowledge

### 2.1.1 The concept of receptance

Before proceeding with a review of structural modification, it is necessary to first define what receptances are because this concept is very important in the following chapters. Receptances are data that quantify the frequency domain relationship between a harmonic excitation force (input) applied to a structure at a specific DoF (degree of freedom) and the resulting displacement (response/output) at a specific DoF dynamic system [7]. The mathematical definition of receptance is explained in the following.

Consider an arbitrary  $n$  DoF undamped system, the matrix form of equations of motion is written as

$$\mathbf{M}\ddot{\mathbf{x}}(t) + \mathbf{K}\mathbf{x}(t) = \mathbf{f}(t) \quad (2.1)$$

where dots denote derivatives with respect to time. The mass and stiffness matrices,  $\mathbf{M}$  and  $\mathbf{K}$ , respectively, are time independent real symmetric  $n \times n$  matrices. Moreover, it is assumed that  $\mathbf{M}$  is positive definite, and  $\mathbf{K}$  are semi-positive definite.  $\mathbf{f}(t)$  is a  $n \times 1$  vector of “ $n$ ” external forces.

If the forces are harmonic with the same frequency and phase (phase is assumed to be zero here), then

$$\mathbf{f}(t) = \begin{bmatrix} f_1 \\ f_2 \\ \cdots \\ \cdots \\ f_n \end{bmatrix} \sin(\omega t) = \mathbf{f} \sin(\omega t) \quad (2.2)$$

where  $f_i$  ( $i = 1, 2, \dots, n$ ) are the amplitudes of the harmonic forces and  $\mathbf{f}$  is a  $n \times 1$  real vector. The system will vibrate harmonically at the same frequency with the excitation forces. Since damping is not concerned here, there is no phase difference between the excitations and responses. Therefore, the displacement vector can be expressed as

$$\mathbf{x}(t) = \begin{bmatrix} v_1 \\ v_2 \\ \cdots \\ v_n \end{bmatrix} \sin(\omega t) = \mathbf{v} \sin(\omega t) \quad (2.3)$$

where  $\mathbf{v}$  denotes the amplitudes of the displacement responses.

Substituting Eqs. (2.2) and (2.3) into Eq. (2.1) yields

$$(\mathbf{K} - \omega^2 \mathbf{M})\mathbf{v} = \mathbf{f} \quad (2.4)$$

Here, matrix  $(\mathbf{K} - \omega^2 \mathbf{M})$  is known as dynamic stiffness matrix and is usually written as

$$\mathbf{Z}(\omega) = \mathbf{K} - \omega^2 \mathbf{M} \quad (2.5)$$

Then Eq. (2.4) can be reformed as

$$\mathbf{Z}(\omega)\mathbf{v} = \mathbf{f} \quad (2.6)$$

or

$$\mathbf{v} = \mathbf{H}(\omega)\mathbf{f} \quad (2.7)$$

The matrix  $\mathbf{H}(\omega)$  in Eq. (2.7), which is the inverse of dynamic stiffness matrix  $\mathbf{H}(\omega) = (\mathbf{K} - \omega^2 \mathbf{M})^{-1}$ , is named receptance matrix.

For a damped system, the equation of motion can be expressed as

$$\mathbf{M}\ddot{\mathbf{x}}(t) + \mathbf{C}\dot{\mathbf{x}}(t) + \mathbf{K}\mathbf{x}(t) = \mathbf{f}(t) \quad (2.8)$$

where damping matrix  $\mathbf{C}$  is assumed to be semi-positive definite and symmetric.

If the excitation force  $\mathbf{f}(t)$  is harmonic and written in a complex form

$$\mathbf{f}(t) = \mathbf{f}e^{i\omega t} \quad (2.9)$$

where  $\mathbf{f}$  is a  $n \times 1$  complex vector. Then the steady state displacement vector is usually written as

$$\mathbf{x}(t) = \mathbf{v}e^{i\omega t} \quad (2.10)$$

Here  $\mathbf{v}$  is also a  $n \times 1$  complex vector.

Substituting Eqs. (2.9) and (2.10) into Eq. (2.8) gives

$$(-\omega^2 \mathbf{M} + i\omega \mathbf{C} + \mathbf{K})\mathbf{v} = \mathbf{f} \quad (2.11)$$

Then the dynamic stiffness matrix and receptance matrix of a damped system are denoted by

$$\mathbf{Z}(\omega) = \mathbf{K} - \omega^2 \mathbf{M} + i\omega \mathbf{C} \quad (2.12)$$

$$\mathbf{H}(\omega) = (\mathbf{K} - \omega^2 \mathbf{M} + i\omega \mathbf{C})^{-1} \quad (2.13)$$

Owing to the existence of damping, the receptance is often denoted by  $\mathbf{H}(i\omega)$ . In general, the receptance matrix  $\mathbf{H}(i\omega)$  is

$$\mathbf{H}(i\omega) = \begin{bmatrix} h_{11}(i\omega) & h_{12}(i\omega) & \dots & h_{1n_f}(i\omega) \\ \vdots & \vdots & \dots & \vdots \\ h_{n_x1}(i\omega) & h_{n_x2}(i\omega) & \dots & h_{n_xn_f}(i\omega) \end{bmatrix} \quad (2.14)$$

Each element  $h_{ij}(i\omega)$  in receptance matrix  $\mathbf{H}(i\omega)$  gives the relationship between the  $i$ th displacement and the  $j$ th excitation force. When the excitation force and measured displacement are at the same location in the same direction, that is to say  $i = j$ , the receptance  $h_{ij}$  is called point receptance. And  $h_{ij}$  is called cross receptance when  $i \neq j$ . In addition,  $\mathbf{H}(i\omega)$  is a Hermitian matrix  $\mathbf{H}(i\omega) = \mathbf{H}(i\omega)^T$ , which means  $h_{ij}(i\omega) = \overline{h_{ji}(i\omega)}$ .

### 2.1.2 Structural modification and active control targets

Structural modification and active control aim to modify the dynamic behaviour of a system so as to satisfy certain requirements in real applications. More specifically, the targets of structure modification and active control, concerned in this literature, can be roughly examined in the following aspects: frequency assignment, anti-resonance assignment, eigenstructure assignment, partial eigenvalue assignment, and partial eigenstructure assignment.

Frequency assignment, is a special case of eigenvalue assignment or pole assignment. It is to shift unwanted frequencies to desired locations [8-10]. Anti-resonance assignment is also called zero assignment. A vibration absorber is actually a good example of the application of the assignment of zero, as introduced by Inman [11] and Sun et al. [12]. The concepts of pole and zero are often used in control theory. Poles



are global properties while zeros are local properties of an individual receptance. Specially, for a particular receptance, a pole and a zero can coincide at a frequency, leaving one peak invisible from the receptance and one node in the mode or eigenvector. This is called a pole-zero cancellation [13].

All eigenvalues and eigenvectors (i.e., eigenpairs), together, constitute the eigenstructure of a system. Eigenstructure assignment techniques allow the modified system to have desired eigenvalues and eigenvectors (or frequencies and mode shapes) and have been widely used for vibration suppression in structures, especially in large space structures [14-17].

In practical applications, it is very common that only a small number of eigenvalues need to be relocated, for example, to avoid resonance. The modification of a subset of the natural frequencies, however, may lead to unexpected changes of other eigenvalues. This phenomenon is known as frequency spill-over. To avoid or minimize the unexpected changes of the other eigenvalues, partial eigenvalue assignment methods have been developed [18]. In addition, partial eigenstructure assignment is another hot topic in this field which is more challenging [19].

The above-mentioned topics in the field of structural modification and active control have been studied by numerous researchers. A detailed review on the existing techniques is presented in the following subsections.

## **2.2 Structural modification**

Structural modification is usually referred to as a technique to study the effects of physical parameters changes of a vibrating system on its dynamic characteristics. The data necessary to solve the structural modification problem are the dynamic behaviour of the original structure and the modifications [20]. The modifications can take various forms. For a simple mass-spring system, the modification parameters are usually the mass and stiffness quantities of physical elements. For a practical system such as a cantilever, the modification parameters can be the thickness or length of a section of the beam. Besides, additional structure, such as beams or plates, can also be added to modify the original system. These modifications are not mass or stiffness quantities but their changes affect both mass and stiffness properties. The dynamic behaviour of the structure can be described by

(1) Spatial model obtaining from finite element model, which refers to mass, stiffness and damping matrices ( $\mathbf{M}$ ,  $\mathbf{K}$ ,  $\mathbf{C}$ ) of a system [21-23].

(2) Modal model, made of natural frequencies, damping ratio and mode shapes identified by a curve-fitting of experimental data or determined from a theoretical analysis [24].

(3) Response model, which can be directly obtained from experimental modal analysis (EMA) on a structure and is often expressed by frequency response functions (FRFs) [1].

Table 2.1 Relationship among the three models [25]

	Spatial model	Modal model	Response model
Spatial model ( $\mathbf{M}$ , $\mathbf{K}$ , $\mathbf{C}$ )	----	Eigenvalue problem $(-\omega^2\mathbf{M} + i\omega\mathbf{C} + \mathbf{K})\mathbf{v} = \mathbf{0}$	$\mathbf{H}(\omega) = (-\omega^2\mathbf{M} + i\omega\mathbf{C} + \mathbf{K})^{-1}$
Modal model $\text{diag}(\omega_i^2)$ , $\mathbf{V}$	$\mathbf{M} = (\mathbf{V}\mathbf{V}^T)^{-1}$ $\mathbf{K} = \mathbf{M}\mathbf{V}\text{diag}(\omega_i^2)\mathbf{V}^T\mathbf{M}$	---	$\mathbf{H}(\omega) = \mathbf{V}\text{diag}([\omega_i^2 - \omega^2]^{-1})\mathbf{V}^T$
Response model $\mathbf{H}(\omega)$	$\mathbf{K} = \mathbf{H}(\omega)^{-1} _{\omega=0}$ $\mathbf{M} = \frac{\mathbf{H}(\omega_1)^{-1} - \mathbf{H}(\omega_2)^{-1}}{\omega_2^2 - \omega_1^2}$	Modal analysis	---

The three models are interchangeable as shown in Table 2.1 and the structural modification methods varies depending on the model adopted. The spatial model identification is usually difficult when dealing with complex structure, such as an engine or a tower. Also, the estimation of complete modal model usually runs into ill-condition problem and modal truncation error. In contrast, the directly use of measured receptance can partially avoid the requirement of accurate spatial model and the incompleteness of modal model.

On the other hand, the form of modifications will also lead to different structural modification methods. Structural modification can be a forward/direct problem or an inverse problem. A detailed introduction on the structural modification methods is given in the following sections.

### 2.2.1 Forward problem

The forward problem is the one that predicts dynamic property changes once mass or stiffness changes are given.

Baldwin and Hutton [26] provided a detailed review about structural modification techniques that had been proposed before the 1980s. These techniques can be grouped into three categories based on the assumptions of the form of modifications: techniques based on small modifications [27, 28], techniques based on localized modifications [29-31] and techniques based on modal approximation [32]. Elliott and Mitchell [33] examined the effects of modal truncation on modal modifications. The results of their study showed the modified modal vector can be a weighted linear sum of the original modal vectors and modal truncation might affect almost any mode in a modification process. Ram et al. [34] derived the Rayleigh-Ritz approximations for some of the eigenpairs of a modified structure. This method is applicable when using truncated modal testing data and finite element analysis for modified structures.

The effects of system modification on the dynamic behaviour of the system were investigated by Ram and Blech [35]. It was shown that the consequence of connecting a vibratory system to the ground through a simple oscillator is to increase the natural frequencies of the unmodified system which are lower than the natural frequencies of the oscillator, and to decrease the natural frequencies which are above the natural frequency of the oscillator. Ram [36] determined the eigenvalues of damped subsystems with known connections using transfer function or spectral and modal data from the separate subsystems. Cafeo et al. [37] explored the utilization of beam elements in structural dynamics modification based on experimental modal data including rotational degrees of freedom. Hang et al. [38] investigated approaches of efficiently predicting the effects of distributed structural modifications on dynamic response of a complex structure.

Apart from predicting the dynamic property of a structure with known modifications, there are also a number of articles on predicting dynamic behaviours of assembled structures. An assembled structure usually consists of several substructures. Substructure coupling methods have been widely used to couple substructures and predict their dynamic responses [39-42]. Those methods, although their initial purpose is not frequency assignment, could also be used to solve forward structural

modification problem [43]. There are mainly two types of substructure-coupling methods: modal synthesis methods [44], and frequency domain methods [45]. Modal synthesis methods usually would produce modal truncation errors, while frequency domain methods, using the measured FRFs directly, could avoid this problem [46]. De Klerk et al. [47] presented a general framework which allowed for classification of substructuring methods and highlighted the interrelations between those methods. A reformulation and generalization of the classical frequency-based substructuring method was introduced by De Klerk et al. [46]. D'Ambrogio et al. [48] analysed the feasibility of assembling different substructures' models, such as FRF models, modal models and FE (finite element) models, for predicting the dynamic behaviour of assembled structures. Liu and Ewins et al. [40] reviewed some FRF-coupling methods and then proposed a general joint description method for FRF-coupling analysis. The FRFs of a plate connected with a beam via a steel bolt were predicted. Matthias et al. [49] predicted the FRFs at the tool tip of a holder-tool assembly based on receptance-coupling substructure analysis. Latini et al. [50] used modal substructuring methods to get the behaviour of complex linear systems which are coupled through a nonlinear interface.

### **2.2.2 Inverse problem**

The inverse problem is to determine the structure parameters such that the modified systems could have desired dynamic behaviour, such as shifting the troublesome natural frequency away from the driving frequency, creating a vibration node or decreasing the vibration amplitudes. Compared with forward methods, the inverse methods are more intuitive in practical problems and more appealing in practice.

Some inverse methods rely on system spatial model [21-23] or modal data [51-53]. Ram and Braun [53] proposed a method for approximating the necessary changes in the mass and stiffness matrices of a linear system to reach a desired dynamic behaviour based on incomplete modal model of the unmodified system. Bucher and Braun [52] proposed an inverse structural modification method that computed the necessary mass and stiffness modifications using modal test results only, even when only a partial set of eigensolutions is available for such tests. Braun and Ram [24] considered the inverse problem of determining the structural modifications which could assign a desired spectrum and developed physically realisable solutions. They showed that it is possible

to solve the inverse structural modification problem without truncation error if both left and right eigenvectors of the system are available. Wu [22] transferred the problems of inverse eigenvalues design of lumped linear parameters system into that of solving algebra equations.

Another important and interesting application of structural modification is called zero/anti-resonance assignment. Zeros are as important as the natural frequencies since they are the frequencies at which vibration disappears to zero, or to low amplitudes when damping is present. Zeros of the system can be determined mathematically by solving for the eigenvalues of the adjoint system, obtained by deleting a row and a column from the original dynamic stiffness matrix.

Some researchers used sensitivity method to assign poles (natural frequency) and zeros (antiresonances). For example, Mottershead [54] studied the relationship between the sensitivity of the zeros and the sensitivities of natural frequencies and mode-shapes of structural systems. The zeros can be determined by solving a ‘subsidiary’ eigenvalue problem. A big drawback of the sensitivity approach is that it is based on a linear truncation of the Taylor series, and is therefore limited to small modifications. Mottershead and Lallement [13] established the necessary and sufficient conditions for pole-zero cancellations and achieved pole-zero cancellation in structures by unit-rank modifications. They also concluded that it is not possible to produce a pole-zero cancellation by a point modification at the same DoF. Li and He [55] realized pole-zero cancellation of a vibrating system using linear modification method. This method was also extended to several pole-zero cancellations for a single receptance or to the same pole-zero cancellation for several receptances.

In terms of partial eigenvalue assignment problem (no spill-over), Ouyang and Zhang [56] made a first attempt to achieve the partial assignment of natural frequencies of mass-spring systems with passive modifications. Two kinds of lumped mass-spring systems, simply in-line mass-spring systems and multiple-connected mass-spring systems were analysed and physically realisable passive modifications can be found for those two kinds of systems. Motivated by the work by Ouyang and Zhang, Belotti et al. [57] proposed a new partial frequency assignment method for general structures with passive modifications. Physically realizable modifications were determined through a three-step procedure. First of all, a system that has the desired eigenvalues

is found, regardless of the physical constraints. After that, an equivalent system is computed. Finally, the system is projected onto the feasibility constraints to obtain an optimal physically realizable structure.

- **Receptance-based methods**

Some practitioners argue that the direct use of FRFs seems more logical than the indirect use of modal parameters derived from the FRF data because the modal data derived from finite element model (FEM) or experimental modal analysis (EMA) form an incomplete set of eigenvalues and eigenvectors. Wei et al. [58] showed that, when using modal parameters, the accuracy of the modified dynamic properties is largely affected by the quality of the modal model derived from experimental data. Moreover, when dealing with complex structures, knowledge of the main dynamic parameters is usually poor and the system must be supposed to be a black box, whose dynamics can be characterised by modal testing. Therefore, a great deal of attention has been devoted to black box structures, dynamically described by receptance data.

Early work in the field of receptance-based inverse structural modification theory can be traced back to Duncan [59]. Sestieri and D'Ambrogio [60] solved the structural modification problem using a raw set of experimentally determined FRFs and avoiding any identification process aimed at the creation of either a modal or a physical model of the structure. Several dynamic requirements, such as FRF modulus, response modulus, response power spectral density and response mean square value, can be imposed, depending on the specifications to be satisfied and on the information available about the excitation forces. Tsuei and Yee [61] presented a method for shifting a particular natural frequency of an undamped mechanical system to a desired value. This technique was based on the FRFs of the original dynamic system and gave a global picture for the behaviour of the system with respect to the mass and stiffness parameters. Later on, the same authors, Yee and Tsuei [62] extended this technique for damped structures. The required mass modifications or stiffness modifications could be obtained through an iteration process. Park and Park [63] used a substructure coupling concept to extend the application of the receptance-based structural modification method to large modal changes. Mottershead [1] showed a method that can assign zeros using measured receptances. Only a small number of measurements on the original structures was needed. This method is very useful and convenient in

zero assignment problem and has been proved on several laboratory experimental structures [64, 65].

Kyprianou et al. [66] assigned natural frequencies to a multi-degree-of-freedom undamped system using added mass-spring oscillators. New degrees of freedom were introduced during the modification. The parameters of the mass-spring subsystems were determined by solving multivariate polynomials using the theory of Groebner bases. Later on, the same authors [64] applied the receptance-based structural modification method to a  $\Gamma$ -shaped beam structure. An additional beam was added on the original structure and the dimensions of the cross-section of the added beam were obtained by solving several multivariate polynomials. Only the receptances at the modification coordinates are needed. In particular, the rotational receptances are very important for the frequency or anti-resonance assignment. A rotational receptance estimation method was also introduced by the same authors [67]. Mottershead et al. [68] explored the structural modification of a Lynx Mark 7 helicopter tailcone. A full  $6 \times 6$  receptance matrix at the modification point, including the rotational receptances, was measured using a X-block attachment. The modification in this experiment was in the form of a large overhanging mass.

Ouyang et al. [69] addressed the eigenstructure assignment problem for undamped vibrating systems by formulating the problem as a convex-constrained optimization problem. The method only requires receptances of unmodified system and experimental work on a five-degree-of-freedom undamped test structure with mass and spring modifications was demonstrated to validate the proposed method. This work motivated Liu et al. [70] to assign eigenstructure by adding multiple mass-spring oscillators to some locations of the original structure.

Zarraga et al. [71] reported a theoretical and experimental work on the prediction and suppression of squeal noise of a brake-clutch model. In order to suppress squeal noise, a receptance-based inverse method was applied to shift one of the frequencies of the doublet mode to avoid mode coupling. Tsai et al. [65] presented an experimental validation to the receptance-based structural modification method using a laboratory geared rotor-bearing system. Experimental results showed that more than one natural frequency or antiresonance can be assigned using only the measured receptances.

Liu et al. [72] summarized the receptance-based assignment with entry modifications and extended it to solve frequencies and modes assignment problems by adding subsystems. Three methods different in computational efficiency were proposed in this paper for assignment by arbitrarily complex subsystems and connections. A special case of inverse modification problem is to preserve a specific natural frequency of the structure after modifications. A method based on the Sherman-Morrison formula was proposed by Cakar [73] to keep any one of the natural frequencies of a real structure constant after mass and stiffness modifications.

It is usually assumed the system matrices of engineering structures are symmetric and mass matrix  $\mathbf{M}$  is positive definite and stiffness matrix  $\mathbf{K}$  and damping matrix  $\mathbf{C}$  are semi-positive definite. The structural modification problems on those structures have been well studied. However, in a more general case, engineering structures may have asymmetrical stiffness matrix or damping matrix, such as gyroscopic and circulatory systems [74]. The asymmetry is usually not from the structure itself, but from external loads such as aeroelastic flutter problems or friction in brakes noise problems [75]. Structural modification for structures with asymmetric stiffness matrices or damping matrices are usually more difficult.

An interesting work on the structural modification of damped asymmetric system was studied by Ouyang [76]. This work considered the asymmetry introduced in the stiffness matrix by friction. The author first showed a method that can predict the latent roots of damped asymmetric system from the receptance of damped symmetric system. Then the inverse problem of assigning latent roots to the damped asymmetric system was solved based on the receptance of the unmodified damped symmetric system. Different types of modifications, such as point mass, stiffness and damping modifications, were discussed in this work.

### **2.3 Active control**

Mottershead and Ram said that in 2006 “Control of vibratory systems by passive elements, i.e., by adding springs or dampers to the system, necessitates the system to satisfy the reciprocity law that the force at the  $j$ th DoF due to a unit displacement at the  $k$ th DoF is equal to the force at the  $k$ th DoF due to a unit displacement at the  $j$ th DoF” [77]. This property actually limits the application of passive modification in



vibration control, while the active control method can overcome this limitation. In theory, any desirable forces can be applied on a structure by actuators. Therefore, active control can give much more freedoms when designing the forces to be applied on the structure and has been widely used in the field of vibration control. On the other hand, it should be noted that, in practical applications, passive modifications are usually more desirable because it is more stable and does not need power supply. Before go into the literatures, a simple introduction on the active control is given below.

The dynamic behaviour of a vibrating system can be modified by active control implementing state feedback

$$\mathbf{M}\ddot{\mathbf{x}}(t) + \mathbf{C}\dot{\mathbf{x}}(t) + \mathbf{K}\mathbf{x}(t) = \mathbf{B}\mathbf{u}(t) \quad (2.15)$$

where matrix  $\mathbf{B} \in \mathcal{R}^{n \times n_b}$  is the force distribution matrix ( $n_b$  is the number of actuators/inputs) and  $\mathbf{u}(t)$  represents the control inputs and

$$\mathbf{u}(t) = \mathbf{F}^T \dot{\mathbf{x}}(t) + \mathbf{G}^T \mathbf{x}(t) \quad (2.16)$$

where  $\mathbf{u}(t) \in \mathcal{R}^{n_b \times 1}$  and matrices  $\mathbf{F}$  and  $\mathbf{G}$  are  $n \times n_b$  matrices.

The problem in active control is to determine the required feedback control gains matrices  $\mathbf{F}$  and  $\mathbf{G}$  which can lead to desired closed-loop eigenvalues or eigenvectors.

As said above, pole or eigenvalue assignment has been widely studied in active control theory. For a general case in control theory, pole assignment problem is often stated in a first-order form

$$\mathbf{y}(t) = \mathbf{A}\dot{\mathbf{y}}(t) + \widehat{\mathbf{B}}\widehat{\mathbf{u}}(t) \quad (2.17)$$

There have been numerous methods that achieve pole assignment for systems describing in a first-order equation form. It is easy to think about converting the second-order differential equation in Eq. (2.15) to first-order state-space form such that the pole assignment methods in control theory can be utilized in a vibrating system.

Eq. (2.15) can be written in a first-order state-space form by defining

$$\begin{aligned} \mathbf{A} &= \begin{bmatrix} \mathbf{0} & \mathbf{I} \\ -\mathbf{M}^{-1}\mathbf{K} & -\mathbf{M}^{-1}\mathbf{C} \end{bmatrix}_{2n \times 2n} & \widehat{\mathbf{B}} &= \begin{bmatrix} \mathbf{0} \\ \mathbf{M}^{-1}\mathbf{B} \end{bmatrix}_{2n \times n_b} \\ \mathbf{y}(t) &= \begin{bmatrix} \mathbf{x}(t) \\ \dot{\mathbf{x}}(t) \end{bmatrix}_{2n \times 1} & \widehat{\mathbf{u}}(t) &= \mathbf{u}(t) \in \mathcal{R}^{n_b \times 1} \end{aligned} \quad (2.18)$$

Although the first-order state-space form is often used in control theory, it will inevitably involve dealing with matrices of  $2n$  dimension and thus results in very large computational efforts and possibly poor computational conditioning. In addition, the first-order state space form will lose some natural properties of the system matrices such as symmetry and definiteness. Therefore, in vibrating system, it is preferable to work with the dynamic equations in the second-order form rather than in the first order state-space form.

This subsection gives a detailed review on active control methods. The active control methods in this literature are generally classified into four groups based on their purposes: pole/eigenvalue assignment methods, eigenstructure assignment methods, partial eigenvalue assignment methods and partial eigenstructure assignment methods.

### **2.3.1 Pole/eigenvalue assignment**

Earlier reliable pole placement techniques were derived by Miminis et al. [78, 79]. Those techniques can accurately compute the required feedback in single input case, while the feedback is underdetermined in multiple-input case. Kautsky et al. [80] solved the multiple-input state feedback pole placement problem for first-order systems. Robust solutions were obtained with four algorithms by defining a solution space of linearly independent eigenvectors corresponding to the desired eigenvalues. Carotenuto and Franzè [81] derived a new characteristic polynomial equation for the closed-loop system with static output feedback. Robust solutions of pole assignment can be obtained by an efficient algorithm of global optimization.

Chu and Datta [82] adapted the pole assignment method of first-order systems by Kautsky et al. [80] to pole assignment of second-order systems. They also extended the feedback stabilization of a non-modal approach by Datta and Rincón [83] to a generalization version. The robustness was guaranteed by minimising the condition numbers of the closed-loop eigenvectors. Abdelaziz and Valasek [84] presented a computationally efficient algorithm for solving the pole placement of linear multiple-input systems with non-singular system matrix by state-derivative feedback. Both time-invariant and time-varying systems were considered and this work was believed by the authors to be the first general treatment for multiple-input pole placement by state-derivative feedback.

The receptance method, which was usually used in passive modification, was first introduced into active vibration control by Ram and Mottershead [2]. It was demonstrated that all the poles/zeros might be assigned by single input state feedback control without the knowledge of  $\mathbf{M}$ ,  $\mathbf{C}$ , and  $\mathbf{K}$  matrices. Then a receptance-based output feedback control method was derived by Mottershead et al. [4]. Compared with state feedback control, the output feedback control allows to use collocated actuators and sensors in multiple-input-multiple-output (MIMO) systems. They also demonstrated experiments of poles or zeros assignment of a T-shaped plate.

Ouyang [85] extended the receptance-based method to the complex pole assignment of asymmetric systems using state feedback control. The real part of the complex poles, which reflect the stability of dynamic systems, were particularly designed to improve the stability of asymmetric dynamic systems. Later on, this author [86] proposed a two-stage, passive modification and state feedback control combined, hybrid control method to assign complex poles with negative real parts to asymmetric systems to suppress flutter instability. The hybrid method can result in lower energy cost than sole active control. Singh and Ouyang [87] considered the time-delay problem in the state feedback control loop for pole assignment of damped asymmetric systems. This method is based on the receptances of the symmetric part of the asymmetric open-loop system. Liang et al. [88] assigned not only desired complex poles for asymmetric systems but also eigen-sensitivities at the same time. By assigning eigen-sensitivities, the deviations of obtained eigenvalues from desired eigenvalues, which are usually caused by uncertainties in system parameters, can be minimized.

Tehrani et al. [89] considered errors in receptance measurements and estimated the eigenvalue sensitivities to the errors of receptances. In addition, a sequential multiple-input state feedback control approach was explained. A different eigenvalue can be assigned in each step without affecting the previous assigned eigenvalues. This sequential multiple-input approach was shown to be more robust to measurement noise than the single-input method. Tehrani et al. [90] also extended the receptance-based active control method to a class of single-degree-of-freedom nonlinear systems. An iterative form of the Sherman-Morrison receptance method was required for accurate assignment of peak resonances. Mokrani et al. [91] minimized the control effort required for partial pole placement in multiple-input, multiple-output systems with receptance method. Adamson et al. [92] derived the sensitivity expressions of assigned

closed-loop poles regarding of the FRF misfitting. A robustness metric was defined and optimized by assigning poles within rectangular regions in the complex plane.

Richiedei et al. [93] studied the inverse dynamic modification problem of simultaneous assignment of some resonances and antiresonances with higher-rank modifications. The higher-rank modifications mean the modifications of more parameters. This method allows to reverse the sequence of resonances and antiresonance in cross-receptance, named pole-zero flipping. Pole-zero flipping can be useful in shaping the frequency response or in feedback-controlled systems. Later on, Richiedei and Tamellin [94] developed a novel method which can achieve antiresonance assignment and regional pole placement simultaneously. Instead of assigning accurate poles, all the closed-loop poles were designed to ensure the systems possess desired transient properties such as damping or decay rate. This method can be applied to linear, asymmetric or unstable systems. Antiresonance assignment in lightweight systems was studied by Richiedei et al. [95] using a unit-rank output feedback control. Furthermore, two method extensions were also proposed in the same work. One is to perform pole-zero assignment by using an additional sensor and the other one is a passive-active hybrid strategy which can allow larger frequency shifts without reducing too much the stability margins.

### **2.3.2 Eigenstructure assignment**

Eigenvalues and eigenvectors both play an important role in determining the dynamic behaviour of a vibrating system. Although the control theory usually targets on the assignment of eigenvalues, assigning the eigenvectors too can have more advantageous for vibration control [96]. Eigenstructure assignment is a very useful tool in many field such as finite element model updating [97] and aircraft control.

Calvo-Ramon [14] used the concepts of eigenvalue sensitivity to minimize the distance between the closed-loop eigenstructure of a vibrating system and the predetermined eigenstructure. An output feedback controller can be designed by this method. Rew et al. [15] proposed a new eigenstructure assignment method based on a pole placement method for first-order systems. A symmetric eigenstructure assignment algorithm was employed to make improvement of structural finite element models by Zimmerman and Widengren [98]. This approach was developed for linear vibrating structures with nonproportional damping. Triller and Kammer [99] proposed an active control method

which combined the advantages of the reduced Craig-Bampton substructure representation technique and the eigenstructure assignment control method. The designed controller using this approach was shown to produce more accurate closed-loop eigenstructure.

Kim et al. [99] considered the eigenstructure assignment for vibrating systems represented by second-order differential equations. The computation efforts were reduced and the numerical accuracy of the solutions was improved, compared with the methods with first-order systems. Datta [100] presented a brief review on finite element model updating approaches using eigenstructure assignment or eigenvalue embedding. Duan and Liu [101] used proportional-plus-derivative feedback controller to achieve eigenstructure assignment in second-order linear systems. Simple and complete parametric forms for both the closed eigenvector matrix and the feedback gains are established under a very weak condition. Rastgaar et al [102] gave a review of eigenstructure assignment methods for vibration cancellation in large space structures. Those methods could confine the vibrations close to the source of disturbance while suppressing the vibrations away from disturbance. An eigenstructure assignment theory was adapted to reduce vibration and avoid shimmy on landing gears by Laporte et al. [103]. This method was used to stabilise the landing gear with better vibration response and reduce vibration in near-shimmy operational conditions.

Belotti and Richiedei [104] proposed a passive-active combined, hybrid approach to improve the attainability of the desired eigenstructure. Suitable passive modification was used to enlarge the set of assignable eigenvectors that can be achieved by active control. The required passive modification was obtained using rank minimization techniques. However, system matrices ( $\mathbf{M}$ ,  $\mathbf{C}$ , and  $\mathbf{K}$ ) are needed in this method. Then this hybrid method was further developed by Belotti et al. [105] with an experimental validation, which aims to assign a mode shape and a frequency to a cantilever beam controlled by a piezoelectric actuator. They assigned eigenstructure to the beam to reduce vibrations near the clamped end, while magnifying the vibration near the free end.

### 2.3.3 Partial eigenvalue assignment

Partial eigenvalue assignment is to assign a set of desired eigenvalues while keep the other eigenvalues unchanged so as to avoid spill-over problem.

Datta et al. [106] derived an explicit solution to the partial eigenvalue assignment problem based on orthogonality relations for the symmetric definite linear pencil with single input control. This method is able to work directly in a second-order differential equation which can preserve the structural properties and requires the knowledge of system matrices. Then the multiple-input partial pole placement problem was addressed by Datta and Sarkissian in [107]. They also discussed the necessary and sufficient conditions for the existence of a solution. Ram and Elhay [108] considered the multiple-input partial pole assignment problem as a sequence of pole assignments by single-input control. The closed-loop poles were modified gradually from their initial values to desired locations. A closed-form, non-iterative solution was obtained by using the natural framework of second-order differential equations.

Qian and Xu [109] also discussed the partial eigenvalue assignment problem and derived the robust closed-loop system by minimizing the condition number of the eigenvectors matrix of the closed-loop system. Later, the authors [110] discussed some robustness measurement methods and proposed a numerical method that can improve the robustness. Cai et al. [111] proposed an algorithm for solving the partial quadratic eigenvalue assignment problems. They established a mathematical condition on the existence of solutions for the partial quadratic eigenvalue assignment problems. Ram et al. [112] solved the partial pole placement problem of single-input vibrating systems when there is a time delay between the measured state and actuation of the control. This method requires both the receptance and system matrices. Bai et al. [113] tackled the partial eigenvalue assignment problem of multiple-input vibrating systems by a multiple-step hybrid method. They also extended the work to the time delay problem. The robustness of the partial eigenvalue assignment with time delay was studied by Bai et al. [114]. They proposed an optimization method that can minimize the eigenvalue sensitivity and feedback norm simultaneously.

Then receptance-based active control method described in [2] was extended into a partial pole placement method by Tehrani et al. [115]. This method for single-input and multiple-input were demonstrated experimentally on a lightweight glass-fibre

beam and a heavy modular structure. The multiple-input was a sequential pole placement procedure with single-input. A new multiple-input active vibration control by the method of receptance for partial pole assignment problem was derived by Ram and Mottershead [116]. This method was able to complete multiple-input control in a single application and was superior to the sequential application of single-input control. Motivated by the practical engineering problems, Wei et al. [117] studied the partial eigenvalue assignment by active control with inaccessible degrees of freedom. They proposed a new double input control method which involves displacement, velocity and acceleration feedback. Mokrani et al. [91] minimized the control effort required for the partial pole placement in multiple-input multiple-output systems. The norm of feedback gain matrix was expressed in a form of inverse Rayleigh quotient. This expression greatly reduced the complexity of norm minimization.

Tehrani and Ouyang [118] studied the partial pole assignment for asymmetric systems using state-feedback. A number of complex poles can be assigned with only receptances at a small number of DoFs of symmetric system.

Zhang et al. [119] proposed a novel and explicit partial eigenvalue assignment method with output feedback control. This method was derived from an important work by Brauer [120]. Araújo and Santos [121] were also inspired by the work of Brauer and proposed a multiplicative perturbation method which result in partial eigenvalue perturbation. The proposed method was successfully applied to model updating and partial natural frequency assignment. De Almeida and Araújo [122] provided a method to solve the partial eigenvalue assignment problem for regional assignment. The target eigenvalues were assigned to a given D-region. Dantas et al. [123] considered the time delay problem in the receptance based partial pole placement method using rank-one state feedback control. The feedback gains were obtained using genetic algorithm and the stability of the closed-loop system was optimized based on the Nyquist stability criterion. Xie [124] proposed a receptance method for partial quadratic eigenvalue assignment problem using receptance matrices and the unwanted eigenpairs of open-loop system. The norms of feedback gain matrices and the condition number of closed-loop system were simultaneously minimized.

### 2.3.4 Partial eigenstructure assignment

Partial eigenstructure assignment is also an important topic in vibration control and has been studied by numerous researchers. Lu et al. [125] explained the meaning of partial eigenstructure assignment and derived an effective numerical algorithm for partial eigenstructure assignment of first-order large scale systems. Kim and Kim [126] used null space approach to compute the admissible eigenspace so that desired eigenvalues and several elements of eigenvectors can be assigned to prescribed values. Then additional feedback control was adopted to stabilize the remaining eigenpairs so as to reduce the spill-over problem. The proposed method was applied to a flight control system of an aircraft model. Datta et al. [127] achieved partial eigenstructure assignment for second-order vibrating systems by properly choosing the input influence matrix  $\mathbf{B}$ , and the gain matrices  $\mathbf{F}$  and  $\mathbf{G}$ . This method was developed based on the authors' previous work on the single-input partial pole assignment problem [106]. Sarkissian [19] proposed a "direct and partial modal approach" for the solution of partial eigenvalue assignment and partial eigenstructure assignment. The "direct" means the systems are described by second-order differential equations without reformulation to a first-order form. And the approach is partial modal in the sense that it requires only partial knowledge of eigenvalues and eigenvectors of the open-loop systems.

Alexandridis [128] presented a generalised formulation of the necessary and sufficient conditions for the solution of the eigenstructure assignment of first-order systems by output feedback control. A simple and unified solution was derived and this solution can result in a solution of partial eigenstructure assignment. Baddou et al. [129] proposed a new partial eigenstructure assignment method for first-order systems. This method is based on a method called inverse procedure which was introduced by Benzaouia [130].

Zhang et al. [131] derived a partial eigenstructure assignment method for undamped vibrating system using acceleration and displacement feedback. First, they derived a necessary and sufficient condition for mass and stiffness matrices perturbations that can satisfy partial eigenstructure assignment. Then the required control gain matrices were determined based on the condition. Bajodah and Mibar [132] extended the work in [126] to continuous-time linear quadratic regulator control systems. Yu [133]



established two new orthogonality relations to construct an acceleration-velocity feedback control law which can solve partial eigenstructure assignment problem. Minimum controller gains, which mean the minimum energy consumption, were obtained through an optimization algorithm.

## **2.4 Receptance measurement**

The research work in this thesis is based on receptance data which can be obtained from experiments. Therefore, it is important to learn how to get accurate and sufficient receptance data.

From an experiment point of view, there are still some difficulties in receptance measurement. For example, an excitation force may not be able to be applied on the structure due to physical limitations in some cases. Moreover, the receptance associated with rotational DoFs is unable to be measured directly. There are mainly two issues in the rotational receptance measurement: (1) the measurement rotational response (2) the excitation and the measurement of a pure moment. The following subsection first presents a brief review on the rotational receptance measurement, which is often needed in the application of receptance method.

Another thing is the modal analysis methods. Although the advanced software can provide several modal analysis methods to users to get the fitted FRF and modal parameters, knowing the theories of different methods can help engineers to choose an optimal method in different problems.

### **2.4.1 Rotational receptance estimation**

As clarified above, there are two problems in rotational receptance measurement. The first problem, measuring rotational response, is easier than the other one. There are already different sensors available to measure rotational response. Janssens and Britte [134] gave a summary and comparison on different kinds of rotational sensors, such as Laser Doppler vibrometer [135], angular accelerometers [136], or coder-based sensors [137] including magnetic pick-ups, optical sensors and incremental encoders. The sensors for rotational response measurement are usually more expensive than translational sensors.

For the second problem, exciting and measuring a pure moment are still unsolved yet. However, researchers have proposed some alternative approaches to apply a force which simultaneously imparts a moment excitation.

Earlier work for the measurement of rotational receptances can be seen in the papers by Ewins and Sainsbury [138] and Ewins and Gleeson [139]. They used a rigid attachment, such as a T-block, and expressed the receptance matrix in terms of the measured translational receptances, a coordinate transformation matrix and the mass matrix of the attachment. Then Cheng and Qu [140] and Qu et al. [141] used an L-shaped beam tip fixed at one point of the original structure for measuring the rotational compliance of a thin-walled plane structure. Sattinger [142] showed the rotational mobilities of structures are equivalent to spatial derivatives of their translational mobilities. Then he adapted the finite-difference method to the approximation of spatial derivatives. Therefore, the rotational mobilities were derived from measured translational mobilities. Maia et al. [143] estimated the rotational FRFs using mass uncoupling method and a T-block attachment. Later, the authors [144] implemented their method into a beam structure to explore the difficulties in application.

Ratcliffe and Lieven [145] used a laser system to extract the responses of rotational DoFs by a simple plane-fitting technique. Duarte and Ewins [146] used the finite-difference formulation to establish the rotational data to be used in structural coupling analysis. They particularly considered the residual compensation in the experimental derivation of rotational DoF parameters (i.e., either modal or response). In addition, they gave a comprehensive table which lists several works developed by 2000 on the measurement of rotational DoFs.

Mottershead et al. [67] proposed a multiple-input multiple-output estimator for rotational receptances. A T-block was used in this method and they considered the elasticity of the T-block attachment rather than assuming the attachment is rigid. This method was successfully applied on a beam structure [64]. Mottershead et al. [68] extended this method to determine a full  $6 \times 6$  receptance matrix using a X-block. Lv et al. [147] estimated the torsional receptance of a shafting structure with a T-block attachment. Inspired by Lv's work [147], Tsai et al. [148] proposed a more robust torsional receptance estimation method. The authors also discussed the effects of different choices of excitation locations and response measurement locations.

It has to be mentioned that there are also some advanced rotation receptances measurement techniques which are usually expensive and not easy to implement in general, for example, Zanarini [149] presented three different full-field optical techniques means to obtain rotational receptances using full-field optical and contactless methods.

## 2.4.2 Modal analysis methods

A modal test cannot directly produce the required receptance matrix at the desired eigenvalue. The obtained values from experiments are usually the matrix  $\mathbf{H}(s)$  when the complex parameter  $s$  is limited to points on the imaginary axis. i.e.,  $s = i\omega$ . Therefore, the required receptance data are usually inferred from the measured FRFs using curve fitting methods [150-152].

Curve fitting is a numerical process by which an analytical FRF model is matched to experimental FRF data in a manner that minimizes the squared error between the experimental data and the analytical curve fitting model. The purpose of curve fitting is to estimate the unknown modal parameters of the curve fitting model. More precisely, the modal frequency, damping, and mode shapes of each resonance in the frequency range of the FRFs is estimated by fitting an analytical model to a set of FRFs [25].

For example, the analytical or mathematical model of a structure can be expressed in terms of modal properties [153], as shown below.

- Partial fraction expansion model

The receptance matrix in Eq. (2.14) can also be expressed in partial fraction expansion form. When expressed in this form, any receptance value at any frequency is a summation of terms, each term called the resonance curve of a mode of vibration.

$$\mathbf{H}(i\omega) = \sum_{k=1}^n \frac{\mathbf{A}_k \mathbf{v}_k \mathbf{v}_k^T}{(\omega_k^2 - \omega^2 + 2i\zeta\omega\omega_k)} \quad (2.19)$$

where  $\omega_k$  is the  $k$ th natural frequency,  $\mathbf{v}_k$  is the mode shape for the  $k$ th mode, and  $\mathbf{A}_k$  scaling constant.

Maia and Silva [154] presented a very detailed review work on the modal analysis identification techniques. There are a number of modal analysis methods. Those

methods can be grouped into frequency domain modal analysis [155, 156] and time domain analysis [157-159]. In each group, they can be further classified by the number of inputs and outputs. In this literature, the modal analysis methods will not be reviewed in detail and only two typical frequency domain methods are introduced to help readers gain a basic understanding on the modal analysis methods.

Rational fractional polynomial method is a well-known modal analysis method and was proposed by Richardson and Formenti [150]. They expressed an FRF in terms of rational fraction polynomials, as shown below.

- Rational fraction polynomial model

The receptance matrix in Eq. (2.14) can also be expressed analytically as a ratio of two polynomials. This is called rational fraction polynomial matrix form of the transfer function matrix. Expressed in terms of  $n$ -modes, the denominator polynomial has  $(2n+1)$  terms.

$$h_{ij}(s) = \frac{b_0 s^m + b_1 s^{m-1} + \dots + b_m}{a_0 s^{2n} + a_1 s^{2n-1} + \dots + a_{2n}} \quad (2.20)$$

where  $n$  is the number of modes in the analytical curve fitting model and  $m$  is the number of zeros,  $a_0 s^{2n} + a_1 s^{2n-1} + \dots + a_{2n}$  is the characteristic polynomial. Also,  $(a_0, a_1, \dots, a_{2n})$  and  $(b_0, b_1, \dots, b_m)$  are real valued coefficients

Each receptance  $h_{ij}(i\omega)$  in matrix  $\mathbf{H}(i\omega)$  has a unique numerator polynomial and the same denominator polynomial, called characteristic polynomial. Through numerical manipulations, the coefficients of these polynomials can be identified and then the modal parameters can be determined using the obtained function.

Guillaume et al. [160] proposed a poly-reference least-squares complex frequency-domain (LSCF) method. This method can produce very clean stabilisation diagrams, easing dramatically the problem of selecting the model order and the best structural system poles. Moreover, the poly-reference LSCF method is superior for closed-coupled modes resulting in good modal parameter estimations. This method has been implemented into the software Test.Lab by LMS, named ‘‘PloyMAX’’.

### **2.4.3 Simple assessment of measured data**

Although many modal analysis methods were developed to minimize the effects of inaccuracy carried in measured data, it is impossible to overcome all errors. To minimize the errors caused by some avoidable mistakes such as, human mistakes or sensor errors, and improve the confidence on measured data, some simple but quite useful techniques can be used to check the quality of measured data [161].

- **Repeatability check**

The simplest, but not the least useful, assessment is to check the repeatability of the measurement. A linear structure should yield identical FRF curves for every measurement when the input forces and response locations are unchanged. Each FRF curve can be derived from the average of a number of measurements. This property is usually assessed using a coherence coefficient function, which is widely used in common commercial modal analysis software.

- **Reciprocity check**

The reciprocity property means that for a single input, the FRF data should be identical if one exchange the locations of force and response. From mathematical point of view, this property is originated from the symmetry of mass, stiffness and damping matrices. With this property, it could reduce the efforts for receptance matrix measurement and only a part of receptances is needed to measure if they are reliable.

- **Linearity check**

One property that is usually omitted but is very important is the linearity of the test structure. When applying modal analysis on a structure, it is assumed that the structure behaves linearly. The linearity of a structure can be checked easily in a modal test. For example, FRF data from same locations can be measured repeatedly with different but uncontrolled excitation amplitudes. The measured FRF data can be overlaid to verify the uniformity of the curves.

## **2.5 Conclusion**

A review of structural modification, active control and receptance measurement has been presented in this chapter. It can provide readers a basic understanding of the frequency assignment and partial assignment problems, which will be discussed in the

following chapters. In addition, some difficulties and useful methods in receptance measurement are introduced to help readers get accurate and sufficient receptance data.

## **Chapter 3**

### **Receptance-based Frequency assignment for assembled structures**

An engineering structure usually consists of several or many substructures, such as a ship, a car or a washing machine. Those substructures are assembled into a whole structure through joints or links. With the increasing requirements on vibration control from customers or safety considerations, the assembled structures are usually supposed to satisfy some dynamic behaviours, for example, avoiding resonance.

In many cases, the substructures, which may come from different manufactures or have specific functions, are difficult or not allowed to be modified. On the other hand, those links or joints between substructures have great influences on the dynamic behaviours of the assembled structures. Therefore, designing proper links or joints, is crucially important to achieve the desired dynamic behaviours of assembled structures. This chapter aims to establish a receptance-based frequency assignment method, which assigns frequencies to an assembled structure and finds the optimal links between the substructures. Those links are usually much simpler than the uncoupled substructures and are much easier to be modelled.

Frequency assignment for assembled structures is a special case for structural modifications. Therefore, the receptance-based structural modifications method introduced by Mottershead and Ram [77] is presented in this chapter first to help readers understand the receptance method. Then, the theory on the receptance-based frequency assignment method for assembled structures is explained. Only part of the receptances of substructures and theoretical models of links are needed in this method. Then two numerical examples are presented to demonstrate the performance of the proposed method.

A large part of this chapter was reported in the following journal paper by the author of this thesis and his supervisor, Ouyang Huajiang [162]:

S. Zhang, H. Ouyang, Receptance-based frequency assignment for assembled structures, *Journal of Vibration and Control*, 27 (2020) 1573-1583.

### **3.1 Introduction**

Frequency assignment is a very effective way to achieve vibration control by shifting the affected natural frequencies to desired locations. The assignment can be achieved through forward and inverse methods. For assembled structures, substructure-coupling methods have been widely used to couple substructures and predict their dynamic responses [39, 41, 42, 46]. Those methods, although their initial purpose is not frequency assignment, could also be used to solve forward frequency assignment problems for assembled structures by repeating the coupling process with different links until the requirements are met [43, 67].

However, the forward methods are usually time-consuming and an inverse method (that would avoid a trial-and-error process) would be more appealing in practice. There are only a few publications about the inverse assignment problems of assembled structures. For example, Birchfield et al. [163] predicted the dynamic response of a coupled-rotor-system using the receptance functions of individual subsystems. The subsystems were coupled using springs and dampers and critical speed of coupled-rotor-system was changed to a desired value by modifying the link. No additional degree of freedom was introduced in this method. Tsai et al. [164] presented a theoretical study of the frequency assignment problem of a coupled system via structural modification of one of its subsystems. The proposed technique was derived based on receptance coupling technique and formulated as an optimization problem.

In the above inverse methods, those links would be treated as substructures/subsystems so that the coupling method could be applied. However, this is not efficient and intuitive when there are multiple links. The links in this research are treated as modifications of uncoupled substructures so the idea of structural modification is employed. The links could be discrete components (masses, springs and dampers) or continuous structures (beams, plates or even more complicated structures). The



properties of those links are optimized based on the receptances of substructures and finite element models of links.

## 3.2 Receptance-based structural modification theory

Structural modification is a technique to study the physical parameter changes of a structural system on its dynamic properties which are in the forms of natural frequencies and mode shapes. A typical structural modification problem, which is also the focus of this research, is to assign a number of eigenvalues and zeros by modifying the structure, such as by adding point masses, springs, beams or plates. In this way the natural frequencies of a structure may be shifted to desired locations, or antiresonances moved so that the vibration response vanishes at chosen coordinates and frequencies. Alternatively, if the excitation frequency is a narrow-banded range rather than an individual frequency, structural modification can be used to rearrange the natural frequencies so that no natural frequency falls within the band.

As reviewed in chapter 2, there are many structural modification methods. Among those methods, the receptance-based method is very efficient in practice because it can overcome the incompleteness of the modal representation of complex systems and the need for accurate physical models [69]. The receptance-based frequency assignment method for assembled structures proposed in this chapter is an extension of the receptance-based structural modification method. Therefore, to help readers gain a better understanding on the proposed method, the principles of receptance-based structural modification for passive modification is explained in this section. The general theory of this receptance-based method is based on the paper by Mottershead and Ram [77].

### 3.2.1 Introductory theory

The equation of motion of a  $n$  DoFs system under excitations can be written in the usual form

$$\mathbf{M}\ddot{\mathbf{x}}(t) + \mathbf{C}\dot{\mathbf{x}}(t) + \mathbf{K}\mathbf{x}(t) = \mathbf{f}(t) \quad (3.1)$$

Taking the Laplace transform from Eq. (3.1) yields

$$(s^2\mathbf{M} + s\mathbf{C} + \mathbf{K})\mathbf{v} = \mathbf{f}(s) \quad (3.2)$$

Then the  $2n$  eigenvalues  $\lambda_k$  ( $k = 1, 2, \dots, 2n$ ) of the system are can be obtained by solving the characteristic polynomial equation

$$\det(s^2\mathbf{M} + s\mathbf{C} + \mathbf{K}) = 0 \quad (3.3)$$

The eigenvector  $\mathbf{v}_k$ , which is associated with the eigenvector  $\lambda_k$ , can be obtained by substituting  $\lambda_k$  into the following equation

$$(s^2\mathbf{M} + s\mathbf{C} + \mathbf{K})\mathbf{v} = \mathbf{0} \quad (3.4)$$

The eigenvalue  $\lambda_k$  and associated eigenvector  $\mathbf{v}_k$  together,  $(\lambda_k, \mathbf{v}_k)$  is named an eigenpair.

The dynamic behaviour of a system can be determined from the eigenvalues and eigenvectors. The imaginary part of an eigenvalue determines the frequency of oscillation, named damped frequency. If the frequency coincidence with an excitation frequency, it will lead to resonance and the structure may suffer excessive vibrations.

Therefore, one important objective of structural modification is to shift natural frequencies away from excitation frequencies to avoid resonance. This objective can be achieved by passive modification which is physically changing system properties or by active control which is applying external forces based on the real-time measurements of the system states. In this chapter, only passive modification is discussed. The active control problem will be discussed in chapter 5 and 6.

### 3.2.2 Receptance-based structural modification method

The matrix  $(s^2\mathbf{M} + s\mathbf{C} + \mathbf{K}) \in \mathbb{C}^{n \times n}$  in Eq. (3.2) is called a dynamic stiffness matrix, which is usually denoted by  $\mathbf{Z}(s)$ . The receptance matrix  $\mathbf{H}(s)$  is defined by the inverse of the dynamic stiffness matrix

$$\mathbf{H}(s) = (s^2\mathbf{M} + s\mathbf{C} + \mathbf{K})^{-1} \quad (3.5)$$

In practice, the dynamic stiffness matrix  $\mathbf{Z}(s)$  is usually obtained from a finite element (FE) model. And the receptance matrix is obtained from the measured receptance frequency response function  $\mathbf{H}(i\omega)$ . Each element in this matrix can be measured individual, for example,  $h_{ij}(s)$  shows the relation between the displacement response at  $i$ th DoF and the force applied at  $j$ th DoF.

In the general case, a modification of arbitrary rank can be expressed as

$$\Delta\mathbf{Z}(s) = s^2\Delta\mathbf{M} + s\Delta\mathbf{C} + \Delta\mathbf{K} \quad (3.6)$$

If a general modification is applied on the system described in Eq. (3.2), the dynamic equation of the modified system may be expressed as

$$(\mathbf{Z}(s) + \Delta\mathbf{Z}(s))\mathbf{v} = \mathbf{f}(s) \quad (3.7)$$

Pre-multiplying Eq. (3.7) by the receptance matrix on both sides yields

$$(\mathbf{I} + \mathbf{H}(s)\Delta\mathbf{Z}(s))\mathbf{v} = \mathbf{H}(s)\mathbf{f}(s) \quad (3.8)$$

Here,  $\mathbf{I}$  is an identity matrix of suitable dimension. The receptance matrix of modified system can be expressed in terms of the receptance matrix of the original system and the general modification

$$\hat{\mathbf{H}}(s) = (\mathbf{I} + \mathbf{H}(s)\Delta\mathbf{Z}(s))^{-1}\mathbf{H}(s) = \frac{\text{adj}(\mathbf{I} + \mathbf{H}(s)\Delta\mathbf{Z}(s))\mathbf{H}(s)}{\det(\mathbf{I} + \mathbf{H}(s)\Delta\mathbf{Z}(s))} \quad (3.9)$$

Here the term ‘adj’ means the adjugated matrix.

The receptance of modified system  $\hat{\mathbf{H}}(s)$  can also be obtained using Woodbury formula [165]. The Woodbury formula can be stated as

$$(\mathbf{A}_w + \mathbf{U}\mathbf{V}^T)^{-1} = \mathbf{A}_w^{-1} - \mathbf{A}_w^{-1}\mathbf{U}(\mathbf{I} + \mathbf{V}^T\mathbf{A}_w^{-1}\mathbf{U})^{-1}\mathbf{V}^T\mathbf{A}_w^{-1} \quad (3.10)$$

where  $\mathbf{I}$  is an identity matrix;  $\mathbf{U}$  and  $\mathbf{V}$  can be any matrices or column vectors. They all need to have compatible dimensions with  $\mathbf{A}_w$ . This formula is particularly useful when  $\mathbf{U}$  and  $\mathbf{V}$  are of much lower ranks than that of  $\mathbf{A}_w$ , which is always the case in structural modification under this investigation.

According to Eq. (3.7), the receptance matrix of the mass-modified system is defined as

$$\hat{\mathbf{H}}(s) = (\mathbf{Z}(s) + \Delta\mathbf{Z}(s))^{-1} \quad (3.11)$$

And the receptance matrix of original system is denoted as  $\mathbf{H}(s) = \mathbf{Z}(s)^{-1}$ . By replacing matrices  $\mathbf{A}_w$ ,  $\mathbf{U}$  and  $\mathbf{V}$  in Eq. (3.10) with matrices  $\mathbf{Z}(s)$ ,  $\Delta\mathbf{Z}(s)$  and  $\mathbf{I}$  respectively, the following equation can be obtained

$$\hat{\mathbf{H}}(s) = \mathbf{H}(s) - \mathbf{H}(s)\Delta\mathbf{Z}(s)(\mathbf{I} + \mathbf{H}(s)\Delta\mathbf{Z}(s))^{-1}\mathbf{H}(s) \quad (3.12)$$

Therefore, the receptance matrix of the modified system can be derived from the assignment receptance matrix of the original system using Eq. (3.12). Please note that  $\Delta\mathbf{Z}$  is of a very low rank and hence all the non-zero elements make up a small diagonal matrix block. Therefore,  $(\mathbf{I} + \mathbf{H}(s)\Delta\mathbf{Z}(s))^{-1}$  in Eq. (3.12) is relatively very easy to calculate.

In fact, the two equations, Eq. (3.9) and Eq. (3.12), give identical results. One good thing that can be found from both equations is that not the full receptance matrix is needed. The number of required receptances is usually small, especially when the modifications are only applied at a few locations.

The eigenvalues of the modified system  $\hat{\lambda}_k, k = 1, 2, \dots, 2n$  are defined as the roots of the characteristic equation

$$\det(\mathbf{I} + \mathbf{H}(s)\Delta\mathbf{Z}(s)) = 0 \quad (3.13)$$

And the eigenvectors of corresponding to each of the eigenvalues are obtained by solving the following equation

$$(\mathbf{I} + \mathbf{H}(s)\Delta\mathbf{Z}(s))\mathbf{v} = \mathbf{0}, k = 1, 2, \dots, 2n \quad (3.14)$$

If the desired eigenvalue or frequency is prescribed, the required structural modification  $\Delta\mathbf{Z}$  can be obtained by solving Eq. (3.13). However, directly solving the equation could be challenging especially when the number of modifications is large or there are multiple desired eigenvalues or frequencies. In fact, there is no need to get an exact solution. An approximate solution is good enough when the exact solution is hard to compute or does not exist due to physical limitations. Therefore, the eigenvalue assignment problem is usually cast as an optimization problem provides a relatively flexible way to find a solution. The basic objective function for the eigenvalue assignment problem is reformed as

$$\begin{aligned} & \min_{\Delta\mathbf{Z}} \left\{ \sum_{k=1}^{n_d} \det(\mathbf{I} + \mathbf{H}(\hat{\lambda}_k)\Delta\mathbf{Z}(\hat{\lambda}_k)) \right\} \\ & \text{subject to } \Delta\mathbf{Z} \in \Gamma \end{aligned} \quad (3.15)$$

where  $n_d$  is the number of desired eigenvalues and  $\Gamma$  represents the physical constraints on passive modifications.

Apart from eigenvalues, zero assignment is also a desired objective for structural modification. The zeros of modified system can also be obtained from the matrix in the numerator in Eq. (3.9). The zeros define those frequencies at which vibrations on certain locations can disappear. For example, to suppress the vibration at  $i$ th DoF when the force is applied at  $j$ th DoF at frequency  $\omega$ , a zero of the  $ij$ th modified receptance at frequency  $\omega$  can be expected. In order to achieve this objective, the following equation can be adopted

$$[\text{adj}(\mathbf{I} + \mathbf{H}(\omega)\Delta\mathbf{Z}(\omega))\mathbf{H}(\omega)]_{ij} = 0 \quad (3.16)$$

where the subscript  $ij$  represents the  $ij$ th element of the matrix in square brackets. A detailed discussion on the zero assignment using measured receptances can be found in [1].

### 3.2.3 Numerical Example

A 3-DoF system is considered as shown in Fig. 3.1. The system matrices are shown below (Proportional damping is considered here for simplicity).

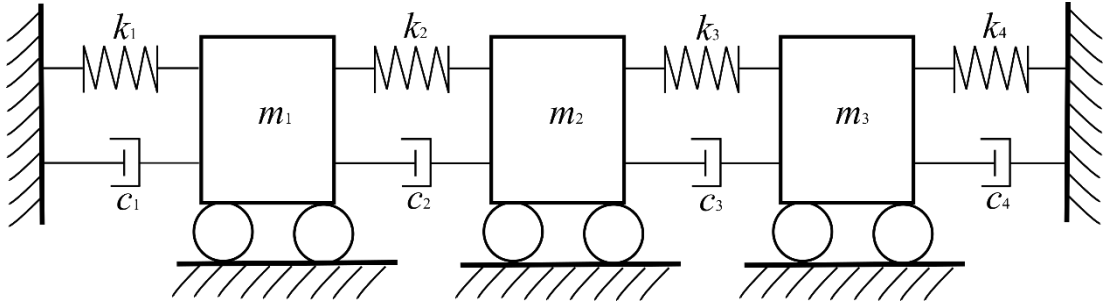


Fig. 3.1 A 3-DoF system

$$\mathbf{M} = \begin{bmatrix} 1 & & \\ & 2 & \\ & & 1 \end{bmatrix}, \quad \mathbf{K} = 10^5 \times \begin{bmatrix} 6 & -5 & \\ -5 & 8 & -3 \\ & -3 & 5 \end{bmatrix}, \quad \mathbf{C} = 10^{-5} \times \mathbf{K}$$

The system presents its three natural frequencies at  $\omega_1 = 252.48$  rad/s,  $\omega_2 = 724.62$  rad/s and  $\omega_3 = 954.54$  rad/s. (1) The first problem is to assign a natural frequency at 300 rad/s by adding modification on the ground spring  $k_1$  and the modification is denoted as  $\delta k_1$ . (2) In the second problem, a natural frequency at 300 rad/s and a zero

to the point receptance  $h_{11}$  at 400 rad/s are supposed to be assigned by modifying the ground spring  $k_1$  and the spring  $k_2$  between  $m_1$  and  $m_2$ . Those modifications are denoted by  $\delta k_1$  and  $\delta k_2$ , respectively. (3) The last problem is to assign two natural frequencies at 300 rad/s and 750 rad/s with the same modification locations as problem (2).

The physical constraints on those modifications are defined by  $0 < \delta k_1 < 5 \times 10^5$  N/m and  $-4 \times 10^5 < \delta k_2 < 5 \times 10^5$  N/m in all three problems.

Solutions: (1) For the assignment of natural frequency at 300 rad/s, since the modification happens on  $m_1$ , only the receptance  $h_{11}$  is required in this problem. By substituting the desired natural frequency into Eq. (3.13), the solution for  $\delta k_1$  can be found to be a complex number  $\delta k_1 = (1.14 - 0.01i) \times 10^5$  N/m.

There is in fact an imaginary part present in this solution. This existence of imaginary component is due to the damping. However, in real cases, especially with steel structures that are lightly damped, the imaginary part can be just ignored. The receptances of original system and modified system are presented in Fig. 3.2. Apparently, the desired natural frequency 300 rad/s is assigned as expected.

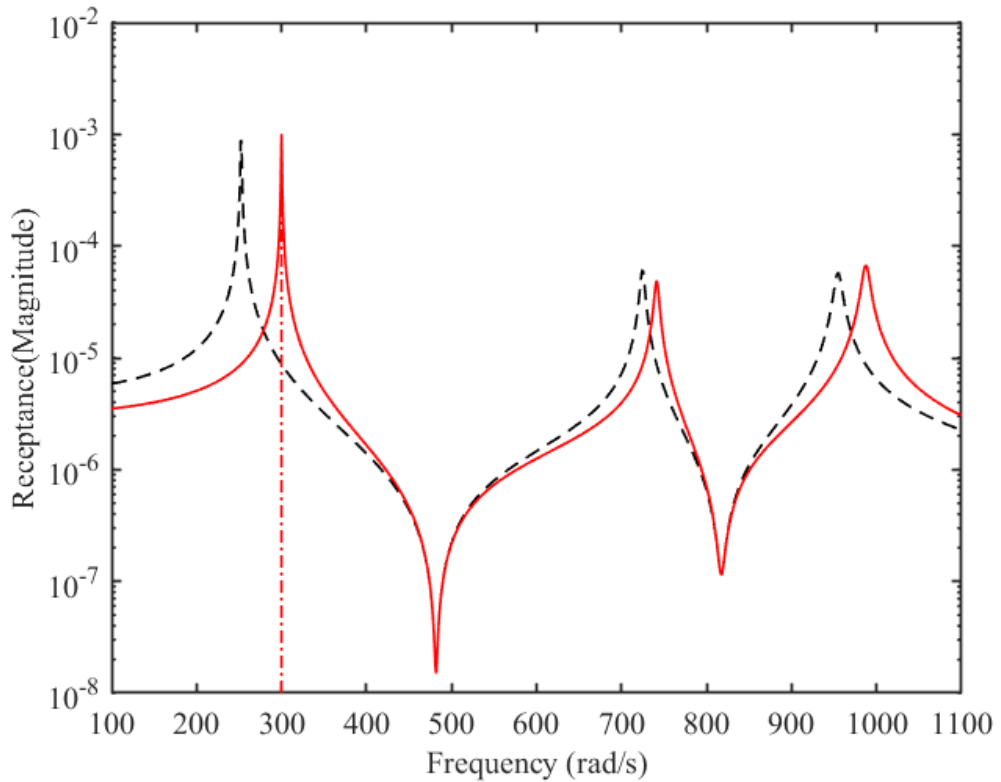


Fig. 3.2 Original (black dash line) and modified (red line) receptances  $h_{11}$ :  
assignment of a natural frequency at 300 rad/s

(2) For the assignment of a natural frequency and zero at the same time, both Eq. (3.15) and Eq. (3.16) are applied. The obtained modifications are  $\delta k_1 = 1.43 \times 10^5$  N/m and  $\delta k_2 = -2.17 \times 10^5$  N/m. The modified receptance  $h_{11}$  is shown in Fig. 3.3. Clearly, a natural frequency at 300 rad/s and a zero at 400 rad/s are achieved.

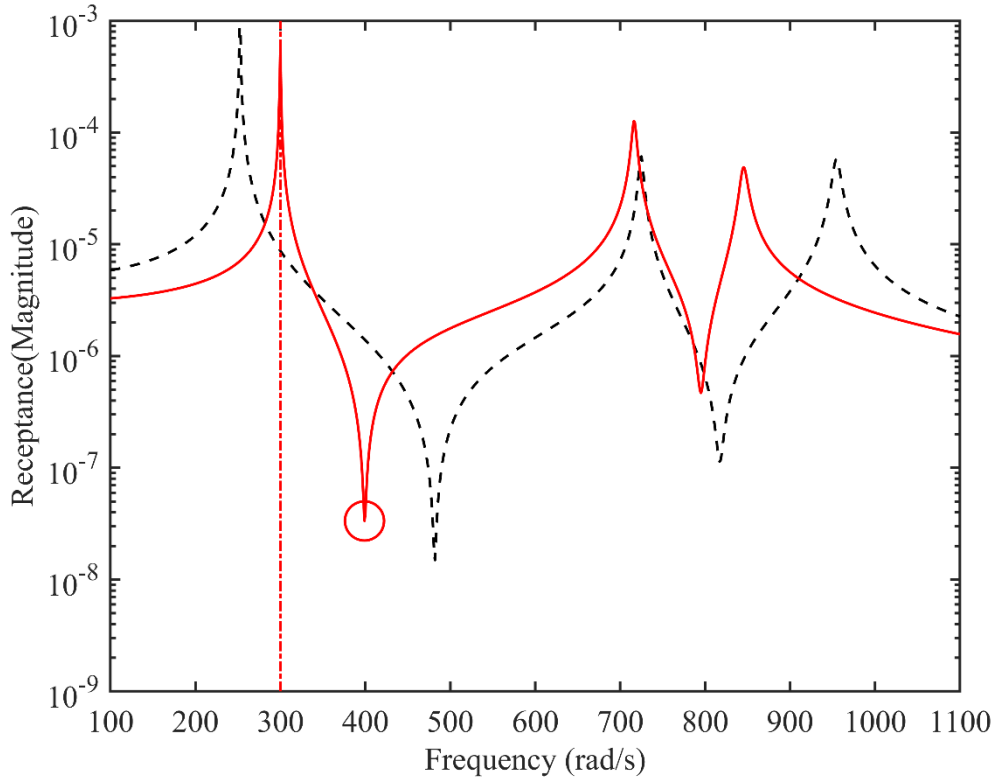


Fig. 3.3 Original (black dash line) and modified (red line) receptances  $h_{11}$ :  
assignment of a natural frequency at 300 rad/s and a zero at 400 rad/s

(3) For the assignment of two natural frequencies 300 rad/s and 750 rad/s, modifications are related with  $m_1$  and  $m_2$ . Only the receptances at the modification locations are needed, which can form a  $2 \times 2$  receptance matrix in this problem. The required modifications can be obtained by solving the optimization problem in Eq. (3.15). The obtained modifications are  $\delta k_1 = 1.04 \times 10^5$  N/m and  $\delta k_2 = 2.76 \times 10^5$  N/m. Fig. 3.4 shows the modified receptances with a natural frequency at 300.0 rad/s and a natural frequency at 748.8 rad/s, which are very close to the expected natural frequencies.

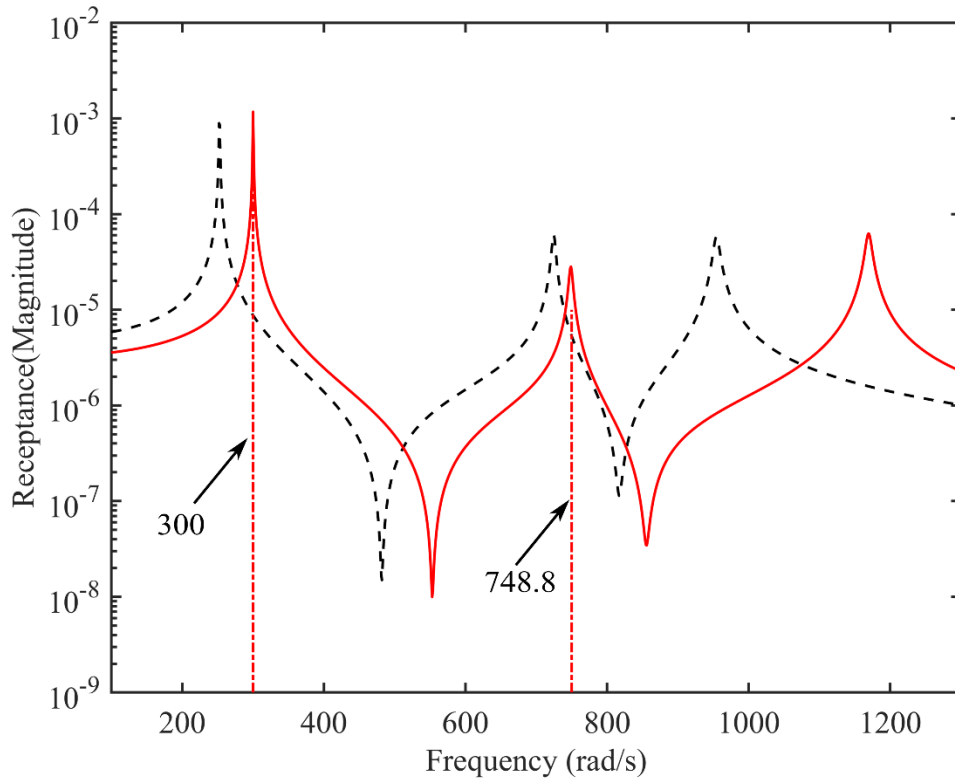


Fig. 3.4 Original (black dash line) and modified (red line) receptances  $h_{11}$ :  
assignment of the natural frequencies at 300 rad/s and 750 rad/s

### 3.3 Receptance-based frequency assignment for assembled structures

The receptance-based structural modification theory explained in section 3.2 has already been studied or developed by many researchers, which have been reviewed in chapter 2. However, there was usually one structure involved, which was to be modified by changing the existing structural properties of or adding a simple structure to an original structure, in those aforementioned investigations. For assembled structures, there would be more than one substructure involved. Those receptance-based methods could not be directly applied to assign frequencies for assembled structures, especially when the substructures are not allowed or difficult to be modified and only the links between substructures could be changed. Therefore, this section extends the receptance-based structural modification theory into a frequency assignment method for assembled structures.



The following derivation is based on two substructures and two links. However, it is apparently applicable to an assembled structure with any number of substructures and links. As shown in Fig. 3.5, substructure A and substructure B are connected through two links C and D. The DoFs of substructure A, ‘ $p$ ’, are coupled with the DoFs of substructure B, ‘ $q$ ’, by link C. Similarly, the DoFs of substructure A, ‘ $i$ ’, are coupled with DoFs of substructure B, ‘ $j$ ’, through link D. All the other DoFs of substructure A and B are denoted by ‘ $a$ ’ and ‘ $b$ ’, respectively. The internal DoFs of links C and D are denoted by ‘ $c$ ’ and ‘ $d$ ’. It should be noted that there is no restriction on the complexity of these substructures and links, though links are more likely to be less complex than substructures in practice. Those links C and D, are modifications of this “assembled structure” in order that the modified structure could have certain desired natural frequencies.

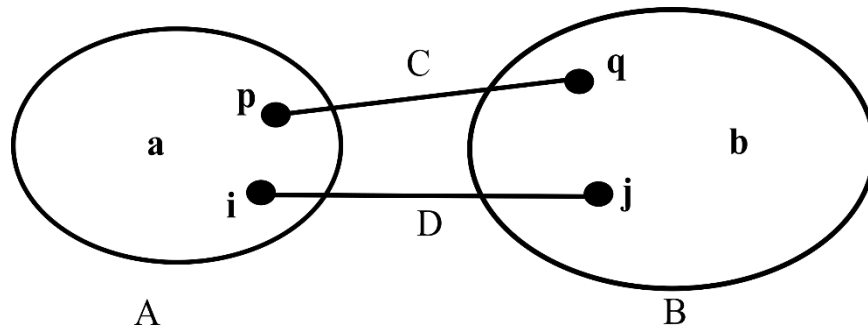


Fig. 3.5 Substructure A and B connected by links C and D

When substructure A and B are connected through links C and D, there will be internal forces, denoted by force vectors  $\mathbf{f}$ , at the interface DoFs  $p$ ,  $q$ ,  $i$ , and  $j$ , are shown in Fig. 3.6.

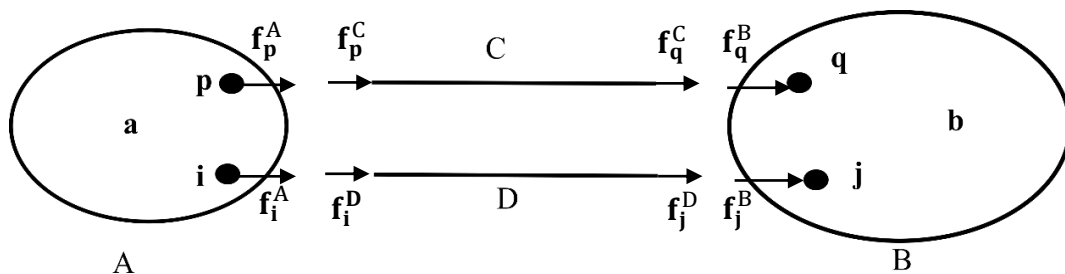


Fig. 3.6 Internal forces at the interfaces DoFs

The equations of motion for substructures A and B in frequency domain can be

expressed as

$$\begin{bmatrix} \mathbf{Z}_{aa}^A & \mathbf{Z}_{ap}^A & \mathbf{Z}_{ai}^A & \mathbf{0} & \mathbf{0} & \mathbf{0} \\ \mathbf{Z}_{pa}^A & \mathbf{Z}_{pp}^A & \mathbf{Z}_{pi}^A & \mathbf{0} & \mathbf{0} & \mathbf{0} \\ \mathbf{Z}_{ia}^A & \mathbf{Z}_{ip}^A & \mathbf{Z}_{ii}^A & \mathbf{0} & \mathbf{0} & \mathbf{0} \\ \mathbf{0} & \mathbf{0} & \mathbf{0} & \mathbf{Z}_{qq}^B & \mathbf{Z}_{qj}^B & \mathbf{Z}_{qb}^B \\ \mathbf{0} & \mathbf{0} & \mathbf{0} & \mathbf{Z}_{jq}^B & \mathbf{Z}_{jj}^B & \mathbf{Z}_{jb}^B \\ \mathbf{0} & \mathbf{0} & \mathbf{0} & \mathbf{Z}_{bq}^B & \mathbf{Z}_{bj}^B & \mathbf{Z}_{bb}^B \end{bmatrix} \begin{bmatrix} \mathbf{x}_a^A \\ \mathbf{x}_p^A \\ \mathbf{x}_i^A \\ \mathbf{x}_q^B \\ \mathbf{x}_j^B \\ \mathbf{x}_b^B \end{bmatrix} = \begin{bmatrix} \mathbf{0} \\ \mathbf{f}_p^A \\ \mathbf{f}_i^A \\ \mathbf{f}_q^B \\ \mathbf{f}_j^B \\ \mathbf{0} \end{bmatrix} \quad (3.17)$$

The nine matrix blocks at the top left corner and the nine matrix blocks at the bottom right corner in the matrix of Eq. (3.17) can be grouped respectively as

$$\mathbf{Z}^A = \begin{bmatrix} \mathbf{Z}_{aa}^A & \mathbf{Z}_{ap}^A & \mathbf{Z}_{ai}^A \\ \mathbf{Z}_{pa}^A & \mathbf{Z}_{pp}^A & \mathbf{Z}_{pi}^A \\ \mathbf{Z}_{ia}^A & \mathbf{Z}_{ip}^A & \mathbf{Z}_{ii}^A \end{bmatrix}, \mathbf{Z}^B = \begin{bmatrix} \mathbf{Z}_{qq}^B & \mathbf{Z}_{qj}^B & \mathbf{Z}_{qb}^B \\ \mathbf{Z}_{jq}^B & \mathbf{Z}_{jj}^B & \mathbf{Z}_{jb}^B \\ \mathbf{Z}_{bq}^B & \mathbf{Z}_{bj}^B & \mathbf{Z}_{bb}^B \end{bmatrix} \quad (3.18)$$

Here  $\mathbf{Z}^A$  and  $\mathbf{Z}^B$  are the dynamic stiffness matrices of substructure A and substructure B respectively, when they are considered as separate structures. For convenience, the dependence on frequency is omitted in the above and following equations.

Similarly, the equations of motion for links C and D can be written as

$$\begin{bmatrix} \mathbf{Z}_{pp}^C & \mathbf{Z}_{pc}^C & \mathbf{Z}_{pq}^C & \mathbf{0} & \mathbf{0} & \mathbf{0} \\ \mathbf{Z}_{cp}^C & \mathbf{Z}_{cc}^C & \mathbf{Z}_{cq}^C & \mathbf{0} & \mathbf{0} & \mathbf{0} \\ \mathbf{Z}_{qp}^C & \mathbf{Z}_{qc}^C & \mathbf{Z}_{qq}^C & \mathbf{0} & \mathbf{0} & \mathbf{0} \\ \mathbf{0} & \mathbf{0} & \mathbf{0} & \mathbf{Z}_{ii}^D & \mathbf{Z}_{id}^D & \mathbf{Z}_{ij}^D \\ \mathbf{0} & \mathbf{0} & \mathbf{0} & \mathbf{Z}_{di}^D & \mathbf{Z}_{dd}^D & \mathbf{Z}_{dj}^D \\ \mathbf{0} & \mathbf{0} & \mathbf{0} & \mathbf{Z}_{ji}^D & \mathbf{Z}_{jd}^D & \mathbf{Z}_{jj}^D \end{bmatrix} \begin{bmatrix} \mathbf{x}_p^C \\ \mathbf{x}_c^C \\ \mathbf{x}_q^C \\ \mathbf{x}_i^D \\ \mathbf{x}_d^D \\ \mathbf{x}_j^D \end{bmatrix} = \begin{bmatrix} \mathbf{f}_p^C \\ \mathbf{0} \\ \mathbf{f}_q^C \\ \mathbf{f}_i^D \\ \mathbf{0} \\ \mathbf{f}_j^D \end{bmatrix} \quad (3.19)$$

Besides, the conditions of displacement compatibility should be satisfied

$$\mathbf{x}_p^A = \mathbf{x}_p^C, \mathbf{x}_q^B = \mathbf{x}_q^C, \mathbf{x}_i^A = \mathbf{x}_i^D, \mathbf{x}_j^B = \mathbf{x}_j^D \quad (3.20)$$

and the conditions of force equilibrium must stand as

$$\mathbf{f}_p^A + \mathbf{f}_p^C = \mathbf{0}, \mathbf{f}_q^B + \mathbf{f}_q^C = \mathbf{0}, \mathbf{f}_i^A + \mathbf{f}_i^D = \mathbf{0}, \mathbf{f}_j^B + \mathbf{f}_j^D = \mathbf{0} \quad (3.21)$$

Therefore, based on the above two conditions, Eq. (3.17) and Eq. (3.19) could be assembled into one equation below, which is the equation of motion of the assembled structure when with an external force vector  $\mathbf{f}_{\text{ext}}$

$$(\tilde{\mathbf{Z}} + \Delta\tilde{\mathbf{Z}})\mathbf{x} = \mathbf{f}_{\text{ext}} \quad (3.22)$$

where

$$\tilde{\mathbf{Z}} = \begin{bmatrix} \mathbf{Z}_{aa}^A & \mathbf{Z}_{ap}^A & \mathbf{Z}_{ai}^A & \mathbf{0} & \mathbf{0} & \mathbf{0} & \mathbf{0} & \mathbf{0} \\ \mathbf{Z}_{pa}^A & \mathbf{Z}_{pp}^A & \mathbf{Z}_{pi}^A & \mathbf{0} & \mathbf{0} & \mathbf{0} & \mathbf{0} & \mathbf{0} \\ \mathbf{Z}_{ia}^A & \mathbf{Z}_{ip}^A & \mathbf{Z}_{ii}^A & \mathbf{0} & \mathbf{0} & \mathbf{0} & \mathbf{0} & \mathbf{0} \\ \mathbf{0} & \mathbf{0} & \mathbf{0} & \mathbf{0} & \mathbf{0} & \mathbf{0} & \mathbf{0} & \mathbf{0} \\ \mathbf{0} & \mathbf{0} & \mathbf{0} & \mathbf{0} & \mathbf{0} & \mathbf{0} & \mathbf{0} & \mathbf{0} \\ \mathbf{0} & \mathbf{0} & \mathbf{0} & \mathbf{0} & \mathbf{0} & \mathbf{Z}_{qq}^B & \mathbf{Z}_{qj}^B & \mathbf{Z}_{qb}^B \\ \mathbf{0} & \mathbf{0} & \mathbf{0} & \mathbf{0} & \mathbf{0} & \mathbf{Z}_{jq}^B & \mathbf{Z}_{jj}^B & \mathbf{Z}_{jb}^B \\ \mathbf{0} & \mathbf{0} & \mathbf{0} & \mathbf{0} & \mathbf{0} & \mathbf{Z}_{bq}^B & \mathbf{Z}_{bj}^B & \mathbf{Z}_{bb}^B \end{bmatrix}$$

$$\Delta\tilde{\mathbf{Z}} = \begin{bmatrix} \mathbf{0} & \mathbf{0} & \mathbf{0} & \mathbf{0} & \mathbf{0} & \mathbf{0} & \mathbf{0} & \mathbf{0} \\ \mathbf{0} & \mathbf{Z}_{pp}^C & \mathbf{0} & \mathbf{Z}_{pc}^C & \mathbf{0} & \mathbf{Z}_{pq}^C & \mathbf{0} & \mathbf{0} \\ \mathbf{0} & \mathbf{0} & \mathbf{Z}_{ii}^D & \mathbf{0} & \mathbf{Z}_{id}^D & \mathbf{0} & \mathbf{Z}_{ij}^D & \mathbf{0} \\ \mathbf{0} & \mathbf{Z}_{cp}^C & \mathbf{0} & \mathbf{Z}_{cc}^C & \mathbf{0} & \mathbf{Z}_{cq}^C & \mathbf{0} & \mathbf{0} \\ \mathbf{0} & \mathbf{0} & \mathbf{Z}_{di}^D & \mathbf{0} & \mathbf{Z}_{dd}^D & \mathbf{0} & \mathbf{Z}_{dj}^D & \mathbf{0} \\ \mathbf{0} & \mathbf{Z}_{qp}^C & \mathbf{0} & \mathbf{Z}_{qc}^C & \mathbf{0} & \mathbf{Z}_{qq}^C & \mathbf{0} & \mathbf{0} \\ \mathbf{0} & \mathbf{0} & \mathbf{Z}_{ji}^D & \mathbf{0} & \mathbf{Z}_{jd}^D & \mathbf{0} & \mathbf{Z}_{jj}^D & \mathbf{0} \\ \mathbf{0} & \mathbf{0} & \mathbf{0} & \mathbf{0} & \mathbf{0} & \mathbf{0} & \mathbf{0} & \mathbf{0} \end{bmatrix}$$

$$\mathbf{x} = [\mathbf{x}_a^A \quad \mathbf{x}_p^A \quad \mathbf{x}_i^A \quad \mathbf{x}_c^C \quad \mathbf{x}_d^D \quad \mathbf{x}_q^B \quad \mathbf{x}_j^B \quad \mathbf{x}_b^B]^T$$

In Eq. (3.22),  $\tilde{\mathbf{Z}}$  only consists of the dynamic stiffness matrices of the substructures and  $\Delta\tilde{\mathbf{Z}}$  only concerns the dynamic stiffness matrices of the links. However, it is usually hard to obtain accurate dynamic stiffness matrices of substructures, which would require detailed faithful models corrected by experimental results through, for example, model updating techniques. In contrast, receptance matrix, which is the inverse of dynamic stiffness matrix, can be easily and accurately measured from experiment. Therefore, using receptance matrices of substructures would be much appealing.

Define a receptance-related matrix  $\tilde{\mathbf{H}}$  as

$$\tilde{\mathbf{H}} = \begin{bmatrix} \mathbf{H}^A & \mathbf{0} & \mathbf{0} & \mathbf{0} \\ \mathbf{0} & \beta\mathbf{I}_c & \mathbf{0} & \mathbf{0} \\ \mathbf{0} & \mathbf{0} & \beta\mathbf{I}_d & \mathbf{0} \\ \mathbf{0} & \mathbf{0} & \mathbf{0} & \mathbf{H}^B \end{bmatrix} \quad (3.23)$$

where  $\mathbf{I}_c$  and  $\mathbf{I}_d$  are identity matrices of suitable dimensions,  $\beta$  is a scaling number which is used to keep the elements in matrix  $\tilde{\mathbf{H}}$  in similar orders of magnitude to those of  $\mathbf{H}^A$  and  $\mathbf{H}^B$  to avoid ill-conditioning, and

$$\mathbf{H}^A = (\mathbf{Z}^A)^{-1} = \begin{bmatrix} \mathbf{H}_{aa}^A & \mathbf{H}_{ap}^A & \mathbf{H}_{ai}^A \\ \mathbf{H}_{pa}^A & \mathbf{H}_{pp}^A & \mathbf{H}_{pi}^A \\ \mathbf{H}_{ia}^A & \mathbf{H}_{ip}^A & \mathbf{H}_{ii}^A \end{bmatrix} \quad (3.24)$$

$$\mathbf{H}^B = (\mathbf{Z}^B)^{-1} = \begin{bmatrix} \mathbf{H}_{qq}^B & \mathbf{H}_{qj}^B & \mathbf{H}_{qb}^B \\ \mathbf{H}_{jq}^B & \mathbf{H}_{jj}^B & \mathbf{H}_{jb}^B \\ \mathbf{H}_{bq}^B & \mathbf{H}_{bj}^B & \mathbf{H}_{bb}^B \end{bmatrix} \quad (3.25)$$

which are the receptance matrices of the uncoupled substructures A and B, respectively.

Then, Eq. (3.22) is pre-multiplied by this receptance-related matrix  $\tilde{\mathbf{H}}$  to yield

$$(\tilde{\mathbf{I}} + \tilde{\mathbf{H}}\Delta\tilde{\mathbf{Z}})\mathbf{x} = \tilde{\mathbf{H}}\mathbf{f}_{\text{ext}} \quad (3.26)$$

where

$$\tilde{\mathbf{I}} = \begin{bmatrix} \mathbf{I}^A & \mathbf{0} & \mathbf{0} & \mathbf{0} \\ \mathbf{0} & \mathbf{0} & \mathbf{0} & \mathbf{0} \\ \mathbf{0} & \mathbf{0} & \mathbf{0} & \mathbf{0} \\ \mathbf{0} & \mathbf{0} & \mathbf{0} & \mathbf{I}^B \end{bmatrix} = \begin{bmatrix} \mathbf{I}_a & \mathbf{0} & \mathbf{0} & \mathbf{0} & \mathbf{0} & \mathbf{0} & \mathbf{0} & \mathbf{0} \\ \mathbf{0} & \mathbf{I}_p & \mathbf{0} & \mathbf{0} & \mathbf{0} & \mathbf{0} & \mathbf{0} & \mathbf{0} \\ \mathbf{0} & \mathbf{0} & \mathbf{I}_i & \mathbf{0} & \mathbf{0} & \mathbf{0} & \mathbf{0} & \mathbf{0} \\ \mathbf{0} & \mathbf{0} & \mathbf{0} & \mathbf{0} & \mathbf{0} & \mathbf{0} & \mathbf{0} & \mathbf{0} \\ \mathbf{0} & \mathbf{0} & \mathbf{0} & \mathbf{0} & \mathbf{0} & \mathbf{0} & \mathbf{0} & \mathbf{0} \\ \mathbf{0} & \mathbf{0} & \mathbf{0} & \mathbf{0} & \mathbf{0} & \mathbf{I}_q & \mathbf{0} & \mathbf{0} \\ \mathbf{0} & \mathbf{0} & \mathbf{0} & \mathbf{0} & \mathbf{0} & \mathbf{0} & \mathbf{I}_j & \mathbf{0} \\ \mathbf{0} & \mathbf{0} & \mathbf{0} & \mathbf{0} & \mathbf{0} & \mathbf{0} & \mathbf{0} & \mathbf{I}_b \end{bmatrix} \quad (3.27)$$

Then the receptance of the assembled structure can be expressed as

$$\mathbf{H}_{\text{ass}} = (\tilde{\mathbf{I}} + \tilde{\mathbf{H}}\Delta\tilde{\mathbf{Z}})^{-1}\tilde{\mathbf{H}} \quad (3.28)$$

As explained in section 3.2.2, the eigenvalues of assembled structure can be determined by

$$\det(\tilde{\mathbf{I}} + \tilde{\mathbf{H}}\Delta\tilde{\mathbf{Z}}) = 0 \quad (3.29)$$

The above Eq. (3.29) could be simplified as

$$\begin{aligned} & \det(\tilde{\mathbf{I}}_s + \tilde{\mathbf{H}}_s(\omega)\Delta\tilde{\mathbf{Z}}_s(\omega)) = \\ & \det\left(\begin{bmatrix} \tilde{\mathbf{I}}^C & \mathbf{0} \\ \mathbf{0} & \tilde{\mathbf{I}}^D \end{bmatrix} + \begin{bmatrix} \tilde{\mathbf{H}}_{CC} & \tilde{\mathbf{H}}_{CD} \\ \tilde{\mathbf{H}}_{DC} & \tilde{\mathbf{H}}_{DD} \end{bmatrix} \begin{bmatrix} \mathbf{Z}^C & \mathbf{0} \\ \mathbf{0} & \mathbf{Z}^D \end{bmatrix}\right) = 0 \end{aligned} \quad (3.30)$$

where

$$\begin{aligned}\tilde{\mathbf{I}}^C &= \begin{bmatrix} \mathbf{I}_p^A & \mathbf{0} & \mathbf{0} \\ \mathbf{0} & \mathbf{0} & \mathbf{0} \\ \mathbf{0} & \mathbf{0} & \mathbf{I}_q^B \end{bmatrix}, \quad \tilde{\mathbf{H}}_{CC} = \begin{bmatrix} \mathbf{H}_{pp}^A & \mathbf{0} & \mathbf{0} \\ \mathbf{0} & \beta \mathbf{I}_c & \mathbf{0} \\ \mathbf{0} & \mathbf{0} & \mathbf{H}_{qq}^B \end{bmatrix}, \quad \tilde{\mathbf{H}}_{CD} = \begin{bmatrix} \mathbf{H}_{pi}^A & \mathbf{0} & \mathbf{0} \\ \mathbf{0} & \mathbf{0} & \mathbf{0} \\ \mathbf{0} & \mathbf{0} & \mathbf{H}_{qj}^B \end{bmatrix} \\ \tilde{\mathbf{I}}^D &= \begin{bmatrix} \mathbf{I}_i^A & \mathbf{0} & \mathbf{0} \\ \mathbf{0} & \mathbf{0} & \mathbf{0} \\ \mathbf{0} & \mathbf{0} & \mathbf{I}_j^B \end{bmatrix}, \quad \tilde{\mathbf{H}}_{DC} = \begin{bmatrix} \mathbf{H}_{ip}^A & \mathbf{0} & \mathbf{0} \\ \mathbf{0} & \mathbf{0} & \mathbf{0} \\ \mathbf{0} & \mathbf{0} & \mathbf{H}_{jq}^B \end{bmatrix}, \quad \tilde{\mathbf{H}}_{DD} = \begin{bmatrix} \mathbf{H}_{ii}^A & \mathbf{0} & \mathbf{0} \\ \mathbf{0} & \beta \mathbf{I}_d & \mathbf{0} \\ \mathbf{0} & \mathbf{0} & \mathbf{H}_{jj}^B \end{bmatrix}\end{aligned}$$

Detailed derivations from Eq. (3.29) to Eq. (3.30) could be found in the Appendix A. It should be noticed that the number of rows or columns in the matrices in Eq. (3.29) is the total number of DoFs of the assembled structure, which is usually very large in practice, while the number of rows or columns in the matrices in Eq. (3.30) is the number of DoFs of the connection DoFs between substructures A and B together and links C and D together, which is much smaller.

In Eq. (3.30),  $\omega$  is the desired natural frequency. The desired natural frequency could be assigned by solving Eq. (3.30) for  $\Delta\tilde{\mathbf{Z}}_s$ . However, as explained in section 3.2.2, in reality, it is usually difficult to solve Eq. (3.30) directly. Instead, converting this problem into an optimization problem would be more convenient to find a solution. Therefore, Eq. (3.30) is converted into

$$\min_{\Delta\tilde{\mathbf{Z}}_s} \left\{ \sum_{i=1}^{n_d} \det(\tilde{\mathbf{I}}_s + \tilde{\mathbf{H}}_s(\omega_i) \Delta\tilde{\mathbf{Z}}_s(\omega_i)) \right\} \quad (3.31)$$

Here  $n_d$  is the number of desired natural frequencies. There are many optimization methods. Since the optimization algorithm is not the focus of this paper, the detailed optimization process is not presented here. This equation is very similar with Eq. (3.15) which is introduced in subsection 3.2.2.

Suppose that there is only one link C in Fig. 3.5, Eq. (3.30) would be recast as

$$\det(\tilde{\mathbf{I}}^C + \tilde{\mathbf{H}}_{CC} \mathbf{Z}^C) = 0 \quad (3.32)$$

Similarly, if there are  $r$  independent links (that is, they do not have shared DoFs), denoted by  $L_1, L_2, \dots, L_r$ , Eq. (3.30) would be written as

$$\det \left( \begin{bmatrix} \tilde{\mathbf{I}}^{L_1} & \mathbf{0} & \dots & \mathbf{0} \\ \mathbf{0} & \tilde{\mathbf{I}}^{L_2} & \dots & \mathbf{0} \\ \vdots & \vdots & \ddots & \vdots \\ \mathbf{0} & \mathbf{0} & \dots & \tilde{\mathbf{I}}^{L_r} \end{bmatrix} + \begin{bmatrix} \tilde{\mathbf{H}}_{L_1 L_1} & \tilde{\mathbf{H}}_{L_1 L_2} & \dots & \tilde{\mathbf{H}}_{L_1 L_r} \\ \tilde{\mathbf{H}}_{L_2 L_1} & \tilde{\mathbf{H}}_{L_2 L_2} & \dots & \tilde{\mathbf{H}}_{L_2 L_r} \\ \vdots & \vdots & \ddots & \vdots \\ \tilde{\mathbf{H}}_{L_r L_1} & \tilde{\mathbf{H}}_{L_r L_2} & \dots & \tilde{\mathbf{H}}_{L_r L_r} \end{bmatrix} \begin{bmatrix} \mathbf{Z}^{L_1} & \mathbf{0} & \dots & \mathbf{0} \\ \mathbf{0} & \mathbf{Z}^{L_2} & \dots & \mathbf{0} \\ \vdots & \vdots & \ddots & \vdots \\ \mathbf{0} & \mathbf{0} & \dots & \mathbf{Z}^{L_r} \end{bmatrix} \right) = 0 \quad (3.33)$$

Therefore, this method could be applied to frequency assignment of assembled structure with any number of links. This receptance-based method does not require the system models of substructures. Only receptance matrices of substructures at the connection DoFs are needed and they are easier to be measured, compared with mass matrices and more importantly, stiffness matrices.

The zeros of the assembled structures are also given from the matrix in the numerator in Eq. (3.28). Therefore, zeros can also be assigned for the assembled structures. An equation that is similar with Eq. (3.16) can be obtained

$$[\text{adj}(\tilde{\mathbf{I}}(\omega) + \tilde{\mathbf{H}}(\omega)\Delta\tilde{\mathbf{Z}}(\omega))\tilde{\mathbf{H}}(\omega)]_{ij} = 0 \quad (3.34)$$

A zero can be assigned to  $h_{ij}$  of assembled structure at the frequency  $\omega$  by solving Eq. (3.34).

### 3.4 Numerical examples

In this section, two simulated examples are analysed using the proposed method in section 3.3. The first example has two discrete substructures, which are to be connected using a spring-mass-spring link. The second one is about two frame structures connected through 4 beams. Damping is not considered in either example. In the following simulations, the required receptances are obtained from theoretical models. However, they will be directly measured in practice.

#### 3.4.1 Discrete structure with one link

Two discrete substructures A and B are connected using a spring-mass-spring link, as shown in Fig. 3.7. The connection points are  $m_3$  and  $m_4$ . The parameters of these substructures are given in Table 3.1. Table 3.2 shows the natural frequencies of substructures A and B. It is required to (1) assign a natural frequency  $\omega = 30\pi$  rad/s to the assembled structure (2) assign a natural frequency  $\omega = 30\pi$  rad/s and a zero to the cross receptance  $h_{12}$  at  $40\pi$  rad/s for the assembled structure by designing the link.

The physical constraints on the link C are defined as  $0 < k_{c1}, k_{c2} < 5 \times 10^5$  N/m and  $0 < m_0 < 10$  kg.

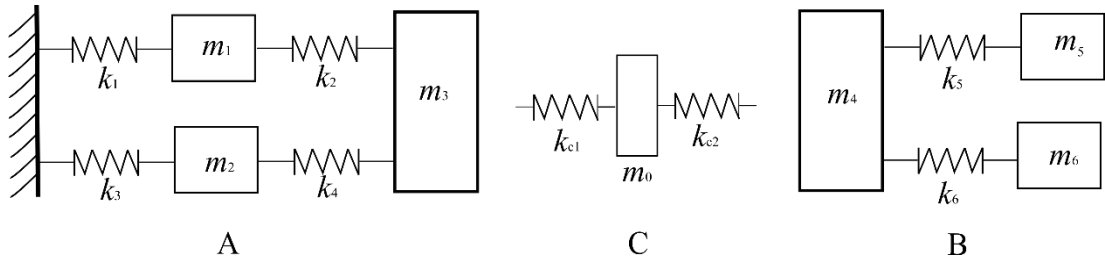


Fig. 3.7 Substructure A and B coupled through link C

Table 3.1 Substructures' parameters

Mass elements (kg)	$m_1 = 5, m_2 = 4, m_3 = 7,$ $m_4 = 4, m_5 = 2, m_6 = 1$
Stiffness elements (N/m)	$1 \times 10^5$ for all

In this example, link C takes the form of spring-mass-spring, as shown in Fig. 3.7. Suppose the parameters of this link are denoted by  $(k_{c1}, k_{c2}, m_0)$ , the dynamic stiffness matrix of this link is

$$\mathbf{Z}^C(\omega) = \begin{bmatrix} k_{c1} & -k_{c1} & 0 \\ -k_{c1} & k_{c1} + k_{c2} - m_0(\omega)^2 & -k_{c2} \\ 0 & -k_{c2} & k_{c2} \end{bmatrix}$$

Table 3.2 Natural frequencies of substructure A and B

Mode	1	2	3
Substructure A (Hz)	15.98	33.34	40.46
Substructure B (Hz)	0	40.47	58.55

For the first problem, the receptance matrix at the desired frequency value is

$$\tilde{\mathbf{H}}_{CC}(\omega) = \begin{bmatrix} h_{33}^A & 0 & 0 \\ 0 & \beta 1 & 0 \\ 0 & 0 & h_{44}^B \end{bmatrix} = 10^{-5} \begin{bmatrix} 7.84 & 0 & 0 \\ 0 & 1 & 0 \\ 0 & 0 & -1.50 \end{bmatrix}$$

According to Eq. (3.32), the optimization problem in this example would be

$$\min\{\det(\tilde{\mathbf{I}}^c + \tilde{\mathbf{H}}_{cc}(\omega)\mathbf{Z}^c(\omega))\} \quad (3.35)$$

This optimization problem can be solved using MATLAB built-in function *fmincon*. If  $k_{c1} = 1 \times 10^5$  N/m, the obtained result is  $k_{c2} = 0.28 \times 10^5$  N/m,  $m_0 = 6.75$  kg.

Fig. 3.8 shows the FRF  $h_{12}$  of the assemble structure. Apparently, the obtained natural frequency is exactly the desired frequency  $\omega = 30\pi$  rad/s (or 15 Hz).

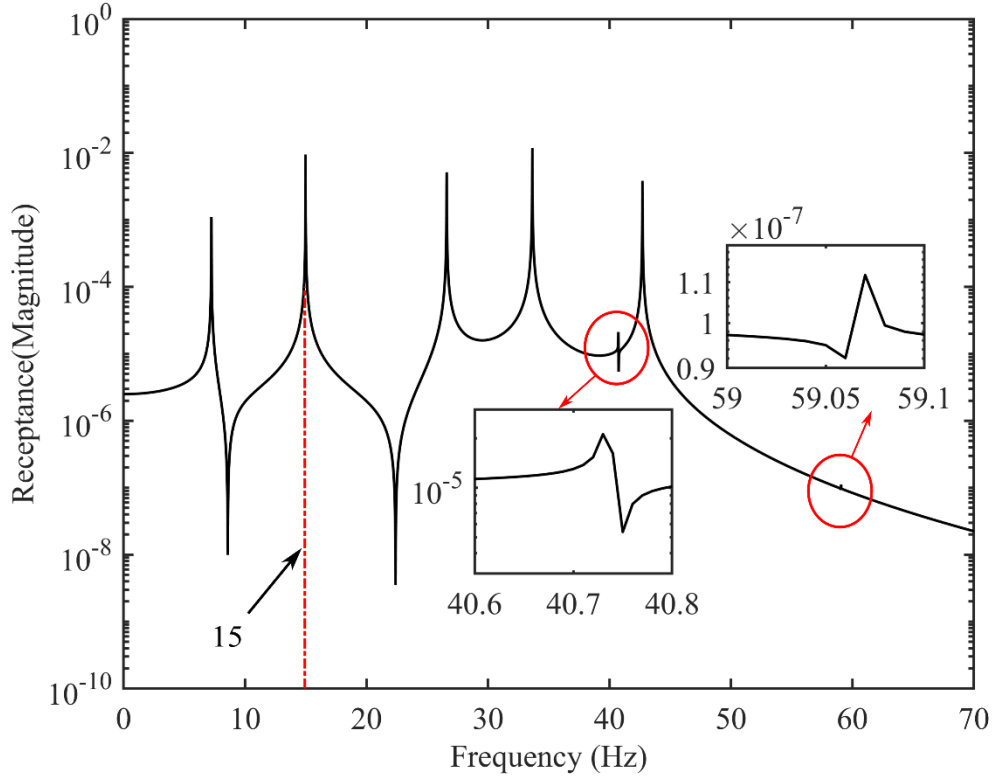


Fig. 3.8 FRF  $h_{12}$  of the assembled structure with a natural frequency at  $30\pi$  rad/s

Table 3.3 Natural frequencies of the assembled structure (a desired frequency 15 Hz)

Mode	1	2	3	4	5	6	7
Frequency (Hz)	7.23	15.00	26.60	33.65	40.73	42.71	59.06

In fact, there are multiple solutions in this optimization problem. One could choose a desired solution based on other criteria, such as a restriction on the value of the mass or stiffness.

For the second problem, a zero is supposed to be assigned to  $h_{12}$  at 20 Hz with a natural frequency at 15 Hz. This problem is solved using Eq. (3.31) and (3.34). The obtained results are  $k_{c1} = 1 \times 10^5$  N/m,  $k_{c2} = 0.34 \times 10^5$  N/m and  $m_0 = 9.33$  kg.



Fig. 3.9 shows the receptance  $h_{12}$  of the assembled structure with a zero at  $40\pi$  rad/s and a natural frequency at  $30\pi$  rad/s.

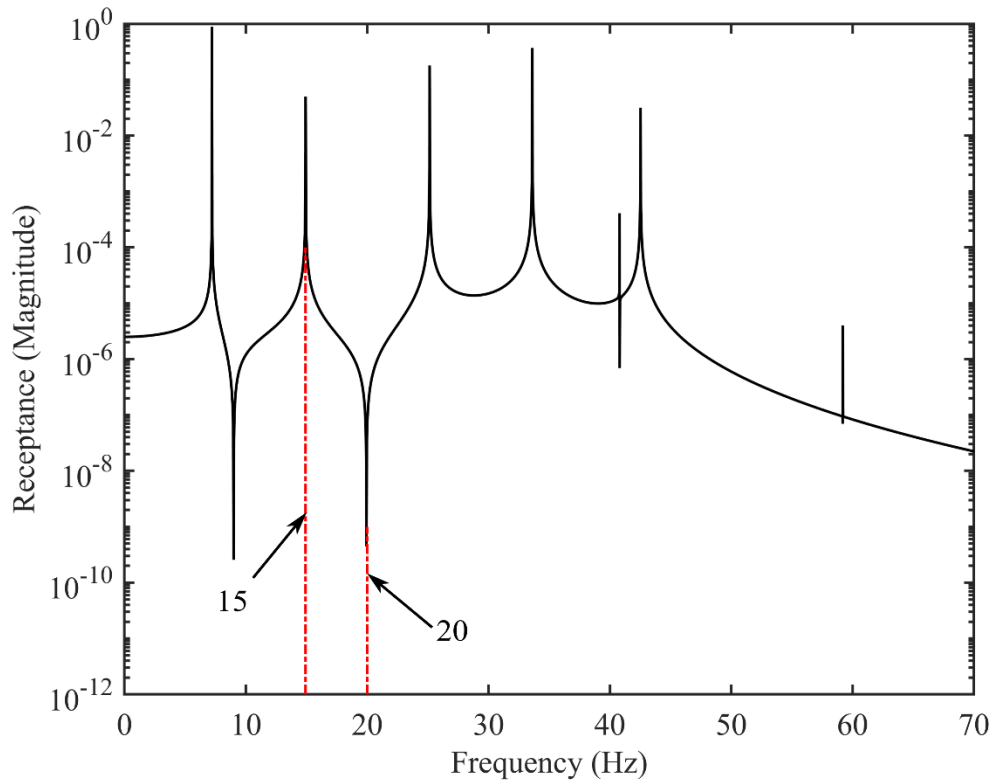


Fig. 3.9 FRF  $h_{12}$  of the assembled structure with a natural frequency at 15 Hz and a zero at 20 Hz.

Table 3.4 Natural frequencies of the assembled structure (a desired frequency at 15 Hz and a zero at 20 Hz)

Mode	1	2	3	4	5	6	7
Frequency (Hz)	7.21	15.00	25.14	33.60	40.79	42.52	59.18

### 3.4.2 Continuous structure with multiple continuous links

Consider two frame structures A (in dark colour) and B (in light colour), which are composed of mild steel beams, are connected by four links at the mid-points of their four sides. Frame B is placed at the centre of frame A. The corresponding finite element models are shown in Fig. 3.10. The finite element model of frame A has 14 nodes and 6 beams with two of them grounded. The finite element model of frame B

has 12 nodes and 4 beams. Each node has 3 degrees of freedom (a horizontal translation and a vertical translation, and a rotation). The material properties of frames A and B, and links C are the same. The Young's modulus is 210GPa and the density is 7850 kg/m<sup>3</sup>. The cross-sectional areas of frames A and B are described in Table 3.5. The four links consist of two horizontal beams and two vertical beams. The cross-sectional areas of those link beams are optimized to assign (1) one natural frequency  $f = 35$  Hz, and (2) two natural frequencies simultaneously,  $f_1 = 35$  Hz and  $f_2 = 100$  Hz.

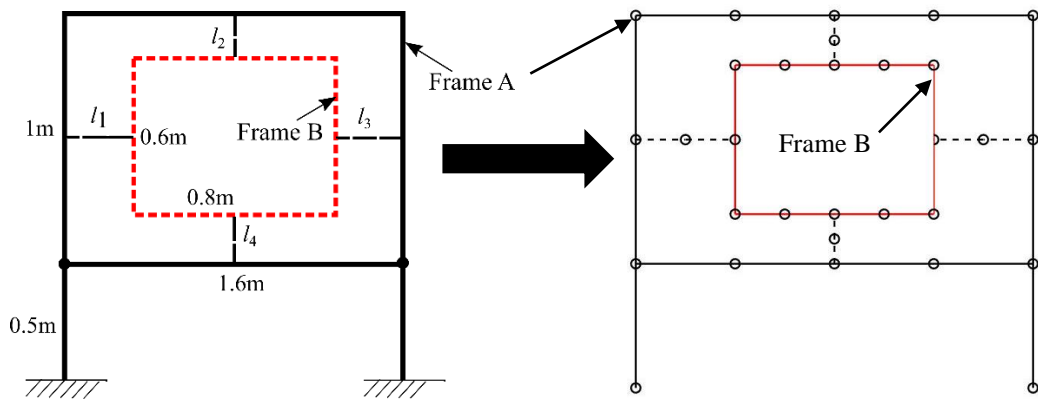


Fig. 3.10 Finite element model of frames A and B and links

Table 3.5 Cross-sectional areas of frames A and B

Cross area of Frame A		Cross area of Frame B	
width (m)	height(m)	width (m)	height(m)
0.08	0.06	0.05	0.04

In this example, the lengths of the four links  $l_i$  ( $i = 1,2,3,4$ ) are prescribed. The cross section areas of the four links are all square, as shown in Fig. 3.11.

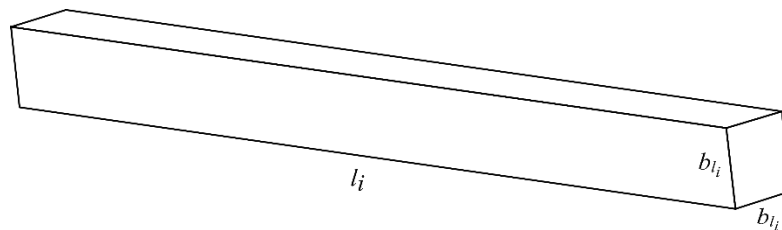


Fig. 3.11 The profile of a link

The design variables are the breadths  $b_{l_i}$  of the cross-sections of the four links, which are denoted by  $(b_{l_1}, b_{l_2}, b_{l_3}, b_{l_4})$  respectively. The simulated annealing algorithm is adopted in this example.

For the first problem, assuming  $b_{l_1} = b_{l_3}$  and  $b_{l_2} = b_{l_4}$ , which means the two horizontal links are identical and the two vertical links are identical too, so there are only two design variables  $(b_{l_1}, b_{l_2})$ . The lower bound and upper bound of these design variables are 0.01m and 0.1m. Then substituting the receptance matrices of frames A and B into Eq. (3.30), the values of  $b_{l_1} = 0.037$  m,  $b_{l_2} = 0.039$  m are obtained. Receptance  $h_{38,44}$  of the assembled structure is shown in Fig. 3.12 with a natural frequency at 34.99 Hz. The first 5 natural frequencies of assembled structure are collected in Table 3.6. (The bold number in Table 3.6 indicates the assigned frequency for the assembled structure. The bold numbers in Table 3.7 and Table 3.8 have the same meaning).

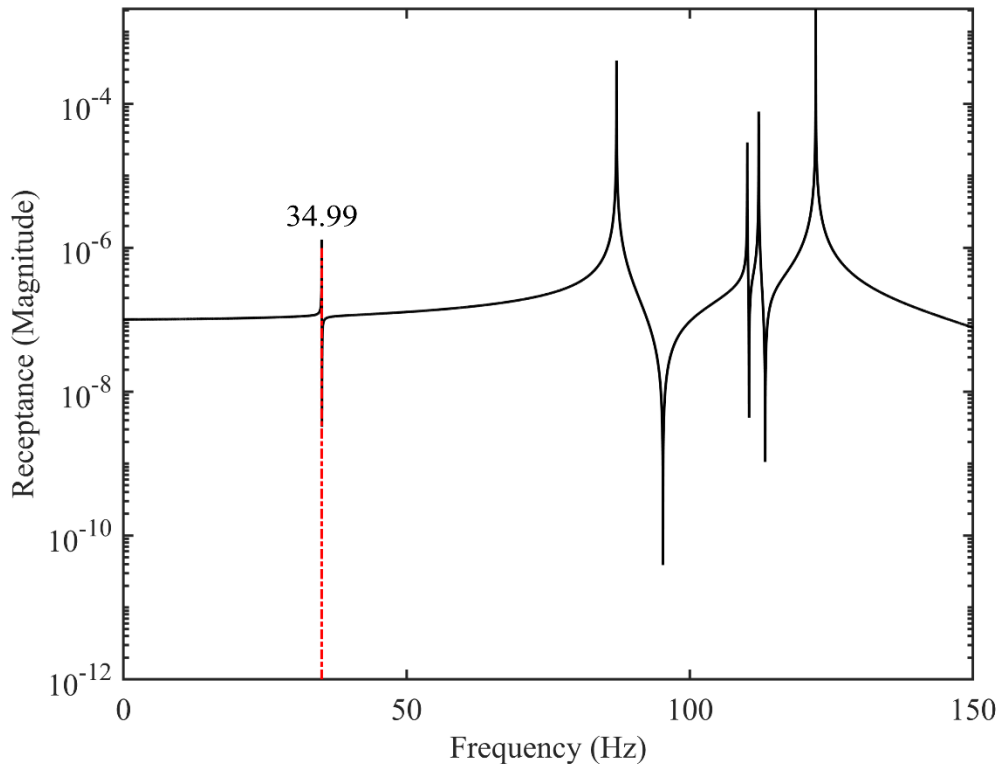


Fig. 3.12 FRF  $h_{38,44}$  with one assigned frequency

Table 3.6 First 5 natural frequencies of assembled structure with one assigned frequency at 34.99 Hz

Mode	1	2	3	4	5
Frequency (Hz)	<b>34.99</b>	87.06	110.15	112.16	122.23

In the second problem, two frequencies are to be assigned to the assembled structure. Let  $b_{l_2} = b_{l_4}$ , which leaves 3 design variables ( $b_{l_1}, b_{l_2}, b_{l_3}$ ) in this optimization problem. If the lower bound and upper bound of those design variables are still 0.01m and 0.1m, from Eq. (3.30), the optimized results obtained are  $b_{l_1} = 0.058\text{m}$ ,  $b_{l_2} = 0.03\text{ m}$ , and  $b_{l_3} = 0.043\text{ m}$ . Fig. 3.13 shows receptance  $h_{38,44}$  of the assembled structure with optimized links. This figure indicates that the first two natural frequencies of the assembled structure are 35.40Hz and 100 Hz, which are very close to the desired frequencies. The first 5 natural frequencies of this assembled structure are listed in Table 3.7.

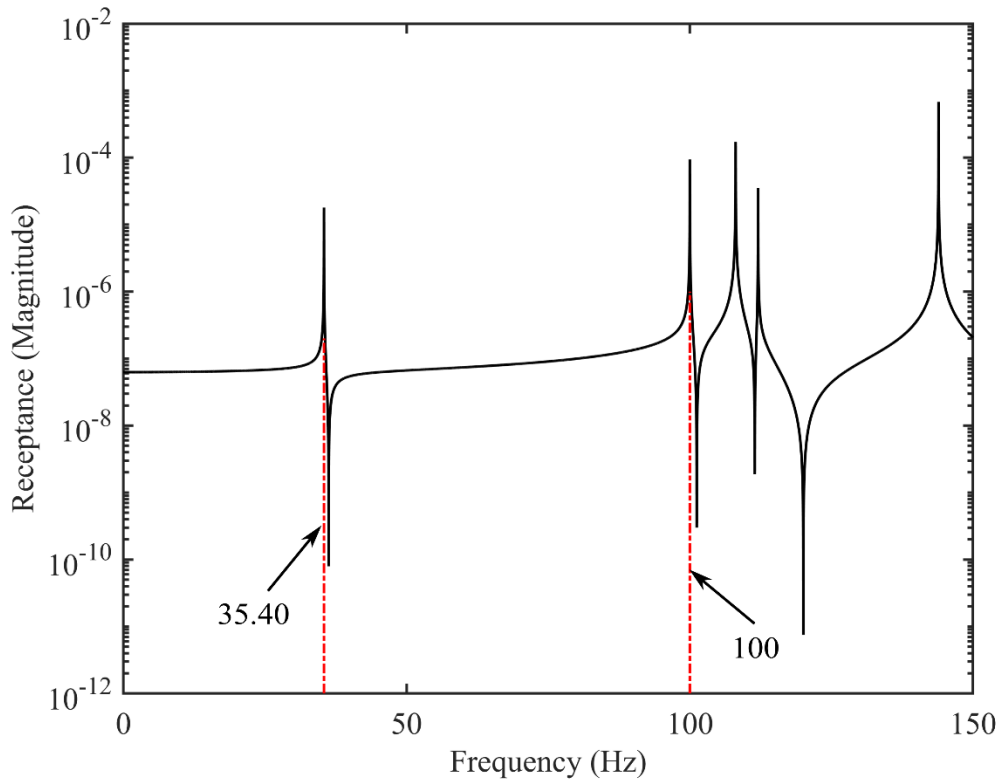


Fig. 3.13 FRF  $h_{38,44}$  with two assigned frequencies

Table 3.7 First 5 natural frequencies of assembled structure with two assigned frequencies at 35.40 Hz and 100.00 Hz

Mode	1	2	3	4	5
Frequency (Hz)	<b>35.40</b>	<b>100.00</b>	108.08	112.05	143.91

On the other hand, if the lower bound and upper bound of those design variables are 0.003m and 0.04m, the obtained results are  $b_{l_1} = 0.008\text{m}$ ,  $b_{l_2} = 0.014\text{m}$ , and  $b_{l_3} = 0.003\text{m}$ . The first 5 natural frequencies of this new assembled structure are presented in Table 3.8. It should be noticed that the assigned frequencies 34.99 Hz and 101.31 Hz, are the second and fifth natural frequencies, respectively.

Table 3.8 First 5 natural frequencies of assembled structure with two assigned frequencies at 34.99 Hz and 101.31 Hz

Mode	1	2	3	4	5
Frequency (Hz)	21.91	<b>34.99</b>	69.34	91.04	<b>101.31</b>

### 3.5 Discussion

In those examples in section 3.4, there are usually more than one solution for each assignment problem. As shown in subsection 3.4.2, two different solutions are found with different lower bounds and upper bounds. Although both solutions could assign the desired frequencies, the actually assigned frequencies correspond to different modes in the two solutions and thus the resulting assembled structures will have different dynamic behaviours. This is because mode shapes are not involved in this frequency assignment method, unlike a previous method reported in [69]. Therefore, a further optimization, determining which solution is optimal among a number of feasible solutions that all assign the desired frequencies should be useful. This optimal solution could be determined based on other specific requirements, such as the restrictions on the parameters of links, or the corresponding mode shapes, as constraints to the optimization problem described in Eq. (3.31).

One drawback of this method is that it requires the theoretical models (usually finite element models) of the links. However, this is unavoidable for an inverse assignment method because the modifications are unknown and cannot be measured beforehand. A theoretical model allows its frequencies to be associated with its structural properties and thus can be used in the optimization algorithm used, which requires a repeated use

of the theoretical model with different structural properties in the iterations. For simple links, such as mass-spring systems, beams or rods, it is quite easy to build theoretical models for them. On the other hand, it is difficult to model complex links accurately. However, the links are usually much simpler than the uncoupled substructures. Their possible lack of modelling accuracy would not have a big impact on the accuracy of frequency assignment, in the context of very complicated assembled structures. There are ways to reduce the inaccuracy of the theoretical models of complex links. For example, if a link is to be a complex structure, one can divide the link into modifiable parts and unmodifiable parts. The unmodifiable parts could be measured by building real structures for them so that those structures would become another substructures. The modifiable parts should be as simple as possible. It would be easier to build accurate theoretical models for these simple modifiable parts. An experimental work on this method will be introduced in next chapter.

### **3.6 Conclusions**

This chapter presents a receptance-based frequency assignment method for assembled structures. This method maintains the original substructures designed for specific requirements and the assignment is achieved through modifying the links that connect the uncoupled original substructures. Those added links can be discrete structures or continuous structures. This method only requires the receptances of the uncoupled substructures at the connection points of the links which can be measured accurately and easily in practice, and the theoretical models of links which are usually much simpler than the uncoupled substructures are thus easy to build and accurate.

Assigning frequencies for an assembled structure using this method involves multiple substructures. The modifications in this paper, as links, introduce extra degrees of freedom for the whole assembled structure. The proposed methodology works well for any number of links and substructures. Two numerical examples are presented to validate this proposed method.

## **Chapter 4**

### **Experimental work on frequency assignment of an assembled structure**

#### **4.1 Introduction**

This chapter presents experimental work on frequency assignment of an assembled structure. The test structure in this chapter is a simplified model of a part of a ship hull.

An unwanted side effect of building faster and lighter ships is their increasing level of noise and vibration. In order to retain the full benefit of building faster ships without compromising the comfort and safety concerns, effective vibration control needs to be implemented to ship structures. A floating raft system, which is usually modelled as a two-stage vibration isolation system, as shown in Fig. 4.1, has been widely used in ships due to its excellent performance on vibration isolation [166-168]. Rotatory machines, such as diesel engines, pumps, and electric generators are installed on floating raft systems so that the vibration sources are integrated on the floating raft platforms. Noise and vibration of rotatory machines are generally dominated by several peaks. Therefore, a floating raft system has to be designed carefully to avoid resonances. In addition, in some cases, new machines may be added onto an in-use floating raft platform. Structural modification might be needed to reduce the unwanted vibration effects of these new machines.

A floating raft platform is usually installed on the ship hull through several isolators (The lower isolators shown in Fig. 4.1). The properties of these lower isolators will affect the isolation performance of the whole floating raft system. Therefore, proper isolators between the floating raft platform and the ship hull must be designed so as to make sure the whole floating raft system can have desired dynamic behaviour after installation. In order to validate the method proposed in chapter 3 and simplify the experiments, a simple structure based on the floating raft system is designed in this

chapter. This laboratory structure is composed of two substructures and six beam-type simple links.

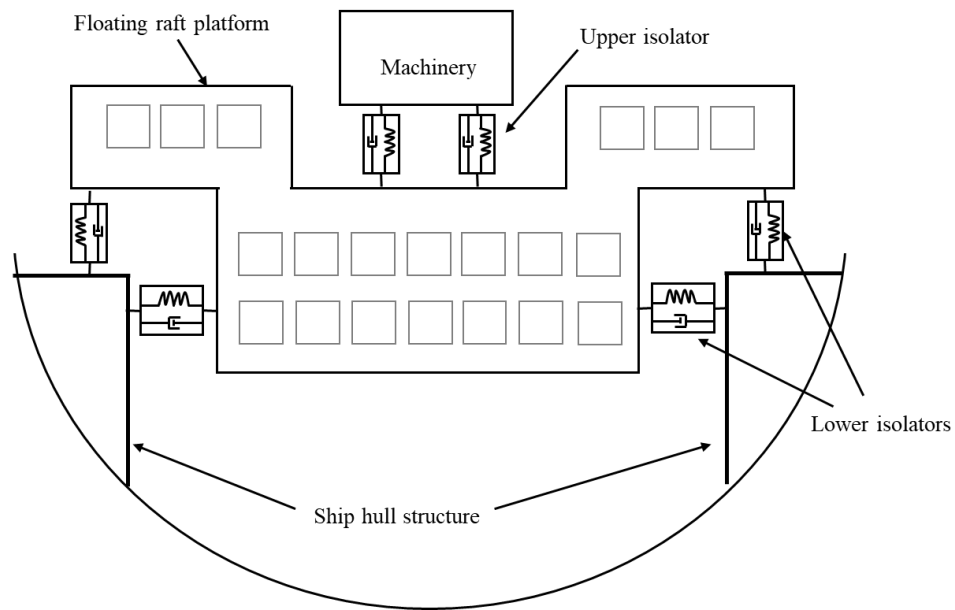


Fig. 4.1 A schematic diagram of a floating raft system

This chapter begins with an introduction of the designed test structure in this experimental work. Then a rotational receptance estimation method is presented. After that, the required finite element models of an auxiliary structure and links are built using Abaqus. Several modal tests are conducted to get the natural frequencies of the assembled structure and to measure the receptances at connection points on the two substructures. The frequency assignment method proposed in chapter 3 is adopted to assign desired natural frequencies for the assembled structures using the measured receptances and the FE models of the links. It should be acknowledged that the test structures in this chapter were manufactured and the experiments were conducted in the Key Laboratory of Ship Vibration and Noise in China.

## 4.2 The tested assembled structure

Fig. 4.2 shows a real floating raft system used on a ship. The floating raft platform is installed on a ship hull through several isolators in different directions, similar to the lower isolators in Fig. 4.1.



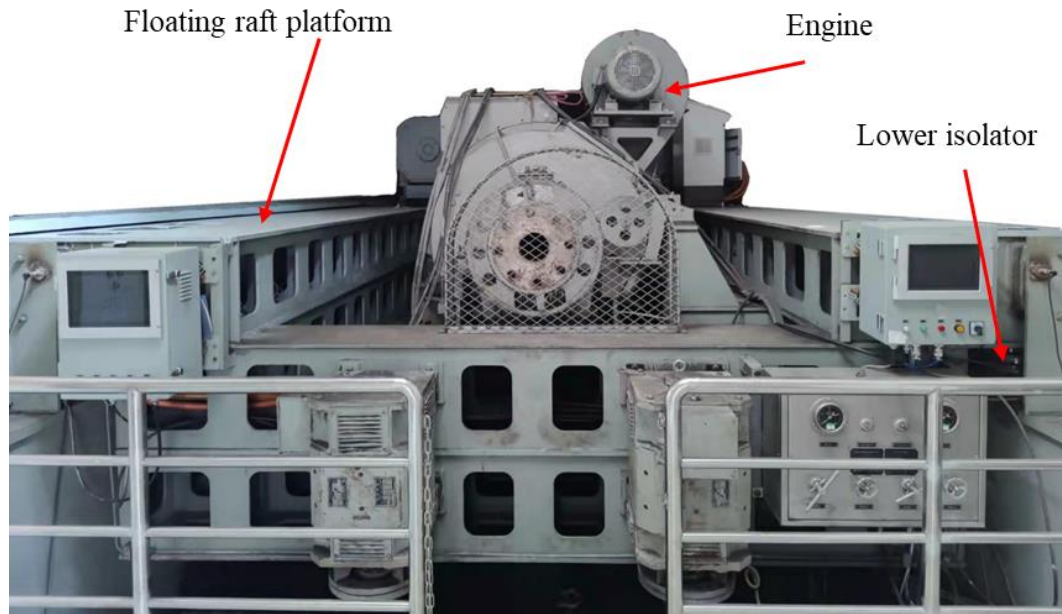


Fig. 4.2 A floating raft system (This picture was taken with the kind permission of the national key laboratory of ship vibration and noise in China)

Fig. 4.3 shows the model of the designed structure in this chapter. It consists of two substructures, named substructure S and substructure B, as presented in Fig. 4.4. Substructure S, which represents the ship hull, looks like a door frame with two L-shaped plates/beams. Substructure B represents a floating raft platform and is like an inverted  $\Omega$ .

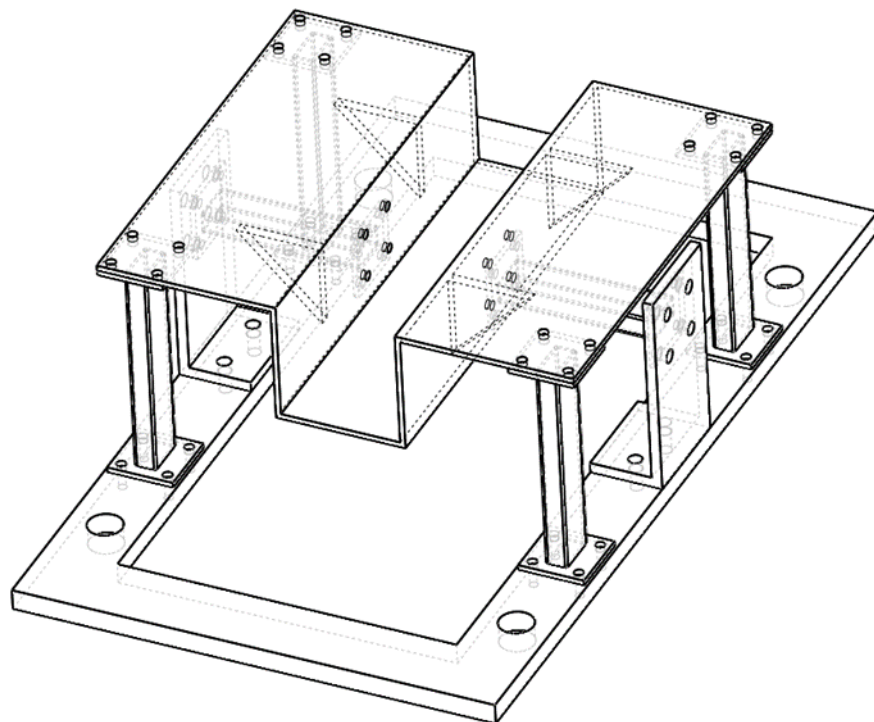


Fig. 4.3 The designed test structure.

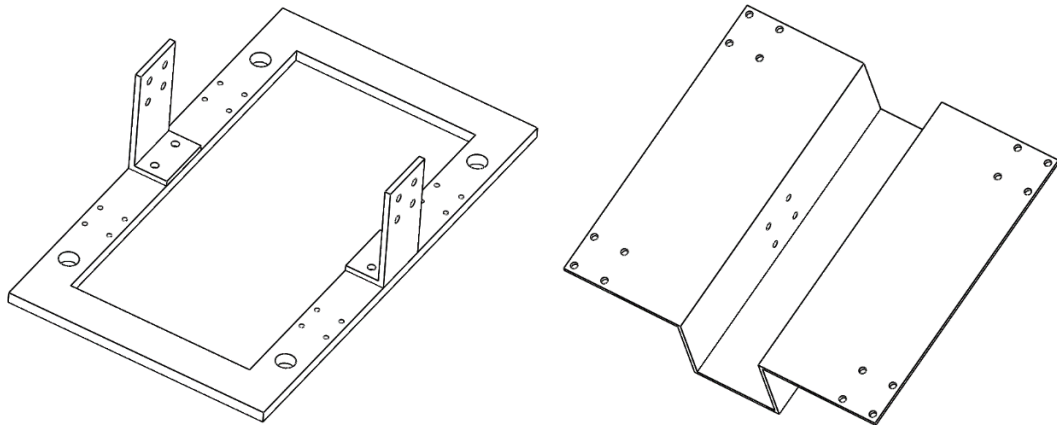


Fig. 4.4 Two Substructures (left: Substructure S, right: Substructure B)

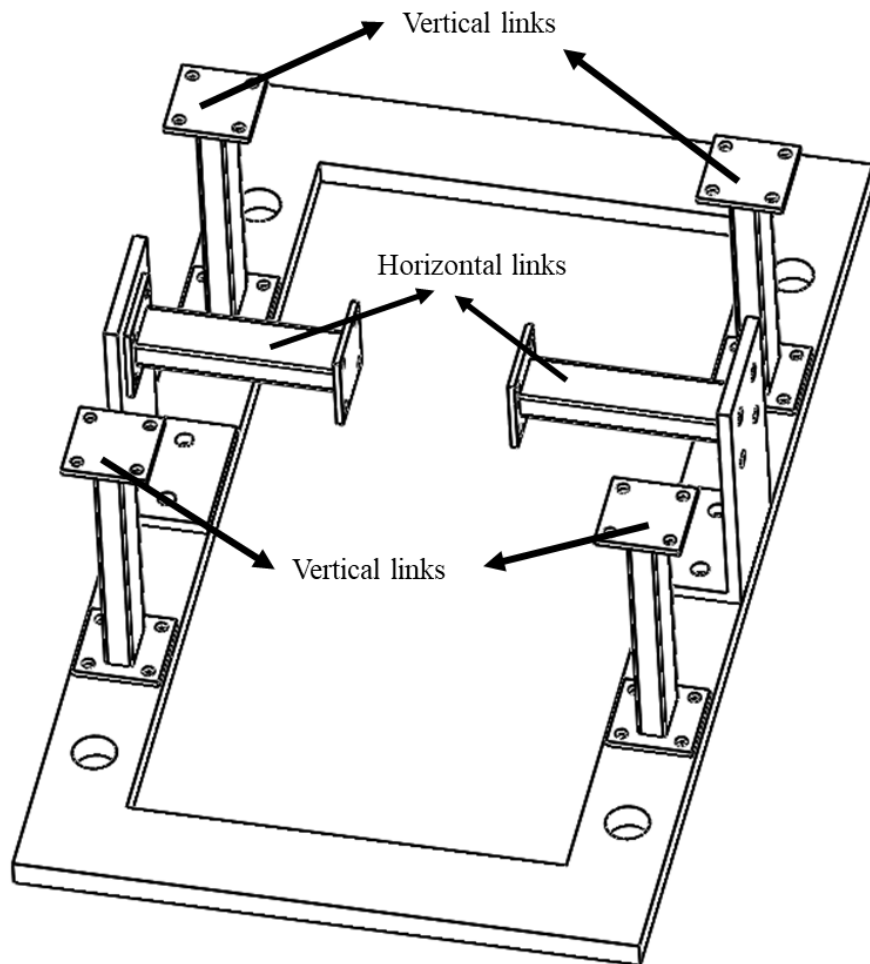


Fig. 4.5 The links between two substructures

The two substructures are connected through six simple links: two identical horizontal links and four identical vertical links, as depicted in Fig. 4.5. Each link is composed of a rectangular tube and two flanges at two ends.

The designed assembled structure has multiple links in different directions. Therefore, this test structure is adequately complicated to explore the performance of the method proposed in chapter 3 and also allow practice of actual structural modification of a real assembled structure.

From Fig. 4.3, it can be seen that each link is bolted onto both substructures on a small area. Compared with the whole assembled structure, the connection area is very small and the interested frequency in this experiment is low (smaller than 200 Hz). So, this small area should behave like a rigid body within the interested frequency range. Therefore, it is reasonable to assume that each substructure is connected with these links at six points. In order to utilise the frequency assignment method presented in chapter 3, it is needed to measure the receptances at the connection points on the two substructures and build theoretical models or FE models of the links.

### 4.3 Rotational receptance estimation

A big challenge in this experimental work is the estimation of rotational receptances. There are two issues for this task. One is that it is usually difficult to apply a pure moment to a structure. The other one is that the measurement of angular displacements is not as easy as the measurement of translational displacements. A number of researchers have made contributions to the study of this topic [67, 147, 148, 169, 170]. The method used in this chapter is mainly based on the work by Tsai et al. [148]. The moment is applied in the form of a force onto an auxiliary structure on the parent structure of which rotational receptances are to be measured. The auxiliary structure is usually very simple and can be modelled accurately using finite element method.

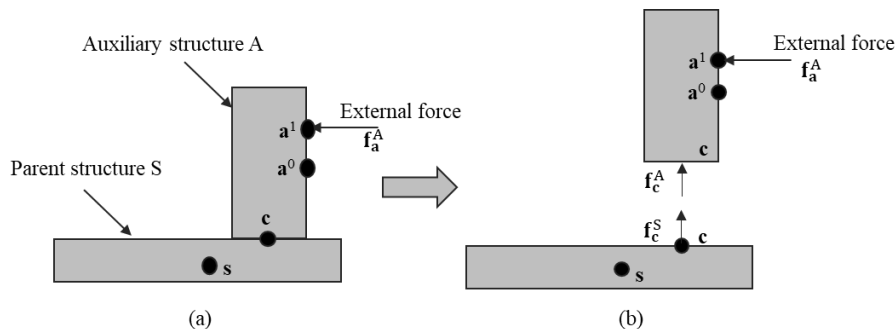


Fig. 4.6 Coupling of an auxiliary structure

As shown in Fig. 4.6, an auxiliary structure A is rigidly connected with the parent structure S through a few connection DoFs denoted as “c” that are shared by the two structures. The DoFs of parent structure S and auxiliary structure A that are not “c” are denoted as “s” and “a”, respectively. In order to estimate the rotational receptances, a few sensors are placed and excitations are applied on the auxiliary structure. The measured DoFs among DoFs “a” are denoted as “a<sup>0</sup>” and the DoFs subject to external forces in DoFs “a” are denoted as “a<sup>1</sup>”. The DoFs a<sup>0</sup> and a<sup>1</sup> may have shared DoFs. The black dots in Fig. 4.6 denote the degrees of freedom of the auxiliary structure or the parent structure.

The dynamic equations of the coupled system and the auxiliary structure A alone in frequency domain can be defined respectively as

$$\begin{bmatrix} \mathbf{x}_c^{SA} \\ \mathbf{x}_a^{SA} \end{bmatrix} = \begin{bmatrix} \mathbf{H}_{cc}^{SA} & \mathbf{H}_{ca}^{SA} \\ \mathbf{H}_{ac}^{SA} & \mathbf{H}_{aa}^{SA} \end{bmatrix} \begin{bmatrix} \mathbf{f}_c^{SA} \\ \mathbf{f}_a^{SA} \end{bmatrix} \quad (4.1)$$

$$\begin{bmatrix} \mathbf{x}_c^A \\ \mathbf{x}_{t^0}^A \\ \mathbf{x}_{t^1}^A \end{bmatrix} = \begin{bmatrix} \mathbf{H}_{cc}^A & \mathbf{H}_{ca^0}^A & \mathbf{H}_{ca^1}^A \\ \mathbf{H}_{a^0c}^A & \mathbf{H}_{a^0a^0}^A & \mathbf{H}_{a^0a^1}^A \\ \mathbf{H}_{a^1c}^A & \mathbf{H}_{a^1a^0}^A & \mathbf{H}_{a^1a^1}^A \end{bmatrix} \begin{bmatrix} \mathbf{f}_c^A \\ \mathbf{0} \\ \mathbf{f}_{a^1}^A \end{bmatrix} \quad (4.2)$$

where the superscript “SA” denotes the coupled structure and superscript “A” represents the auxiliary structure A.

Based on Eq. (4.2), the following two equations can be established

$$\mathbf{f}_c^A = \mathbf{H}_{a^0c}^A{}^{-1} (\mathbf{x}_{a^0}^A - \mathbf{H}_{a^0a^1}^A \mathbf{f}_{a^1}^A) \quad (4.3)$$

$$\mathbf{x}_c^A = \mathbf{H}_{cc}^A \mathbf{H}_{a^0c}^A{}^{-1} (\mathbf{x}_{a^0}^A - \mathbf{H}_{a^0a^1}^A \mathbf{f}_{a^1}^A) + \mathbf{H}_{ca^1}^A \mathbf{f}_{a^1}^A \quad (4.4)$$

The receptance matrices  $\mathbf{H}_*^A$  in the above equations, are from the finite element model of the auxiliary structure. According to the free-body diagram of uncoupled structure in the right side in Fig. 4.6, the force equilibrium and displacement compatibility conditions applied at DoFs c can be defined as

$$\mathbf{x}_c^{SA} = \mathbf{x}_c^A = \mathbf{x}_c^S, \mathbf{f}_c^{SA} = \mathbf{f}_c^A + \mathbf{f}_c^S \quad (4.5)$$

Since there is no external force applied at DoFs  $\mathbf{c}$ , the forces (including moments) applied on the parent structure  $S$  at DoFs  $\mathbf{c}$  can be easily obtained  $\mathbf{f}_c^S = -\mathbf{f}_c^A$ . Eq. (4.4) can give the responses of the parent structure  $S$  at DoFs  $\mathbf{c}$ .

The auxiliary structure used in this experimental work is shown in Fig. 4.7. In addition, two angular accelerometers were adopted to help reduce the difficulty of rotational receptance estimation. One angular accelerometer was attached on the auxiliary structure and the other one was attached on the parent structure  $S$ .

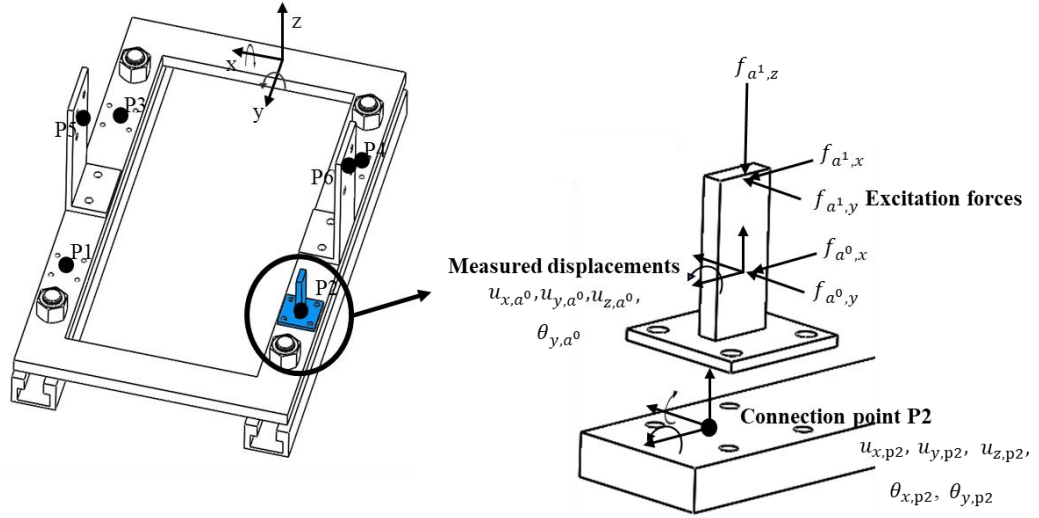


Fig. 4.7 The auxiliary structure used in this experiment

Each substructure has six connection points. At each connection point, there are 5 DoFs. Taking connection point P2 as example, shown in Fig. 4.7, the 5 DoFs are denoted by  $(u_{x,p2}, u_{y,p2}, u_{z,p2}, \theta_{x,p2}, \theta_{y,p2})$  ( $\theta_{z,p2}$  is not considered in this experiment and the reason will be explained in section 4.5). Therefore, a  $5 \times 5$  receptance matrix needs to be measured at point P2 and this matrix can be written as

$$\mathbf{H}_{p2p2}^S = \begin{bmatrix} h_{2x2x} & h_{2x2y} & h_{2x2z} & h_{2x2\theta_x} & h_{2x2\theta_y} \\ h_{2y2x} & h_{2y2y} & h_{2y2z} & h_{2y2\theta_x} & h_{2y2\theta_y} \\ h_{2z2x} & h_{2z2y} & h_{2z2z} & h_{2z2\theta_x} & h_{2z2\theta_y} \\ h_{2\theta_x2x} & h_{2\theta_x2y} & h_{2\theta_x2z} & h_{2\theta_x2\theta_x} & h_{2\theta_x2\theta_y} \\ h_{2\theta_y2x} & h_{2\theta_y2y} & h_{2\theta_y2z} & h_{2\theta_y2\theta_x} & h_{2\theta_y2\theta_y} \end{bmatrix} \quad (4.6)$$

The nine receptances at the top left corner are only translational displacements related and can be measured directly using an impact hammer and accelerometers, without the aid of the auxiliary structure.

$$(\mathbf{H}_{p2p2}^S)_{translational} = \begin{bmatrix} h_{2x2x} & h_{2x2y} & h_{2x2z} \\ h_{2y2x} & h_{2y2y} & h_{2y2z} \\ h_{2z2x} & h_{2z2y} & h_{2z2z} \end{bmatrix}$$

Only receptances at the last two rows or columns in Eq. (4.6), which are rotational displacements related or moment excitation related, are to be measured using the auxiliary structure in Fig. 4.7. (The other six receptances at the top right corner or bottom left corner can be obtained according to the reciprocity of receptances).

During the experiment, a tri-axial accelerometer and an angular accelerometer are placed on the auxiliary structure at point “a0” and excitation forces are applied at points “a0” and “a1” in different directions. The excitation forces and measured responses on the auxiliary structure are collected into vectors

$$\mathbf{f}_{a1}^A = [f_{a1,x} \quad f_{a1,y} \quad f_{a1,z} \quad f_{a0,x} \quad f_{a0,y}]^T \quad (4.7)$$

$$\mathbf{x}_{a0}^A = [u_{x,a0} \quad u_{y,a0} \quad u_{z,a0} \quad \theta_{y,a0}]^T \quad (4.8)$$

The excitation forces  $f_{a1,x}$ ,  $f_{a1,y}$ ,  $f_{a1,z}$ ,  $f_{a0,x}$ , and  $f_{a0,y}$  are applied on the auxiliary structure consecutively in five separate tests. For example, in the first test, only the first element in  $\mathbf{f}_{a1}^A$  is non-zero and in the second test, only the second element in  $\mathbf{f}_{a1}^A$  is non-zero. In each test, the internal forces  $\mathbf{f}_{p2}^S$  at the connection point P2 can be calculated using Eq. (4.3) and

$$\mathbf{f}_{p2}^S = [f_{p2,x} \quad f_{p2,y} \quad f_{p2,z} \quad f_{p2,\theta_x} \quad f_{p2,\theta_y}] \quad (4.9)$$

An angular accelerometer is attached at point P2 on substructure S so as to get the rotational displacement of substructure S at point P2. The angular accelerometer can only measure one rotational displacement at one test. If the angular accelerometer measures the angular displacement  $\theta_{y,p2}$ , the relationship between measured rotational displacement response and the internal force acting at point P2 can be written as

$$\theta_{y,p2} = [h_{2\theta_y,2x} \quad h_{2\theta_y,2y} \quad h_{2\theta_y,2z} \quad h_{2\theta_y,2\theta_x} \quad h_{2\theta_y,2\theta_y}] (\mathbf{f}_{p2}^S)^T \quad (4.10)$$

After five tests, the following equation could be established

$$\boldsymbol{\theta}_{y,p2} = \mathbf{h}_{2\theta_y} \mathbf{F}_{p2}^S \quad (4.11)$$

where

$$\left(\mathbf{h}_{2\theta_y}\right)^T = \begin{bmatrix} h_{2\theta_y 2x} \\ h_{2\theta_y 2y} \\ h_{2\theta_y 2z} \\ h_{2\theta_y 2\theta_x} \\ h_{2\theta_y 2\theta_y} \end{bmatrix}, \quad \left(\mathbf{F}_{p2}^S\right)^T = \begin{bmatrix} \mathbf{f}_{p2}^{S(1)} \\ \mathbf{f}_{p2}^{S(2)} \\ \mathbf{f}_{p2}^{S(3)} \\ \mathbf{f}_{p2}^{S(4)} \\ \mathbf{f}_{p2}^{S(5)} \end{bmatrix}, \quad \left(\boldsymbol{\theta}_{y,p2}\right)^T = \begin{bmatrix} \theta_{y,p2}^{(1)} \\ \theta_{y,p2}^{(2)} \\ \theta_{y,p2}^{(3)} \\ \theta_{y,p2}^{(4)} \\ \theta_{y,p2}^{(5)} \end{bmatrix} \quad (4.12)$$

The numbers in the superscript in (4.12) denote the sequence of tests. and  $\mathbf{F}_{p2}^S \in \mathbb{C}^{5 \times 5}$ ,  $\mathbf{h}_{2\theta_y} \in \mathbb{C}^{5 \times 1}$ ,  $\boldsymbol{\theta}_{y,p2} \in \mathbb{C}^{5 \times 1}$ . Then the receptances  $\mathbf{h}_{2\theta_y}$  could be obtained

$$\mathbf{h}_{2\theta_y} = \left(\mathbf{F}_{p2}^S\right)^{-1} \boldsymbol{\theta}_{y,p2} \quad (4.13)$$

It can be noticed that  $\mathbf{h}_{2\theta_y}$  is actually the last row of  $\mathbf{H}_{p2p2}^S$ . Similarly, when the angular accelerometer measures the angular displacement  $\theta_{x,p2}$ , the fourth row in matrix  $\mathbf{H}_{p2p2}^S$  can be obtained. The remaining 6 receptances at the top right corner can be obtained using the reciprocity of receptances, for example,  $h_{2x2\theta_y} = h_{2\theta_y 2x}$ .

The above-mentioned measurements are the rotational receptances when the excitations and the rotational displacements are at the same connection points. It is also required to measure the rotational receptances when the excitations and responses are not at the same point, for example,  $\mathbf{H}_{p1p2}^S$ . In this case, the auxiliary structure was attached at point P2 and an angular accelerometer was attached at point P1. The procedure is as same as the measurement of  $\mathbf{H}_{p2p2}^S$ .

#### 4.4 Finite element models

As mentioned in section 4.3, a FE model of the auxiliary structure is needed to estimate the rotational receptances at connection points of each substructure. In addition, the receptance-based frequency assignment method introduced in chapter 3 requires theoretical models or FE models of the links. In this section, the FE models of the auxiliary structure and the links are built and discussed.

#### 4.4.1 Material properties

In this work, the two substructures, six links and the auxiliary structure are all made of carbon steel. The most important material properties concerned in this experiment are the density and the Young's modulus.

In order to estimate the accurate material properties, a simple modal test was applied on a small plate, as shown in Fig. 4.8. The important dimensions of this plate are given in Table 4.1. This plate is made of the same material as the test structure. Five single axial accelerometers were placed on this plate and an excitation was applied at location 3 using an impact hammer. The first natural frequency of this small plate was 1257.3 Hz, reading from the measured receptances.

Table 4.1 Important dimensions of the test small plate

	thickness	width	length	diameter of holes
(mm)	9.9	80	200	9

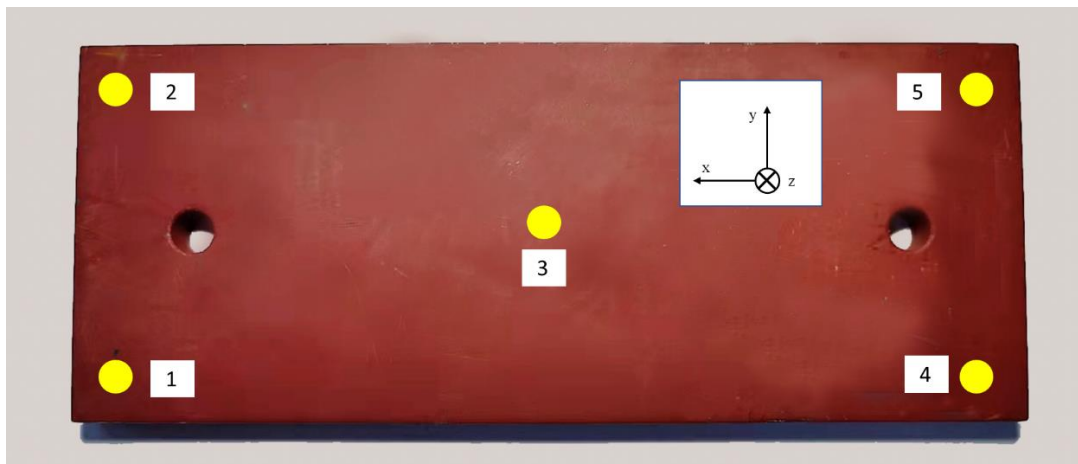


Fig. 4.8 The small plate and sensor locations

The mass of this small plate is 1.214 kg and the volume is calculated as  $1.57 \times 10^{-4} \text{ m}^3$ . So, the density of this material is  $7.73 \times 10^3 \text{ kg/m}^3$ .

A finite element model of this plate, as given in Fig. 4.9, was first established with a material whose Young's modulus is 210 GPa and density is  $7.73 \times 10^3 \text{ kg/m}^3$ . A structural damping was included in this FE model. It was found that the first natural frequency of this plate is 1263.2 Hz from the FE model. Therefore, the Young's



modulus was adjusted to be 208.04 GPa to match the measured data. Fig. 4.10 shows the receptances of this small plate obtained from experiment and updated finite element model. A quite good match can be found from the two receptances.

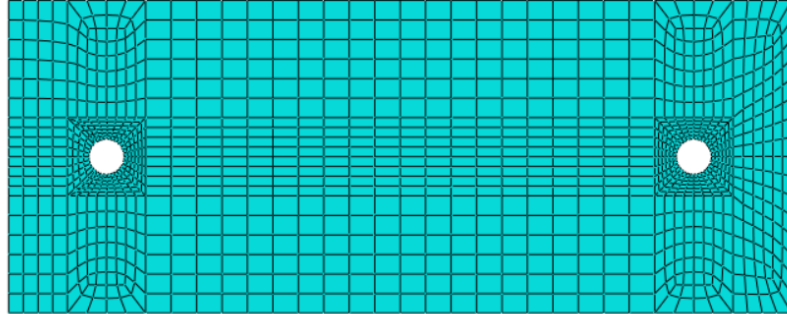


Fig. 4.9 The FE model of the small plate

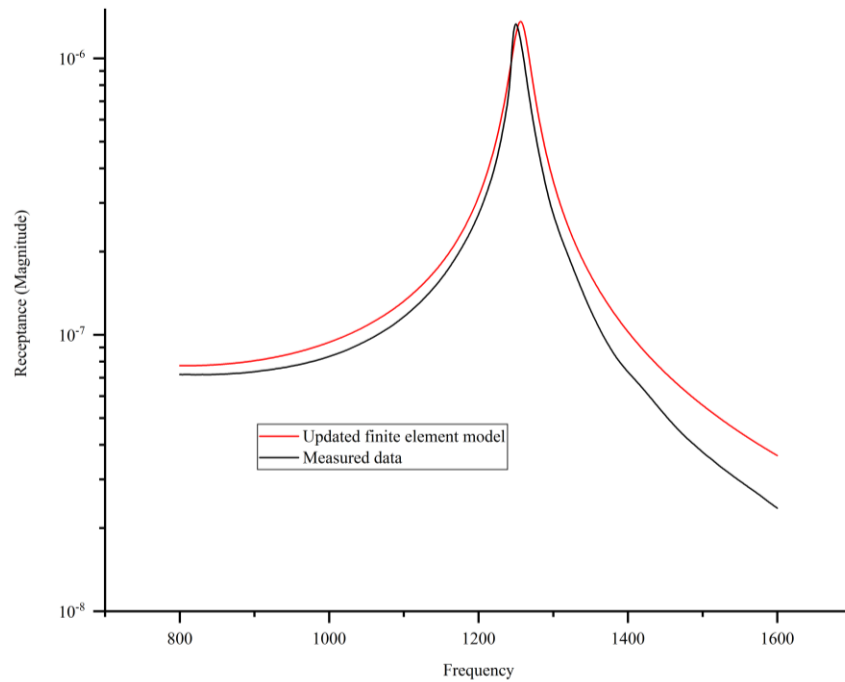


Fig. 4.10 Receptance  $h_{1z3z}$

#### 4.4.2 The auxiliary structure

The auxiliary structure, which was used to help measure the rotational receptances in practice, is shown in Fig. 4.11. This structure includes a square flange and a vertical block. As explained in section 4.3, a finite element model of this auxiliary structure needs to be built.

During the measurement, different excitations were applied on this structure. When an excitation was applied at the centre point of the vertical block, only a translation accelerometer was glued on this structure at the centre point of the vertical block, as shown in Fig. 4.12. If an excitation was applied at the tip of the vertical block, an angular accelerometer was also adopted. To avoid drilling a hole on this auxiliary structure and the test substructures, the angular accelerometer was attached to a ‘cushion’ made of hard plastic by a single socket head cap screw. Then the cushion was glued at the centre point of the vertical block.

The used translational tri-axial accelerometer and angular accelerometer are Brüel & Kjær 4501 and Kistler 8840, weighing 6.5 g and 28.5 g (including the cushion), respectively. And the mass of this auxiliary structure is 318 g. Therefore, the two accelerometers, especially the angular accelerometer, should be included in the FE model of the auxiliary structure.

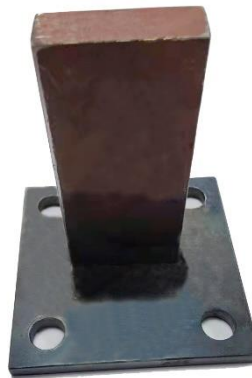


Fig. 4.11 The auxiliary structure



Fig. 4.12 The mounting of this auxiliary structure

(Left: translational accelerometer; Right: translational and angular accelerometers)

A FE model of the auxiliary structure with two accelerometers shown in Fig. 4.13 was built in Abaqus using quadratic hexahedral elements of type C3D20R. The green square spot in the left picture of Fig. 4.13 shows the node with point mass representing translational accelerometers or both the translational and angular accelerometers. The Young's modulus used in this model is 208.04 GPa, the Poisson's ratio is 0.3 and the density is  $7.73 \times 10^3 \text{ kg/m}^3$ .

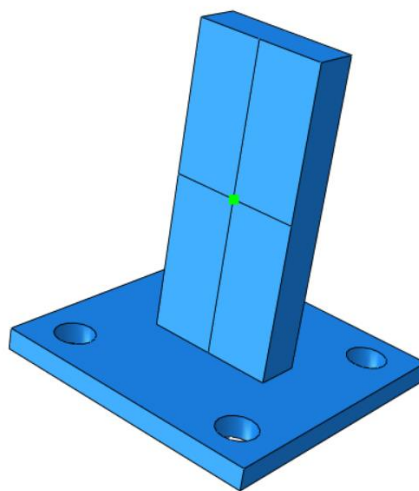


Fig. 4.13 The FE model of the auxiliary structure

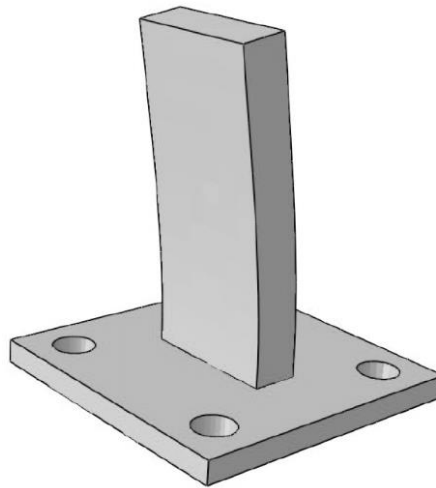


Fig. 4.14 The first mode shape of this auxiliary structure

A modal test was carried out to find the natural frequencies of this auxiliary structure with two accelerometers attached. The measured first flexible natural frequency was 872.9 Hz when the structure is under free-free condition while the first natural frequency from the FE model was 869.8 Hz.

Besides, to minimize the difference between measured receptances and the receptances from the FE model, a structural damping that causes modes to have 2% of damping ratio was considered in this FE model. Fig. 4.15 shows the receptances at the same point from the experiment and the FE model, respectively. It is clear that those two have a good match, which indicates that the FE model is quite accurate.

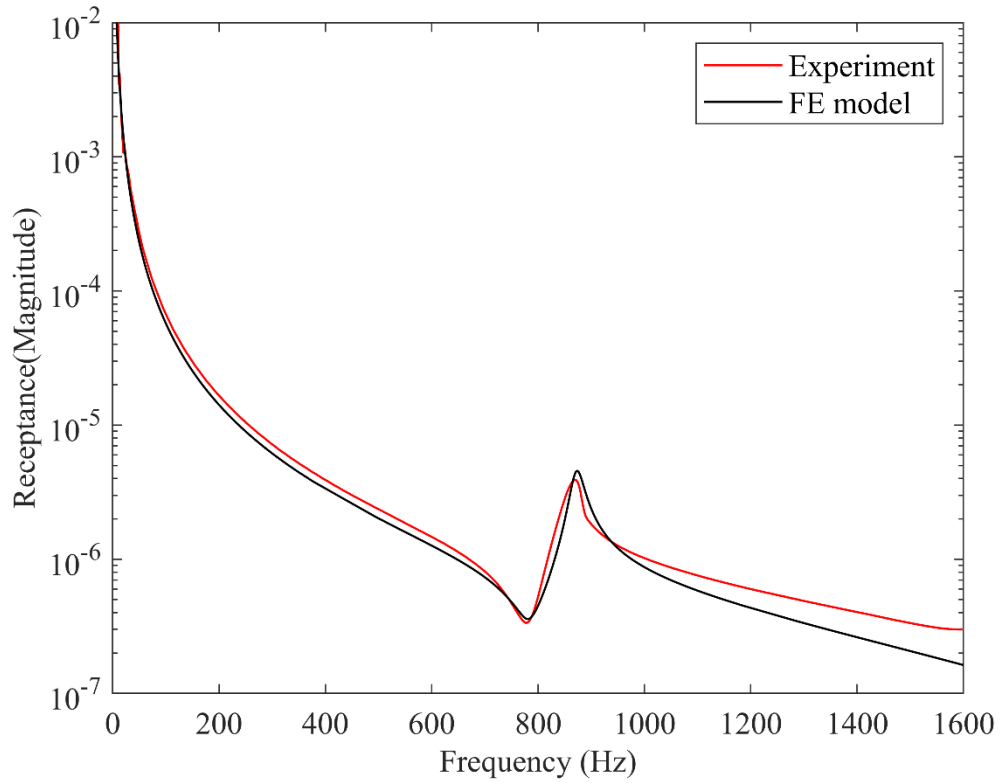


Fig. 4.15 Receptances of the auxiliary structure

### 4.4.3 Links

In this assembled structure, there are 6 links between the two substructures, two identical horizontal links and four identical vertical links. Fig. 4.16 shows a horizontal link and a vertical link. Each link consists of a rectangular tube and two square flanges welded at two ends. The vertical links have the same dimensions as the horizontal links, except that the two horizontal links are shorter than the vertical links. Some important dimensions of the links are given in Table 4.2.

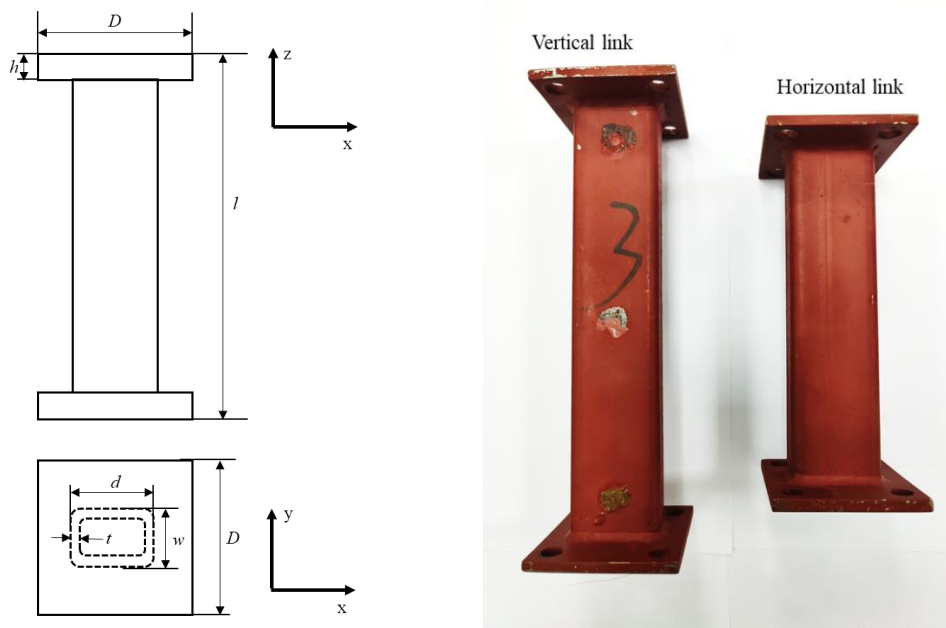


Fig. 4.16 Schematic diagram of the link and the real links

Table 4.2 Some important dimensions of links

	Cross-section			Flange		$l$
	$d$	$w$	$t$	$D$	$h$	
Horizontal links (mm)	40.8	20.5	2.5	64	5	210
Vertical links (mm)	40.8	20.5	2.5	64	5	162

According to the method explained in chapter 3, the FE models of the links are required to achieve frequency assignment. In this work, FE models of the links were built using Abaqus.

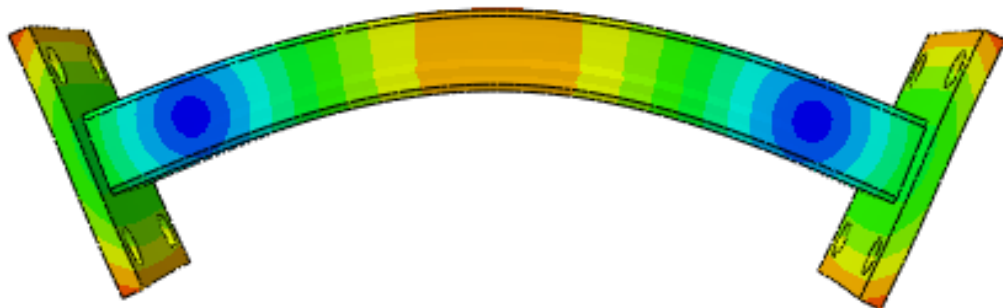


Fig. 4.17 The first mode shape of a vertical link (free-free condition)

First, the detailed FE models of links with solid elements were created and the first mode shape of the link is found to be the bending of the rectangular tube in its local  $y$ - $z$  plane, as pictured in Fig. 4.17. It can be noticed that there is almost no deflection on the two square flanges when only considering those flanges. Therefore, the two square flanges can be modelled as rigid bodies. Please note that because of the frequency range of interest of the assembled structure, only the first bending mode of the links will be involved.

Simple modal tests were conducted to obtain the dynamic behaviours of the links. Three uniaxial accelerometers were attached on the links to measure the natural frequencies of a link, as shown in Fig. 4.18. This link was placed on a cushion of foam such that the link can be considered as being under free-free condition.



Fig. 4.18 Modal test on the link

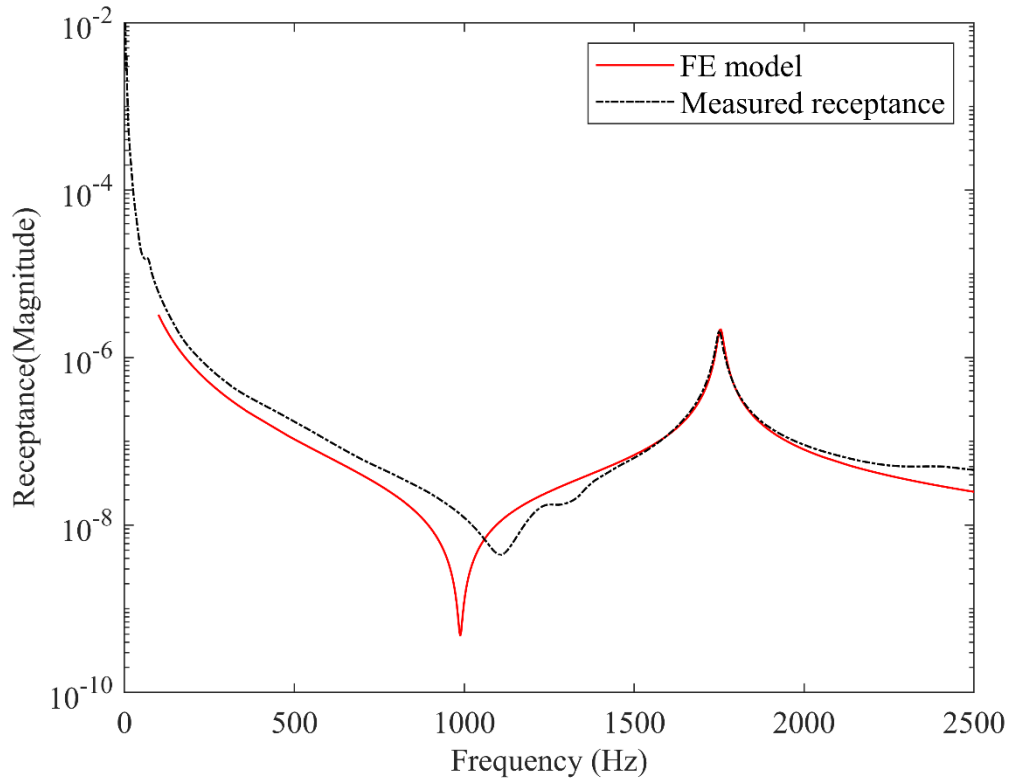


Fig. 4.19 Receptance  $h_{31}$  of a vertical link

Fig. 4.19 shows the receptances obtained from the experiment and the FE model. It is obvious that the receptance from the FE model has a good match with the measured receptance, which indicates that the FE model is accurate enough.

In general, the FE model of a link, although it is much simpler than substructures, may have many degrees of freedom. However, only the degrees of freedom at the connection points are important. Therefore, to save computation time, the internal degrees of freedom can be eliminated by using an efficient tool in Abaqus, *substructure generation*. A reduced model, with much fewer degrees of freedom, can be created by defining the link as a *substructure*.

In this work, the links were only connected with substructures at the two ends. Therefore, the finite element model of the link can be replaced with a reduced model, which has only two retained nodes and all the other nodes have been eliminated before analysis. Each node has 5 degrees of freedom and the dynamic stiffness matrix of each link is a  $10 \times 10$  matrix. One thing that needs attention is that the local coordinate system of each link, as shown in Fig. 4.16, is different from the global coordinate



system defined in substructure S or B. A linear transformation of the dynamic stiffness matrix of the link is needed before it is used in the following calculations.

## **4.5 Experimental results**

Both the substructures and the links were manufactured and modal tests were conducted on the assembled structure and substructures A and B. The natural frequencies of the assembled structure were then used as target values to be assigned using receptance data from the substructures. Application of the method described in chapter 3 was expected to result in the known dimensions of the links.

A general measurement set-up in a modal test should have three parts. The first part is to generate the excitation force and apply it to the test structure. Two most common excitation equipment are shaker and hammer. In this work, due to the lack of suitable shakers, all the experiments were conducted with an impact hammer.

The second part is responsible for measuring and acquiring the response data. Accelerometers are the most common sensors for a modal test, which can measure the acceleration of a test structure. A force transducer is also needed in a modal test. In this work, the force transducer is located at the hammer tip and is compressed when impact is applied to.

The third part provides signal processing capacity to derive FRF data from the measured force and response data.

The equipment used in those experiments were: Brüel & Kjær LAN-XI data acquisition system, impact hammer 8206, triaxial accelerometers 4501, single-axial accelerometers 4533/4534, and angular accelerometer Kistler 8840. Fig. 4.20 shows some of the equipment used in the experiments.



Fig. 4.20 The measurement set-up used in this work

#### 4.5.1 Assembled structure

The test rig in this work is shown in Fig. 4.21. A modal test was conducted to measure the natural frequencies of this assembled structure.

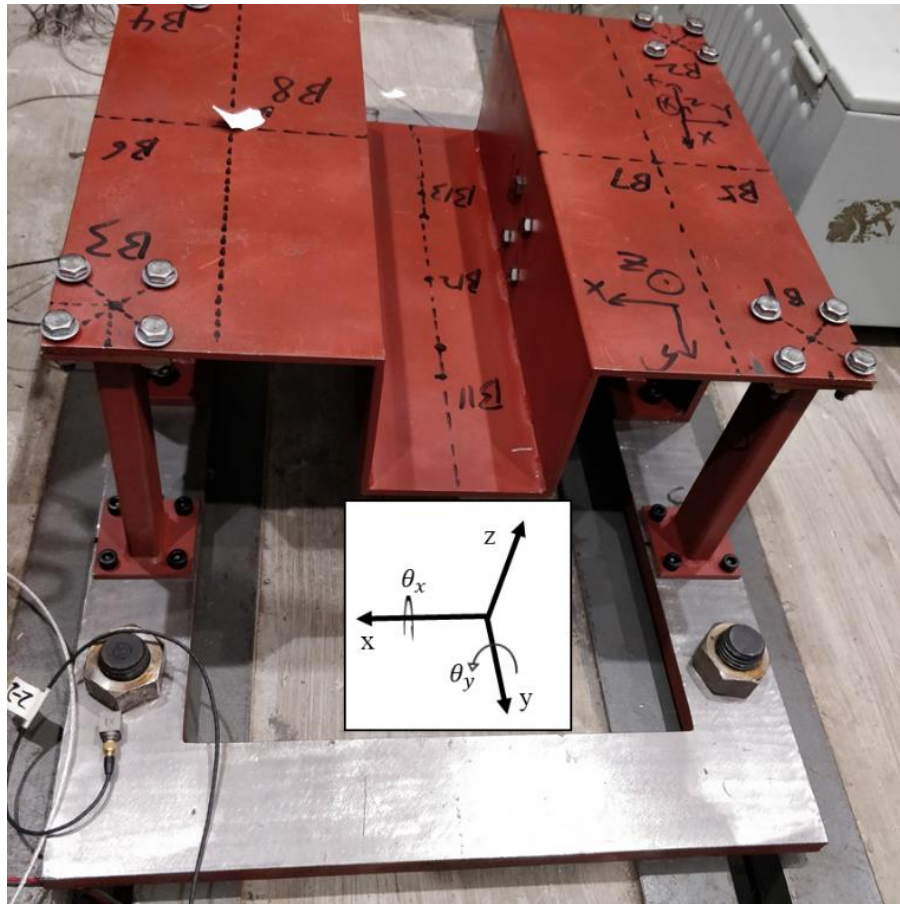


Fig. 4.21 The test rig and measured locations

Six tri-axial accelerometers and two single axial accelerometers were used in this experiment and the locations of these sensors are shown in Fig. 4.22. P3 was symmetric with point P4 with respect to the  $y$ - $z$  plane and P5 was symmetric with point P6 with respect to the  $y$ - $z$  plane.

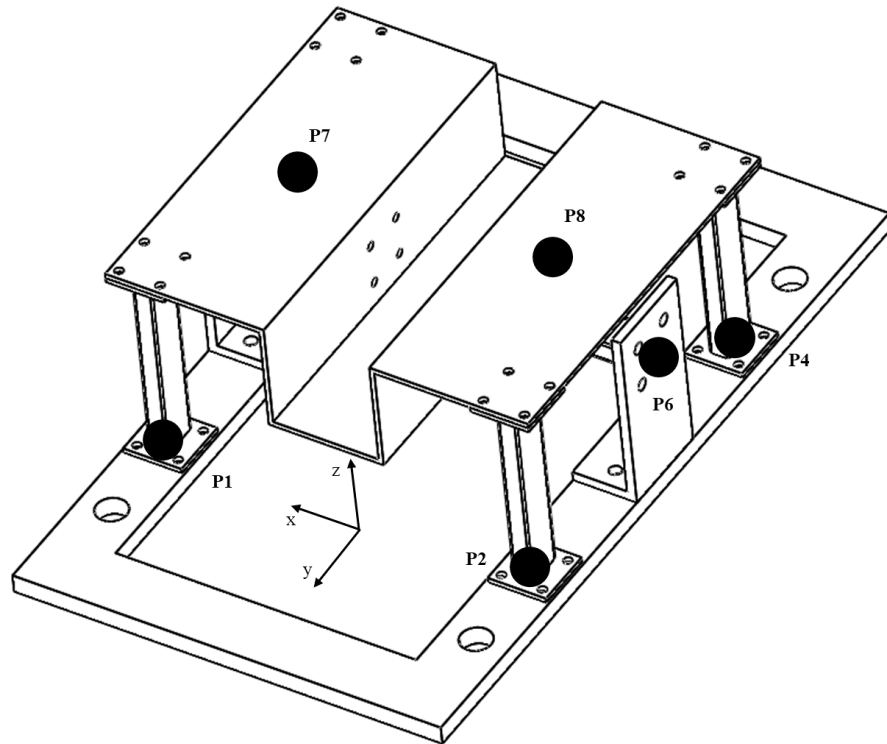
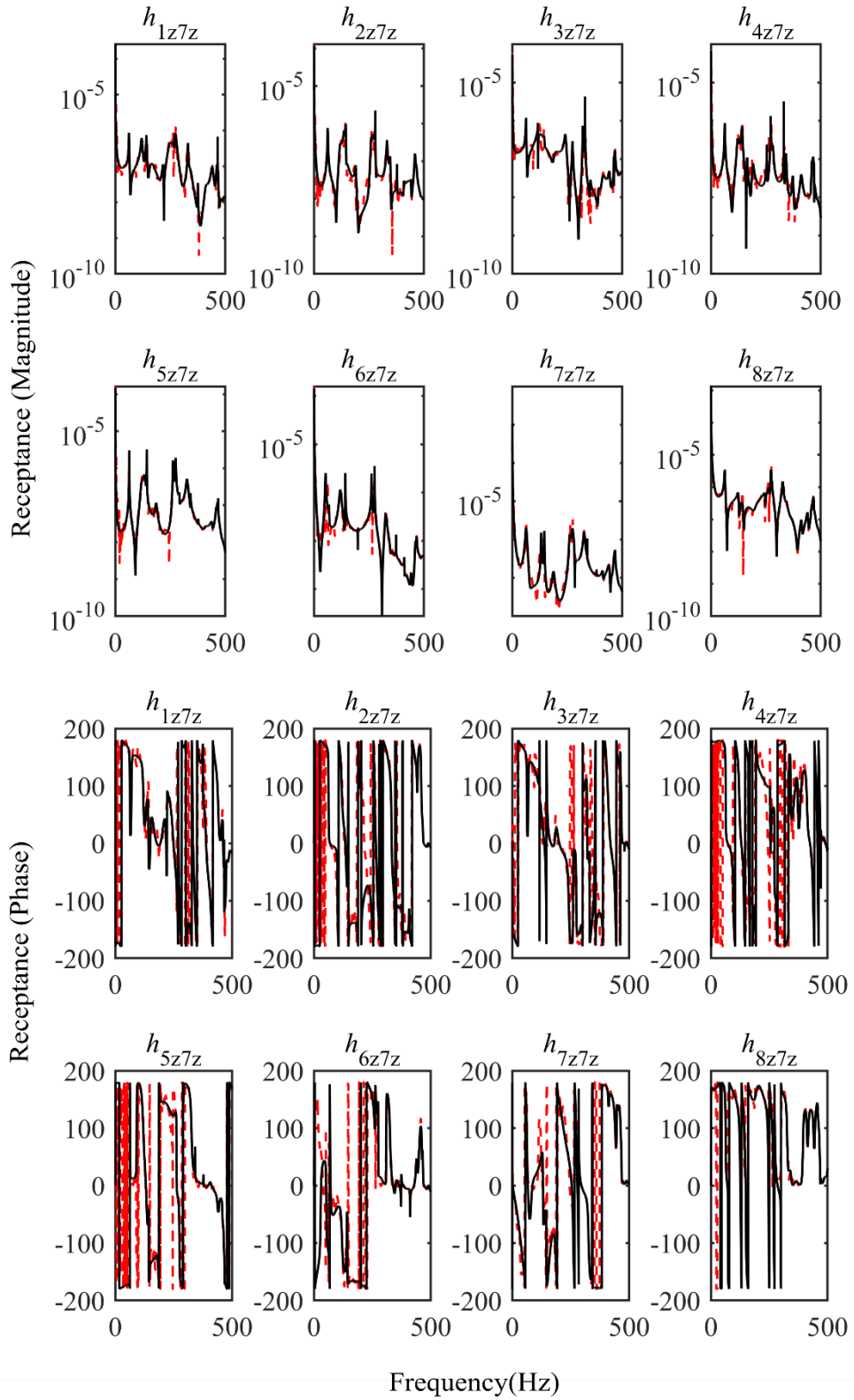


Fig. 4.22 Sensor locations

Two external excitations were applied separately at point P7 along  $-z$  direction and point P6 along  $x$  direction. Fig. 4.23 shows the moduli of some of the measured receptances of the assembled structure. Each receptance was derived from the average of 5 measured FRFs.



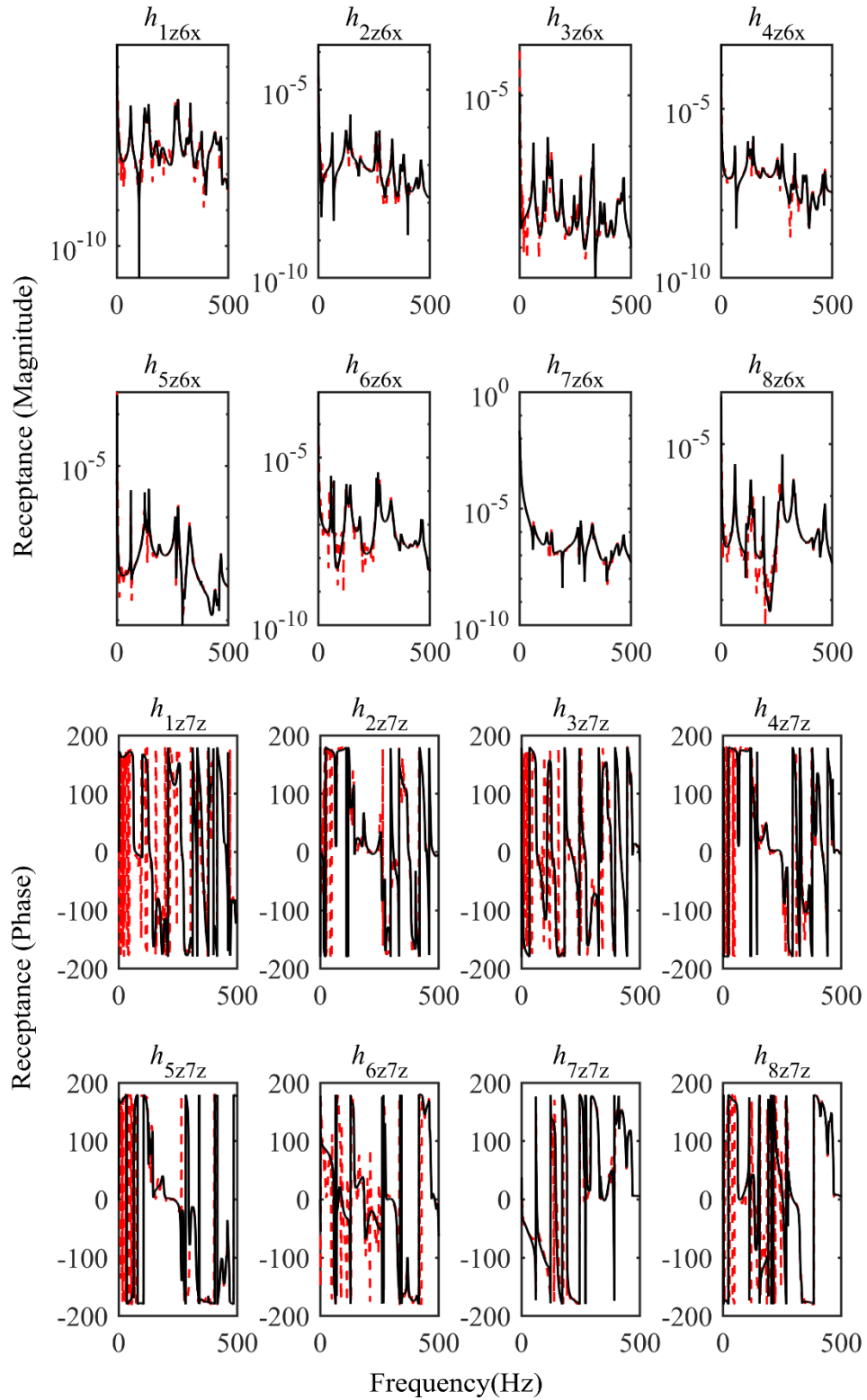


Fig. 4.23 Measured receptances of the assembled structure

The natural frequencies of this assembled structure were read from the measured receptances, as listed in the third row in Table 4.3.

Table 4.3 Natural frequencies of the assembled structure

Mode	1	2	3	4	5	6
FE model (Hz)	68.8	118.9	142.2	195.5	231.4	269.9
Experiment (Hz)	63.3	124.8	142.9	187.5	262.1	274.7

A finite element model of this assembled structure was built in Abaqus in order to have a better understanding on the mode shapes of the assembled structure. The natural frequencies obtained from the FE model are given in the second row in Table 4.3. There are some differences between the natural frequencies from the experiment and the FE model and the differences may come from the way of installation or the weight of bolts and screws. However, this FE model was only used to provide assistance and the requirement on the accuracy of this FE model does not need to be very high. Therefore, the above FE model of the assembled structure was considered good enough in this work. The first 6 FE modes are presented in Fig. 4.24.

From Fig. 4.24, it can be seen, in the first two modes, the deformations of the links are mainly the bending in the  $x$ - $z$  plane. The torsional displacements  $\theta_z$  at the first four connection points (P1, P2, P3 and P4) and the torsional displacements  $\theta_x$  at connection points P5 and P6 can be ignored so as to reduce the number of required receptances. Therefore, to decrease the difficulties in this experimental work, the first two natural frequencies will be used as target natural frequencies in the following assignment.

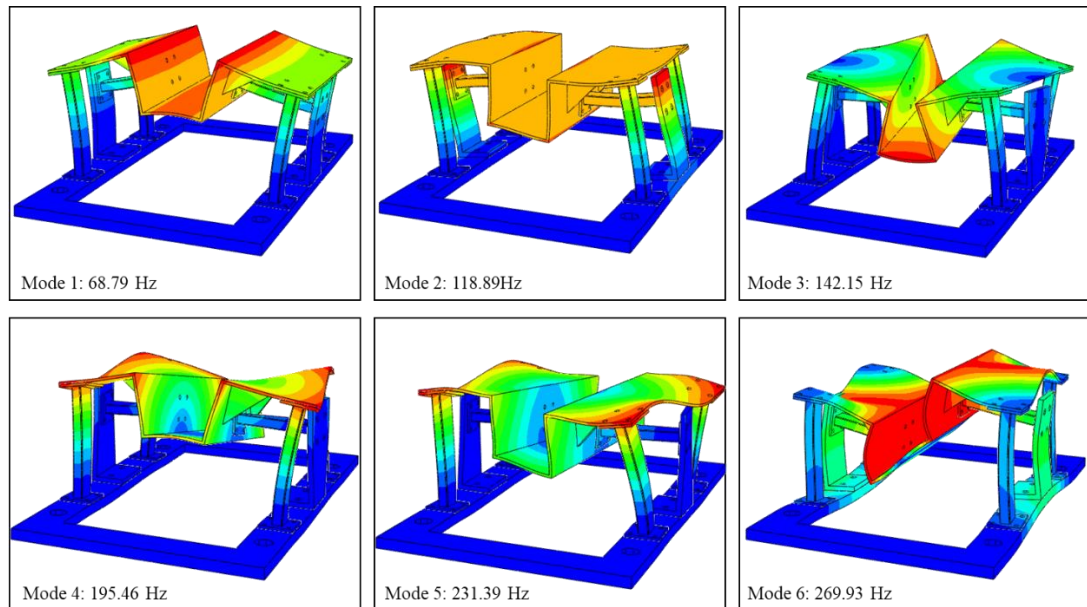


Fig. 4.24 Mode shapes of the assembled structure



#### 4.5.2 Substructure S

Substructure S was bolted on the ground at four locations. If substructure S is directly bolted on the ground, it will be hard to excite the door frame of the structure S. Then the vibrations of the first two or three modes may be only related with the two L-shaped beams. Since the concerned frequencies in this experiment is not high, it is wanted the door frame of substructure S can behave as a flexible structure, instead of a rigid one. Therefore, to decrease the dynamic stiffness of substructure S, three washers were placed between substructure S and the ground, as shown in Fig. 4.25. By doing this, substructure S is supported by four feet and it is easier to excite the door frame of substructure S at low frequencies.

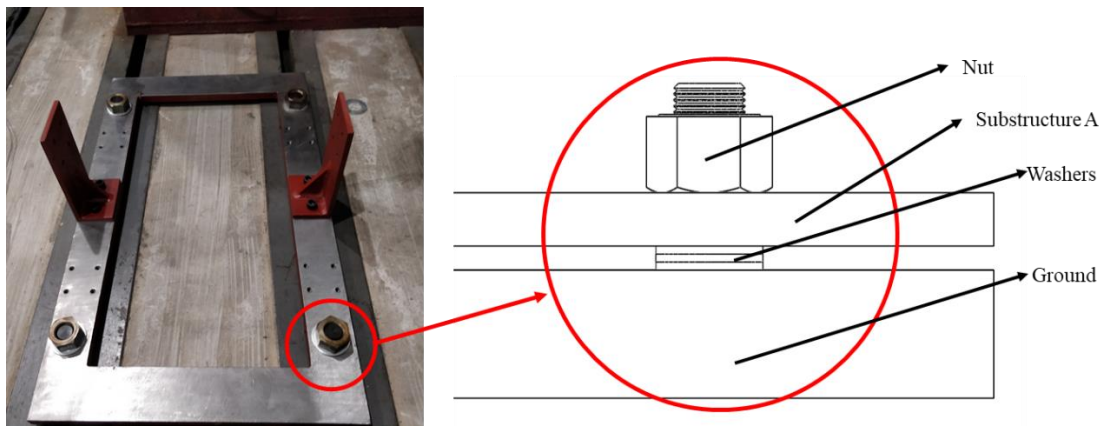


Fig. 4.25 Installation of substructure S



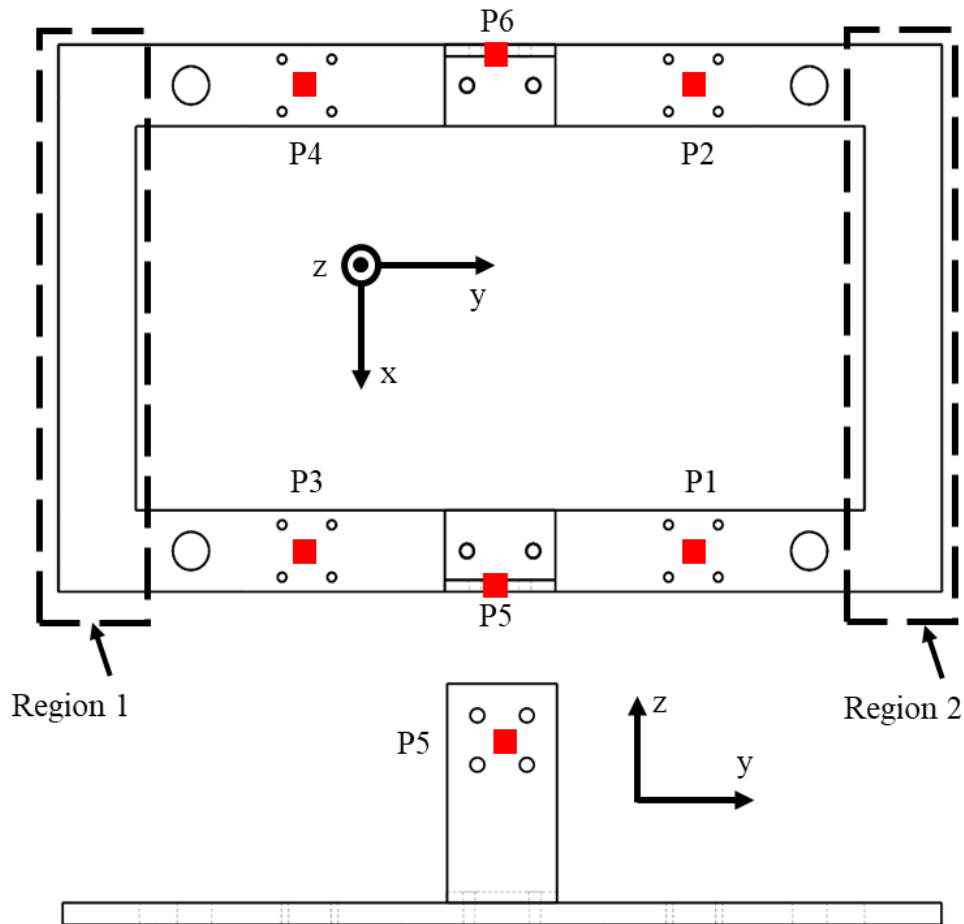
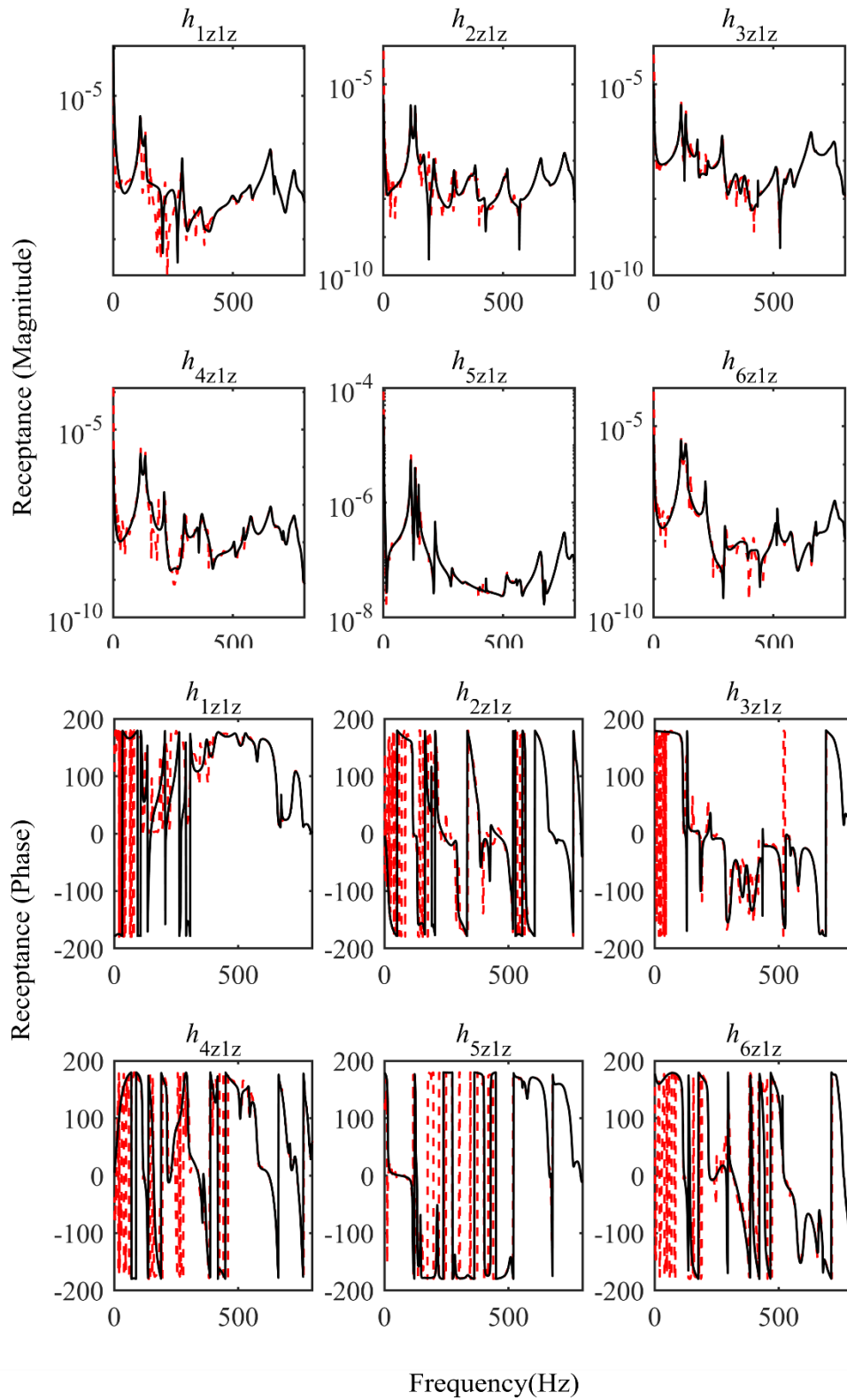


Fig. 4.26 Locations of sensors (red squares) and coordinate system on substructure S

Several tests were conducted to measure all the required receptances. Fig. 4.26 shows the sensor locations and the coordinate system. Each connection point has 5 DoFs. For example, the DoFs at point 1 were denoted as  $(u_{1x}, u_{1y}, u_{1z}, \theta_{1x}, \theta_{1y})$ . The translational receptances were measured directly by applying excitations sequentially at the six points along the  $x$ ,  $y$  and  $z$  axes. However, it should be noted that excitations cannot be applied at the first four points along the  $y$  direction because of physical limitations.

The moduli of a group of measured translational receptances are given in Fig. 4.27. Each receptance was obtained from the average of 5 measurements. Fig. 4.28 shows the coherence coefficients during the measurements.



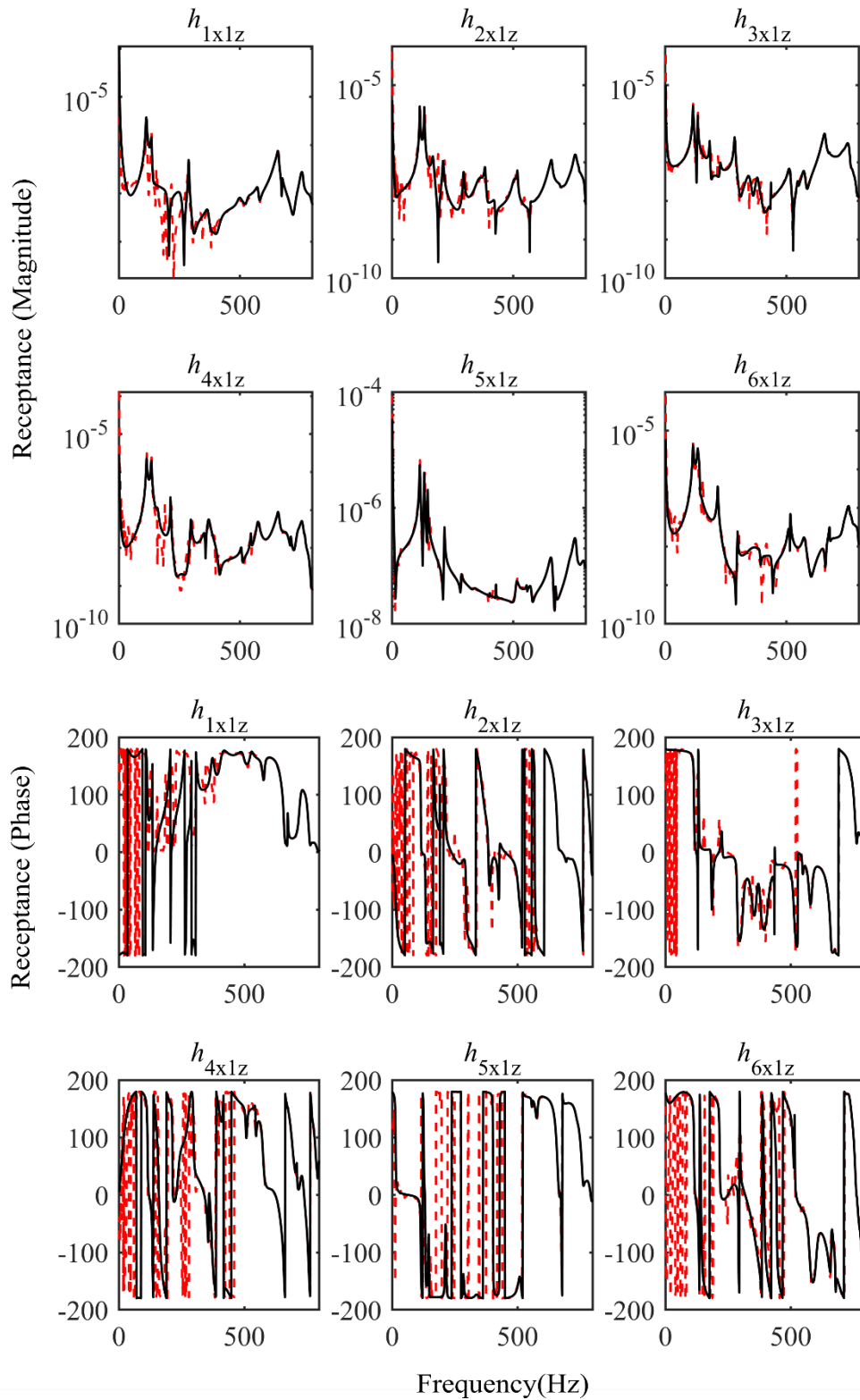


Fig. 4.27 A group of translational receptances  
 (Red dashed lines: measured receptances; black solid lines: fitted receptances)

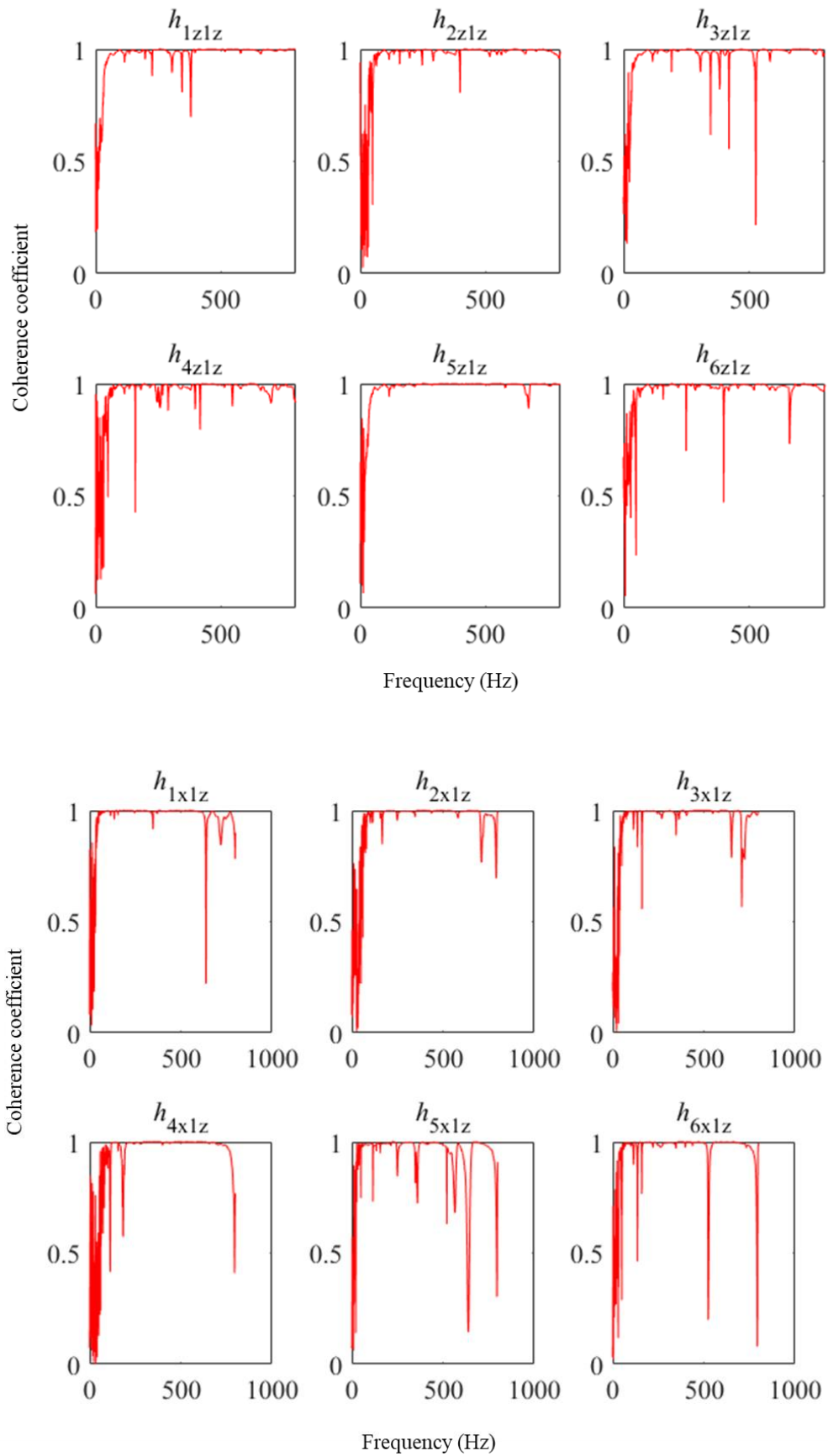


Fig. 4.28 Coherence coefficients

The quality of the measurements could also be assessed by checking the reciprocity of receptances, as shown in Fig. 4.29.

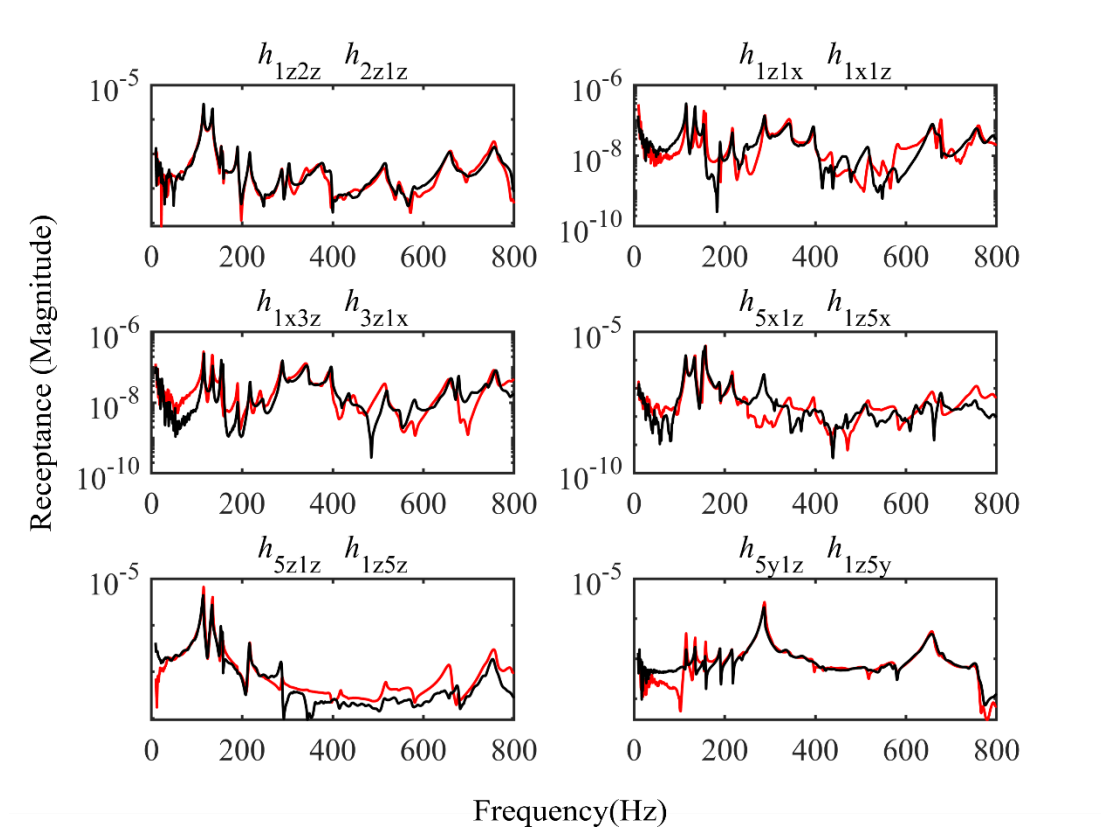


Fig. 4.29 Receptances reciprocity of substructure S

Fig. 4.30 shows a group of measured translational receptances and the results indicate that substructure S has geometrical symmetry with respect to the  $x$ - $z$  plane and  $y$ - $z$  plane, especially when the excitation frequency is smaller than 300 Hz. This property could reduce the efforts when measuring the rotational receptances. Measuring a half of the rotational receptances was enough to get all the required information.

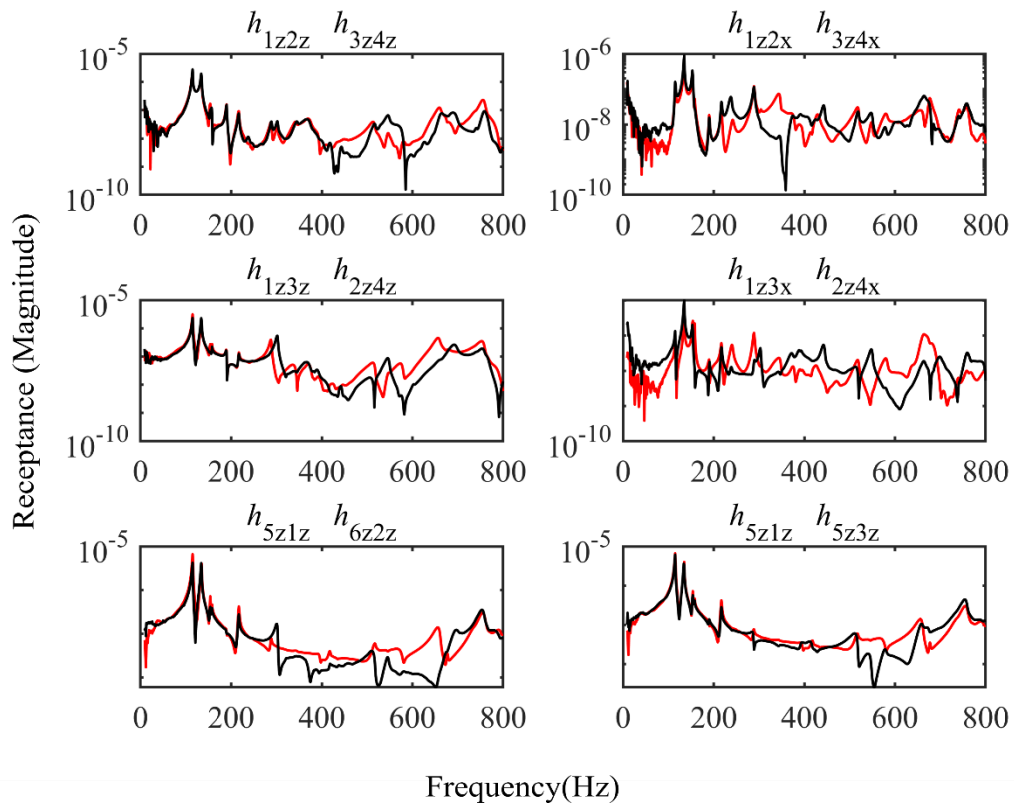


Fig. 4.30 The geometrical symmetry property of substructure S

The rotational receptances were measured with the aid of the auxiliary structure and two angular accelerometers. For example, Fig. 4.31 shows the measurement of the response at DoF  $\theta_{2x}$  when an excitation was applied on point 4.

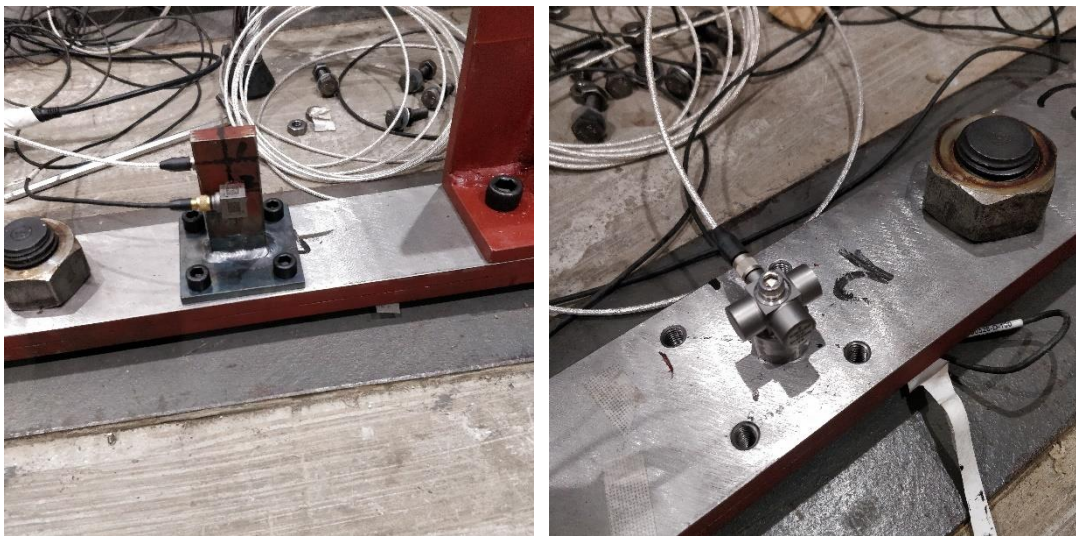


Fig. 4.31 The measurement of rotational receptances

By applying the method explained in section 4.3, the rotational receptances of substructure S at the connection points could be obtained. A part of the measured rotational receptances is given in Fig. 4.32.

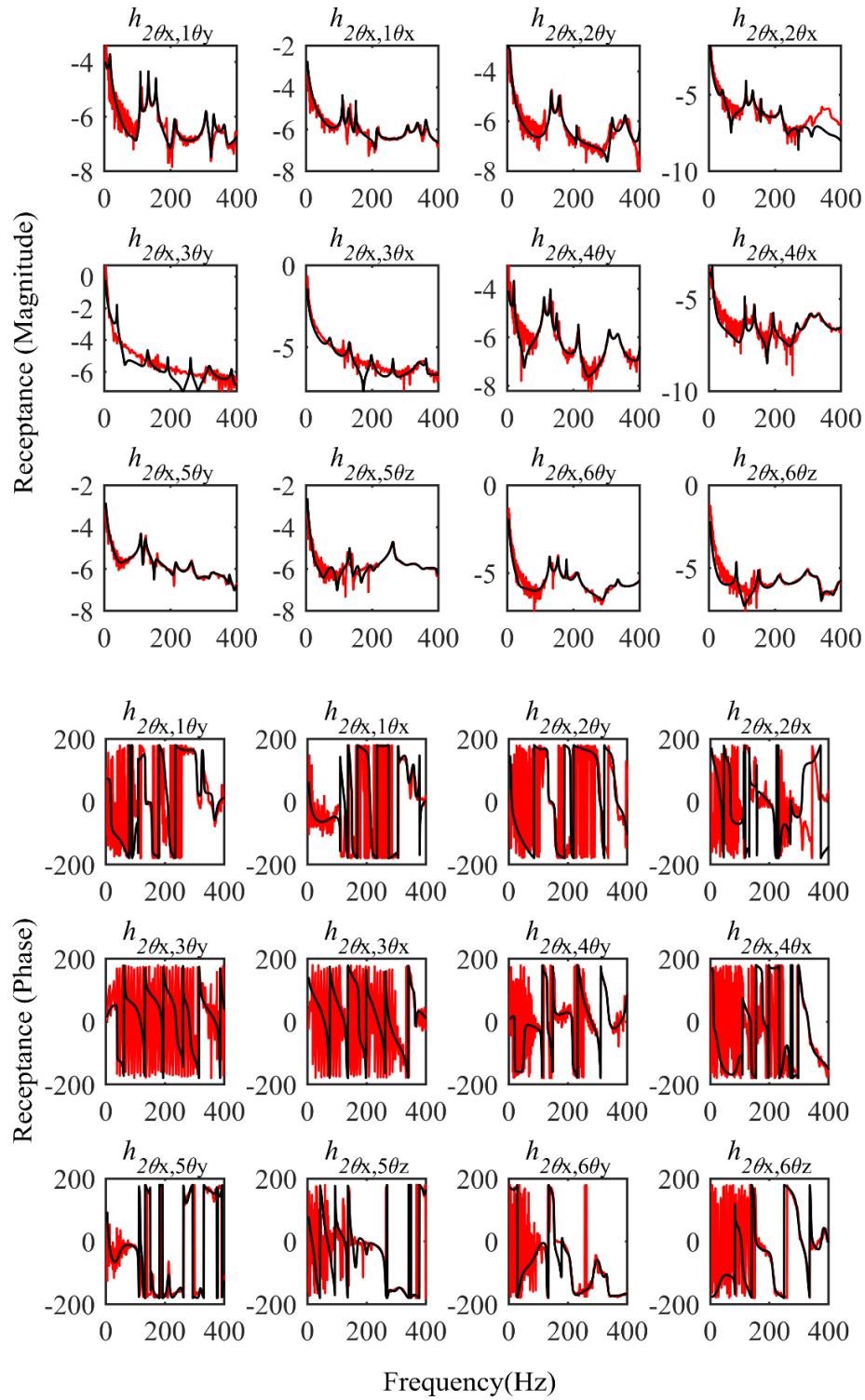


Fig. 4.32 Rotational receptances of substructure S

(Red dash lines: measured receptances; black lines: fitted receptances)



The first six natural frequencies of substructure S read from the measured receptances are listed in Table 4.4. And the first 6 natural frequencies obtained from the finite element model are given in Table 4.5. The mode shapes corresponding to the first 6 natural frequencies from the FE model are presented in Fig. 4.33.

Table 4.4 First six natural frequencies of substructure S (Experiment)

Mode	1	2	3	4	5	6
Frequency (Hz)	38.9	114.8	135.8	153.4	189.1	214.8

Table 4.5 First six natural frequencies of substructure S (Finite element model)

Mode	1	2	3	4	5	6
Frequency (Hz)	35.6	60.45	118.7	149.4	159.46	169.39

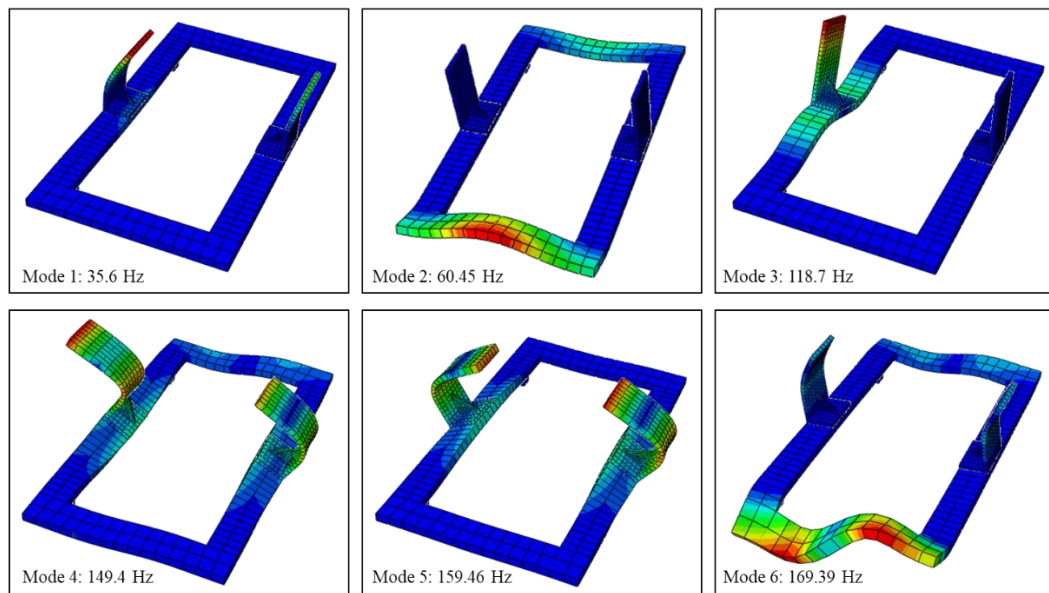


Fig. 4.33 Mode shapes of substructure S

It can be noticed that the second natural frequency from the FE model was not obtained from the measured data. This is because the mode shape of the second natural frequency in the FE model is mainly related with the short beams of the door frame. Those regions were denoted as region 1 and region 2 in Fig. 4.26. During the experiment, no sensor was placed in those regions. Therefore, this mode cannot be observed from the measured data. However, this missing mode shape will not affect



the frequency assignment of the assembled structure in the following procedure because the receptance method does not rely on the modal information.

### 4.5.3 Substructure B

In the assembled structure, substructure B is not connected with any other structures except those links, so the receptances of substructure B should be measured under free-free condition. In this experiment, substructure B was hanged on a heavy rigid structure using four relatively soft springs and ropes at four corners, as shown in Fig. 4.34.



Fig. 4.34 Substructure B under free-free condition

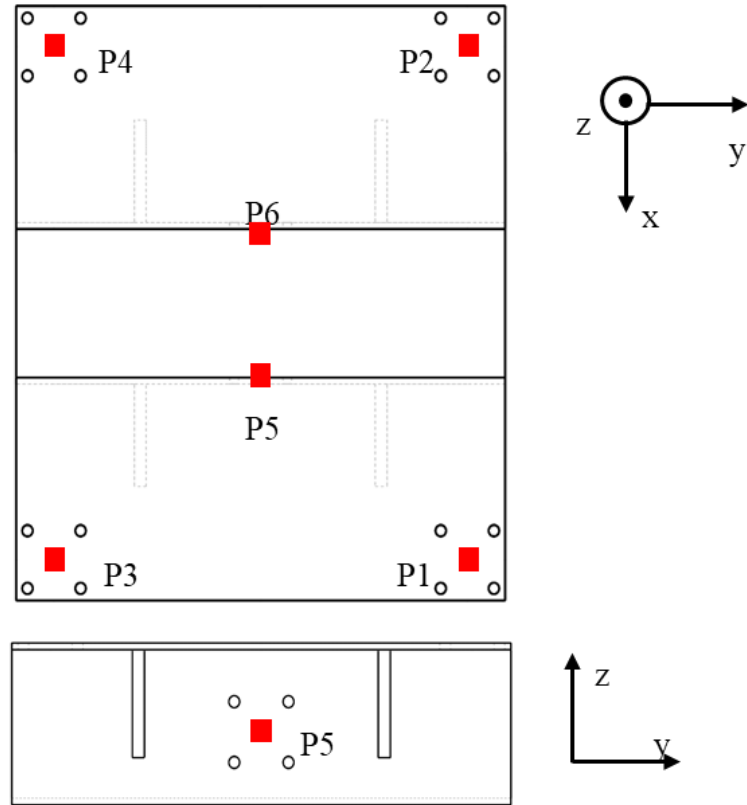


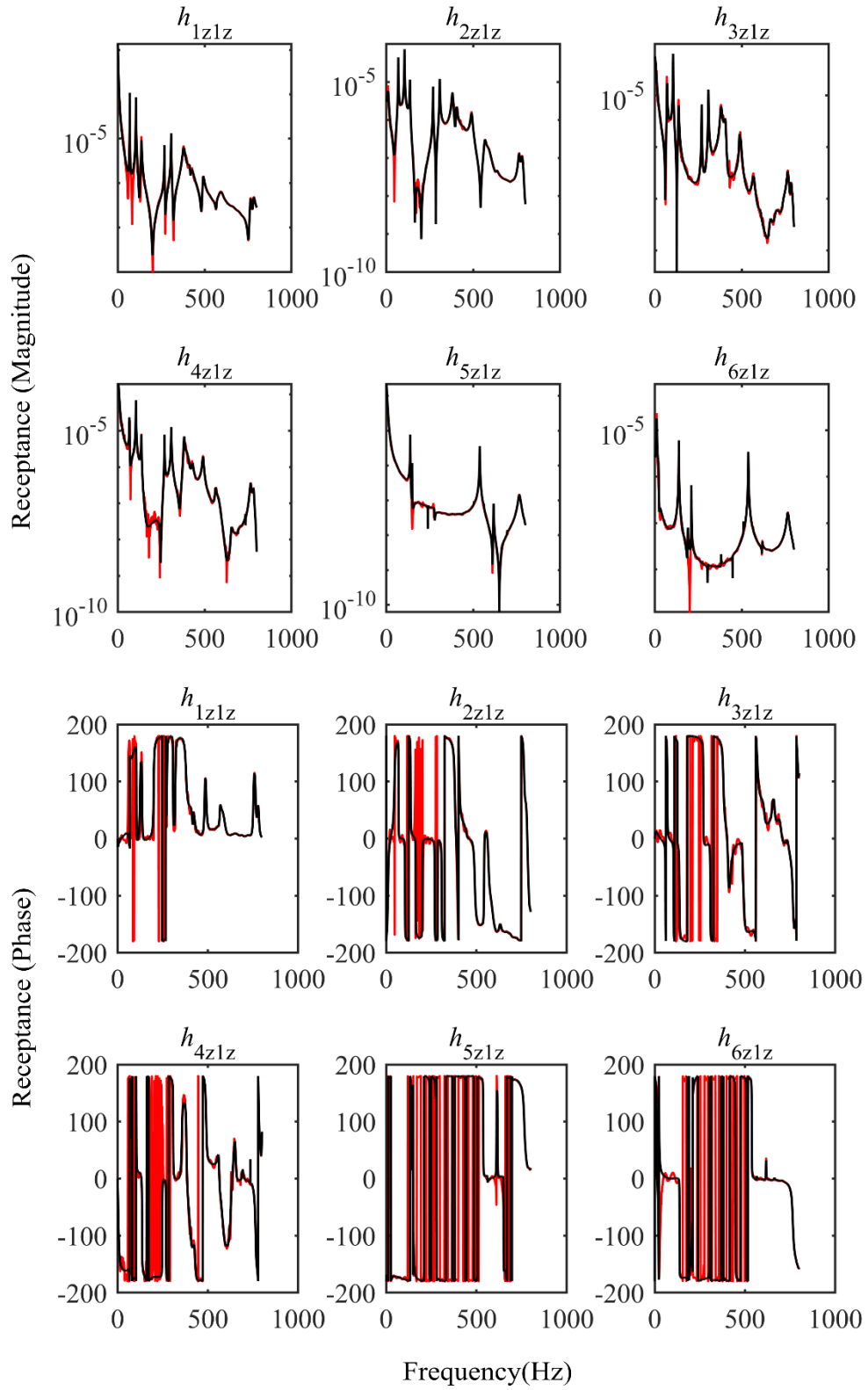
Fig. 4.35 Sensor locations and coordinate system

The stiffness of each spring in Fig. 4.34 is around 1.5 kN/m and the weight of substructure B is 11.2 kg. Therefore, in theory, the natural frequency of the ‘rigid-body’ mode of substructure B would be

$$\frac{1}{2\pi} \sqrt{\frac{k}{m}} = \frac{1}{2\pi} \sqrt{\frac{6000}{11.2}} \approx 3.68 \text{ Hz} \quad (4.14)$$

Fig. 4.35 shows the coordinate system and the measured points. Each point has 5 DoFs,  $(u_x, u_y, u_z, \theta_x, \theta_y)$  for the first four points and  $(u_x, u_y, u_z, \theta_y, \theta_z)$  for points P5 and P6. Again, at first, the translational receptances were measured using an impact hammer and accelerometers, while excitations cannot be applied at points 5 and 6 along the y direction due to physical limitations.

The moduli of part of the translational receptances of substructure B at the connection points are given in Fig. 4.36.



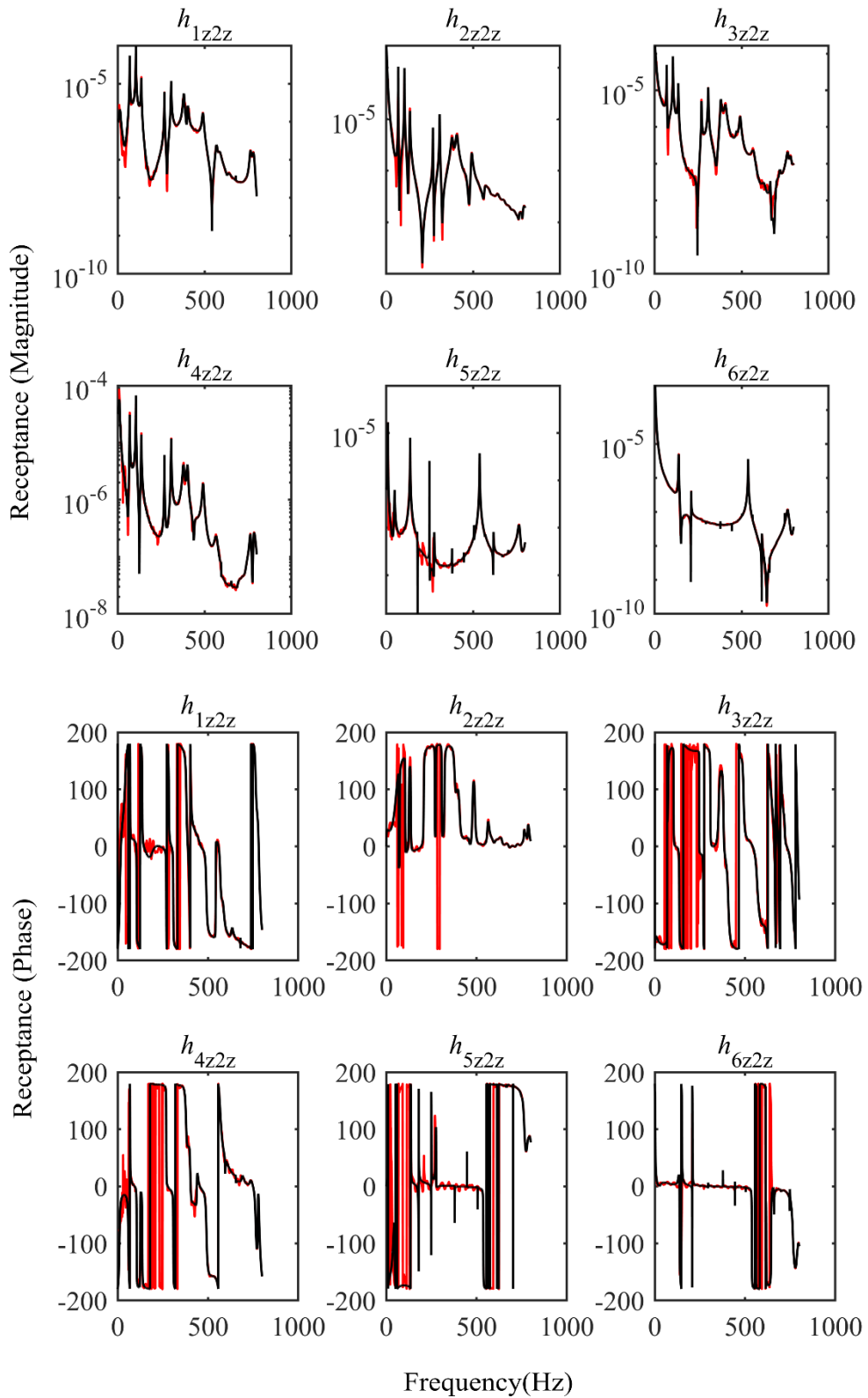


Fig. 4.36 Part of measured translation receptances of substructure B (Red dash lines: measured receptances; black lines: fitted receptances)

It should be mentioned, as shown in Fig. 4.37, that the measured receptance has a peak at 3 Hz, at which substructure B behaves like a rigid body, as expected. Therefore, it is reasonable to assume substructure B in this experiment is under free-free condition.

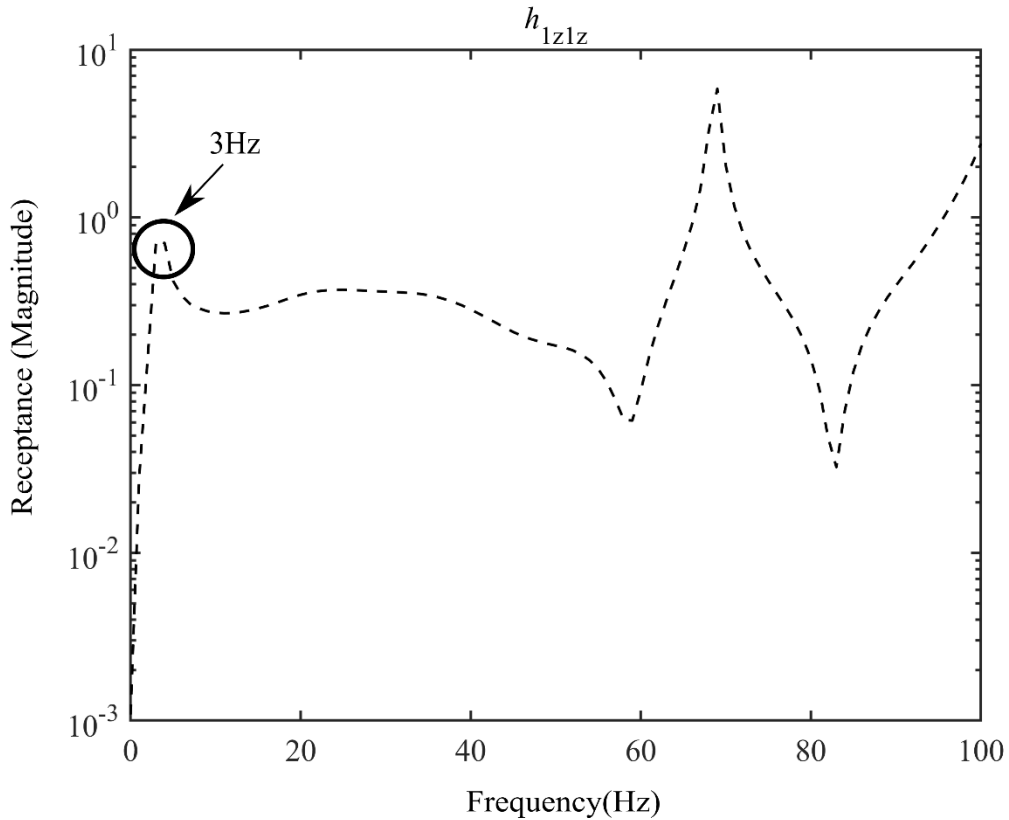


Fig. 4.37 Rigid body mode

Similarly, the quality of the measurements could be validated by checking their reciprocities, as shown in Fig. 4.38. And the geometrical symmetry of substructure B could also be seen from the measured receptances, as presented in Fig. 4.39.

The rotational receptances of substructure B at the connection points were measured by applying the method in section 4.3. Fig. 4.40 shows some of the measured rotational receptances of substructure B.

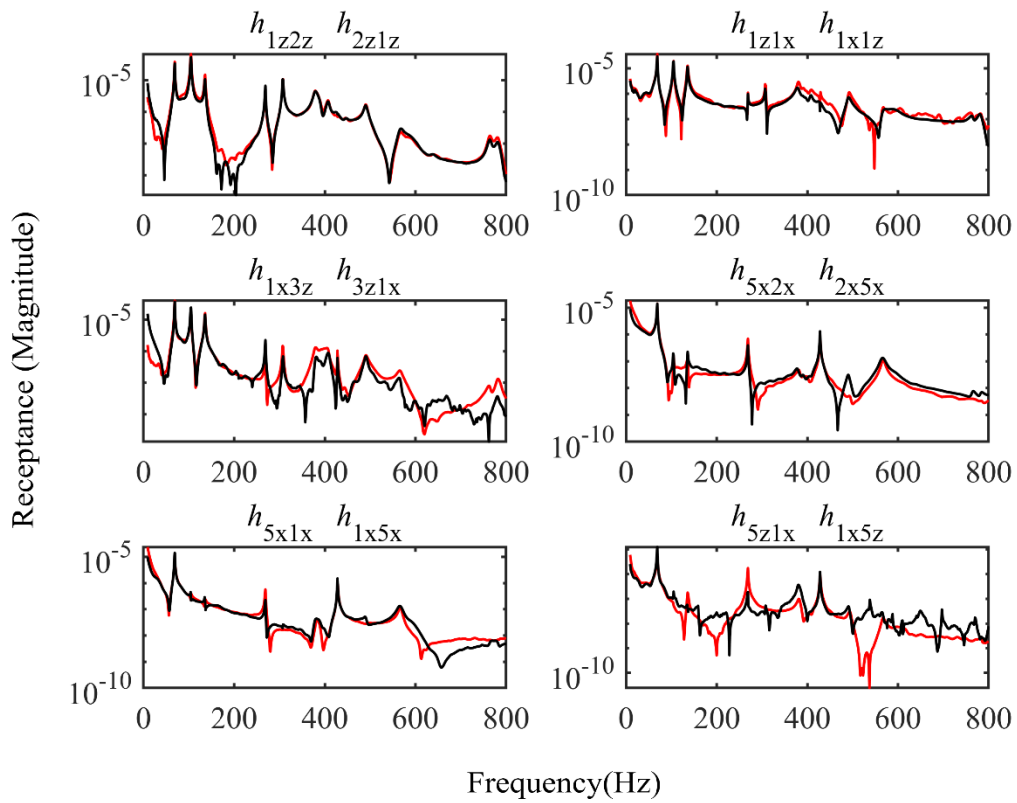


Fig. 4.38 Receptances reciprocity of substructure B

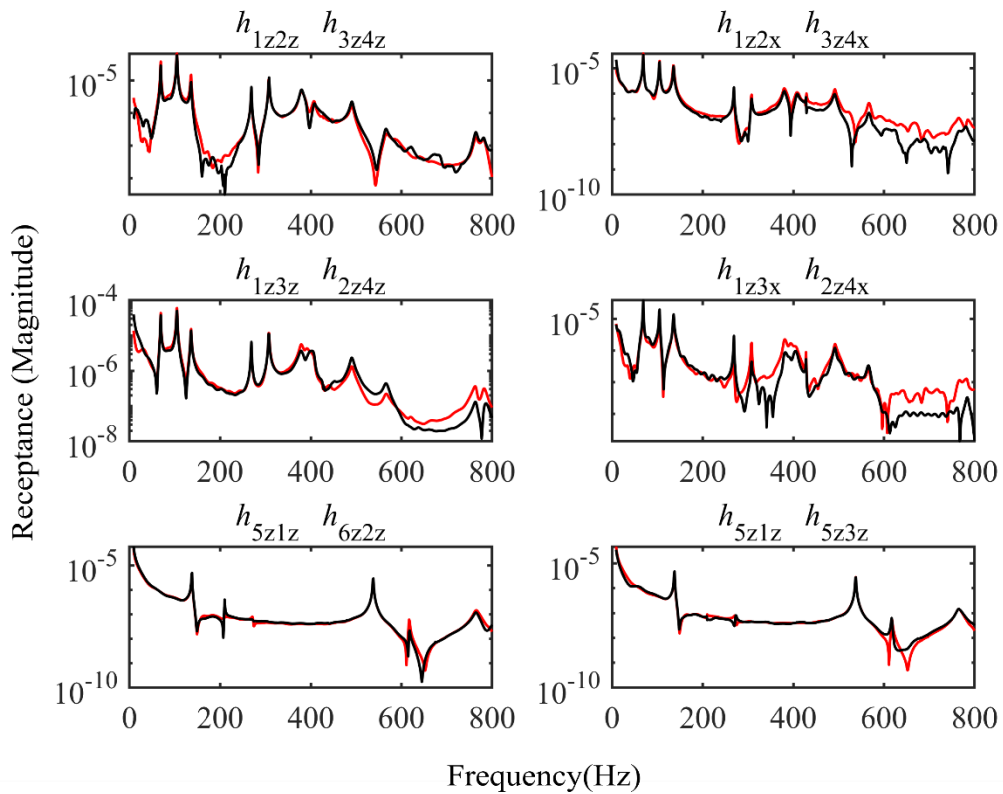


Fig. 4.39 The geometrical symmetry property of substructure B

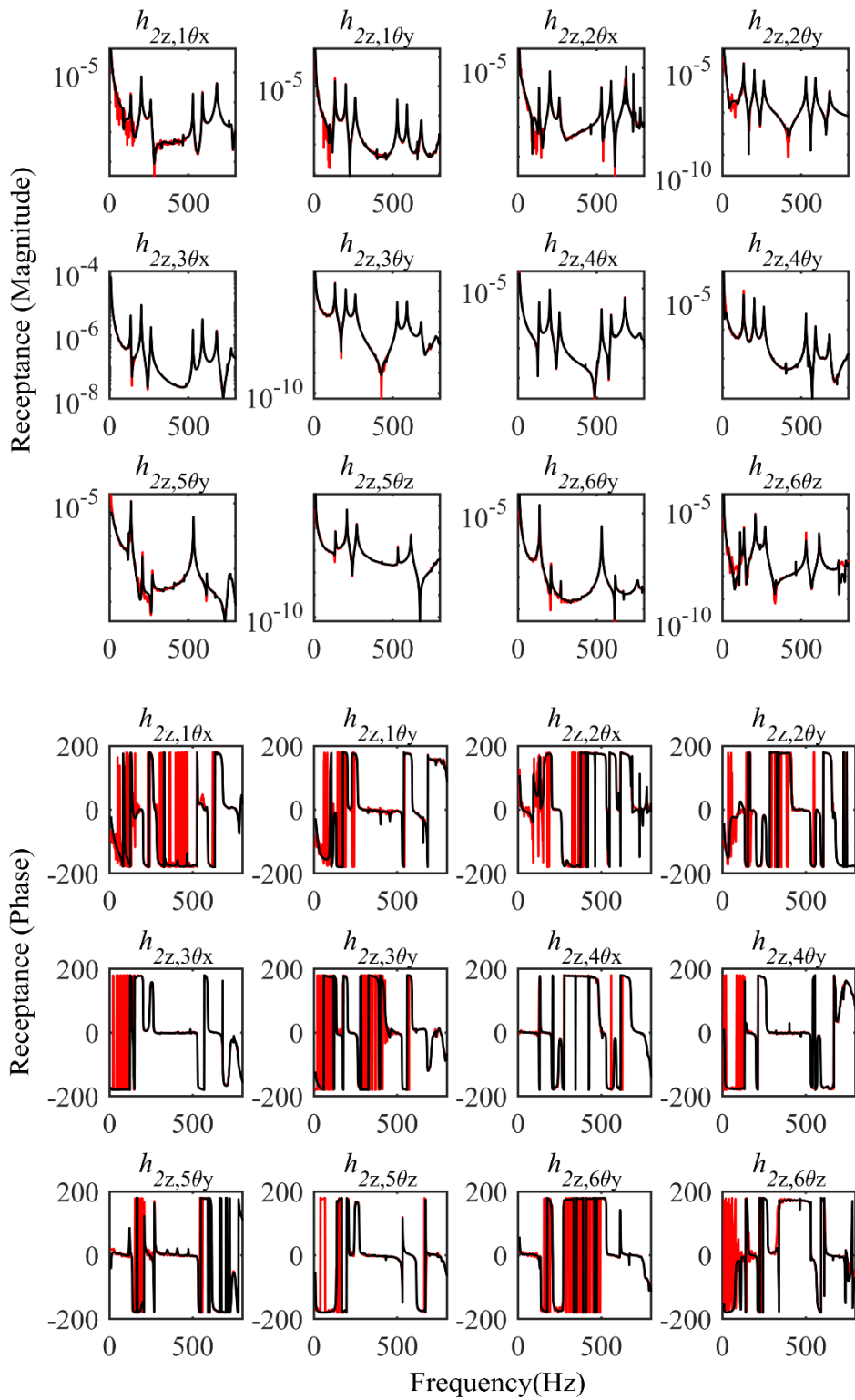


Fig. 4.40 Some rotational receptances of substructure B

(Red dashed lines: measured receptances; black solid lines: fitted receptances)

Since angular accelerometers are available in this experiment, it should be noticed that some of the rotational-related receptances, which could be formulated as

$$h_{rt} = \frac{\text{angular displacement}}{\text{force excitation}}$$

can be measured without the using of the auxiliary structure. According to the reciprocity of receptance matrix, the following formulation is obtained

$$h_{rt} = h_{tr} = \frac{\text{translational displacement}}{\text{moment excitation}}$$

As introduced in section 4.3, the receptances  $h_{tr}$  can be measured with the help of the auxiliary structure. In this experiment, the above mentioned two groups of receptances are measured with two approaches. And it is able to check the quality of the rotational estimation method described in section 4.3. Fig. 4.41 shows the comparison between the measured receptances with or without the auxiliary structure. It can be seen that the two approaches are quite close.

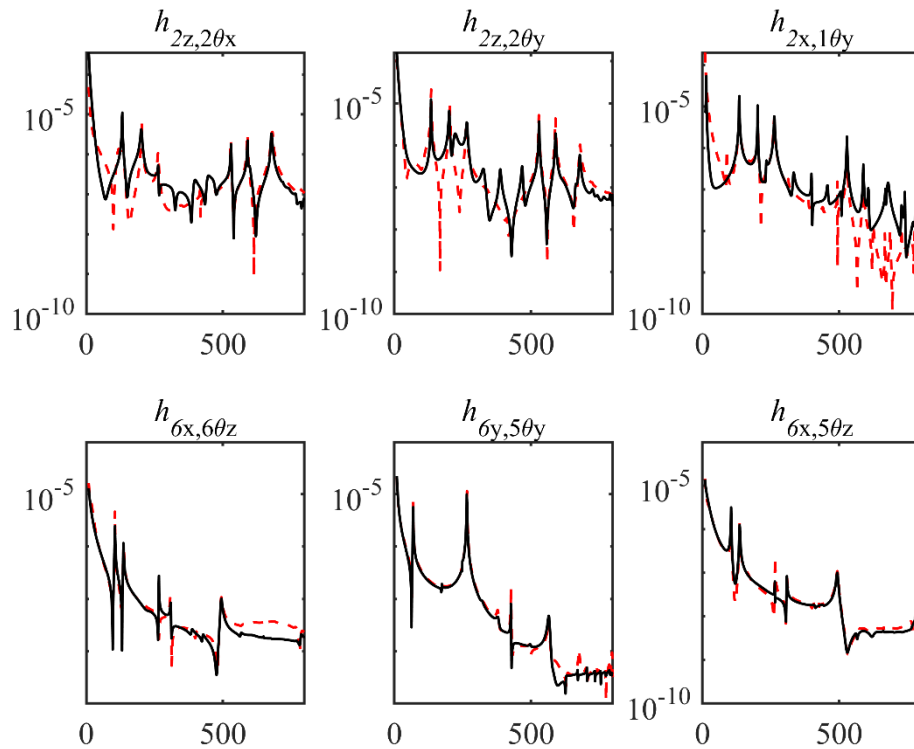


Fig. 4.41 The comparison of measured receptances using two approaches

(Red dash line:  $h_{tr}$ , black line:  $h_{rt}$ )



The natural frequencies of substructure B, obtained from the FE model and the measured receptances, are listed in Table 4.6, with the corresponding mode shapes depicted in Fig. 4.42.

Table 4.6 The first 5 natural frequencies of substructure B

Mode	1	2	3	4	5
FE model (Hz)	69.7	104.7	127.2	216.1	262.9
Experiment (Hz)	69.3	105.6	135.9	210.8	269.8

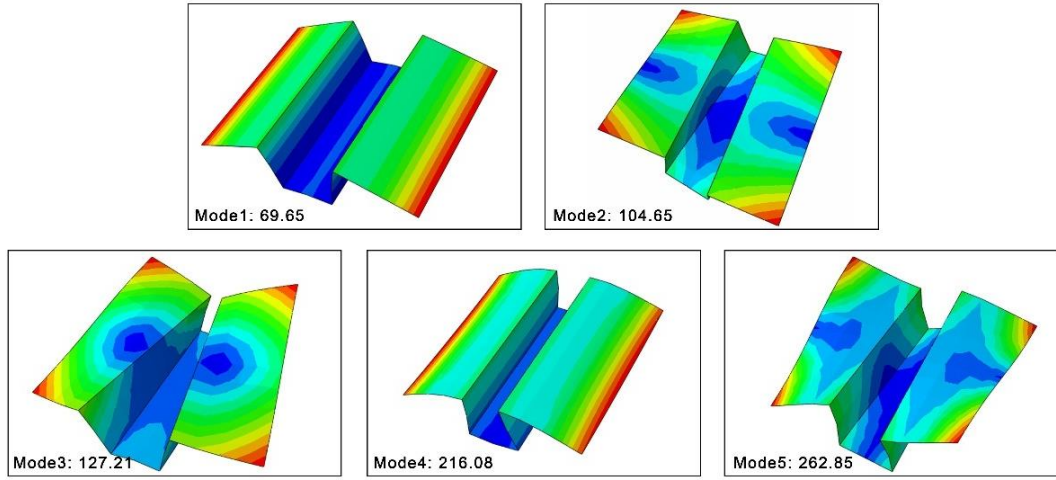


Fig. 4.42 The first 5 mode shapes of substructure B

## 4.6 Frequency assignment

Based on the theory in chapter 3, the frequency assignment of an assembled structure with  $n_L$  links, can be achieved by solving the following optimization problem

$$\min \sum_{i=1}^{n_d} \varepsilon_i |\det(\tilde{\mathbf{I}}_s + \tilde{\mathbf{H}}_s(\omega_i) \Delta \tilde{\mathbf{Z}}_s(\omega_i, \boldsymbol{\gamma}))| \quad (4.15)$$

where  $n_d$  is the number of desired frequencies,  $\varepsilon_i$  is a weighting coefficient for  $i$ th desired natural frequency and  $\boldsymbol{\gamma}$  represents the design variables.  $\tilde{\mathbf{H}}_s(\omega_i)$  is a receptance-related matrix and is constructed using the measured receptances at the connection points.  $\Delta \tilde{\mathbf{Z}}_s(\omega_i)$  is a matrix which contains the dynamic stiffness matrices of all the links.

$$\tilde{\mathbf{H}}_s(\omega_i) = \begin{bmatrix} \tilde{\mathbf{H}}_{L_1L_1} & \tilde{\mathbf{H}}_{L_1L_2} & \cdots & \tilde{\mathbf{H}}_{L_1L_{n_L}} \\ \tilde{\mathbf{H}}_{L_2L_1} & \tilde{\mathbf{H}}_{L_2L_2} & \cdots & \tilde{\mathbf{H}}_{L_2L_{n_L}} \\ \vdots & \vdots & \ddots & \vdots \\ \tilde{\mathbf{H}}_{L_{n_L}L_1} & \tilde{\mathbf{H}}_{L_{n_L}L_2} & \cdots & \tilde{\mathbf{H}}_{L_{n_L}L_{n_L}} \end{bmatrix}, \quad \Delta\tilde{\mathbf{Z}}_s(\omega_i, \boldsymbol{\gamma}) = \begin{bmatrix} \mathbf{Z}^{L_1} & \mathbf{0} & \cdots & \mathbf{0} \\ \mathbf{0} & \mathbf{Z}^{L_2} & \cdots & \mathbf{0} \\ \vdots & \vdots & \ddots & \vdots \\ \mathbf{0} & \mathbf{0} & \cdots & \mathbf{Z}^{L_{n_L}} \end{bmatrix}$$

However, due to the nonlinearity of the objective function in Eq. (4.15)  $[\det(\tilde{\mathbf{I}}_s + \tilde{\mathbf{H}}_s(\omega_i)\Delta\tilde{\mathbf{Z}}_s(\omega_i, \boldsymbol{\gamma}))]$ , its value can vary drastically, especially when the desired natural frequency is high or the number of DoFs is big. Therefore, a variant equation of Eq. (4.15), which is numerically better conditioned for optimization algorithms, is adopted.

$$\min \sum_{i=1}^{n_d} \varepsilon_i \log_{10} \left| \det \left( \tilde{\mathbf{I}}_s + \tilde{\mathbf{H}}_s(\omega_i)\Delta\tilde{\mathbf{Z}}_s(\omega_i, \boldsymbol{\gamma}) \right) \right| \quad (4.16)$$

In this experiment, all six links have the same cross sections. The design variables in this optimization problem are the geometrical dimensions of the cross section, as shown in Fig. 4.16.

#### 4.6.1 Assignment of one natural frequency

The first natural frequency of the assembled structure of 63.3 Hz is the target frequency in this subsection. The design variable is the thickness  $t$  and the other dimensions of the cross section are assumed to be known. The goal is to find  $t$  that minimizes Eq. (4.16) when  $\omega = 2\pi \times 63.3$  rad/s. The physical constraint of the thickness was defined as  $1\text{mm} \leq t \leq 4\text{mm}$ .

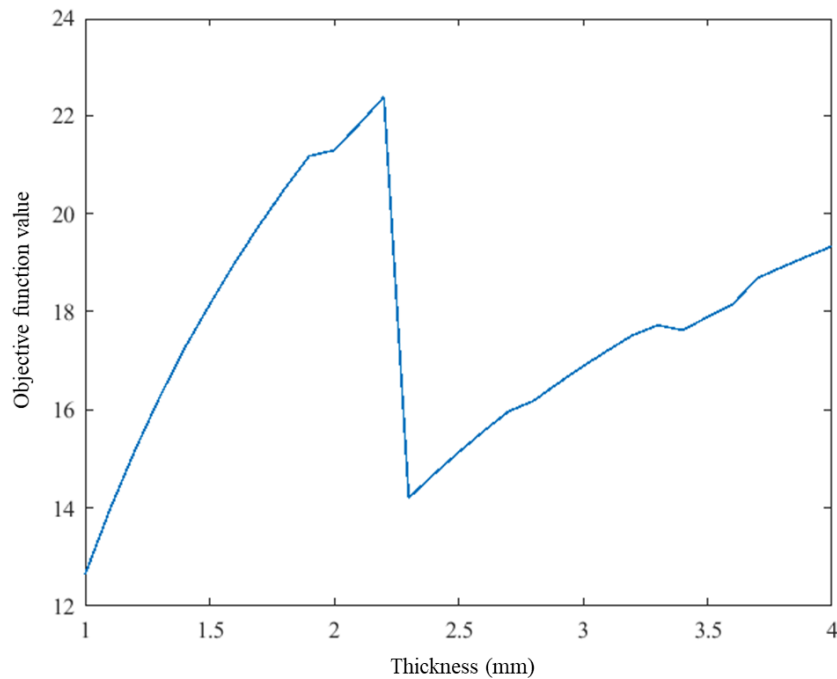


Fig. 4.43 The objective function values versus thickness  $t$

A general optimal function was not easy to implement in this work because of a combination of MATLAB and Abaqus scripts. Also, the optimization algorithm is not the focus of this chapter. Therefore, an alternative way, which is easier to implement but low in efficiency, is used in this work. This method is to get the objective function values with different thicknesses, as shown in Fig. 4.43. From Fig. 4.43, it could be found that when the thickness  $t = 2.3$  mm, the value of the objective function drops drastically and it reaches a local minimum. This indicates that a solution of the frequency assignment at 63.3 Hz is found to be  $t = 2.3$  mm. Although this value is quite close to the true value, 2.5 mm, there is a small difference between the two numbers. The difference between the obtained value and true value may come from the noise of measured receptances, especially the rotational receptances or the optimization algorithm.

#### 4.6.2 Assignment of two natural frequencies

In this subsection, the first two natural frequencies of the assembled structure, 63.3 Hz and 124.8 Hz, are to be assigned simultaneously. Two design variables, the thickness  $t$  and the breadth  $w$ , are used to minimize the objective function in Eq. (4.16). The weighting coefficients were chosen to be  $\varepsilon_i = 1$  ( $i = 1, 2$ ). Physical constraints of the design variables were defined by  $1\text{mm} \leq t \leq 4\text{mm}$  and  $18\text{mm} \leq w \leq 25\text{mm}$ .

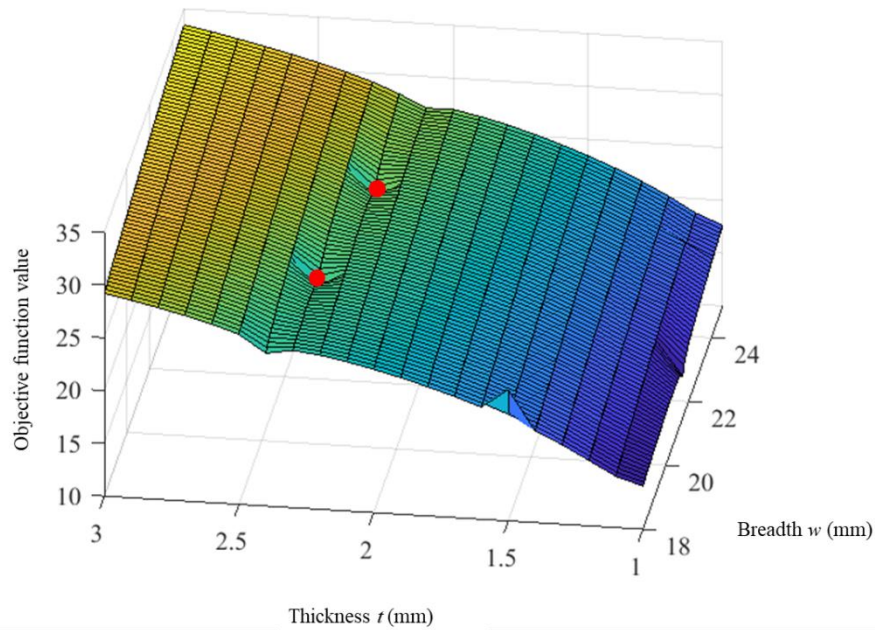


Fig. 4.44 The objective function values in terms of thickness  $t$  and breadth  $w$

The same method in the last subsection is adopted and the objective function values are plotted with varied thickness  $t$  and breadth  $w$ , as shown in Fig. 4.44. Two local minimum points were found, denoted by red circles in Fig. 4.44. Therefore, two solutions that can minimize the objective function were found to be  $w = 20.2$  mm,  $t = 2.3$  mm or  $w = 22.8$  mm,  $t = 2.2$  mm.

The first solution is quite close to the true values  $w = 20.5$  mm,  $t = 2.5$  mm. For the other solution, a new FE model of the assembled structure was built. The properties of links in this new FE model were chosen to be  $w = 22.8$  mm,  $t = 2.2$  mm. The first 5 natural frequencies of the assembled structure with new links are given in Table 4.7.

Table 4.7 Natural frequencies of the assembled structure (FE model)

Mode	1	2	3	4	5	6
FE model (Hz)	66.1	105.4	119.4	143.1	198.1	216.8

The obtained frequencies fall in the first and third modes and the third natural frequency of the new FE model is very close to the second natural frequency of the previous FE model, as shown in Table 4.3.. Although there is difference between the desired natural frequencies and the obtained ones, it can still show the proposed

method is able to assign frequencies for assembled structures by optimizing the properties of links.

In addition, compared with the previous FE model of the assembled structure, the new FE model has a new mode at 105.4 Hz. The mode shapes obtained from the two FE models are also different. Fig. 4.45 shows the first 3 mode shapes of the assembled structure with the new links.

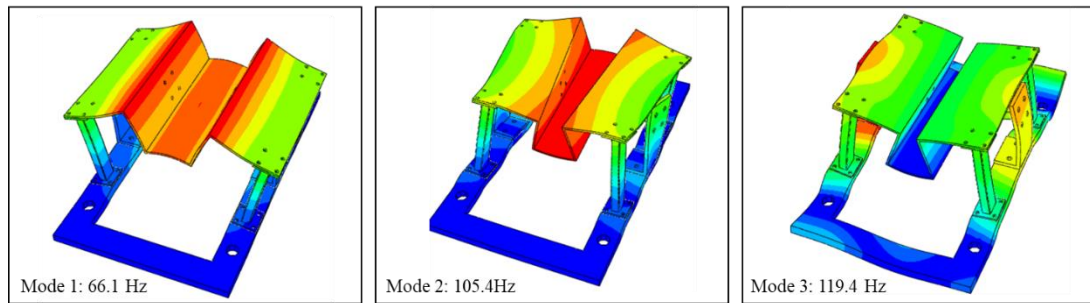


Fig. 4.45 The first 3 mode shapes of the assembled structure

Clearly, this proposed frequency assignment method for the assembled structure may give multiple solutions which will lead to different modal behaviours of the assembled structure. This is because the mode shapes are not considered in the optimization problem, as discussed in chapter 3. The final optimal solution should be chosen by other criteria which is defined case-by-case.

In conclusion, from the obtained results, it is validated that the proposed method can achieve the frequency assignment of assembled structures using measured receptances.

## 4.7 Conclusions

Experimental work on frequency assignment of an assembled structure is presented in this chapter. The laboratory test structure is a simplified model of a ship hull. There are two substructures and six simple links in this assembled structure. The receptances of substructures at connection points must be measured.

One big problem during the receptance measurement is the estimation of rotational receptances. In this work, the rotational receptances were measured with the aid of an auxiliary structure. This auxiliary structure is relatively very simple such that an accurate finite element model of the auxiliary structure can be built. Besides, in order

to reduce the efforts to measure the rotational receptances, two angular accelerometers were used to measure the rotational responses.

All the substructures and links were manufactured and modal tests were conducted on the assembled structure. The natural frequencies of the assembled structure were then used as target values to be assigned using the measured receptance data from the substructures.

Then several modal tests were conducted to measure the natural frequencies of the substructures and the receptances of each substructure at the connection points. The first one or two natural frequencies of the assembled structure were assigned by optimizing the geometrical properties of the links using the measured receptances and the FE models of the links, and applying the frequency assignment method proposed in chapter 3. It was found that the obtained solutions are quite close to the true values, which means this experimental work can validate the method proposed in chapter 3.

## Chapter 5

### Receptance-based partial eigenstructure assignment using hybrid control

Eigenvalues and eigenvectors play an important role in determining the dynamic behaviour of a vibrating system. Generally, the eigenvalues determine the stability and the rate at which the free-vibration response decays or grows, while the eigenvectors determine the “relative shape” of the transient response [125]. In chapter 3, a receptance-based frequency assignment method for assembled structures is presented. It has been pointed out in chapter 3 that, when only frequency assignment is considered, a desired natural frequency value for an assembled structure may associate with different modes when making different physical modifications such that the assembled structure has different dynamic behaviours, although the same desired frequency value is achieved. Therefore, only considering frequency/eigenvalue assignment may not be good enough for some vibrating systems. In some cases, the system transient response is to be altered or nodes are expected at certain locations. Both eigenvalue placement as well as eigenvector placement should be considered. The problem of assigning both the eigenvalues and the eigenvectors is known as the *eigenstructure assignment problem*. Eigenstructure assignment techniques have been proved critical in the solution of a variety of control problems, including monotonic tracking control [171], fault detection [172], damping controller design [173] and model updating [98, 100].

In many applications, especially for large scale systems and structures, it is usually only a small part of eigenvalues/eigenvectors that significantly affects the stability and other performances of the system and thus needs to be relocated. Meanwhile, it is required to keep other eigenvalues unaffected by the assignment. The problem of replacing a small number of eigenvalues and eigenvectors while leaving the remaining eigenpairs unchanged is called *partial eigenstructure assignment*. Such a control measure is said to satisfy the no spill-over property in an engineering practice.

There are already many researchers who have worked or are working on partial eigenstructure assignment methods [19, 127, 129, 131, 133, 174-176], as reviewed in chapter 2. However, previous methods require the system matrices (mass, stiffness and damping matrices) which are not easy to obtain in real applications, especially for complex structures, such as an engine or a pump. Since the receptance method can overcome this drawback, it is very appealing to establish a receptance-based method to solve partial eigenstructure assignment problem.

A receptance-based partial eigenstructure assignment method using hybrid control is proposed in this chapter. This method is the first one that can achieve partial eigenstructure assignment of a second-order system with receptance. One thing that should be clarified is the force distribution matrix  $\mathbf{B}$  in this chapter is predefined by engineers. In practice, people usually would prefer predefine the matrix  $\mathbf{B}$  according to the number of actuators and feasible locations. So, the case which determines the matrix  $\mathbf{B}$  based on the measured data is not considered in this chapter while it will be discussed in chapter 6.

The outline of this chapter is as the following. First, a receptance-based partial eigenvalue assignment method with state feedback control is explained. This active control method could assign desired eigenvalues while keeping the other eigenvalues unchanged. Then it is explained why the existing receptance-based active control method cannot directly achieve partial eigenstructure assignment. A numerical example is simulated to prove this point. After that, the theory on the receptance-based partial eigenstructure assignment method using hybrid control is presented. Numerical examples are given to reveal the performances of this proposed method. Some discussions and conclusions are given in the end.

A part of this chapter was reported in the following conference paper by the author of this thesis and his supervisor, Ouyang Huajiang [162]:

S. Zhang, H. Ouyang, 2021. *Receptance-based partial eigenstructure assignment using hybrid control* [Online]. The 27th International Congress on Sound and Vibration, 2021 online: Silesian University Press, Gliwice, Poland. Available: [https://iiav.org/content/archives\\_icsv\\_last/2021\\_icsv27/content/papers/papers/full\\_paper\\_601\\_20210430132307842.pdf](https://iiav.org/content/archives_icsv_last/2021_icsv27/content/papers/papers/full_paper_601_20210430132307842.pdf) [Accessed]



## 5.1 Introduction

In many situations, especially when dealing with large DoFs systems, it is desirable to assign only a subset of the eigenvalues with their corresponding eigenvectors, while leaving the rest unchanged from the original system. This is named a partial eigenstructure assignment problem. Due to the limitations of passive modifications, it is difficult to set up a general passive modification method for this problem. The existing partial eigenstructure assignment methods usually use an active control method. It should be noted that there are some passive modification methods for *eigenstructure assignment problem* [69, 70] or *partial eigenvalue assignment problem* [56, 57].

Over the last decades, several effective methods have been proposed to perform partial eigenstructure assignment. For example, pioneering work in the field of partial eigenstructure assignment via state feedback was done by Lu et al. [125] in 1991. Datta et al. [127] developed a method for partial eigenstructure assignment by determining proper force distribution matrix  $\mathbf{B}$  and gain matrices. Recently, some researchers combined partial eigenstructure assignment with some other control techniques [132, 177]. However, existing methods require system matrices  $\mathbf{M}$ ,  $\mathbf{C}$  and  $\mathbf{K}$ , which can be called a model-based approach. In addition, some methods [129, 132, 176] need to convert the second-order equations of motion into a first-order realisation, which cannot preserve some good properties of a second-order system. A receptance-based method that does not need to use or evaluate the system matrices, will be very useful.

A receptance-based partial eigenvalue assignment method was proposed by Ram and Mottershead [116]. This method can successfully assign desired eigenvalues while keeping the other eigenvalues unchanged. However, it cannot solve the partial eigenstructure assignment problem because the desired eigenvectors are not always assignable by this active control method. A wise passive modification can widen the set of eigenvectors that can be achieved through active control. Therefore, a hybrid control method is formulated in this chapter. This hybrid method consists of two steps: (1) to find feasible passive modifications such that desired eigenvectors are assignable, and (2) to get the required gain matrices in active control. Several simulated examples are presented in this chapter to explain the limitation of the pure active control method and show the performance of this new hybrid control method.

## 5.2 Receptance-based partial eigenvalue assignment

A receptance-based active control method [116] was proposed to solve the partial eigenvalue assignment problem. This method can assign desired eigenvalues while keeping the other eigenvalues unchanged. Whether this active control method can be used to achieve partial eigenstructure assignment remains to be known. Therefore, the theory of this receptance-based active control method is explained in this section.

### 5.2.1 Problem description

Consider a linear, time-invariant,  $n$  DoFs damped vibration system. Its equation of motion can be written as

$$\mathbf{M}\ddot{\mathbf{x}} + \mathbf{C}\dot{\mathbf{x}} + \mathbf{K}\mathbf{x} = \mathbf{0} \quad (5.1)$$

Eq. (5.1) can lead to the following eigenvalue equation

$$(\lambda^2\mathbf{M} + \lambda\mathbf{C} + \mathbf{K})\mathbf{v} = \mathbf{0} \quad (5.2)$$

The  $2n$  eigenvalues and eigenvectors are denoted by  $\{\lambda_k\}_{k=1}^{2n}$  and  $\{\mathbf{v}_k\}_{k=1}^{2n}$ . Those eigenvalues can be partitioned into two mutually exclusive subsets  $\Lambda_1 = \{\lambda_1, \lambda_2, \dots, \lambda_{2p}\}$  and  $\Lambda_2 = \{\lambda_{2p+1}, \lambda_{2p+2}, \dots, \lambda_{2n}\}$ . The corresponding eigenvectors are denoted as  $\mathbf{V}_1 = \{\mathbf{v}_1, \mathbf{v}_2, \dots, \mathbf{v}_{2p}\}$  and  $\mathbf{V}_2 = \{\mathbf{v}_{2p+1}, \mathbf{v}_{2p+2}, \dots, \mathbf{v}_{2n}\}$ . It is assumed that there are no repeated eigenvalues.

For a partial eigenvalue assignment problem, without loss of generality, it is wanted to change the first subset of eigenvalues  $\Lambda_1$  to another subset of targeted eigenvalues  $\Sigma_1 = \{\mu_1, \mu_2, \dots, \mu_{2p}\}$  and keep the other subset of eigenvalues  $\Lambda_2$  unchanged, that is,  $\Sigma_2 = \Lambda_2$ . Notice that an assumption  $\Lambda_1 \cap \Sigma_1 = \emptyset$  is made in the chapter.

To achieve this partial eigenvalue assignment, the system described in Eq. (5.1) is modified by applying a control force. This control force is expressed as

$$\mathbf{f}(t) = \mathbf{B}\mathbf{u}(t) \quad (5.3)$$

where  $\mathbf{B} = [\mathbf{b}_1 \ \dots \ \mathbf{b}_{n_b}] \in \mathcal{R}^{n \times n_b}$  is the control force distribution matrix ( $n_b$  indicates the number of actuators), and  $\mathbf{u}(t)$  is a time-dependent control force. Then the equation of motion in Eq. (5.1) becomes

$$\mathbf{M}\ddot{\mathbf{x}} + \mathbf{C}\dot{\mathbf{x}} + \mathbf{K}\mathbf{x} = \mathbf{B}\mathbf{u}(t) \quad (5.4)$$

The special choice of  $\mathbf{u}(t)$  is formed from a linear combination of the states of the system

$$\mathbf{u}(t) = \mathbf{F}^T \dot{\mathbf{x}}(t) + \mathbf{G}^T \mathbf{x}(t) \quad (5.5)$$

where  $\mathbf{F} = [\mathbf{f}_1 \ \dots \ \mathbf{f}_{n_b}]$  and  $\mathbf{G} = [\mathbf{g}_1 \ \dots \ \mathbf{g}_{n_b}]$  are  $n \times n_b$  matrices. It should be noticed that the choice of  $\mathbf{u}(t)$  in Eq. (5.5) applies state feedback control using displacement and velocity. This kind of control method is called *state feedback control*.

The eigenvalues of the closed-loop are characterised by

$$(\mu^2 \mathbf{M} + \mu(\mathbf{C} - \mathbf{B}\mathbf{F}^T) + (\mathbf{K} - \mathbf{B}\mathbf{G}^T))\mathbf{w} = \mathbf{0} \quad (5.6)$$

where  $\mu$  and  $\mathbf{w}$  denote the eigenvalue and eigenvector of the closed-loop system. Then the partial eigenvalue problem is to determine the gain matrices  $\mathbf{F}$  and  $\mathbf{G}$  such that the closed-loop system in Eq. (5.6) can have the newly prescribed eigenvalues  $\boldsymbol{\Sigma}_1$  and the original eigenvalues  $\boldsymbol{\Sigma}_2 = \boldsymbol{\Lambda}_2$ .

### 5.2.2 Receptance-based partial eigenvalue assignment method

The theory of the receptance-based partial eigenvalue assignment method is explained briefly in this section, based on the paper by Ram and Mottershead [116].

The quadratic eigenvalue problem associated with the open-loop and closed-loop systems, respectively, are

$$(\lambda_k^2 \mathbf{M} + \lambda_k \mathbf{C} + \mathbf{K})\mathbf{v}_k = \mathbf{0}, \quad k = 1, 2, \dots, 2n \quad (5.7)$$

$$(\mu_k^2 \mathbf{M} + \mu_k \mathbf{C} + \mathbf{K})\mathbf{w}_k = \mathbf{B}(\mu_k \mathbf{F}^T + \mathbf{G}^T)\mathbf{w}_k, \quad k = 1, 2, \dots, 2n \quad (5.8)$$

For those unchanged eigenvalues

$$\mu_k = \lambda_k, k = 2p + 1, 2p + 2, \dots, 2n \quad (5.9)$$

Substituting Eq. (5.9) into Eq. (5.8) gives

$$(\lambda_k^2 \mathbf{M} + \lambda_k \mathbf{C} + \mathbf{K})\mathbf{w}_k = \mathbf{B}(\lambda_k \mathbf{F}^T + \mathbf{G}^T)\mathbf{w}_k, \quad k = 2p + 1, \dots, 2n \quad (5.10)$$

According to Eq. (5.7), a no-trivial solution to Eq. (5.10) is

$$\mathbf{w}_k = \mathbf{v}_k, k = 2p + 1, \dots, 2n \quad (5.11)$$

and

$$\mathbf{B}(\lambda_k \mathbf{F}^T + \mathbf{G}^T) \mathbf{w}_k = \mathbf{0}, k = 2p + 1, \dots, 2n \quad (5.12)$$

Eq. (5.12) can be reformed as

$$\begin{aligned} & \left( \mathbf{b}_1(\lambda_k \mathbf{f}_1^T + \mathbf{g}_1^T) + \mathbf{b}_2(\lambda_k \mathbf{f}_2^T + \mathbf{g}_2^T) + \dots + \mathbf{b}_{n_b}(\lambda_k \mathbf{f}_{n_b}^T + \mathbf{g}_{n_b}^T) \right) \mathbf{v}_k = \mathbf{0}, \\ & k = 2p + 1, \dots, 2n \end{aligned} \quad (5.13)$$

The  $(2n - 2p)$  equations in Eq. (5.13) are satisfied whenever

$$\begin{bmatrix} \lambda_k \mathbf{v}_k^T & \mathbf{0} & \dots & \mathbf{0} & \mathbf{v}_k^T & \mathbf{0} & \dots & \mathbf{0} \\ \mathbf{0} & \lambda_k \mathbf{v}_k^T & \dots & \mathbf{0} & \mathbf{0} & \mathbf{v}_k^T & \dots & \mathbf{0} \\ \vdots & \vdots & \vdots & \vdots & \vdots & \vdots & \vdots & \vdots \\ \mathbf{0} & \mathbf{0} & \dots & \lambda_k \mathbf{v}_k^T & \mathbf{0} & \mathbf{0} & \dots & \mathbf{v}_k^T \end{bmatrix} \begin{bmatrix} \mathbf{f}_1 \\ \vdots \\ \mathbf{f}_{n_b} \\ \mathbf{g}_1 \\ \vdots \\ \mathbf{g}_{n_b} \end{bmatrix} = \begin{bmatrix} 0 \\ 0 \\ \vdots \\ 0 \end{bmatrix} \quad (5.14)$$

or in a compact form

$$\mathbf{Q}_k \mathbf{y} = \mathbf{0}, k = 2p + 1, \dots, 2n \quad (5.15)$$

with the obvious definitions of  $\mathbf{Q}_k$  and  $\mathbf{y}$ .

For those  $2p$  eigenvalues that are to be changed, pre-multiplying Eq. (5.8) by receptance matrix  $\mathbf{H}(\mu_k)$  gives

$$\mathbf{w}_k = \mathbf{H}(\mu_k) \mathbf{B}(\mu_k \mathbf{F}^T + \mathbf{G}^T) \mathbf{w}_k, k = 1, 2, \dots, 2p \quad (5.16)$$

which can be expanded as

$$\begin{aligned} & \mathbf{w}_k = \mathbf{H}(\mu_k) \left( \mathbf{b}_1(\mu_k \mathbf{f}_1^T + \mathbf{g}_1^T) + \mathbf{b}_2(\mu_k \mathbf{f}_2^T + \mathbf{g}_2^T) + \dots + \mathbf{b}_{n_b}(\mu_k \mathbf{f}_{n_b}^T + \mathbf{g}_{n_b}^T) \right) \mathbf{w}_k \\ & k = 1, 2, \dots, 2p \end{aligned} \quad (5.17)$$

By introducing a scaling vector  $\boldsymbol{\alpha}_k = [\alpha_{k1}, \alpha_{k2}, \dots, \alpha_{k,n_b}]^T$

$$\alpha_{kj} = (\mu_k \mathbf{f}_j^T + \mathbf{g}_j^T) \mathbf{w}_k, j = 1, 2, \dots, n_b \quad (5.18)$$

and a new matrix  $\mathbf{R}_k = [\mathbf{r}_{k1}, \mathbf{r}_{k2}, \dots, \mathbf{r}_{k,n_b}]$

$$\mathbf{r}_{kj} = \mathbf{H}(\mu_k)\mathbf{b}_j, j = 1, 2, \dots, n_b \quad (5.19)$$

Eq. (5.17) can be recast as

$$\mathbf{w}_k = \alpha_{k1}\mathbf{r}_{k1} + \alpha_{k2}\mathbf{r}_{k2} + \dots + \alpha_{k,n_b}\mathbf{r}_{k,n_b}, k = 1, 2, \dots, 2p \quad (5.20)$$

It should be noted that the scaling vector  $\boldsymbol{\alpha}_k$  can be chosen differently since the eigenvector  $\mathbf{w}_k$  can be scaled arbitrarily. Also, the obtained eigenvector of the closed-loop system is a linear combination of  $\{\mathbf{r}_{kj}\}_{j=1}^{n_b}$ . This is actually a limitation for this method to be applied to the partial eigenstructure assignment problem. Detailed discussions on this point will be presented in section 5.3.

Eq. (5.18) can be written in a matrix form

$$\begin{bmatrix} \mu_k \mathbf{w}_k^T & \mathbf{0} & \dots & \mathbf{0} & \mathbf{w}_k^T & \mathbf{0} & \dots & \mathbf{0} \\ \mathbf{0} & \mu_k \mathbf{w}_k^T & \dots & \mathbf{0} & \mathbf{0} & \mathbf{w}_k^T & \dots & \mathbf{0} \\ \vdots & \vdots & \vdots & \vdots & \vdots & \vdots & \vdots & \vdots \\ \mathbf{0} & \mathbf{0} & \dots & \mu_k \mathbf{w}_k^T & \mathbf{0} & \mathbf{0} & \dots & \mathbf{w}_k^T \end{bmatrix} \begin{bmatrix} \mathbf{f}_1 \\ \vdots \\ \mathbf{f}_{n_b} \\ \mathbf{g}_1 \\ \vdots \\ \mathbf{g}_{n_b} \end{bmatrix} = \begin{bmatrix} \alpha_{k1} \\ \alpha_{k2} \\ \vdots \\ \alpha_{k,n_b} \end{bmatrix} \quad (5.21)$$

or in a compact form

$$\mathbf{P}_k \mathbf{y} = \boldsymbol{\alpha}_k, k = 1, 2, \dots, 2p \quad (5.22)$$

The procedure of the receptance-based partial eigenvalue assignment method can be summarized as the following.

Given a system whose eigenvalues are  $\{\lambda_k\}_{k=1}^{2n}$  and the  $2p$  ( $p < n$ ) desired eigenvalues  $\boldsymbol{\Sigma}_1 = \{\mu_k\}_{k=1}^{2p}$ ,

- a) Get those unchanged eigenvalues and corresponding eigenvectors, and form the matrices  $\mathbf{Q}_k, k = 2p + 1, 2p + 2, \dots, 2n$ .
- b) Get the receptance matrices  $\{\mathbf{H}(\mu_k)\}_{k=1}^{2p}$  at those desired eigenvalues and calculate the matrices  $\mathbf{R}_k, k = 1, 2, \dots, 2p$ .
- c) Choose arbitrarily the scaling vectors  $\{\boldsymbol{\alpha}_k\}_{k=1}^{2p}$  and obtain the eigenvectors of the closed-loop system  $\{\mathbf{w}_k\}_{k=1}^{2p}$  using Eq. (5.20).
- d) Form the matrices  $\mathbf{P}_k, k = 1, 2, \dots, 2p$  using Eq. (5.21).
- e) Get the gain matrices  $\mathbf{F}$  and  $\mathbf{G}$  by solving the following equation

$$\begin{bmatrix} \mathbf{P}_1 \\ \vdots \\ \mathbf{P}_{2p} \\ \mathbf{Q}_{2p+1} \\ \vdots \\ \mathbf{Q}_{2n} \end{bmatrix} \begin{bmatrix} \mathbf{f}_1 \\ \vdots \\ \mathbf{f}_{n_b} \\ \mathbf{g}_1 \\ \vdots \\ \mathbf{g}_{n_b} \end{bmatrix} = \begin{bmatrix} \boldsymbol{\alpha}_1 \\ \vdots \\ \boldsymbol{\alpha}_{2p} \\ \mathbf{0} \\ \vdots \\ \mathbf{0} \end{bmatrix} \quad (5.23)$$

Although the scaling vectors  $\{\boldsymbol{\alpha}_k\}_{k=1}^{2p}$  can be chosen arbitrarily, in theory, they can be defined so as to achieve other targets or satisfy other requirements. For example, Mokrani et al. [91] minimized the norm of feedback gain matrix by choosing optimal scaling vectors.

### 5.2.3 Numerical examples

The 3-DoF system in chapter 3 is considered here.

$$\mathbf{M} = \begin{bmatrix} 1 & & \\ & 2 & \\ & & 1 \end{bmatrix}, \quad \mathbf{K} = 10^5 \times \begin{bmatrix} 6 & -5 & \\ -5 & 8 & -3 \\ & -3 & 5 \end{bmatrix}, \quad \mathbf{C} = 10^{-5} \times \mathbf{K}$$

The eigenvalues of the open-loop system are

$$\lambda_{1,2} = -0.32 \pm 252.48i, \quad \lambda_{3,4} = -2.63 \pm 724.62i, \quad \lambda_{5,6} = -4.56 \pm 954.54i,$$

It is wanted to change the eigenvalues  $\lambda_{1,2}$  to the new values  $\mu_{1,2} = -3.00 \pm 300i$ , while keeping the other four eigenvalues unchanged.

The eigenvectors corresponding to the unchanged eigenvectors are

$$\mathbf{x}_{3,4} = [-0.56 \quad -0.08 \quad 1]^T$$

$$\mathbf{x}_{5,6} = [1 \quad -0.62 \quad 0.45]^T$$

(1) Single input

Only one actuator is employed. Then the force distribution vector is taken to be

$$\mathbf{b} = [1 \quad 0 \quad 1]^T$$

The receptance matrices  $\mathbf{H}(\mu_1)$  and  $\mathbf{H}(\mu_2)$  can be easily obtained and the vectors  $\mathbf{r}_1$  and  $\mathbf{r}_2$  are

$$\mathbf{r}_1 = \mathbf{H}(\mu_1)\mathbf{b} = 10^{-4} \times [-0.17 + 0.01i \quad -0.19 + 0.01i \quad -0.11 + 0.01i]^T$$

$$\mathbf{r}_2 = \mathbf{H}(\mu_2)\mathbf{b} = 10^{-4} \times [-0.17 - 0.01i \quad -0.19 - 0.01i \quad -0.11 - 0.01i]^T$$

For those desired eigenvalues, choose

$$\alpha_1 = (\mu_1 \mathbf{f}^T + \mathbf{g}^T) \mathbf{w}_1 = 1$$

$$\alpha_2 = (\mu_2 \mathbf{f}^T + \mathbf{g}^T) \mathbf{w}_2 = 1$$

Then the eigenvectors  $\mathbf{w}_1$  and  $\mathbf{w}_2$  can be obtained from Eq. (5.20). Then the gain vectors  $\mathbf{f}$  and  $\mathbf{g}$  are calculated by solving Eq. (5.23), which are

$$\mathbf{f} = [-3.09 \quad -6.62 \quad -2.28]^T$$

$$\mathbf{g} = 10^4 \times [-1.51 \quad -3.24 \quad -1.11]^T$$

Fig. 5.1 shows the FRFs of original system and controlled system.

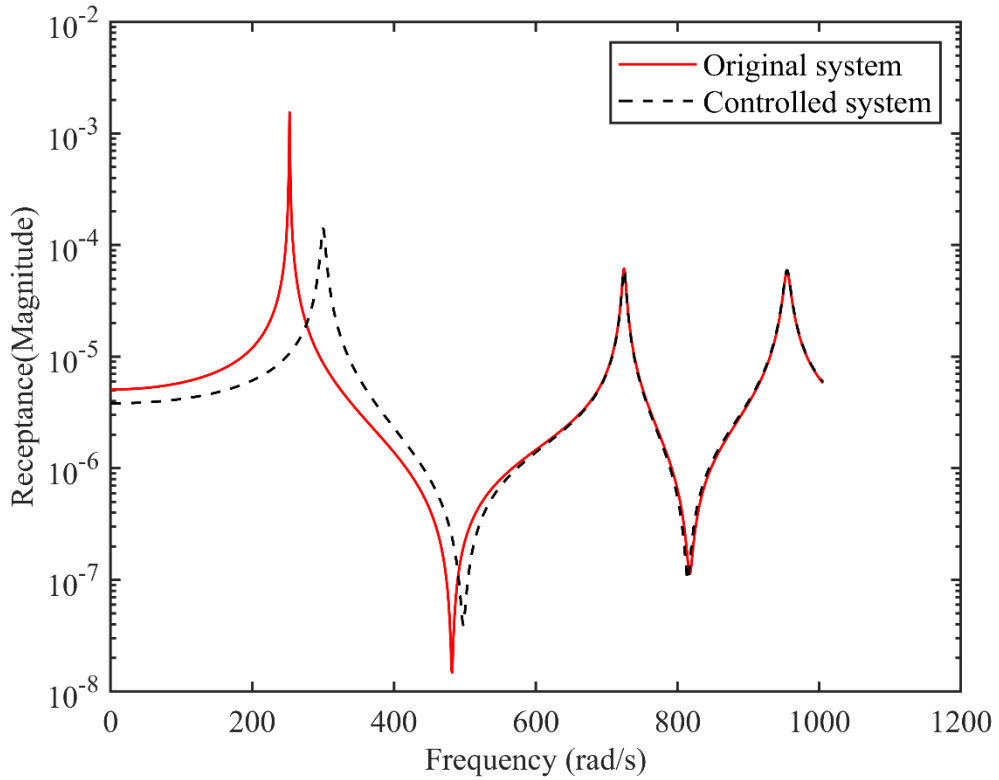


Fig. 5.1 FRF  $h_{11}$

The eigenvalues and eigenvectors of the closed-loop system are given in

$$\mu_{1,2} = -3.00 \pm 300.00i, \mu_{3,4} = -2.63 \pm 724.62i, \mu_{5,6} = -4.56 \pm 954.54i$$

Table 5.1 Eigenvalues and eigenvectors of the controlled system

	$\mu_{1,2}$	$\mu_{3,4}$	$\mu_{5,6}$
	$-3.00 \pm 300.00i$	$-2.63 \pm 724.62i$	$-4.56 \pm 954.54i$
$\mathbf{w}_k$	0.88	-0.56	1
	1.00	-0.08	-0.62
	0.60	1	0.45

Apparently, the desired eigenvalues are achieved and the other eigenvalues are kept.

## (2) Multiple inputs

Two actuators are adopted, and the force distribution matrix is taken to be

$$\mathbf{B} = \begin{bmatrix} 1 & 0 \\ 0 & 1 \\ 1 & -1 \end{bmatrix}$$

The scaling vectors are chosen as

$$\boldsymbol{\alpha}_1 = [1 \quad -1]^T$$

$$\boldsymbol{\alpha}_2 = [0.5 \quad 1]^T$$

Following the procedure in subsection 5.2.2, the gain matrices  $\mathbf{F}$  and  $\mathbf{G}$  can be obtained as

$$\mathbf{F} = \begin{bmatrix} -3.03 & -0.32 \\ -6.49 & -0.68 \\ -2.23 & -0.23 \end{bmatrix} \text{ and } \mathbf{G} = 10^4 \times \begin{bmatrix} -1.48 & -0.15 \\ -3.18 & -0.33 \\ -1.09 & -0.11 \end{bmatrix}$$

The closed-loop system can be characterized as

$$(\mu_k^2 \mathbf{M} + \mu_k (\mathbf{C} - \mathbf{B}\mathbf{F}^T) + \mathbf{K} - \mathbf{B}\mathbf{G}^T) \mathbf{w}_k = \mathbf{0}$$

with the eigenvalues as expected.

The above results show that this receptance-based partial eigenvalue assignment can be applied with a single input or multiple inputs.



### 5.3 Receptance-based partial eigenstructure assignment by active control

In subsections 5.2.2 and 5.2.3, it has been explained and verified that the receptance-method can be used to achieve partial eigenvalue assignment with state feedback control. However, for partial eigenstructure assignment, which aims to assign desired eigenvalues and eigenvectors, the receptance-based active control method is not able to successfully assign desired eigenvectors. A detailed discussion on this point is presented in the following.

#### 5.3.1 Existence of solutions for partial eigenstructure assignment with state feedback control

From Eq. (5.20), it has been found that the eigenvector of the closed-loop system  $\mathbf{w}_k$  corresponding to the desired eigenvalue  $\mu_k$  is a linear combination of  $\{\mathbf{r}_{kj}\}_{j=1}^{n_b}$ , where  $k = 1, 2, \dots, 2p$ . This relationship can also be written in a compact form

$$\mathbf{w}_k = \mathbf{R}_k \boldsymbol{\alpha}_k, k = 1, 2, \dots, 2p \quad (5.24)$$

For a damped system, the elements in the above equation are usually complex. In general, it can be transformed into an equivalent real equation of twice the dimension. It is straightforward to prove that Eq. (5.24) is equivalent to

$$\begin{bmatrix} \text{Real}(\mathbf{w}_k) \\ \text{Imag}(\mathbf{w}_k) \end{bmatrix} = \begin{bmatrix} \text{Real}(\mathbf{R}_k) & -\text{Imag}(\mathbf{R}_k) \\ \text{Imag}(\mathbf{R}_k) & \text{Real}(\mathbf{R}_k) \end{bmatrix} \begin{bmatrix} \text{Real}(\boldsymbol{\alpha}_k) \\ \text{Imag}(\boldsymbol{\alpha}_k) \end{bmatrix} \quad (5.25)$$

where  $\text{Real}(\ast)$  denotes the real part and  $\text{Imag}(\ast)$  denotes the imaginary part. For simplicity, Eq. (5.24) is still used in the following derivations, because the method can be adapted to Eq. (5.25) with minor modifications.

For partial eigenstructure assignment problem, the desired eigenvector  $\mathbf{w}_k$  is prescribed and  $\mathbf{R}_k$  can be obtained using measured receptance. Based on the Rouché-Capelli theorem, the desired eigenvector can be assigned if and only if

$$\text{rank}([\mathbf{R}_k \ \mathbf{w}_k]) = \text{rank}(\mathbf{R}_k) \quad (5.26)$$

Eq. (5.24) can be recast as

$$[\mathbf{I} \mid \beta_k \mathbf{R}_k] \begin{bmatrix} \mathbf{w}_k \\ -\frac{1}{\beta_k} \boldsymbol{\alpha}_k \end{bmatrix} = \mathbf{0} \quad (5.27)$$

Here,  $\beta_k$  is a scaling coefficient which is used to keep the elements in the same matrix in similar orders of magnitude to avoid ill-conditioning. Therefore, the desired eigenvector  $\mathbf{w}_k$  is assignable if and only  $\mathbf{w}_k$  belongs to the following vector space

$$\psi(\mu_k) = \left\{ \mathbf{w}_k \in \mathbb{C}^{n \times 1} \text{ and } \begin{bmatrix} \mathbf{w}_k \\ -\frac{1}{\beta_k} \boldsymbol{\alpha}_k \end{bmatrix} \in \ker([\mathbf{I} \mid \beta_k \mathbf{R}_k]) \right\} \quad (5.28)$$

Here, ‘ker’ denotes the null space. However, it is not guaranteed and it is usually unlikely that the desired eigenvector  $\mathbf{w}_k$  happens to lie in the allowable space  $\psi(\mu_k)$ . For instance, in the case of single input, the eigenvector of the closed-loop system  $\mathbf{w}_k$  corresponding to the desired eigenvalue  $\mu_k$  should follow

$$\mathbf{w}_k = \alpha_k \mathbf{r}_k, k = 1, 2, \dots, 2p \quad (5.29)$$

This means the desired eigenvector  $\mathbf{w}_k$  should be parallel to  $\mathbf{r}_k$ , which is usually unlikely to be satisfied.

Since the desired eigenvector  $\mathbf{w}_k$  usually does not belong to the allowable space  $\psi(\mu_k)$ , one way that is often used to get the desired eigenvector is to assign the projection of  $\mathbf{w}_k$  onto  $\psi(\mu_k)$ , rather than  $\mathbf{w}_k$  itself. For example, if the columns of matrix  $\mathbf{S}_k \in \mathbb{C}^{(n+n_b) \times n_b}$  span the allowable space  $\psi(\mu_k)$ , it can be partitioned as

$$\mathbf{S}_k = \begin{bmatrix} \mathbf{S}_{k,1} \\ \mathbf{S}_{k,2} \end{bmatrix}, \mathbf{S}_{k,1} \in \mathbb{C}^{n \times n_b} \text{ and } \mathbf{S}_{k,2} \in \mathbb{C}^{n_b \times n_b} \quad (5.30)$$

Then the projection of eigenvector  $\mathbf{w}_k$  onto the allowable space  $\psi(\mu_k)$  can be defined as [178]

$$\tilde{\mathbf{w}}_k = \mathbf{S}_{k,1} (\mathbf{S}_{k,1}^T \mathbf{S}_{k,1})^{-1} \mathbf{S}_{k,1}^T \mathbf{w}_k \quad (5.31)$$

Fig. 5.2 shows the relationship between the desired eigenvector and its projection.

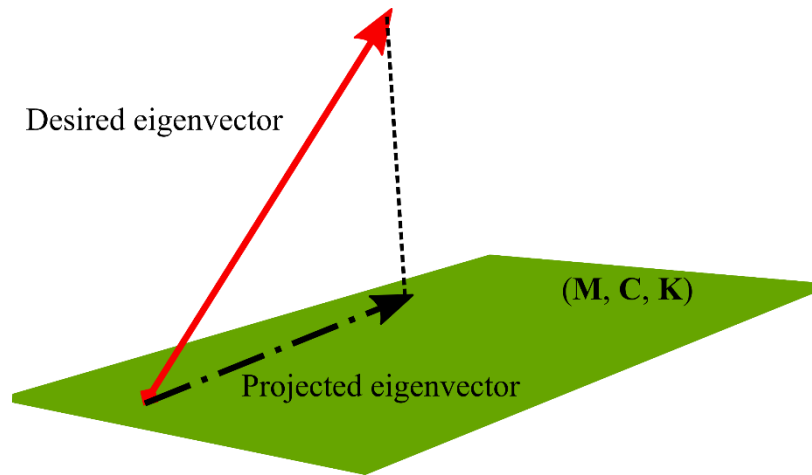


Fig. 5.2 Eigenvector projection

However, this approach may lead to poor dynamic performances which are much different from the desired performances, because the projection might have big differences from the desired eigenvector. A numerical example is presented here to demonstrate this point.

### 5.3.2 Numerical Example

A five-DoF undamped system, as shown in Fig. 5.3, is considered here. This example was used in other papers to validate some eigenvalue assignment or eigenstructure assignment methods [69, 70, 104]. The values of the masses and stiffnesses are shown in Table 5.2. Table 5.3 gives the natural frequencies and eigenvectors of the original system. It is wanted to assign two desired eigenpairs to the second and fourth modes and keep the other eigenpairs unchanged. The desired natural frequencies and corresponding eigenvectors are shown in Table 5.4. Since no damping is considered in this example, only displacement feedback is adopted.

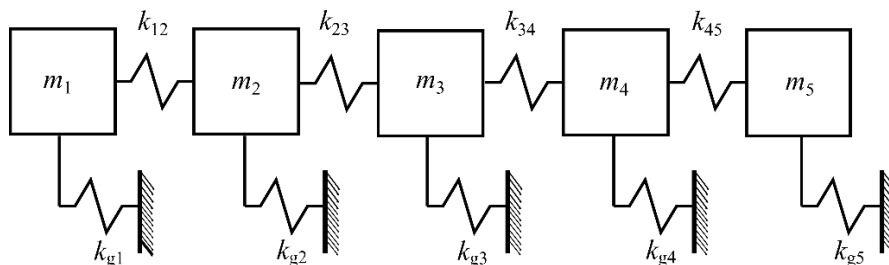


Fig. 5.3 A 5-dof system

Table 5.2 System parameters

$m_1$ [kg]	1.34	$k_1$ [kN/m]	82.1
$m_2$ [kg]	2.61	$k_2$ [kN/m]	73.5
$m_3$ [kg]	8.21	$k_3$ [kN/m]	68.2
$m_4$ [kg]	5.12	$k_4$ [kN/m]	73.6
$m_5$ [kg]	1.73	$k_{g,i}, i = 1, \dots, 5$ [kN/m]	98.9

Table 5.3 Eigenstructure of the open-loop system

Mode number	1	2	3	4	5
$f_{k,\text{origin}}$ [Hz]	22.28	32.61	42.92	52.71	64.57
$x_{k,1}$	0.244	-0.222	-0.983	-0.019	-1.000
$x_{k,2}$	0.460	-0.337	-1.000	-0.008	0.482
$x_{k,3}$	1.000	-0.417	0.218	0.025	-0.030
$x_{k,4}$	0.673	1.000	-0.060	-0.235	0.004
$x_{k,5}$	0.358	0.737	-0.094	1.000	-0.003

Table 5.4 Desired eigenpairs

Mode number	2	4
$f_{k,\text{origin}}$ [Hz]	39.00	55.00
$w_{k,1}$	0.050	1.000
$w_{k,2}$	0.000	0.800
$w_{k,3}$	0.200	-0.100
$w_{k,4}$	-0.55	0.010
$w_{k,5}$	1	0.000

(1) single input

Only one actuator is used, and the force distribution vector is taken to be

$$\mathbf{b} = [1 \ 0 \ 1 \ -1 \ 0]^T$$

The cosines of the angles between the original eigenvectors and the desired eigenvectors are 0.0581 at 39 Hz and 0.0232 at 55 Hz. The obtained values indicate that the desired eigenvectors are almost orthogonal to the original eigenvectors.

By obtaining the receptances at the desired natural frequencies of 39Hz and 55 Hz, the vectors  $\mathbf{r}_k$  ( $k = 2,4$ ) can be calculated

$$\mathbf{r}_2 = 10^{-4} \times [0.15 \quad 0.06 \quad -0.09 \quad 0.11 \quad 0.12]^T$$

$$\mathbf{r}_4 = 10^{-4} \times [0.08 \quad -0.10 \quad -0.01 \quad 0.05 \quad -0.11]^T$$

Then the desired eigenvector  $\mathbf{w}_k$  is projected onto the allowable space  $\psi(f_k)$ . The cosine of the angle between each desired eigenvector and its projection is evaluated. The two desired eigenvectors cannot be assigned through active control with good accuracy, since the computed cosines are 0.1681 at 39 Hz and 0.0093 at 55 Hz, respectively.

By applying the receptance-based active control method, the gain vector is

$$\mathbf{g} = 10^5 \times [-0.03 \quad -0.10 \quad -0.49 \quad 1.00 \quad -0.35]^T$$

and the natural frequencies and eigenvectors of the closed-loop system are presented in Table 5.5. The quantities evaluated to assess the performances of active control method are given in Table 5.6.

The results show the spill-over problem can be avoided since the unchanged eigenpairs are kept, while the desired eigenvectors corresponding to the second and fourth modes are not as expected. It means the receptance-based active control cannot achieve partial eigenstructure assignment with a single input.

Table 5.5 Natural frequencies and eigenvectors of the closed-loop system

Mode number	1	2	3	4	5
$f_k$ [Hz]	22.28	39.00	42.92	55.00	64.57
$w_{k,1}$	0.244	-0.222	-0.983	-0.019	-1.000
$w_{k,2}$	0.460	-0.337	-1.000	-0.008	0.482
$w_{k,3}$	1.000	-0.417	0.218	0.025	-0.030
$w_{k,4}$	0.673	1.000	-0.060	-0.235	0.004
$w_{k,5}$	0.358	0.737	-0.094	1.000	-0.003

Table 5.6 Performance assessment for single input

Desired modes			Unchanged modes			
Mode number	2	4	Mode number	1	3	5
$\delta f = \frac{ f_{k,obt} - f_{k,des} }{\text{Hz}}$	0	0	$\delta f = \frac{ f_{k,obt} - f_{k,origin} }{\text{Hz}}$	0	0	0
$\cos(\mathbf{w}_{k,des}, \mathbf{w}_{k,obt})$	0.17	0.01	$\cos(\mathbf{v}_{k,origin}, \mathbf{w}_{k,obt})$	1.00	1.00	1.00

Although the above example shows the disadvantage of the existing receptance-based active control method, it may still not be convincing. Therefore, several different vectors  $\mathbf{b}$  are predefined to achieve the target eigenstructure. Table 5.7 shows the results of the receptance-based active control method with different vectors  $\mathbf{b}$ .

Table 5.7 The qualities of obtained eigenvectors with different vector  $\mathbf{b}$

vector $\mathbf{b}$	$\cos(\mathbf{w}_{k,des}, \mathbf{w}_{k,obt})$	
	$k=2$	$k=4$
$[1 \ 0 \ 1 \ 0 \ 1]^T$	0.40	0.01
$[1 \ -1 \ 0 \ 1 \ -1]^T$	0.73	0.10
$[1 \ 2 \ -2 \ 1 \ 1]^T$	0.10	0.52

It can be seen from Table 5.7 that the receptance-based active control method usually cannot directly achieve partial eigenstructure assignment with predefined vector  $\mathbf{b}$ .

## (2) Multiple-input

For multiple-input, the force distribution matrix  $\mathbf{B}$  is taken to be

$$\mathbf{B}^T = \begin{bmatrix} 1 & 0 & 0 & 0.5 & 0 \\ 0 & 1 & 0 & 0 & 0.5 \\ 0 & 0 & 1 & 0 & 0 \end{bmatrix}$$

With the receptance matrices at desired natural frequencies, the matrix  $\mathbf{R}_k, k = 2,4$  can be calculated as

$$\mathbf{R}_2 = 10^{-5} \times \begin{bmatrix} 2.32 & 1.60 & -0.49 \\ 1.62 & 1.96 & -0.60 \\ -0.43 & -0.54 & -0.25 \\ -0.14 & -0.12 & 0.12 \\ -0.15 & 0.61 & 0.13 \end{bmatrix}$$

$$\mathbf{R}_4 = 10^{-5} \times \begin{bmatrix} 0.62 & -1.02 & 0.11 \\ -1.06 & -0.26 & 0.03 \\ 0.13 & -0.02 & -0.14 \\ -0.28 & 0.52 & 0.05 \\ 0.60 & -2.58 & -0.10 \end{bmatrix}$$

Since  $\text{rank}([\mathbf{R}_2 \ \mathbf{w}_2]) \neq \text{rank}(\mathbf{R}_2)$  and  $\text{rank}([\mathbf{R}_4 \ \mathbf{w}_4]) \neq \text{rank}(\mathbf{R}_4)$ , the desired eigenvectors cannot be assigned accurately. Therefore, instead of assigning desired eigenvector  $\mathbf{w}_k$  directly, assigning the projection of  $\mathbf{w}_k$  onto  $\psi(\mu_k)$  is a feasible way. The projected/assignable eigenvectors are obtained

$$\tilde{\mathbf{w}}_2 = [-0.57 \quad 0.79 \quad -0.18 \quad -0.00 \quad 1.00]^T$$

$$\tilde{\mathbf{w}}_4 = [0.89 \quad 0.93 \quad -1.00 \quad 0.19 \quad 0.37]^T$$

Then the required gain matrix  $\mathbf{G}$  is calculated as

$$\mathbf{G} = 10^5 \times \begin{bmatrix} 0.05 & 0.03 & -0.50 \\ 0.12 & 0.14 & -1.56 \\ 0.30 & 0.82 & -6.52 \\ 0.10 & -2.09 & 11.10 \\ -1.23 & 1.43 & -0.33 \end{bmatrix}$$

The performance of the active control method with multiple inputs is assessed with two quantities, as shown in Table 5.8.

Table 5.8 Performance assessment for multiple inputs

Desired modes			Unchanged modes			
Mode number	2	4	Mode number	1	3	5
$\delta f =  f_k - f_{k,des} $ Hz	0	0	$\delta f =  f_k - f_{k,origin} $ Hz	0	0	0
$\cos(\mathbf{w}_{k,des}, \mathbf{w}_{k,obt})$	0.57	0.80	$\cos(\mathbf{v}_{k,origin}, \mathbf{w}_{k,obt})$	1.00	1.00	1.00

Clearly, the spill-over problem is avoided by keeping the three natural frequencies and corresponding eigenvectors unchanged. However, the assigned eigenvectors corresponding to the second and fourth modes are still quite different with the desired ones. Therefore, the partial eigenstructure assignment cannot be achieved using the receptance-based multiple inputs active control method. It remains a challenge to develop a receptance-based method which can achieve partial eigenstructure assignment.

## 5.4 Receptance-based partial eigenstructure assignment with hybrid control

It has been demonstrated in section 5.3.1 that  $\mathbf{w}_k$  can only be assigned when  $\mathbf{w}_k$  belongs to the allowable space  $\psi(\mu_k)$ . In this section, passive modifications, which are usually mass and stiffness modifications, are used to get a new allowable space  $\hat{\psi}(\mu_k)$  such that  $\mathbf{w}_k \in \hat{\psi}(\mu_k)$ . The detailed derivation of this hybrid control method is explained in the following.

### 5.4.1 Passive modification

The closed-loop system with passive modifications can be described by the following second-order differential equation

$$(\mu_k^2(\mathbf{M} + \Delta\mathbf{M}) + \mu_k\mathbf{C} + \mathbf{K} + \Delta\mathbf{K})\mathbf{w}_k = \mathbf{B}(\mu_k\mathbf{F}^T + \mathbf{G}^T)\mathbf{w}_k, k = 1, 2, \dots, 2n \quad (5.32)$$

For those desired eigenvalues in subset  $\Sigma_1$ , pre-multiplying Eq. (5.32) by the receptance matrix  $\mathbf{H}(\mu_k)$  yields

$$\begin{aligned} (\mathbf{I} + \mathbf{H}(\mu_k)(\mu_k^2\Delta\mathbf{M} + \Delta\mathbf{K}))\mathbf{w}_k &= \mathbf{H}(\mu_k)\mathbf{B}(\mu_k\mathbf{F}^T + \mathbf{G}^T)\mathbf{w}_k \\ k &= 1, 2, \dots, 2p \end{aligned} \quad (5.33)$$

Eq. (5.33) can be rearranged as

$$(\mathbf{I} + \mathbf{H}(\mu_k)(\mu_k^2\Delta\mathbf{M} + \Delta\mathbf{K}))\mathbf{w}_k = \mathbf{R}_k\boldsymbol{\alpha}_k, \quad k = 1, 2, \dots, 2p \quad (5.34)$$

where  $\boldsymbol{\alpha}_k$  and  $\mathbf{R}_k$  have been defined in Eq. (5.18) and Eq. (5.19).

The goal in this step is to find proper modification matrices  $\Delta\mathbf{M}$  and  $\Delta\mathbf{K}$  so that  $\mathbf{w}_k$  belongs to a new allowable space  $\hat{\psi}(\mu_k)$ . This new space  $\hat{\psi}(\mu_k)$  is defined as

$$\hat{\psi}(\mu_k) = \left\{ \mathbf{w}_k \in \mathbb{C}^{n \times 1} \text{ and } \begin{Bmatrix} \mathbf{w}_k \\ -\boldsymbol{\alpha}_k \end{Bmatrix} \in \ker([\mathbf{I} + \mathbf{H}(\mu_k)(\mu_k^2\Delta\mathbf{M} + \Delta\mathbf{K}) \mid \mathbf{R}_k]) \right\} \quad (5.35)$$

If vector  $\mathbf{d}_k$  is defined as



$$\mathbf{d}_k = \left( \mathbf{I} + \mathbf{H}(\mu_k)(\mu_k^2 \Delta \mathbf{M} + \Delta \mathbf{K}) \right) \mathbf{w}_k, k = 1, 2, \dots, 2p \quad (5.36)$$

Then Eq. (5.34) can be written as

$$\mathbf{R}_k \boldsymbol{\alpha}_k = \mathbf{d}_k, \quad k = 1, 2, \dots, 2p \quad (5.37)$$

Eq. (5.37) is solvable if and only if

$$\text{rank}([\mathbf{R}_k \mid \mathbf{d}_k]) = \text{rank}(\mathbf{R}_k), k = 1, 2, \dots, 2p \quad (5.38)$$

If  $\mathbf{R}_k^+$  is the Moore-Penrose inverse of  $\mathbf{R}_k$ , the following equation can be obtained

$$\mathbf{R}_k \mathbf{R}_k^+ \mathbf{R}_k = \mathbf{R}_k \quad (5.39)$$

Pre-multiplying Eq. (5.37) by  $\mathbf{R}_k \mathbf{R}_k^+$  on both sides yield

$$\mathbf{R}_k \mathbf{R}_k^+ \mathbf{R}_k \boldsymbol{\alpha}_k = \mathbf{R}_k \mathbf{R}_k^+ \mathbf{d}_k \quad (5.40)$$

It can be reformed as

$$\mathbf{d}_k = \mathbf{R}_k \mathbf{R}_k^+ \mathbf{d}_k \quad (5.41)$$

Therefore,

$$(\mathbf{R}_k \boldsymbol{\alpha}_k - \mathbf{d}_k) = (\mathbf{I} - \mathbf{R}_k \mathbf{R}_k^+) \mathbf{d}_k \quad (5.42)$$

It is wanted to make sure  $(\mathbf{R}_k \boldsymbol{\alpha}_k - \mathbf{d}_k) = \mathbf{0}$  such that the desired eigenvector  $\mathbf{w}_k$  is assignable. From Eq. (5.42), a sufficient and necessary condition to achieve this is

$$(\mathbf{I} - \mathbf{R}_k \mathbf{R}_k^+) \mathbf{d}_k = \mathbf{0} \quad (5.43)$$

However, this condition is not guaranteed to be obtained due to the physical feasibility and restrictions. Thus, it is more proper to convert Eq. (5.43) into an optimization problem

$$\begin{aligned} & \text{minimize} \quad \sum_{k=1}^{2p} \varepsilon_k \|\mathbf{I} - \mathbf{R}_k \mathbf{R}_k^+\| \mathbf{d}_k \|^2 \\ & \text{subject to} \quad (\Delta \mathbf{M}, \Delta \mathbf{K}) \in \Gamma \end{aligned} \quad (5.44)$$

where  $\varepsilon_k$  are weighting coefficients and  $\Gamma$  represents the physical constraints on passive modifications.

For those unchanged eigenvalues, the corresponding eigenvectors are assumed to be unchanged too, thus

$$\mu_k = \lambda_k, \mathbf{w}_k = \mathbf{v}_k, k = 2p + 1, \dots, 2n \quad (5.45)$$

Substituting Eq. (5.45) into Eq. (5.32) gives

$$\begin{aligned} (\lambda_k^2(\mathbf{M} + \Delta\mathbf{M}) + \lambda_k\mathbf{C} + \mathbf{K} + \Delta\mathbf{K})\mathbf{v}_k &= \mathbf{B}(\lambda_k\mathbf{F}^T + \mathbf{G}^T)\mathbf{v}_k \\ k &= 2p + 1, \dots, 2n \end{aligned} \quad (5.46)$$

Then Eq. (5.46) can be organized as

$$(\lambda_k^2\Delta\mathbf{M} + \Delta\mathbf{K})\mathbf{v}_k = \mathbf{B}(\lambda_k\mathbf{F}^T + \mathbf{G}^T)\mathbf{v}_k, \quad k = 2p + 1, \dots, 2n \quad (5.47)$$

By defining vector  $\mathbf{t}_k$  as

$$\mathbf{t}_k = (\lambda_k^2\Delta\mathbf{M} + \Delta\mathbf{K})\mathbf{v}_k, k = 2p + 1, \dots, 2n \quad (5.48)$$

Then Eq. (5.47) can be recast as

$$\mathbf{B}\boldsymbol{\alpha}_k = \mathbf{t}_k, k = 2p + 1, \dots, 2n \quad (5.49)$$

According to the Rouché-Capelli theorem, Eq. (5.49) can be solved if and only if the rank of matrix  $\mathbf{B}$  is equal to the rank of the augmented matrix  $[\mathbf{B} \mid \mathbf{t}_k]$ . Therefore, Eq. (5.49) can be solved for all indices  $k = 2p + 1, \dots, 2n$  if and only if

$$\text{rank}([\mathbf{B} \mid \mathbf{T}]) = \text{rank}(\mathbf{B}) \quad (5.50)$$

with  $\mathbf{T} = [\mathbf{t}_{2p+1} \ \mathbf{t}_{2p+2} \ \dots \ \mathbf{t}_{2n}]$ .

It has been proved in reference [179] that

$$\text{rank}([\mathbf{B} \mid \mathbf{T}]) = \text{rank}(\mathbf{B}) + \text{rank}((\mathbf{I} - \mathbf{B}\mathbf{B}^+)\mathbf{T}) \quad (5.51)$$

where  $\mathbf{B}^+$  is the Moore-Penrose inverse of  $\mathbf{B}$ . According to Eq. (5.51), Eq. (5.50) can be satisfied if

$$\text{rank}((\mathbf{I} - \mathbf{B}\mathbf{B}^+)\mathbf{T}) = 0 \quad (5.52)$$

The only exact solution of Eq. (5.52) is  $(\mathbf{I} - \mathbf{B}\mathbf{B}^+)\mathbf{T} = \mathbf{0}$ . Again, this solution is not guaranteed to be obtained due to the physical feasibility and restrictions. The

minimization of the 2-norm of a matrix can be considered as an approximation of the minimization of the rank of a matrix. Thus, it is more proper to convert Eq. (5.52) into an optimization problem

$$\begin{aligned} & \text{minimize} && \|(\mathbf{I} - \mathbf{B}\mathbf{B}^+)\mathbf{T}\|^2 \\ & \text{subject to} && (\Delta\mathbf{M}, \Delta\mathbf{K}) \in \Gamma \end{aligned} \quad (5.53)$$

Then the suitable passive modifications can be obtained by minimizing the objective functions in Eq. (5.47) and Eq. (5.53). If  $\Gamma$  is a convex subset, the optimization problems in Eq. (5.47) and Eq. (5.53) are convex programs. Therefore, they can be solved by means of proper state-of-the-art quadratic programming techniques.

### 5.4.2 Eigenvector projection

Once the suitable passive modifications are obtained by solving the optimization problems in Eq. (5.47) and Eq. (5.53), the new space  $\hat{\psi}(\mu_k)$  can be defined by Eq. (5.35). However, due to the physical constraints represented by  $\Gamma$  and the numerical errors caused by the optimization algorithm, it is still not guaranteed that the desired eigenvector  $\mathbf{w}_k$  belongs to the new allowable space  $\hat{\psi}(\mu_k)$ . Therefore, the goal remains to assign the projection of the desired eigenvectors onto the new allowable space  $\hat{\psi}(\mu_k)$ , as explained in section 5.3.

Although this hybrid control method also assigns the projection of a desired eigenvector on allowable space  $\hat{\psi}(\mu_k)$  rather than the desired eigenvector itself, this projection is a better approximation of  $\mathbf{w}_k$  than the projection onto  $\psi(\mu_k)$ . This point will be shown in this chapter with numerical examples. Fig. 5.4 schematically represents the meaning of the passive modification. The passive modification is to allow the desired eigenvector to be assigned with a much better accuracy by state feedback control.

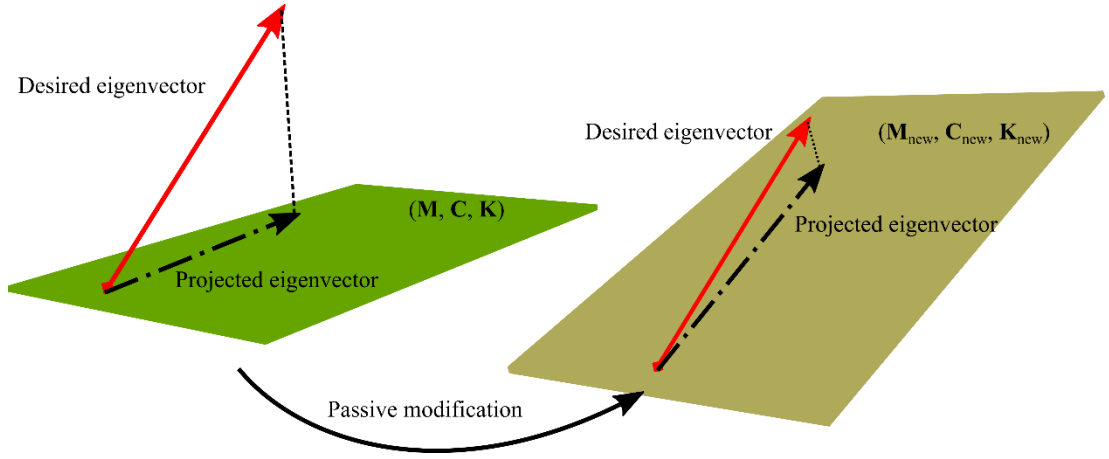


Fig. 5.4 The purpose of passive modification

### 5.4.3 Active control

After the feasible passive modifications are found such that the desired eigenvector  $\mathbf{w}_k$  belongs to a new allowable space  $\hat{\psi}(\mu_k)$ , the desired eigenpairs are to be assigned by active control. Now the problem is to find the gain matrices which can assign desired eigenpairs and keep the other eigenpairs unchanged. This step is similar to the receptance-based partial eigenvalue assignment method already covered in subsection 5.2.2.

For the desired eigenvalues, the scaling vectors  $\{\alpha_k\}_{k=1}^{2p}$  can be determined using Eq. (5.37) when the feasible passive modifications are found. Similarly, for those unchanged eigenvalues, the scaling vectors  $\{\alpha_k\}_{k=2p+1}^{2n}$  can be determined using Eq. (5.49).

Since the scaling vector is defined by

$$\alpha_k = (\mu_k \mathbf{F}^T + \mathbf{G}^T) \mathbf{w}_k, k = 1, 2, \dots, 2n \quad (5.54)$$

Eq. (5.54) can be reformed as

$$\begin{bmatrix} \mu_k \mathbf{w}_k^T & \mathbf{0} & \dots & \mathbf{0} & \mathbf{w}_k^T & \mathbf{0} & \dots & \mathbf{0} \\ \mathbf{0} & \mu_k \mathbf{w}_k^T & \dots & \mathbf{0} & \mathbf{0} & \mathbf{w}_k^T & \dots & \mathbf{0} \\ \vdots & \vdots & \ddots & \vdots & \vdots & \vdots & \ddots & \vdots \\ \mathbf{0} & \mathbf{0} & \dots & \mu_k \mathbf{w}_k^T & \mathbf{0} & \mathbf{0} & \dots & \mathbf{w}_k^T \end{bmatrix} \begin{bmatrix} \mathbf{f}_1 \\ \vdots \\ \mathbf{f}_{n_b} \\ \mathbf{g}_1 \\ \vdots \\ \mathbf{g}_{n_b} \end{bmatrix} = \begin{bmatrix} \alpha_{k1} \\ \alpha_{k2} \\ \vdots \\ \alpha_{k,n_b} \end{bmatrix} \quad (5.55)$$

or in a compact form

$$\mathbf{U}_k \mathbf{y} = \boldsymbol{\alpha}_k, k = 1, 2, \dots, 2n \quad (5.56)$$

Then the gain matrices can be obtained by solving the following equation

$$\begin{bmatrix} \mathbf{U}_1 \\ \vdots \\ \mathbf{U}_{2n} \end{bmatrix} \begin{bmatrix} \mathbf{f}_1 \\ \vdots \\ \mathbf{f}_i \\ \mathbf{g}_1 \\ \vdots \\ \mathbf{g}_i \end{bmatrix} = \begin{bmatrix} \boldsymbol{\alpha}_1 \\ \vdots \\ \boldsymbol{\alpha}_{2n} \end{bmatrix} \quad (5.57)$$

## 5.5 Numerical examples

The 5-DoF system in section 5.3.2 is reconsidered here. In section 5.3.2, it has been shown that the receptance-based active control method cannot achieve the partial eigenstructure assignment. Here, the hybrid method described in section 5.4 is used to achieve partial eigenstructure assignment.

Passive modifications are allowed to be applied on the five masses and five ground springs. The lower bound and upper bound for mass modifications are -1 kg and 2 kg, and the lower bound and upper bound for stiffness modifications are -50 kN/m and 50 kN/m.

### 5.5.1 Undamped systems

In this example, it is wanted to assign desired second and fourth natural frequencies, 39Hz and 55 Hz, and corresponding eigenvectors, as shown in Table 5.4. Besides, the other eigenpairs are supposed to be unchanged.

(1) Single input

Only one actuator is used and the force distribution vector is taken to be

$$\mathbf{b} = [1 \quad 2 \quad -2 \quad 1 \quad 1]^T$$

The receptance matrices at desired natural frequencies 39Hz and 55 Hz can be easily obtained from numerical simulation in this example. Then the vectors  $\mathbf{r}_k, k = 2, 4$  are obtained as

$$\mathbf{r}_2 = 10^{-4} \times [0.66 \quad 0.69 \quad -0.10 \quad 0.10 \quad 0.04]^T$$

$$\mathbf{r}_4 = 10^{-4} \times [-0.16 \quad -0.16 \quad 0.04 \quad 0.04 \quad -0.38]^T$$

The cosine of the angle between  $\mathbf{r}_k$  and  $\mathbf{w}_k$  is evaluated

$$\cos(\mathbf{w}_2, \mathbf{r}_2) = -0.0970 \text{ and } \cos(\mathbf{w}_4, \mathbf{r}_4) = -0.6513$$

Therefore, the receptance-based active control method cannot assign desired eigenvectors with good accuracy.

So, the hybrid control method is applied to solve this problem. The first step is to find feasible passive modifications such that the desired eigenvectors belong to the new allowable spaces. The required passive modifications are shown in Table 5.9, which are obtained by solving the optimization problems in Eq. (5.47) and Eq. (5.53).

Table 5.9 Structural modifications

Mass modification	$\delta m_1$	$\delta m_2$	$\delta m_3$	$\delta m_4$	$\delta m_5$
[kg]	-0.12	-0.18	0.54	1.60	2.00
Stiffness modification	$\delta k_{g1}$	$\delta k_{g2}$	$\delta k_{g3}$	$\delta k_{g4}$	$\delta k_{g5}$
[kN/m]	-18.4	-28.1	23.2	22.0	8.70

The desired eigenvectors are projected onto the new allowable spaces and the quantities of those projected eigenvectors are assessed with the cosine of the angle between each desired eigenvector and its projection. The computed cosines are 0.9887 and 0.9774, which indicate that the mode shapes can be assigned with good approximation.

Then the required gain vector in this example is

$$\mathbf{g}^T = 10^5 \times [0.24 \quad 0.67 \quad 2.55 \quad -3.27 \quad -2.17]^T$$

The dynamic equation of the closed-loop system is

$$\left( \mathbf{K} + \Delta\mathbf{K} - (2\pi f_k)^2 (\mathbf{M} + \Delta\mathbf{M}) \right) \mathbf{w}_k = \mathbf{b}\mathbf{g}^T \mathbf{w}_k, \quad k = 1, 2, \dots, 5$$

To demonstrate the superiority of the hybrid approach, the performances of the hybrid control method and active control method for the desired eigenpairs are assessed with two quantities, which are presented in Table 5.10. The assessments of the two methods on the spill-over problem are shown in Table 5.11.

Table 5.10 Eigenpair assignment comparison

	Active control		Hybrid control	
	2	4	2	4
Desired Mode	2	4	2	4
$ f_{k,obt} - f_{k,des} $ Hz	0	0	0	0
$\cos(\mathbf{v}_{k,des}, \mathbf{w}_{k,obt})$	0.10	0.52	0.99	0.98

Table 5.11 Spill-over assessment

	Active control			Hybrid control		
	1	3	5	1	3	5
Unchanged Mode	1	3	5	1	3	5
$ f_{k,origin} - f_{k,obt} $ Hz	0	0	0	0.06	0.62	0.13
$\cos(\mathbf{v}_{k,origin}, \mathbf{w}_{k,obt})$	1	1	1	1.00	0.99	1.00

The results show the hybrid control method can assign desired natural frequencies and eigenvectors with very good approximation. The spill-over problem can also be successfully avoided by the hybrid control method, although the active control may give better results.

## (2) Multiple inputs

Multiple inputs are adopted and the force distribution matrix  $\mathbf{B}$  is taken to be

$$\mathbf{B}^T = \begin{bmatrix} 1 & 0 & 0 & 0.5 & 0 \\ 0 & 1 & 0 & 0 & 0.5 \\ 0 & 0 & 1 & 0 & 0 \end{bmatrix}$$

The matrices  $\mathbf{R}_k$  can be easily obtained with the receptances at the desired natural frequencies. Then the suitable passive modifications are determined by solving the optimization problems in Eq. (5.47) and Eq. (5.53). The obtained required modifications  $\Delta\mathbf{M}$  and  $\Delta\mathbf{K}$  obtained are presented in Table 5.12.

With those passive modifications, the desired eigenvectors are projected onto the new allowable spaces  $\hat{\psi}(f_2)$  and  $\hat{\psi}(f_4)$ . The cosine of the angle between each desired eigenvector and its projection onto the new allowable space is evaluated. The mode shapes at 39 Hz and 55 Hz can be assigned with good accuracy, since the computed cosines are 0.99 and 0.98, respectively. This means that the desired eigenvectors are assignable with those passive modifications.

Table 5.12 Structural modifications

Mass modification	$\delta m_1$	$\delta m_2$	$\delta m_3$	$\delta m_4$	$\delta m_5$
[kg]	-0.17	-0.31	0.50	2.00	2.00
Stiffness modification	$\delta k_{g1}$	$\delta k_{g2}$	$\delta k_{g3}$	$\delta k_{g4}$	$\delta k_{g5}$
[kN/m]	-25.9	-47.7	10.0	35.1	12.4

Table 5.13 Eigenpair assignment comparison

	Active control		Hybrid control	
Desired Mode	2	4	2	4
$ f_{k,obt} - f_{k,des} $ Hz	0	0	0	0
$\cos(\mathbf{w}_{k,des}, \mathbf{w}_{k,obt})$	0.57	0.80	0.99	0.98

Table 5.14 Spill-over assessment

	Active control			Hybrid control		
Unchanged Mode	1	3	5	1	3	5
$ f_{k,origin} - f_{k,obt} $ Hz	0	0	0	0	0	0
$\cos(\mathbf{w}_{k,origin}, \mathbf{w}_{k,obt})$	1	1	1	1.00	1.00	1.00

Then the gain matrix  $\mathbf{G}$  can be calculated using Eq. (5.57) as

$$\mathbf{G}^T = 10^5 \times \begin{bmatrix} 0.71 & 1.97 & 7.54 & -9.67 & -6.05 \\ 1.88 & 5.41 & 20.27 & -26.17 & -16.18 \\ -0.91 & -2.51 & -9.38 & 12.03 & 7.42 \end{bmatrix}$$

Therefore, the closed-loop system is governed by

$$\left( \mathbf{K} + \Delta\mathbf{K} - (2\pi f_k)^2 (\mathbf{M} + \Delta\mathbf{M}) \right) \mathbf{w}_k = \mathbf{B}\mathbf{G}^T \mathbf{w}_k, \quad k = 1, 2, \dots, 5$$

Table 5.13 and Table 5.14 give the assessments of the performances of active control method and hybrid control method. It is obvious that the hybrid control method can assign desired eigenvectors with much better approximation than the active control method. Besides, the spill-over problem can also be overcome by the proposed hybrid control method.



### 5.5.2 Damped systems

This example is to assess the capability of the proposed hybrid control method to deal with complex eigenvalues and complex eigenvectors, which occur in the presence of damping. The considered vibrating system here is the same as the previous example, except for the presence of dampers. The damping matrix is chosen as  $\mathbf{C} = 10 \times \mathbf{I}_5$  ( $\mathbf{I}_5$  is the  $5 \times 5$  identity matrix).

The eigenvalues of this damped system are

$$\lambda_{1,2} = -0.41 \pm 139.98i, \lambda_{3,4} = -0.60 \pm 204.88i, \lambda_{5,6} = -1.17 \pm 269.68i$$

$$\lambda_{7,8} = -1.31 \pm 331.20i, \lambda_{9,10} = -1.58 \pm 405.73i$$

Table 5.15 shows the damped frequency and damping ratio for each mode. The desired eigenvalues and eigenvectors are given in Table 5.16. The desired eigenvalues are chosen to shift the damped frequencies to new locations and increase the damping ratios.

Table 5.15 Damped frequencies and damping ratios

	$\lambda_{1,2}$	$\lambda_{3,4}$	$\lambda_{5,6}$	$\lambda_{7,8}$	$\lambda_{9,10}$
$f_{k,\text{damped}}$ [Hz]	22.28	32.61	42.92	52.71	64.57
Damping ratio $\zeta_k$	0.0029	0.0029	0.0043	0.0040	0.0039

Table 5.16 Desired eigenpairs

	$\mu_{3,4} = -3 \pm 245.05i$	$\mu_{7,8} = -4 \pm 345.58i$
$f_{k,\text{damped}}$ [Hz]	39	55
Damping ratio $\zeta_k$	0.0122	0.0116
$w_{k,1}$	$0.0500 \mp 0.0000i$	$1.2000 \pm 0.0000i$
$w_{k,2}$	0	$0.3977 \pm 0.0058i$
$w_{k,3}$	$0.3759 \pm 0.0049i$	$0.1555 \pm 0.007i$
$w_{k,4}$	$2.471 \pm 0.0407i$	$0.1452 \pm 0.0019i$
$w_{k,5}$	$-3.3190 \mp 0.0346i$	0

Both the proposed hybrid control method and the receptance-based active control method are employed to solve the partial eigenstructure assignment problem. Table 5.17 shows the required passive modifications for this damped system with hybrid control method.

Table 5.17 Structural modifications

Mass modification	$\delta m_1$	$\delta m_2$	$\delta m_3$	$\delta m_4$	$\delta m_5$
[kg]	-0.12	0.24	0.25	-1.00	-1.00
Stiffness modification	$\delta k_{g1}$	$\delta k_{g2}$	$\delta k_{g3}$	$\delta k_{g4}$	$\delta k_{g5}$
[kN/m]	15.3	-50.0	7.14	39.7	-43.0

The performances of the two methods are also assessed by the two quantities: absolute eigenvalue error, cosine of the angle between the desired eigenvector and the obtained eigenvector. It is found that all the desired eigenvalues are assigned and the other eigenpairs are kept using the two methods. However, for the desired eigenvectors, for the active control method, the cosine of the angle between each desired eigenvector and the obtained one is

$$\cos(\mathbf{w}_{3,des}, \mathbf{w}_{3,obt}) = \cos(\mathbf{w}_{4,des}, \mathbf{w}_{4,obt}) = 0.79$$

$$\cos(\mathbf{w}_{7,des}, \mathbf{w}_{7,obt}) = \cos(\mathbf{w}_{8,des}, \mathbf{w}_{8,obt}) = 0.99$$

The obtained results show that the assigned eigenvectors corresponding to  $\mu_{7,8}$  are very close to the desired ones. However, the mode shapes corresponding to  $\mu_{3,4}$  are not very good.

With the hybrid control method, the cosines are calculated to be

$$\cos(\mathbf{w}_{3,des}, \mathbf{w}_{3,obt}) = \cos(\mathbf{w}_{4,des}, \mathbf{w}_{4,obt}) = 0.95$$

$$\cos(\mathbf{w}_{7,des}, \mathbf{w}_{7,obt}) = \cos(\mathbf{w}_{8,des}, \mathbf{w}_{8,obt}) = 0.99$$

All the desired eigenpairs can be successfully assigned. So, the hybrid control method can give much better results than the active control method.

### 5.5.3 Cantilever beam

A cantilever beam, which is discretised into three Euler-Bernoulli beam elements, is presented in this example, as pictured in Fig. 5.5. This example was studied by Belotti et al. [104] and it is taken as a benchmark here.

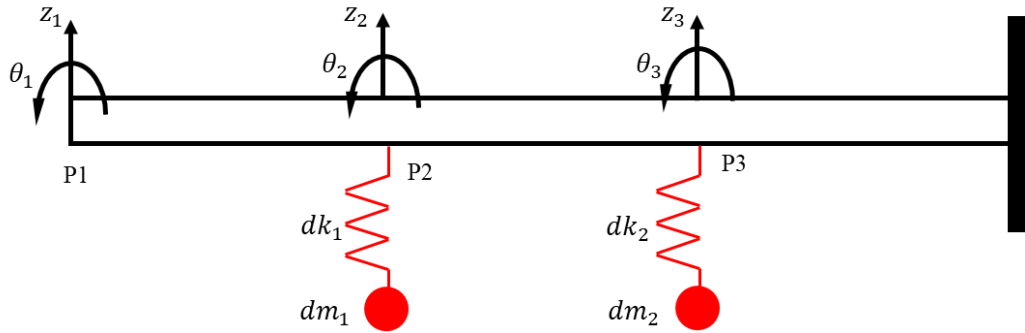


Fig. 5.5 A cantilever beam with two spring-mass modifications

The mass and stiffness matrices of the original cantilever beam are

$$\mathbf{M}_0 = \begin{bmatrix} 1.56 & 0.66 & 0.54 & -0.39 & 0 & 0 \\ 0.66 & 0.36 & 0.39 & -0.27 & 0 & 0 \\ 0.54 & 0.39 & 3.12 & 0 & 0.54 & -0.39 \\ -0.39 & -0.27 & 0 & 0.72 & 0.39 & -0.27 \\ 0 & 0 & 0.54 & 0.39 & 3.12 & 0 \\ 0 & 0 & -0.39 & -0.27 & 0 & 0.72 \end{bmatrix}$$

$$\mathbf{K}_0 = \begin{bmatrix} 12 & 18 & -12 & 18 & 0 & 0 \\ 18 & 36 & -18 & 18 & 0 & 0 \\ -12 & -18 & 24 & 0 & -12 & 18 \\ 18 & 18 & 0 & 72 & -18 & 18 \\ 0 & 0 & -12 & -18 & 24 & 0 \\ 0 & 0 & 18 & 18 & 0 & 72 \end{bmatrix}$$

The second row in Table 5.18 shows the eigenvalues of original system. It is wanted to increase the first eigenvalue to 0.3 while the others remain unchanged.

Table 5.18 Eigenvalues of the cantilever beam (Before and after controlled)

Mode	1	2	3	4	5	6
Original system	0.036	1.437	11.470	58.167	206.023	818.838
Hybrid controlled	<b>0.298</b>	1.444	11.484	58.167	206.027	818.839

Apart from the eigenvalues, it is also expected to change the first mode shape to create a node at point 2. Fig. 5.6 shows the original and desired first mode shapes. The value of the desired eigenvector is given in the second column in Table 5.19.

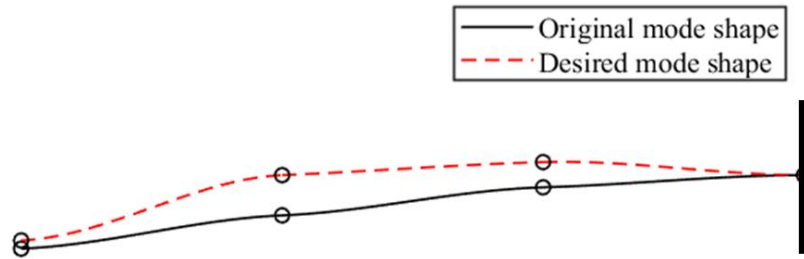


Fig. 5.6 The first mode shape of the cantilever beam

Table 5.19 Desired eigenvector and obtained eigenvector

	Desired eigenvector	Active control	Hybrid control
$\mathbf{w}_1$	0.500	1.000	0.010
	-0.086	-0.114	-0.004
	0	0.628	0
	-0.082	-0.129	-0.003
	-0.100	0.251	-0.004
	-0.057	-0.126	0.001
$\cos(\mathbf{w}_{\text{des}}, \mathbf{w}_{\text{obt}})$	-	0.78	0.95

The hybrid control method is used to achieve the partial eigenstructure assignment. The passive modifications in this example take the form of spring-mass oscillators at point 2 and point 3, as shown in Fig. 5.5. Although additional DoFs are introduced by the passive modifications, the proposed hybrid control method is applicable.

For the active control part, single-input state feedback control is adopted here and the force distribution vector  $\mathbf{b}$  is taken to be

$$\mathbf{b} = [1 \quad 0 \quad 2 \quad 0 \quad -1 \quad 0]^T$$

The needed passive modifications, presented in Table 5.20, are calculated by solving the optimization equations using the MATLAB built-in function *fmincon*.

Table 5.20 The parameters of passive modifications

$dm_1$	$dk_1$	$dm_2$	$dk_2$
7.540	0.031	0.128	0.038

Then the gain vector  $\mathbf{g}$  is obtained by solving Eq. (5.57) to be

$$\mathbf{g} = [0.215 \quad 0.102 \quad 0.266 \quad -0.043 \quad 0.097 \quad -0.029]^T$$

The resulted eigenvector corresponding to the first mode by hybrid control method is given in the fourth column in Table 5.19. It should be clarified that the two new DoFs created by the modifications are not included in the presented eigenvector.

To show the performance of this hybrid control method, the closed-loop eigenvector with only active control is also calculated. The same force distribution vector  $\mathbf{b}$  is used in the active control method.

It can be seen in Table 5.19 that the cosine of the angle between the desired eigenvector and the obtained eigenvector using hybrid control is 0.95, while the value for active control method is only 0.78. Therefore, the hybrid method can produce a much better approximation of the desired eigenvector than the active control method alone.

As for the unchanged eigenpairs, both hybrid control method and active control method can give good results. Table 5.21 shows the assessments of the spill-over with the two methods.

Table 5.21 Spill-over assessments

	Hybrid control				
Unchanged Mode	2	3	4	5	6
$ \omega_{k,origin}^2 - \omega_{k,obt}^2 $ Hz	0.01	0.02	0	0.01	0
$\cos(\mathbf{w}_{k,origin}, \mathbf{w}_{k,obt})$	1	1	1	1	1
	Active control				
Unchanged Mode	2	3	4	5	6
$ \omega_{k,origin}^2 - \omega_{k,obt}^2 $ Hz	0	0	0	0	0
$\cos(\mathbf{w}_{k,origin}, \mathbf{w}_{k,obt})$	1	1	1	1	1

## 5.6 Equivalent active control

The hybrid control method presented in section 5.4, employs both passive modification and active control. Since in theory any passive modification can be achieved by active control, it is easy to convert this hybrid method into a sole active control method. That is to say, the partial eigenstructure assignment can be achieved through a three-step active control method.

- (1) To find suitable passive modification which allows desired eigenvectors are achievable.
- (2) To get the required gain matrices of active control after passive modification.
- (3) To replace the passive modification with an equivalent active control.

Apparently, the sole active control method will usually require more energy or have high requirements on the inputs. A simple comparison between the hybrid control method and the three-step active control method is given in the following through a numerical example.

As shown in the example in subsection 5.5.1, the hybrid control can successfully achieve partial eigenstructure assignment with single input. The dynamic equation of the system with hybrid control is

$$\left( \mathbf{K} + \Delta\mathbf{K} - (2\pi f_k)^2 (\mathbf{M} + \Delta\mathbf{M}) \right) \mathbf{w}_k = \mathbf{b} \mathbf{g}^T \mathbf{w}_k$$

where the passive modifications  $\Delta\mathbf{M}$  and  $\Delta\mathbf{K}$  are given in Table 5.9.

The gain vector  $\mathbf{g}$  and the force distribution vector  $\mathbf{b}$  are

$$\mathbf{g}^T = 10^5 \times [0.24 \quad 0.67 \quad 2.55 \quad -3.27 \quad -2.17]^T$$

If a sole active control method is expected, the passive modification can be replaced by active control. To get an equivalent result, the active control will need to use the acceleration feedback because mass modifications are involved in the hybrid control method.

The passive modification can be written in the form of

$$\Delta \mathbf{M} = \mathbf{b}_2 \mathbf{f}_2^T + \mathbf{b}_3 \mathbf{f}_3^T + \mathbf{b}_4 \mathbf{f}_4^T + \mathbf{b}_5 \mathbf{f}_5^T + \mathbf{b}_6 \mathbf{f}_6^T$$

$$\Delta \mathbf{K} = \mathbf{b}_2 \mathbf{g}_2^T + \mathbf{b}_3 \mathbf{g}_3^T + \mathbf{b}_4 \mathbf{g}_4^T + \mathbf{b}_5 \mathbf{g}_5^T + \mathbf{b}_6 \mathbf{g}_6^T$$

By substituting the values in Table 5.9, a no-trivial solution can be found to be

$$[\mathbf{b}_2 \quad \mathbf{b}_3 \quad \mathbf{b}_4 \quad \mathbf{b}_5 \quad \mathbf{b}_6] = \begin{bmatrix} 1 & & & & \\ & 1 & & & \\ & & 1 & & \\ & & & 1 & \\ & & & & 1 \end{bmatrix}$$

$$[\mathbf{f}_2 \quad \mathbf{f}_3 \quad \mathbf{f}_4 \quad \mathbf{f}_5 \quad \mathbf{f}_6] = \begin{bmatrix} -0.12 & & & & \\ & -0.18 & & & \\ & & 0.54 & & \\ & & & 1.60 & \\ & & & & 2.00 \end{bmatrix}$$

$$[\mathbf{g}_2 \quad \mathbf{g}_3 \quad \mathbf{g}_4 \quad \mathbf{g}_5 \quad \mathbf{g}_6] = 10^3 \times \begin{bmatrix} -18.4 & & & & \\ & -28.1 & & & \\ & & 23.2 & & \\ & & & 22.0 & \\ & & & & 8.70 \end{bmatrix}$$

Then the dynamic equation of the closed-loop system with sole active control can be written as

$$\left( \mathbf{K} - \omega_k^2 (\mathbf{M} + \Delta \mathbf{M}) \right) \mathbf{w}_k = \left( \sum_{i=2}^6 \mathbf{b}_i (\omega_k^2 \mathbf{f}_i^T + \mathbf{g}_i^T) + \mathbf{b} \mathbf{g}^T \right) \mathbf{w}_k$$

Apparently, more actuators and the acceleration responses are needed in the sole active control method in this example. Therefore, the hybrid method will be more efficient or convenient when passive modification is allowed.

## 5.7 Discussions

The previous sections show that the hybrid control can achieve partial eigenstructure assignment. However, it is not guaranteed that the hybrid control method can always assign the desired eigenvectors with good approximations. The performances of assignment may be affected by many factors, such as the number of actuators, the number of masses receiving actuations or physical constraints. In this section, the effects of the number of the actuators and the number of masses receiving actuations are discussed through a numerical example.

Since a main purpose of this particular research is to evaluate the effect of the number of actuators, a large-DoF model is used. The vibrating system studied is a mass-spring chain, as shown in Fig. 5.7. The system has 20 degrees of freedom. All the masses are 1 kg and all the stiffnesses are 10 kN/m. Only one eigenpair is assigned, for simplicity of presentation. The desired frequency is 2.5 Hz and the associated eigenvector is shown in Table 5.22. Such values of the eigenvector components have been chosen as uniformly distributed random numbers in the interval of  $[-1, 1]$ .

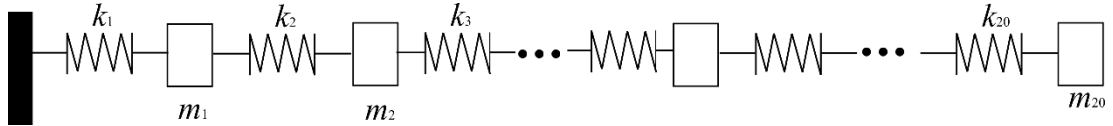


Fig. 5.7 A 20-DoF system

Table 5.22 Desired eigenvector for the twenty-degree of freedom system

$w_1$	$w_2$	$w_3$	$w_4$	$w_5$	$w_6$	$w_7$	$w_8$	$w_9$	$w_{10}$
0.63	0.81	-0.75	0.83	0.26	-0.80	-0.44	0.09	0.92	0.93
$w_{11}$	$w_{12}$	$w_{13}$	$w_{14}$	$w_{15}$	$w_{16}$	$w_{17}$	$w_{18}$	$w_{19}$	$w_{20}$
-0.68	0.94	0.91	-0.03	0.60	-0.72	-0.16	0.83	0.58	0.92

The constraints on the physical modifications are  $-0.5 \leq \delta m_i \leq 2$  kg and  $-0.5 \leq \delta k_i \leq 10$  kN/m, for  $i = 1, 2, \dots, 20$ .

(1) The effect of the number of actuators

The number of actuators is reflected by the number of columns of matrix  $\mathbf{B}$ . In this example, matrix  $\mathbf{B}$  is defined by the first  $n_b$  columns of the identity matrix  $\mathbf{I}_{20}$ . With this definition, the number of actuators also indicates the number of masses receiving actuations.

The performances of the proposed hybrid control method with different numbers of actuators are evaluated through the cosine of the angle between the desired eigenvector and the obtained eigenvector. The results are shown in Fig. 5.8, which indicates that the hybrid control method has a better performance with more actuators.



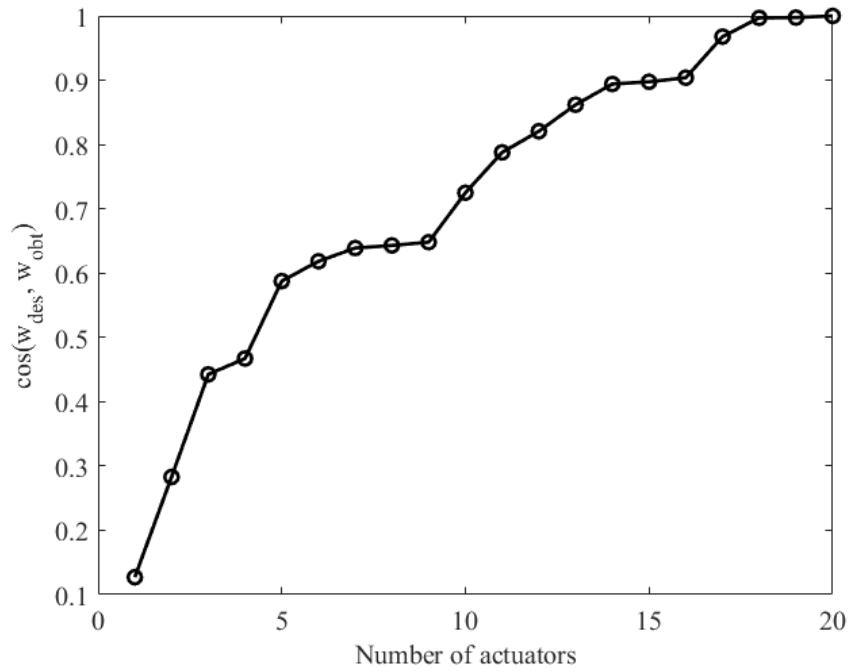


Fig. 5.8 Comparison of the performances with different number of actuators

(2) The effects of the number of masses receiving actuations

In the above example, the number of masses receiving actuations is equal to the number of actuators. With the same number of actuators, the number of masses receiving actuations may also affect the performance of the proposed hybrid control method.

For example, if only one actuator is used, the obtained results will be better if more masses receive actuations, as shown in Fig. 5.9. Although the result is still not very good when 20 masses are under-actuated, the results are still found to be better if more masses are with actuations.

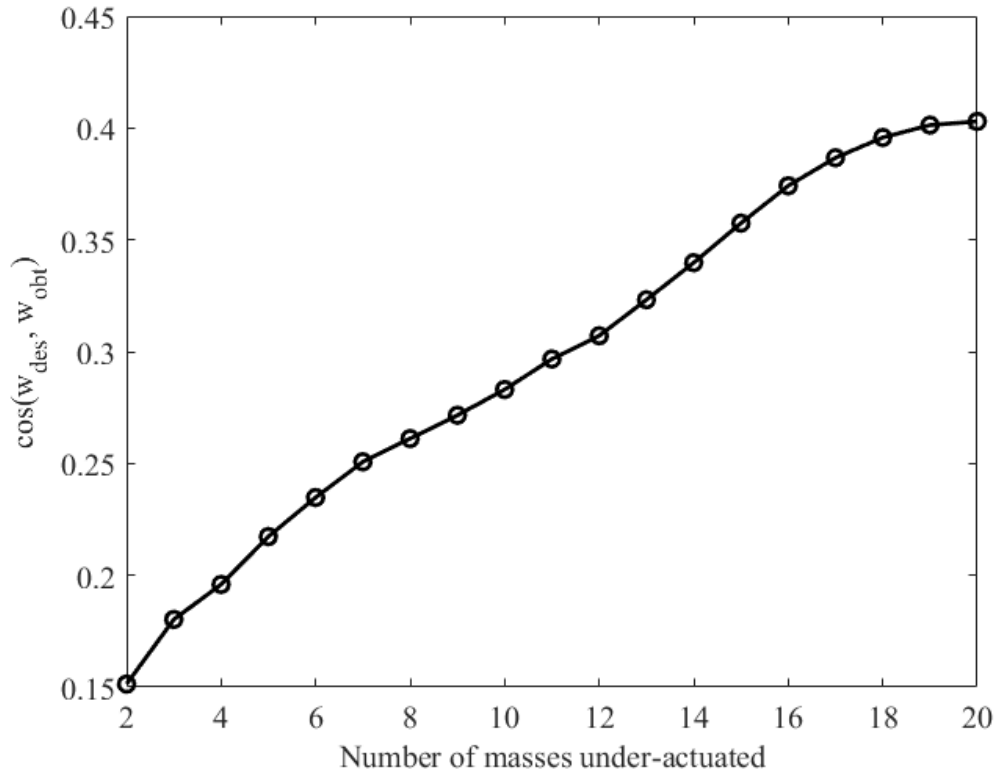


Fig. 5.9 The effects of the number of masses under-actuated

## 5.8 Conclusions

This chapter presents a receptance-based partial eigenstructure assignment method with hybrid control. This method is the first method that can achieve partial eigenstructure assignment with receptance.

Although partial eigenvalue assignment can be easily achieved by receptance-based active control, desired eigenvectors are not guaranteed to be assignable with the existing receptance-based active control methods in general. To overcome the above-mentioned limitation of receptance-based active control method, passive modifications are introduced to combine state feedback control to enable accurate assignment of the desired eigenvectors too. The required structural modifications, which are usually mass and stiffness modifications, are determined by solving optimization equations. It should be noted that it is not guaranteed that the proposed hybrid control method can always assign the desired eigenvectors very accurately. The performances of the hybrid control method may be affected by some factors, such as the number of actuators, the number of masses receiving actuations or physical constraints.

On the other hand, this proposed hybrid control method requires the receptances and the eigenvectors corresponding to those unchanged eigenvalues. Although these eigenvectors could be measured, the efforts to get accurate eigenvectors are big and in practice it is impossible to measure a whole eigenvector. Therefore, the next chapter will present a receptance-based partial eigenstructure assignment method which does not need the knowledge of eigenvectors of the open-loop system.

## Chapter 6

# Receptance-based partial eigenstructure assignment with state feedback control

### 6.1 Introduction

The partial eigenvalue assignment problem is a mathematically challenging problem, particularly when the mathematical description is cast in the second-order formulation framework. Previous methods require either system matrices [19, 107, 109, 110, 119, 131], such as mass, damping or stiffness matrix, or the eigenvectors of open-loop systems [3, 116]. A powerful approach proposed and used in recent years required measured receptances. Following this approach, in chapter 5, a receptance-based partial eigenstructure assignment method with hybrid control is proposed. This hybrid method also needs the eigenvectors of the open-loop system. In practice, not only the system matrices are not easy to obtain or are not very accurate, but also the efforts to get accurate eigenvectors are very big.

To avoid the requirement on eigenvectors of open-loop systems, a new receptance-based partial eigenvalue/eigenstructure assignment method by multiple-input active control is presented in this chapter. Only part of the receptance matrix of the original system is required in this method. In addition, this method can simultaneously assign eigenvalues and the associated eigenvectors, including assigning nodes at desired locations.

One thing that needs to be highlighted in this proposed method is that unlike the method described in chapter 5, the force distribution matrix  $\mathbf{B}$  is not predefined in the method proposed in this chapter and there may be unknown elements in matrix  $\mathbf{B}$  to be determined. This kind of strategy was also used in references [3, 127], in which matrix  $\mathbf{B}$  depends on physical matrices or eigenvectors of the open-loop system. The

method proposed in this chapter determines matrix  $\mathbf{B}$  using receptances as part of its solution procedure.

Three numerical examples are used to validate the proposed method and demonstrate the role of the control efforts. The robustness of the proposed method is analysed through Monte-Carlo simulations. Numerical results show that this method is robust where there are 5% variations of receptance matrices for a four-DoF damped system.

This chapter reports the first attempt to make partial eigenvalue/eigenstructure assignment in the second-order eigenvalue framework using only receptances. A large part of this chapter was written into a paper by the author of this thesis and his supervisor, Huajiang Ouyang as [180]:

S. Zhang, H. Ouyang, Receptance-based partial eigenstructure assignment by state feedback control. This paper was submitted to the journal *Mechanical systems and signal processing*, and it is under review now.

## 6.2 The effect of eigenvectors of open-loop systems on spill-over problem

### 6.2.1 The requirement of eigenvectors of open-loop systems

A receptance-based partial eigenvalue assignment method was introduced by Ram and Mottershead [116], as also briefly described in chapter 5. For simplicity, the method by Ram and Mottershead is named Method RM. Method RM could avoid the requirement on system matrices while it still needs the knowledge of eigenvectors of the open-loop system. A brief review on this method is presented below.

The quadratic eigenvalue problems corresponding to the open-loop and closed-loop systems, respectively, are given by

$$(\lambda_k^2 \mathbf{M} + \lambda_k \mathbf{C} + \mathbf{K}) \mathbf{v}_k = 0, \quad k = 1, 2, \dots, 2n \quad (6.1)$$

$$(\mu_k^2 \mathbf{M} + \mu_k \mathbf{C} + \mathbf{K}) \mathbf{w}_k = \mathbf{B}(\mu_k \mathbf{F}^T + \mathbf{G}^T) \mathbf{w}_k, \quad k = 1, 2, \dots, 2n \quad (6.2)$$

The  $2n$  eigenvalues  $\{\lambda_k\}_{k=1}^{2n}$  with corresponding eigenvectors  $\{\mathbf{v}_k\}_{k=1}^{2n}$  in Eq. (6.1) are the eigenpairs of the open-loop system. Similarly,  $\{\mu_k\}_{k=1}^{2n}$  and  $\{\mathbf{w}_k\}_{k=1}^{2n}$  in Eq. (6.2) are the eigenpairs of the closed-loop system.

A subset of eigenvalues of the open-loop system  $\{\lambda_k\}_{k=1}^{2p}$  is required to be shifted to desired locations  $\{\mu_k\}_{k=1}^{2p}$ . Meanwhile, to avoid spill-over, it is further requested that the other eigenvalues are unchanged.

For the  $2(n - p)$  invariant eigenvalues, it is assumed that

$$\mu_k = \lambda_k, \mathbf{w}_k = \mathbf{v}_k, \quad k = 2p + 1, \dots, 2n \quad (6.3)$$

Substituting Eq. (6.3) into Eq. (6.2) gives

$$(\lambda_k^2 \mathbf{M} + \lambda_k \mathbf{C} + \mathbf{K}) \mathbf{v}_k = \mathbf{B}(\lambda_k \mathbf{F}^T + \mathbf{G}^T) \mathbf{v}_k, \quad k = 2p + 1, \dots, 2n \quad (6.4)$$

Then it can be obtained that

$$\mathbf{B}(\lambda_k \mathbf{F}^T + \mathbf{G}^T) \mathbf{v}_k = \mathbf{0}, \quad k = 2p + 1, \dots, 2n \quad (6.5)$$

Eq. (6.5) could be expanded as

$$\left( \mathbf{b}_1(\lambda_k \mathbf{f}_1^T + \mathbf{g}_1^T) + \dots + \mathbf{b}_{n_b}(\lambda_k \mathbf{f}_{n_b}^T + \mathbf{g}_{n_b}^T) \right) \mathbf{v}_k = \mathbf{0}, \quad k = 2p + 1, \dots, 2n \quad (6.6)$$

Eq. (6.6) can be satisfied whenever

$$\begin{bmatrix} \lambda_k \mathbf{v}_k^T & \mathbf{0} & \dots & \mathbf{0} & \mathbf{v}_k^T & \mathbf{0} & \dots & \mathbf{0} \\ \mathbf{0} & \lambda_k \mathbf{v}_k^T & \dots & \mathbf{0} & \mathbf{0} & \mathbf{v}_k^T & \dots & \mathbf{0} \\ \vdots & \vdots & \vdots & \vdots & \vdots & \vdots & \vdots & \vdots \\ \mathbf{0} & \mathbf{0} & \dots & \lambda_k \mathbf{v}_k^T & \mathbf{0} & \mathbf{0} & \dots & \mathbf{v}_k^T \end{bmatrix} \begin{bmatrix} \mathbf{f}_1 \\ \vdots \\ \mathbf{f}_{n_b} \\ \mathbf{g}_1 \\ \vdots \\ \mathbf{g}_{n_b} \end{bmatrix} = \begin{bmatrix} 0 \\ 0 \\ 0 \\ 0 \\ 0 \\ 0 \end{bmatrix} \quad (6.7)$$

Apparently, to calculate the gain matrices, it is required to know the open-loop eigenvectors  $\{\mathbf{v}_k\}_{k=2p+1}^{2n}$ .

### 6.2.2 The effect of open-loop eigenvectors on spill-over problem

The knowledge of eigenvectors of the open-loop system will affect the performance of the spill-over problem. For example, if the eigenvectors of the open-loop system are not very accurate, the eigenvalues which are expected to be unchanged may not be kept well enough. This is explained through a numerical example below.

**Example:** Consider an open-loop 4-DoF mass-damper-spring system with

$$\mathbf{M} = \begin{bmatrix} 1 & & & \\ & 2 & & \\ & & 2 & \\ & & & 1 \end{bmatrix}, \mathbf{C} = \begin{bmatrix} 1 & -1 & & \\ -1 & 2 & -1 & \\ & -1 & 2 & -1 \\ & & -1 & 1 \end{bmatrix}$$

$$\mathbf{K} = \begin{bmatrix} 2.5 & -0.5 & & \\ -0.5 & 1 & -0.5 & \\ & -0.5 & 2 & -1.5 \\ & & -1.5 & 2 \end{bmatrix}$$

shown in Fig. 6.1.

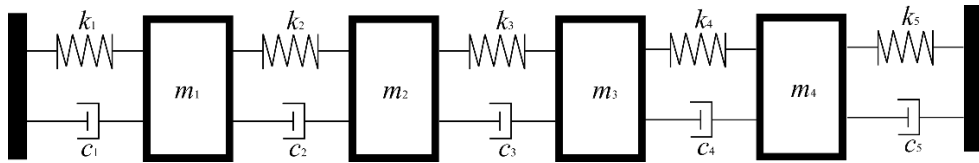


Fig. 6.1 A 4-DoF system

The eigenvalues and their corresponding eigenvectors of this system are listed in Table 6.1.

Table 6.1 Eigenstructure of the open-loop system

	$\lambda_{1,2}$	$\lambda_{3,4}$	$\lambda_{5,6}$	$\lambda_{7,8}$
	$-0.06 + 0.42i$	$-0.67 + 0.60i$	$-0.50 \pm 1.29i$	$-0.77 \pm 1.36i$
$\mathbf{v}_k$	$1.00 \pm 0.00i$	$1.00 \pm 0.00i$	$1.00 \pm 0.00i$	$1.00 \pm 0.00i$
	$3.14 \mp 2.14i$	$-1.18 \mp 2.86i$	$0.01 \mp 0.46i$	$-0.59 \mp 0.23i$
	$4.20 \mp 2.33i$	$0.90 \pm 1.13i$	$0.00 \pm 0.02i$	$-0.10 \mp 1.25i$
	$3.63 \mp 1.66i$	$-0.10 \pm 1.02i$	$-0.25 \pm 0.27i$	$1.33 \pm 2.27i$

It is expected that the first two pairs of eigenvalues are to be changed to desired eigenvalues and the remaining two pairs of eigenvalues stay unchanged, as shown below

$$\mu_{1,2} = -0.50 \pm 0.50i, \quad \mu_{3,4} = -0.90 \pm 0.80i,$$

$$\mu_{5,6} = -0.50 \pm 1.29i, \quad \mu_{7,8} = -0.77 \pm 1.36i$$

With accurate eigenvectors of the original system known, Method RM can certainly find the closed-loop system with expected eigenvalues. However, it is to be considered

the scenario that the measured eigenvectors of the open-loop system are inaccurate. For example, the measured eigenvectors associated with the unchanged eigenvalues  $\lambda_{5,6}$  and  $\lambda_{7,8}$  are

$$\mathbf{v}_5^* = \bar{\mathbf{v}}_6^* = [1.00 + 0.00i \quad 0.02 - 0.69i \quad 0.00 + 0.02i \quad -0.10 + 0.11i]^T$$

$$\mathbf{v}_7^* = \bar{\mathbf{v}}_8^* = [1.00 + 0.00i \quad -0.24 - 0.09i \quad -0.02 - 0.25i \quad 1.33 + 2.27i]^T$$

Each eigenvector has two elements that are different from the true values. The cosines of the angles between the obtained eigenvectors and the true eigenvectors are 0.97 and 0.94, respectively. This means that the obtained eigenvectors are quite close with true eigenvectors, although there are differences.

If the force distribution matrix  $\mathbf{B}$  is predefined as

$$\mathbf{B} = \begin{bmatrix} 1 & -1 & 2 & 1 \\ 0.5 & 1 & 2 & 1 \\ -2 & -1 & 0.5 & 1 \\ -1 & 2 & 1.5 & 0.5 \end{bmatrix}$$

By applying Method RM, the eigenvalues of obtained closed-loop system are

$$\mu_{1,2}^* = -0.50 \pm 0.50i, \quad \mu_{3,4}^* = -0.90 \pm 0.80i,$$

$$\mu_{5,6}^* = -0.52 \pm 1.18i, \quad \mu_{7,8}^* = -0.57 \pm 1.55i$$

The resulting eigenvalues  $\mu_{5,6}^*$  and  $\mu_{7,8}^*$  are not the same as the original values  $-0.50 \pm 1.29i$  and  $-0.77 \pm 1.36i$  (to stay unchanged), though. This means that Method RM is not able to achieve accurate partial eigenvalue assignment when the eigenvectors of the open-loop system are inaccurate and thus it is not robust. In this case, a method which does not need the eigenvectors of open-loop systems, will be more suitable.

### 6.3 Receptance-based partial eigenstructure assignment method

As explained in the last section, Method RM has an assumption that the eigenvectors of the closed-loop system corresponding to invariant eigenvalues are the same as the eigenvectors of the open-loop system. This assumption leads to the requirement of the knowledge of eigenvectors of the open-loop system. Although these eigenvectors could be measured, the efforts to get accurate eigenvectors is very big and in practice



it is impossible to measure a whole eigenvector. Therefore, it is worth exploring a method which does not need the eigenvectors of the open-loop system. For simplicity, the method proposed in this section is named Method NA.

Method NA has major differences compared with Method RM. To help understand this new method, they are listed here.

(a) The eigenvectors of the closed-loop system corresponding to the invariant eigenvalues do not have to be identical to the eigenvectors of the open-loop system in Method NA. During the procedure of Method NA, the eigenvectors of closed-loop system corresponding to the unchanged eigenvalues,  $\{\mathbf{w}_k\}_{k=2p+1}^{k=2n}$  are self-defined. Without knowing the  $\{\mathbf{v}_k\}_{k=2p+1}^{k=2n}$ , there is a very low possibility that  $\{\mathbf{w}_k\}_{k=2p+1}^{k=2n}$  equals  $\{\mathbf{v}_k\}_{k=2p+1}^{k=2n}$ . Method NA is still applicable in this situation. This means Method NA can keep certain eigenpairs unchanged and assign some desired eigenpairs. Compared with Method RM, one advantage in Method NA is that it is not necessary to make sure  $\{\mathbf{w}_k\}_{k=2p+1}^{k=2n} = \{\mathbf{v}_k\}_{k=2p+1}^{k=2n}$ . Therefore, there is no need to evaluate  $\{\mathbf{v}_k\}_{k=2p+1}^{k=2n}$ .

(b) Unlike Method RM which specifies matrix  $\mathbf{B}$  a priori, matrix  $\mathbf{B}$  in this new method is allowed to have unknown elements. In a real engineering application, based on the number of actuators available and the positions (DoFs) of the structure where the actuators can be attached, some elements of  $\mathbf{B}$  are predefined and some other elements are left unknowns. Doing so allows an engineer to take into account the number of actuators available and any restrictions on actuator deployment on the structure, and at the same time retain the freedom of tailoring part of  $\mathbf{B}$  to achieve the goal of partial eigenstructure assignment. In fact, leaving some  $\mathbf{B}$  elements to be determined is found to lead to solutions that need fewer actuators than specifying  $\mathbf{B}$  a priori in Method NA

(c) The desired eigenvectors of the closed-loop system are also be assigned to improve the dynamic behaviour of the vibration system.

(d) Instead of arbitrarily choosing the scaling vectors  $\alpha_k$ , they can be determined during the process.

### 6.3.1 Method derivation

This new method consists of two steps: (1) to determine the force distribution matrix  $\mathbf{B}$  and scaling vectors  $\boldsymbol{\alpha}_k$ ; (2) to calculate the gain matrices  $\mathbf{F}$  and  $\mathbf{G}$ .

- Matrix  $\mathbf{B}$  and scaling vectors  $\boldsymbol{\alpha}_k$

The first step in Method NA is to determine the force distribution matrix  $\mathbf{B}$  and scaling vectors  $\boldsymbol{\alpha}_k$ .

Suppose a known mass modification matrix  $\Delta\mathbf{M}$  is added on the left side of Eq. (6.2), an equilibrium force  $\mu_k^2\Delta\mathbf{M}\mathbf{w}_k$  should be added on the right side to maintain satisfaction of Eq. (6.2). This modification matrix  $\Delta\mathbf{M}$  can be chosen arbitrarily as long as those invariant eigenvalues  $\{\lambda_k\}_{k=2p+1}^{2n}$  are not the eigenvalues of the modified system. One thing that must be made clear is that this mass modification, is only used for the easy determination of matrix  $\mathbf{B}$  and scaling vectors  $\boldsymbol{\alpha}_k$  and it is not applied to the closed-loop system in the actual modification.

For those invariant eigenvalues, Eq. (6.2), with the modification matrix, can be written as

$$(\lambda_k^2(\mathbf{M} + \Delta\mathbf{M}) + \lambda_k\mathbf{C} + \mathbf{K})\mathbf{w}_k = \mathbf{B}(\lambda_k\mathbf{F}^T + \mathbf{G}^T)\mathbf{w}_k + \lambda_k^2\Delta\mathbf{M}\mathbf{w}_k \quad (6.8)$$

where  $k = 2p + 1, \dots, 2n$ .

Define another mass-modified receptance matrix  $\hat{\mathbf{H}}_k = (\lambda_k^2(\mathbf{M} + \Delta\mathbf{M}) + \lambda_k\mathbf{C} + \mathbf{K})^{-1}$ . The receptance matrix of the mass-perturbed system can be (i) obtained from experiments, or (ii) derived from the receptance matrix of the original system directly and easily, by means of the Woodbury matrix identity (please see the subsection 3.2.2). For option (i), although it seems that an extra measurement of a receptance matrix may be needed in this method, the increase of measurement workload is a small price to pay for avoiding the measurement of the open-loop eigenvectors, which is very difficult to achieve.

Pre-multiplying Eq. (6.8) by  $\hat{\mathbf{H}}_k$  gives

$$\mathbf{w}_k = \hat{\mathbf{H}}_k\mathbf{B}(\lambda_k\mathbf{F}^T + \mathbf{G}^T)\mathbf{w}_k + \lambda_k^2\hat{\mathbf{H}}_k\Delta\mathbf{M}\mathbf{w}_k, \quad k = 2p + 1, \dots, 2n \quad (6.9)$$

It can be rearranged as

$$(\mathbf{I} - \lambda_k^2 \widehat{\mathbf{H}}_k \Delta \mathbf{M}) \mathbf{w}_k = \widehat{\mathbf{H}}_k \mathbf{B} (\lambda_k \mathbf{F}^T + \mathbf{G}^T) \mathbf{w}_k, \quad k = 2p + 1, \dots, 2n \quad (6.10)$$

If the eigenvectors of the closed-loop system are pre-defined, the left-hand side of the above equation can be denoted as

$$(\mathbf{I} - \lambda_k^2 \widehat{\mathbf{H}}_k \Delta \mathbf{M}) \mathbf{w}_k = \mathbf{p}_k, \quad k = 2p + 1, \dots, 2n \quad (6.11)$$

Using the scaling vector  $\boldsymbol{\alpha}_k$  defined in Eq. (5.18), Eq. (6.10) and Eq. (6.11) lead to

$$\mathbf{p}_k = \widetilde{\mathbf{H}}_k \mathbf{B} \boldsymbol{\alpha}_k, \quad k = 2p + 1, \dots, 2n \quad (6.12)$$

For those desired eigenvalues, pre-multiplying Eq. (6.2) by receptance matrix  $\mathbf{H}_k$  gives

$$\mathbf{w}_k = \mathbf{H}_k \mathbf{B} \boldsymbol{\alpha}_k, \quad k = 1, 2, \dots, 2p \quad (6.13)$$

where  $\mathbf{H}_k = (\lambda_k^2 \mathbf{M} + \lambda_k \mathbf{C} + \mathbf{K})^{-1}$ .

Eq. (6.12) and Eq. (6.13) can be written into one equation

$$\mathbf{B} \boldsymbol{\alpha}_k = \mathbf{v}_k, \quad k = 1, 2, \dots, 2n \quad (6.14)$$

where  $\mathbf{B} \in \mathcal{R}^{n \times n_b}$ , and

$$\mathbf{v}_k = \begin{cases} \mathbf{H}_k^{-1} \mathbf{w}_k, & k = 1, 2, \dots, 2p \\ \widehat{\mathbf{H}}_k^{-1} \mathbf{p}_k, & k = 2p + 1, 2p + 2, \dots, 2n \end{cases} \quad (6.15)$$

For each pair of complex-conjugate eigenvalues  $\mu_k$  and  $\mu_{k+1}$  ( $k = 1, 3, \dots, 2n - 1$ ), the following equation can be obtained

$$\mu_k = \bar{\mu}_{k+1}, \quad \boldsymbol{\alpha}_{\mu_k} = \bar{\boldsymbol{\alpha}}_{\mu_{k+1}}, \quad \mathbf{v}_k = \bar{\mathbf{v}}_{k+1} \quad (k = 1, 3, \dots, 2n - 1) \quad (6.16)$$

Then the problem is to determine matrix  $\mathbf{B}$  and scaling vectors  $\boldsymbol{\alpha}_k$  by solving the following equation

$$\mathbf{B} \widehat{\mathbf{A}} = \mathbf{Y} \quad (6.17)$$

where  $\widehat{\mathbf{A}} \in \mathbb{C}^{n_b \times n}$ ,  $\mathbf{Y} \in \mathbb{C}^{n \times n}$  and

$$\widehat{\mathbf{A}} = [\boldsymbol{\alpha}_1, \boldsymbol{\alpha}_3, \dots, \boldsymbol{\alpha}_{2n-1}]$$

$$\mathbf{Y} = [\mathbf{v}_1, \mathbf{v}_3, \dots, \mathbf{v}_{2n-1}]$$

In damped vibrating systems, both  $\widehat{\mathbf{A}}$  and  $\mathbf{Y}$  are complex matrices. For simplification, let

$$\widehat{\mathbf{A}}_{\text{real}} = \text{Real}(\widehat{\mathbf{A}}) \text{ and } \widehat{\mathbf{A}}_{\text{imag}} = \text{Imag}(\widehat{\mathbf{A}})$$

$$\mathbf{Y}_{\text{real}} = \text{Real}(\mathbf{Y}) \text{ and } \mathbf{Y}_{\text{imag}} = \text{Imag}(\mathbf{Y})$$

Eq. (6.17) can be rewritten as

$$\mathbf{B}[\widehat{\mathbf{A}}_{\text{real}} \quad \widehat{\mathbf{A}}_{\text{imag}}] = [\mathbf{Y}_{\text{real}} \quad \mathbf{Y}_{\text{imag}}] \quad (6.18)$$

Then Eq. (6.18) is reformed as

$$\mathbf{B}\widetilde{\mathbf{A}} = \widetilde{\mathbf{Y}} \quad (6.19)$$

where  $\widetilde{\mathbf{A}} \in \mathcal{R}^{n_b \times 2n}$ ,  $\widetilde{\mathbf{Y}} \in \mathcal{R}^{n \times 2n}$  with obvious definitions.

Both matrices  $\mathbf{B}$  and  $\widehat{\mathbf{A}}$  may have unknown elements. To guarantee that Eq. (6.19) has solutions, a simple assumption is made that the number of unknowns in Eq. (6.19) is no smaller than the number of equations. There will be multiple solutions under this assumption. On the other hand, if all the elements in matrix  $\mathbf{B}$  and  $\widehat{\mathbf{A}}$  are assumed to be unknown, it is usually difficult to get good solutions.

In this chapter, a  $(n_b \times n_b)$  invertible matrix block in matrix  $\mathbf{B}$ , is pre-determined to simplify the calculations of matrix  $\mathbf{B}$  and scaling matrix  $\widehat{\mathbf{A}}$ . Therefore, the number of inputs  $n_b$  had better satisfy

$$(n \times n_b + n_b \times 2n - n_b^2) \geq n \times 2n \quad (6.20)$$

Eq. (6.20) equals to

$$(n_b - n)(n_b - 2n) \leq 0$$

So, the following requirement on the number of inputs can be obtained

$$n \leq n_b \leq 2n \text{ and } n_b \text{ is an integer number} \quad (6.21)$$

Since the number of inputs should be smaller than or equal to the number of degrees of freedom. It means

$$n_b \leq n \quad (6.22)$$

Therefore, the number of actuators should satisfy  $n_b = n$ ,

It has to be noted that this requirement on the number of inputs is not always necessary. The number of inputs is good enough as long as Eq. (6.19) can be solved. The proposed requirement in this paper is to reduce the efforts of calculations and minimize the numerical errors when solving Eq. (6.19).

The above derivation is based on damped systems while it is also suitable for undamped systems. However, the requirement on the number of actuators for an undamped system is different from the requirement for a damped system. For an undamped system, there is no imaginary part in Eq. (6.17). So, similar to Eq. (6.20), to make sure the number of independent variables is not smaller than the number of equations in Eq. (6.17), the number of actuators had better satisfy the following equation

$$(n \times n_b + n_b \times n - n_b^2) \geq n \times n \quad (6.23)$$

Therefore, the number of actuators should also follow  $n_b = n$  for an undamped system.

- Gain matrices **F** and **G**

In the first step, the force distribution matrix **B** and scaling matrix  $\hat{\mathbf{A}}$  have been obtained. Since  $\alpha_{kj} = (\mu_k \mathbf{f}_j^T + \mathbf{g}_j^T) \mathbf{w}_k$  ( $j = 1, 2, \dots, n_b$ ), it can be obtained that

$$\begin{bmatrix} \mu_k \mathbf{w}_k^T & \mathbf{0} & \cdots & \mathbf{0} & \mathbf{w}_k^T & \mathbf{0} & \cdots & \mathbf{0} \\ \mathbf{0} & \mu_k \mathbf{w}_k^T & \cdots & \mathbf{0} & \mathbf{0} & \mathbf{w}_k^T & \cdots & \mathbf{0} \\ \vdots & \vdots & \vdots & \vdots & \vdots & \vdots & \vdots & \vdots \\ \mathbf{0} & \mathbf{0} & \cdots & \mu_k \mathbf{w}_k^T & \mathbf{0} & \mathbf{0} & \cdots & \mathbf{w}_k^T \end{bmatrix} \begin{bmatrix} \mathbf{f}_1 \\ \vdots \\ \mathbf{f}_{n_b} \\ \mathbf{g}_1 \\ \vdots \\ \mathbf{g}_{n_b} \end{bmatrix} = \begin{bmatrix} \alpha_{k1} \\ \alpha_{k2} \\ \vdots \\ \alpha_{k,n_b} \end{bmatrix} \quad (6.24)$$

or in a compact form

$$\tilde{\mathbf{U}}_k \mathbf{y} = \alpha_k, \quad k = 1, \dots, 2n \quad (6.25)$$

Then gain matrices **F** and **G** can be calculated by solving the following equation

$$\begin{bmatrix} \tilde{\mathbf{U}}_1 \\ \vdots \\ \tilde{\mathbf{U}}_{2n} \end{bmatrix} \begin{bmatrix} \mathbf{f}_1 \\ \vdots \\ \mathbf{f}_{n_b} \\ \mathbf{g}_1 \\ \vdots \\ \mathbf{g}_{n_b} \end{bmatrix} = \begin{bmatrix} \boldsymbol{\alpha}_1 \\ \vdots \\ \boldsymbol{\alpha}_{2n} \end{bmatrix} \quad (6.26)$$

### 6.3.2 Unchanged eigenvalues

In the above derivation, it is wanted to assign certain eigenvalues/eigenpairs and keep all the other eigenvalues unchanged. However, real structures usually have an infinite number of eigenvalues. It is impossible or difficult to keep all the eigenvalues, except the unwanted eigenvalues, with the receptance method. Therefore, it is more practical to alter a subset of eigenvalues/eigenpairs and keep another subset of eigenvalues.

Without loss of generality, it is assumed that the first  $2p < 2n$  eigenvalues of  $\{\lambda_k\}_{k=1}^{2n}$  are required to be changed to predetermined eigenvalues  $\{\mu_k\}_{k=1}^{2p}$  and the next  $2(q - p)$  eigenvalues remain unchanged  $\{\mu_k\}_{k=2p+1}^{2q} = \{\lambda_k\}_{k=2p+1}^{2q}$ ,  $2q \leq 2n$ . These conditions can be written in the form

$$\mu_k = \begin{cases} \mu_k \text{ (desired eigenvalues)} & k = 1, 2, \dots, 2p \\ \lambda_k \text{ (unchanged eigenvalues)} & k = 2p + 1, \dots, 2q \\ \text{not of concern} & k = 2q + 1, \dots, 2n \end{cases} \quad (6.27)$$

For clarify, it should be pointed out that the proposed method in this paper is applicable for  $2q = 2n$  situation. In other words, this new method can be used to assign a subset of eigenvalues and keep all the other eigenvalues unchanged, which is a partial eigenvalue assignment problem studied by a number of researchers, for example, in [106, 107, 181].

However, it is believed that the eigenvalue problem defined in Eq. (6.27) is more useful and realistic than a strict partial eigenvalue assignment. This is because a real structure has a large number of frequencies (or eigenvalues) and thus partial eigenvalue assignment is not only very difficult to achieve but also unnecessary. When a few frequencies are assigned and all the other nearby frequencies stay unchanged, the remaining frequencies that are far away from the frequency range of concern can be left as they would become, with equal or almost equal vibration performance as partial eigenvalue assignment but at a much lower cost.

If only a few eigenvalues need to stay unchanged, the number of actuators, which is equal to the number of concerned modes, can be reduced.

For example, under the condition defined in Eq. (6.27), the number of actuators  $n_b$  should follow

$$(n_b - n)(n_b - 2q) \leq 0 \quad (6.28)$$

Therefore,

$$\min\{n, 2p\} \leq n_b \leq \max\{n, 2p\} \quad (6.29)$$

Since  $n_b \leq n$ ,

$$2p \leq n_b \leq n \text{ or } i = n \quad (6.30)$$

For  $2p \leq n_b \leq n$ , matrix  $\mathbf{B}$  can be partitioned into

$$\mathbf{B} = \begin{bmatrix} \mathbf{B}_e \\ \mathbf{B}_f \end{bmatrix}, \text{ where } \mathbf{B}_e \in \mathcal{R}^{n_b \times n_b}, \text{ and } \mathbf{B}_f \in \mathcal{R}^{(n-n_b) \times n_b}$$

It is easy to define an invertible matrix block matrix  $\mathbf{B}_e$ , leaving matrices  $\mathbf{B}_f$  and scaling vectors  $\boldsymbol{\alpha}_k$  in  $\hat{\mathbf{A}}$  to be determined from Eq. (6.19).

As for undamped system, Eq. (6.23) becomes

$$(p \times n_b + n_b \times p - n_b^2) \geq n \times n \quad (6.31)$$

Then the number of actuators for undamped system should follow  $p \leq n_b \leq n$ .

### 6.3.3 The procedure and requirements

The procedure and some important features of Method NA are summarised below.

- (a). Decide on the desired and unchanged eigenvalues and define the desired eigenvectors.
- (b). Measure receptance matrices of the open-loop system at desired eigenvalues. Make simple mass modifications on the open-loop system and measure the receptance matrices of the mass-modified system at those unchanged eigenvalues.

(c). Choose an invertible matrix  $\mathbf{B}$  or  $\mathbf{B}_1$ . Then calculate the scaling matrix  $\hat{\mathbf{A}}$  using Eq. (6.19).

(d). Determine the gain matrices  $\mathbf{F}$  and  $\mathbf{G}$  by solving Eq. (6.26).

Although Method NA does not need the eigenvectors of the open-loop system, it has a drawback compared with Method RM. The more eigenvalues to be retained, the more inputs are usually required for Method NA. A list of features of Method RM and Method NA are shown in Table 6.2 for comparison.

Table 6.2 Method comparison

	Method RM	Method NA
Required data	Receptance matrices; Eigenvectors of the open-loop system corresponding to the invariant eigenvalues	Receptance matrices
Inputs	Single input or multiple inputs	Multiple inputs
Objectives	Assign a subset of eigenvalues and keep the others unchanged.	Assign a subset of eigenvalues and keep the other eigenvalues unchanged; Assign eigenvectors corresponding to the desired eigenvalues and invariant eigenvalues

## 6.4 Systems with inaccessible degrees of freedom

The derivations in subsection 6.3 are based on a  $n$ -DoF system. In reality, not all the DoFs are physically accessible to actuation or sensing. That is, there exist some inaccessible degrees of freedom. A brief explanation is given here to show that this method is still applicable with inaccessible degrees of freedom.

Considering that only the first  $n_0$  ( $n_0 \leq n$ ) degrees of freedom are accessible to actuation or sensing, Eq. (6.12) can be written as

$$\begin{bmatrix} \mathbf{p}_{k1} \\ \mathbf{p}_{k2} \end{bmatrix} = \begin{bmatrix} \hat{\mathbf{H}}_{k11} & \hat{\mathbf{H}}_{k12} \\ \hat{\mathbf{H}}_{k21} & \hat{\mathbf{H}}_{k22} \end{bmatrix} \begin{bmatrix} \mathbf{B}_1 \\ \mathbf{0} \end{bmatrix} \boldsymbol{\alpha}_k, \quad k = 2p + 1, \dots, 2q \quad (6.32)$$



where  $\mathbf{p}_{k1} \in \mathbb{C}^{n_0 \times 1}$ ,  $\mathbf{p}_{k2} \in \mathbb{C}^{(n-n_0) \times 1}$ ,  $\hat{\mathbf{H}}_{k11} \in \mathbb{C}^{n_0 \times n_0}$ ,  $\hat{\mathbf{H}}_{k12} \in \mathbb{C}^{n_0 \times (n-n_0)}$ ,  $\mathbf{B}_1 \in \mathbb{C}^{n_0 \times n_b}$  and  $\boldsymbol{\alpha}_k \in \mathbb{C}^{n_b \times 1}$ .

Eq. (6.32) could be reformed as

$$\begin{bmatrix} \mathbf{p}_{k1} \\ \mathbf{p}_{k2} \end{bmatrix} = \begin{bmatrix} \hat{\mathbf{H}}_{k11} \mathbf{B}_1 \boldsymbol{\alpha}_k \\ \hat{\mathbf{H}}_{k21} \mathbf{B}_1 \boldsymbol{\alpha}_k \end{bmatrix}, k = 2p + 1, \dots, 2q \quad (6.33)$$

Extracting the first row of Eq. (6.33) results in

$$\mathbf{p}_{k1} = \hat{\mathbf{H}}_{k11} \mathbf{B}_1 \boldsymbol{\alpha}_k, k = 2p + 1, \dots, 2q \quad (6.34)$$

Similarly, Eq. (6.13) can also lead to the following equation

$$\mathbf{w}_{k1} = \mathbf{H}_{k11} \mathbf{B}_1 \boldsymbol{\alpha}_k, k = 2p + 1, \dots, 2q \quad (6.35)$$

where  $\mathbf{w}_{k1}$  is the first  $n_0$  elements in  $\mathbf{w}_k$  and  $\mathbf{H}_{k11}$  is a  $n_0 \times n_0$  matrix block at the left-top corner of the full receptance matrix  $\mathbf{H}_k$ .

Apparently, Eq. (6.34) and Eq. (6.35) are similar to Eq. (6.12) and Eq. (6.13). The procedure of dealing with Eq. (6.12) and Eq. (6.13) is still applicable for Eq. (6.34) and Eq. (6.35). This means that the method can still achieve partial eigenstructure assignment with part of receptance matrices. One thing that needs attention is that the assigned eigenvectors in this case are not the complete eigenvectors. They are part of the eigenvectors, i.e., the eigenvector elements at those accessible degrees of freedom. A 10-DoF undamped system in section 6.6 is demonstrated to prove this method can be applied to a system with inaccessible degrees of freedom.

## 6.5 A 4-DoF damped system

To demonstrate the performance of the proposed method, the 4-DoF mass-damper-spring system in section 6.2 is considered here. The required receptance matrices in the following examples are obtained from simulations, which are usually measured from experiments in engineering applications. This example is used to show the performance of Method NA and three different cases are analysed in this example. In case 1, the first two distinct eigenpairs are assigned while the other two distinct eigenpairs are kept, which is proper partial eigenstructure assignment. The second case is to assign all eight conjugate eigenpairs. Among them, the last two distinct (non-

conjugate) eigenvalues are specially assigned to be equal to the open-loop eigenvalues. So, this looks like eigenstructure assignment but it is more than the conventional eigenstructure assignment in the sense that some eigenvalues are kept at the same time. In case 3, the first two distinct eigenpairs are assigned while the third distinct eigenpair is kept; the remaining (the 4<sup>th</sup>) distinct eigenpair is not controlled. Although case 3 is not a complete partial eigenstructure assignment, it is of particular significance in real applications in which only a small number of eigenpairs need to be changed, several other eigenpairs need to be retained, and all the other eigenpairs are left uncontrolled, which can be a cheaper solution than proper partial eigenstructure assignment.

### 6.5.1 Assign two modes and keep the other modes unchanged

The first two pairs of eigenvalues are to be shifted to desired locations together with desired eigenvectors and the remaining two eigenpairs are kept unchanged, as shown in Table 6.3.

Table 6.3 Desired eigenvalues and eigenvectors

	$\mu_{1,2}$	$\mu_{3,4}$	$\mu_{5,6}$	$\mu_{7,8}$
	$-0.50 \pm 0.50i$	$-0.90 \pm 0.80i$	$-0.50 \pm 1.29i$	$-0.77 \pm 1.36i$
$\mathbf{w}_k$	$1.00 \pm 0.00i$	$1.00 \pm 0.00i$	$1.00 \pm 0.00i$	$1.00 \pm 0.00i$
	$1.00 \mp 4.00i$	$-2.00 \mp 3.00i$	$0.01 \mp 0.46i$	$-0.59 \mp 0.23i$
	$2.00 \mp 2.00i$	$-3.00 \pm 2.00i$	$0.00 \pm 0.02i$	$-0.10 \mp 1.25i$
	$-2.00 \mp 4.00i$	$1.00 \mp 2.00i$	$-0.25 \pm 0.27i$	$1.33 \pm 2.27i$

In this problem, the number of the inputs  $n_b$  is chosen to be 4 and matrix  $\mathbf{B}$  is determined as

$$\mathbf{B} = \begin{bmatrix} 1 & -1 & 2 & 1 \\ 0.5 & 1 & 2 & 1 \\ -2 & -1 & 0.5 & 1 \\ -1 & 2 & 1.5 & 0.5 \end{bmatrix}$$

A mass 0.5 is added on coordinate 1 so the mass modification matrix is  $\Delta\mathbf{M} = \text{diag}([0.5 \ 0 \ 0 \ 0])$ .

Eq. (6.26) gives the gain matrices  $\mathbf{F}$  and  $\mathbf{G}$  as

$$\mathbf{F} = \begin{bmatrix} -0.25 & -0.31 & 0.73 & -1.46 \\ -0.65 & -0.41 & 2.20 & -4.46 \\ 0.71 & -0.14 & -1.62 & 2.44 \\ 0.66 & 0.25 & -1.59 & 2.75 \end{bmatrix}$$

$$\mathbf{G} = \begin{bmatrix} 0.53 & 0.25 & -1.57 & 3.04 \\ -1.42 & -1.06 & 4.16 & -7.95 \\ 1.54 & 0.74 & -3.76 & 6.82 \\ 0.40 & 0.42 & -0.85 & 1.65 \end{bmatrix}$$

The closed-loop system can be described by

$$\mathbf{M}\ddot{\mathbf{x}} + \mathbf{C}\dot{\mathbf{x}} + \mathbf{K}\mathbf{x} - \mathbf{B}\mathbf{F}^T\dot{\mathbf{x}} - \mathbf{B}\mathbf{G}^T\mathbf{x} = \mathbf{0}$$

and the eigenvalue and eigenvectors of the closed-loop system are found to be exactly those as expected.

### 6.5.2 Assign two modes and keep the other eigenvalues unchanged

The first two pairs of eigenvalues are to be changed to desired eigenvalues as shown below and the remaining two pairs of eigenvalues stay unchanged.

$$\mu_{1,2} = -0.50 \pm 0.50i, \quad \mu_{3,4} = -0.90 \pm 0.80i,$$

$$\mu_{5,6} = -0.50 \pm 1.29i, \quad \mu_{7,8} = -0.77 \pm 1.36i$$

Additionally, the following nodes in the four modes shown in Table 6.4 are to be created in the closed-loop system. In this problem, the eigenvectors corresponding to the unchanged eigenvalues are not kept.

Table 6.4 The desired eigenvectors and eigenvalues

	$\mu_{1,2}$	$\mu_{3,4}$	$\mu_{5,6}$	$\mu_{7,8}$
	$-0.50 \pm 0.50i$	$-0.90 \pm 0.80i$	$-0.50 \pm 1.29i$	$-0.77 \pm 1.36i$
$\mathbf{w}_k$	$1.00 \pm 0.00i$	$1.00 \pm 0.00i$	$1.00 \pm 0.00i$	$1.00 \pm 0.00i$
	$3.00 \mp 2.00i$	0	$0.00 \mp 0.80i$	$-0.50 \mp 0.00i$
	0	$0.90 \pm 1.50i$	0	$-0.10 \mp 1.00i$
	$3.00 \mp 2.00i$	$-0.10 \pm 1.00i$	$-0.20 \mp 0.30i$	0

Following the same procedure in subsection 6.5.1 and adopting the same force distribution matrix  $\mathbf{B}$  yield

$$\mathbf{F} = \begin{bmatrix} -1.25 & -0.65 & 0.58 & -2.09 \\ 1.95 & 1.63 & -1.02 & 1.82 \\ -0.46 & -0.52 & 0.05 & -2.14 \\ -1.17 & -1.16 & 1.27 & -2.80 \end{bmatrix},$$

$$\mathbf{G} = \begin{bmatrix} -1.29 & -0.87 & 0.67 & -1.27 \\ -2.38 & -1.32 & 1.92 & -6.73 \\ -1.85 & -1.60 & 0.54 & -4.20 \\ -2.17 & 1.27 & 0.49 & -2.27 \end{bmatrix}$$

The closed-loop system can be described by

$$\mathbf{M}\ddot{\mathbf{x}} + \mathbf{C}\dot{\mathbf{x}} + \mathbf{K}\mathbf{x} - \mathbf{B}\mathbf{F}^T\dot{\mathbf{x}} - \mathbf{B}\mathbf{G}^T\mathbf{x} = \mathbf{0}$$

The eigenvectors and eigenvalues of the closed-loop system are as expected in Table 6.4.

### 6.5.3 Assign two modes and keep one mode

In this problem, the first and second pairs of eigenvalues  $\lambda_{1,2}$  and  $\lambda_{3,4}$  are to be changed to  $\mu_{1,2} = -0.5 + 0.5i$  and  $\mu_{3,4} = -0.90 \pm 0.80i$ , while only the third pair of eigenvalue stays unchanged. The last pair of eigenvalues is not concerned (controlled). The desired eigenvectors corresponding to the first and second pairs of eigenvalues and the unchanged eigenpairs are shown in Table 6.5, which are the same as the eigenvectors shown in Table 6.3.

Table 6.5 The desired eigenvalues and eigenvectors

	$\mu_{1,2}$	$\mu_{3,4}$	$\mu_{5,6}$
	$-0.50 \pm 0.50i$	$-0.90 \pm 0.80i$	$-0.50 \pm 1.29i$
$\mathbf{w}_k$	$1.00 \pm 0.00i$	$1.00 \pm 0.00i$	$1.00 \pm 0.00i$
	$1.00 \mp 4.00i$	$-2.00 \mp 3.00i$	$0.01 \mp 0.46i$
	$2.00 \mp 2.00i$	$-3.00 \pm 2.00i$	$0.00 \pm 0.02i$
	$-2.00 \mp 4.00i$	$1.00 \mp 2.00i$	$-0.25 \pm 0.27i$

In order to compare with the results in case 1, four actuators are adopted here and the invertible force distribution matrix  $\mathbf{B}$  is defined as the same as the matrix  $\mathbf{B}$  in previous problems.

The gain matrices  $\mathbf{F}$  and  $\mathbf{G}$  are calculated as

$$\mathbf{F} = \begin{bmatrix} -1.03 & 0.11 & -0.32 & -0.41 \\ 1.23 & 0.81 & 0.26 & -0.99 \\ 0.63 & -1.57 & 1.22 & -1.40 \\ -1.08 & -0.65 & -0.25 & 0.16 \end{bmatrix},$$

$$\mathbf{G} = \begin{bmatrix} -1.45 & -0.85 & 0.10 & -0.11 \\ -1.10 & 0.82 & 0.48 & -2.88 \\ 2.96 & -0.49 & -0.91 & 3.65 \\ -0.03 & -0.96 & 1.81 & -2.12 \end{bmatrix}$$

Now the closed-loop system becomes

$$\mathbf{M}\ddot{\mathbf{x}} + \mathbf{C}\dot{\mathbf{x}} + \mathbf{K}\mathbf{x} - \mathbf{B}\mathbf{F}^T\dot{\mathbf{x}} - \mathbf{B}\mathbf{G}^T\mathbf{x} = \mathbf{0}$$

with eigenvalues found to be

$$\mu_{1,2} = -0.50 \pm 0.50i, \quad \mu_{3,4} = -0.90 \pm 0.80i,$$

$$\mu_{5,6} = -0.50 \pm 1.29i, \quad \mu_{7,8} = -1.34 \pm 2.12i$$

The eigenvectors of this closed-loop system are presented in Table 6.6. It can be seen that the closed-loop system has those desired eigenvalues and eigenvectors. The only difference between the problem in case 1 and case 3 is that the last pair of eigenvalues is not concerned in case 3.

Table 6.6 Eigenvalues and eigenvectors of the closed-loop system

	$\mu_{1,2}$	$\mu_{3,4}$	$\mu_{5,6}$	$\mu_{7,8}$
	$-0.50 \pm 0.50i$	$-0.90 \pm 0.80i$	$-0.50 \pm 1.29i$	$-1.34 \pm 2.12i$
$\mathbf{w}_k$	$1.00 \pm 0.00i$	$1.00 \pm 0.00i$	$1.00 \pm 0.00i$	$1.00 \pm 0.00i$
	$1.00 \mp 4.00i$	$-2.00 \mp 3.00i$	$0.01 \mp 0.46i$	$0.06 \mp 0.27i$
	$2.00 \mp 2.00i$	$-3.00 \pm 2.00i$	$0.00 \pm 0.02i$	$-0.12 \pm 0.38i$
	$-2.00 \mp 4.00i$	$1.00 \mp 2.00i$	$-0.25 \pm 0.27i$	$-0.39 \mp 0.14i$

If the control effort of active control is defined by the Frobenius norm of the feedback gain matrices, which can be written as

$$En = \left\| \begin{bmatrix} \mathbf{F} \\ \mathbf{G} \end{bmatrix} \right\|_F^2$$

The control efforts in Case 1 and Case 3 can be calculated as 382.05 and 57.61, respectively.

Apparently, the control effort in Case 3 is much smaller than the control effort in Case 1, which means that leaving some unimportant eigenvalues uncontrolled will reduce the control effort.

In the last 3 cases, all the 4 DoFs in this system can be measured or actuated. However, in most engineering cases, not all the DoFs of the system could be measured. The next example is to demonstrate how to deal with a system with inaccessible DoFs and the number of actuators required can be reduced if only a small number of eigenvalues need to be maintained.

### 6.6 An undamped 10-DoF system with inaccessible DoFs

Consider an undamped 10-DoF system, as shown in Fig. 6.2. This example was used by Ouyang and Zhang in [56]. The values of the mass and stiffness parameters are listed in Table 6.7 and the natural frequencies of the open-loop system are presented in Table 6.8.

Table 6.7 System parameters

$m_i, i = 1, \dots, 10$ [kg]	30, 35, 40, 45, 45, 45, 40, 35, 30, 25
$k_i, i = 1, \dots, 25$ [N/m]	$2.4 \times 10^5$

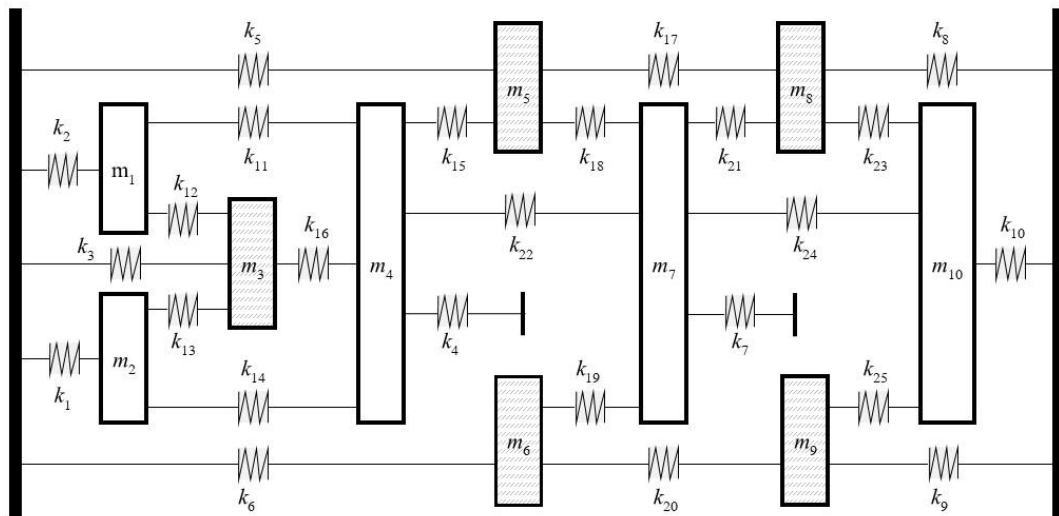


Fig. 6.2 A10-DoF lumped mass system

Table 6.8 Natural frequencies of the open-loop system and the closed-loop system

	1	2	3	4	5
Open-loop [rad/s]	80.0	98.1	120.9	148.7	151.9
Closed-loop [rad/s]	<b>90.0</b>	<b>110.0</b>	<b>120.9</b>	149.0	150.4
	6	7	8	9	10
Open-loop [rad/s]	168.7	179.5	189.1	205.7	221.7
Closed-loop [rad/s]	167.6	190.4	193.0	206.0	221.7

It is wanted that the first two pairs of eigenvalues of the open-loop system are shifted from  $\lambda_{1,2} = \pm 80i$  rad/s and  $\lambda_{3,4} = \pm 98i$  rad/s to  $\mu_{1,2} = \pm 90i$  rad/s and  $\mu_{3,4} = \pm 110i$  rad/s, while the third pair of eigenvalues  $\mu_{5,6} = 120.92$  rad/s is unchanged. In addition, only 5 among the 10 degrees of freedom could be measured or observed. The others are inaccessible. Mass 3, 5, 6, 8, and 9 are chosen as the measurable degrees of freedom in this example. Besides, only displacement feedback matrix  $\mathbf{G}$  is adopted here since no damping is concerned in this problem.

The desired eigenvectors corresponding to first three pairs of eigenvalues are shown in Table 6.9. It should be mentioned that the eigenvectors in this example are not the whole eigenvectors of the system, but the eigenvector elements at the measurable degrees of freedom.

In this example, the number of inputs is chosen as  $n_b = 3$ . Define the control force distribution matrix  $\mathbf{B} \in \mathcal{R}^{5 \times 3}$  as

$$\mathbf{B} = \begin{bmatrix} \mathbf{B}_e \\ \mathbf{B}_f \end{bmatrix} \text{ and } \mathbf{B}_e = \begin{bmatrix} 1 & 1.5 & 1.5 \\ -1.2 & -1 & -0.5 \\ -0.1 & -3 & -1 \end{bmatrix}$$

Two lumped masses 10 kg and 20 kg are placed on mass 3 and 5, respectively. By solving Eq. (6.17), matrix  $\mathbf{B}$  and scaling matrix  $\hat{\mathbf{A}}$  can be obtained

$$\mathbf{B} = \begin{bmatrix} 1 & 1.5 & 1.5 \\ -1.2 & -1 & -0.5 \\ -0.1 & -3 & -1 \\ 3.68 & -4.11 & -0.57 \\ 2.35 & -2.06 & -0.55 \end{bmatrix}$$

$$\hat{\mathbf{A}} = 10^5 \times \begin{bmatrix} 0.13 & 0.67 & -0.30 \\ -0.79 & 1.22 & -0.04 \\ 2.08 & -3.95 & -0.06 \end{bmatrix}$$

Then Eq. (6.26) gives the gain matrix  $\mathbf{G}$  as

$$\mathbf{G}^T = 10^5 \times \begin{bmatrix} 0.50 & -0.12 & -0.22 & -0.25 & -0.06 \\ 1.18 & 0.35 & -0.27 & -0.19 & -0.06 \\ -3.51 & -1.03 & 1.02 & 0.60 & 0.31 \end{bmatrix}$$

The closed-loop system is governed by

$$\mathbf{M}\ddot{\mathbf{x}} + \mathbf{K}\mathbf{x} - \mathbf{B}\mathbf{G}^T\mathbf{x} = \mathbf{0}$$

with the natural frequencies shown in Table 6.8. The eigenvectors associated with the concerned eigenvalues can be seen to be the same as the desired ones presented in Table 6.9.

Table 6.9 Eigenvectors corresponding to the first three modes

Open-loop system			Closed-loop system		
$\lambda_{1,2}$	$\lambda_{3,4}$	$\lambda_{5,6}$	$\mu_{1,2}$	$\mu_{3,4}$	$\mu_{5,6}$
-0.95	0.88	-0.42	-0.70	-0.70	-0.40
-1	-0.11	1.00	-1.00	-0.10	1
-0.96	-1.00	-0.93	-0.90	1.00	-0.60
-0.89	-0.38	0.85	-0.50	0.30	0.70
-0.80	-0.85	-0.59	-0.60	0.60	-0.60

## 6.7 Robustness analysis

Although there is no need to build a finite element model or numerical model of the system in the receptance method and thus the errors associated with modelling can be avoided, the receptance matrix, which is usually obtained from experiment, may suffer from measurement errors, uncertainty of the system or the misfitting of the frequency



response function. The errors contained in the receptance matrix, could lead to poor results for the partial assignment. This section makes an analysis of the robustness of Method NA by using the example in section 6.5.1. The same targets in Case 1, which are to shift the first two pairs of eigenvalues to  $\mu_{1,2} = -0.50 \pm 0.50i$  and  $\mu_{3,4} = -0.90 \pm 0.80i$  and keep the remaining two pairs of eigenvalues unchanged as  $\mu_{5,6} = -0.50 \pm 1.29i$  and  $\mu_{7,8} = -0.77 \pm 1.36i$ , are expected here. Also, the force distribution matrix  $\mathbf{B}$  is defined as the same as the matrix  $\mathbf{B}$  in section 6.5.1. Three different scenarios are considered in this section.

### 6.7.1 Receptance matrices with several contaminated elements

Suppose that the receptance matrices, which are obtained from simulation in this paper, are contaminated at one or two locations. The added numerical perturbation is defined as

$$\tilde{h}_{ij}(\mu_k) = h_{ij}(\mu_k) * \text{rand}(0.95,1.05)$$

where  $\tilde{h}_{ij}(\mu_k)$  is the contaminated receptance,  $h_{ij}(\mu_k)$  is the true receptance and  $\text{rand}(0.95,1.05)$  returns a random number between 0.95 and 1.05 which leads to a 5% variation of the true receptance at most. Besides, to maintain the symmetrical characteristic of a receptance matrix,  $h_{ji}(\mu_k)$  is also perturbed and  $\tilde{h}_{ji}(\mu_k) = \tilde{h}_{ij}(\mu_k)$ .

The receptance matrix at eight eigenvalues needs to be measured or to be simulated in this example. The contaminated elements in each matrix are shown in Table 6.10.

Table 6.10 Contaminated elements in each receptance matrix

Receptance matrix	Contaminated elements
$\tilde{\mathbf{H}}(\mu_{1,2})$	$\tilde{h}_{12} = \tilde{h}_{21}, \tilde{h}_{23} = \tilde{h}_{32},$
$\tilde{\mathbf{H}}(\mu_{3,4})$	$\tilde{h}_{12} = \tilde{h}_{21}$
$\tilde{\mathbf{H}}(\mu_{5,6})$	$\tilde{h}_{23} = \tilde{h}_{32}, \tilde{h}_{43} = \tilde{h}_{34}$
$\tilde{\mathbf{H}}(\mu_{7,8})$	$\tilde{h}_{13} = \tilde{h}_{31}$

Fig. 6.3 shows a Monte-Carlo simulation with 1000 samples. Those eight rectangles represent regions of obtained eigenvalues and they are defined as

$$\text{Region}(\mu_k) = \mu_k + [-0.05, 0.05] \pm [-0.05, 0.05]i$$

It can be seen all the obtained eigenvalues fall into small regions which are close to the nominal values of targeted ones. The variance of each eigenvalue is very small. Also, Fig. 6.3 indicates that the real part of the eigenvalues of closed-loop system, which affect the system damping, are more sensitive to the receptance errors.

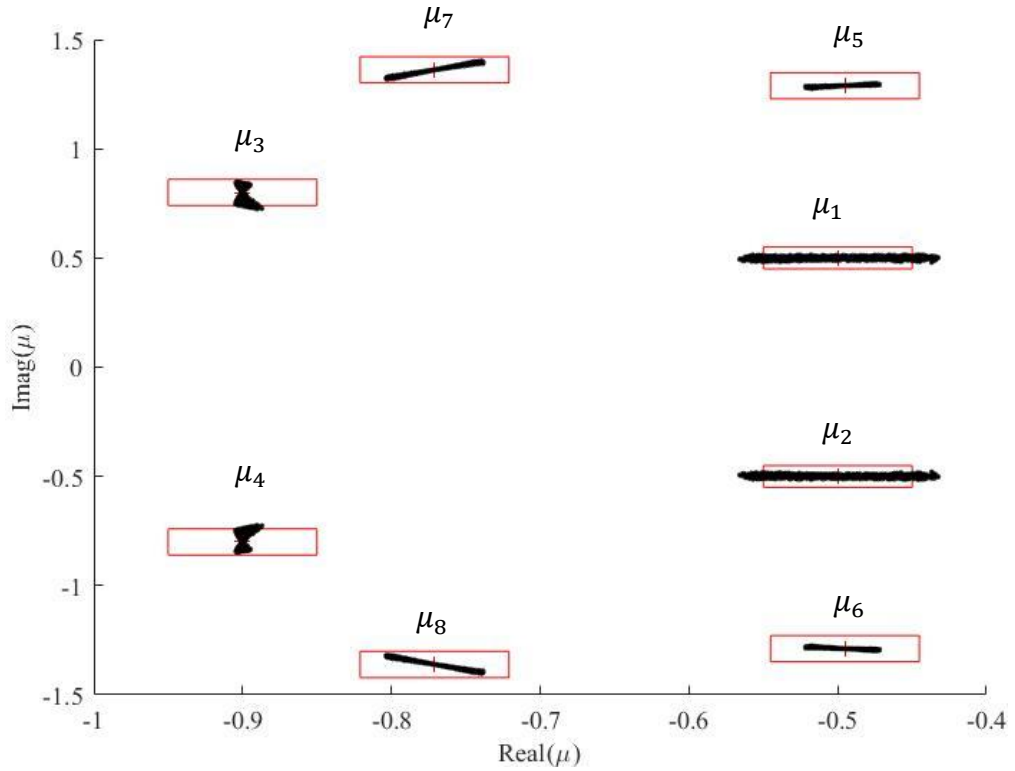


Fig. 6.3 Eigenvalues of the closed-loop system (with a few contaminated elements in receptance matrices)

### 6.7.2 Receptance matrices with one pair of contaminated eigenvalues

Consider the case that the receptance matrices at one pair of eigenvalues are contaminated. It is worth to find out whether the other pairs of eigenvalues will be affected. The receptance matrix with errors is simulated as

$$\tilde{\mathbf{H}}(\mu_k) = \mathbf{H}(\mu_k) * \text{rand}(0.95, 1.05)$$

Suppose that the receptance matrices at the second pair of eigenvalues  $\mathbf{H}(\mu_{3,4})$  are contaminated. A new Monte-Carlo simulation with 1000 samples is conducted. Fig. 6.4 shows the new variability of the obtained eigenvalues. It is clear that only the

eigenvalues  $\mu_{3,4}$  are uncertain and all the other three pairs of eigenvalues are exactly where they are expected. Similarly, if the receptance matrices at the other one or two pairs of eigenvalues are contaminated, only the corresponding eigenvalues are uncertain and the others are unaffected. This is good for the real applications when only a few receptance matrices are uncertain.

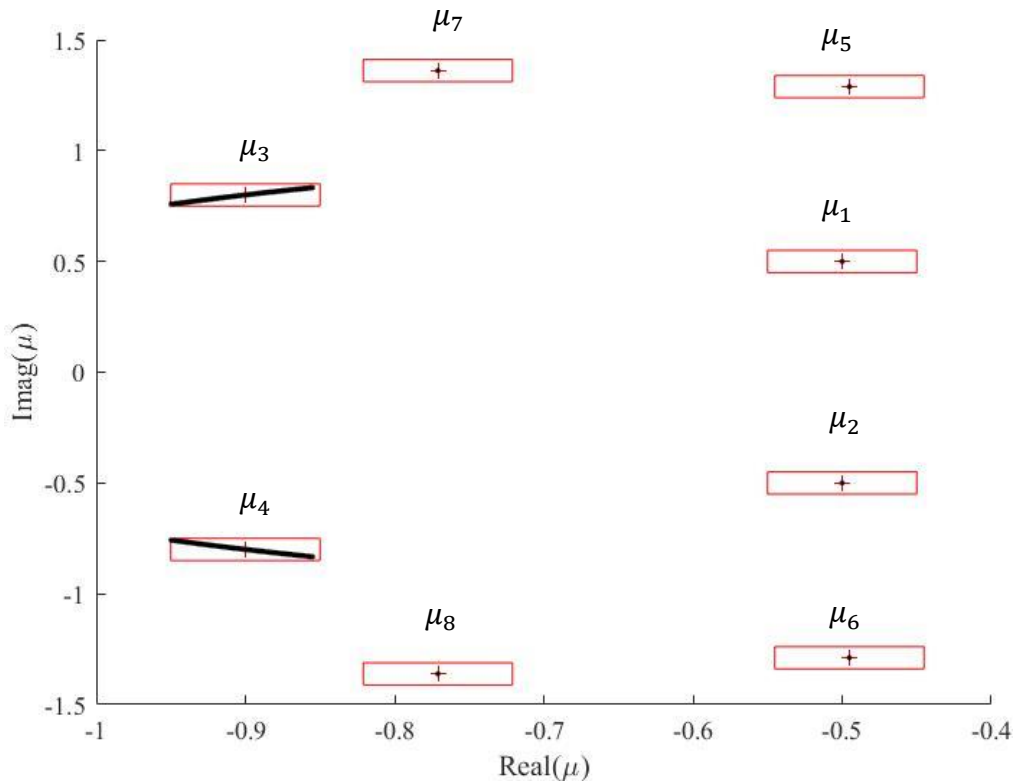


Fig. 6.4 Eigenvalue spread (with contaminated receptance matrices  $\mathbf{H}(\mu_{3,4})$ )

### 6.7.3 Fully contaminated receptance matrices

Now, suppose that all required receptance matrices are variable by as much as 5% of their nominal values. Fig. 6.5 shows the variability of the obtained eigenvalues. By comparison it with Fig. 6.3, the variation of the imaginary part of each eigenvalue is seen to be bigger because more noise is included. However, it still can be seen that most of the obtained eigenvalues are within small regions of frequencies (represented by rectangles). Therefore, this method can be said to be robust in terms of the errors in the measured receptances for the four-DoF damped system.

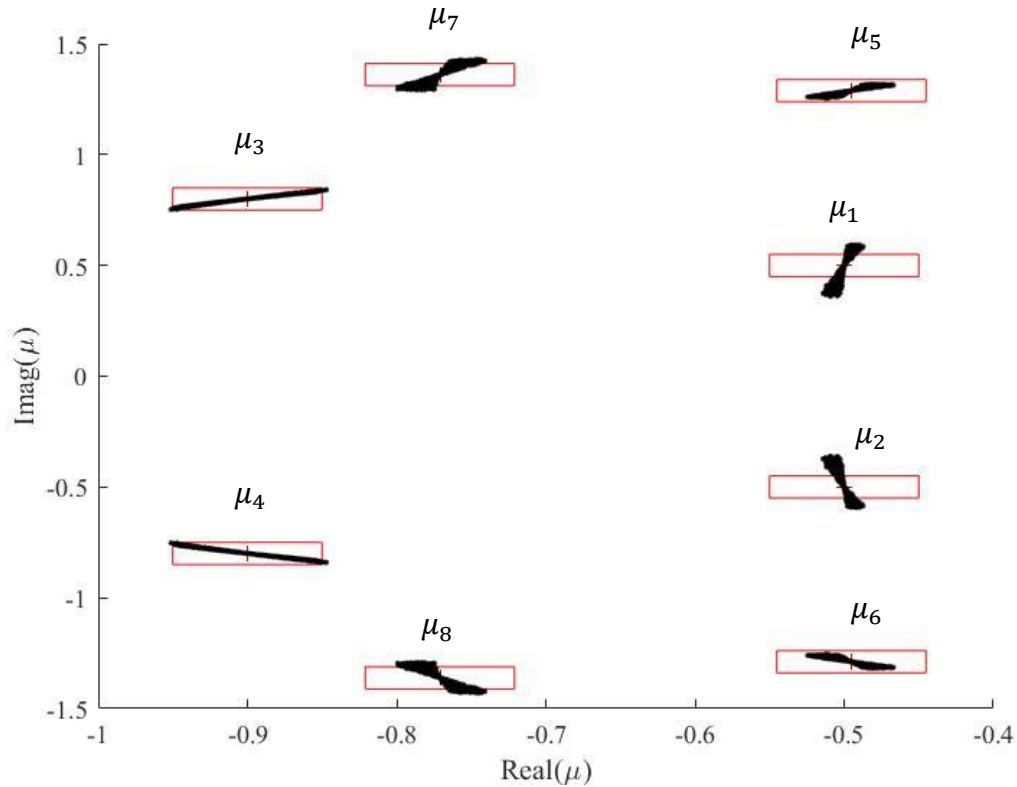


Fig. 6.5 Eigenvalues spread (all receptance matrices are contaminated)

## 6.8 Conclusions

A partial eigenstructure assignment method by state feedback control is proposed in this chapter. This method does not need the physical model (or finite element model) since it is based on measure receptances, and the eigenvectors of the open-loop system. Only part of the receptance matrix is required.

A comparison between this new method and the method proposed by Ram and Mottershead (Multiple-input active vibration control by partial pole placement using the method of receptances, *Mechanical Systems and Signal Processing*, 40 (2013) 727-735) is presented. It shows that this new method has advantages when the open-loop eigenvectors are hard to obtain or inaccurate. It is also verified by means of numerical examples that this method can work efficiently for systems with inaccessible degrees of freedom.

This method can assign some desired eigenpairs and keep all the other or some of the other eigenpairs unchanged. With the same number of actuators and same force distribution matrix  $\mathbf{B}$ , compared with keeping all the other eigenpairs unchanged, the

control effort is smaller if only some of the other eigenpairs are kept. This finding should enable a more cost-effective solution in practice.

The robustness of this method is also analysed. Three scenarios of contaminated receptance matrices are considered. The simulation results show this method is robust where there are 5% variations of receptance matrices for a four-DoF damped system. Besides, if a few receptances are contaminated at certain eigenvalues, all the other eigenvalues are unaffected and only the related eigenvalues are uncertain to a small extent.

However, in this method, the number of the required inputs depends on the total number of the assigned and unchanged eigenvalues, and the number of degrees of freedom. This may restrict the application of this partial eigenstructure assignment method in real applications.

# Chapter 7

## Conclusions and future work

### 7.1 Conclusions

Vibration control is very important for machines and structures. For assembled structures, there are many cases in which modifications to substructures are not allowed or are expensive. In this thesis, frequency assignment for assembled structures is achieved using receptance. The proposed method can optimize the properties of the links between substructures to allow the assembled structure to have desired modal properties as expected. Then this proposed method is validated on a designed laboratory test rig.

In the field of active control, although eigenvalues can be easily assigned with receptance-based method, a general desired eigenvector is not guaranteed to be achievable. The partial eigenstructure assignment problem is discussed in this thesis and two receptance-based partial eigenstructure assignment methods are proposed. One is a passive-active combined hybrid control method which allows a general desired eigenvector can be achieved. The other method is an active control method with state feedback control that can avoid the requirement of open-loop eigenvectors.

The important results drawn from the research work in this PhD project are presented in the following.

1. A receptance-based frequency assignment method for assembled structures: This method is very efficient for assembled structures with any number of links. Unlike the common frequency assignment of a structure, more than one structure are involved in this problem. Only receptance at connection points and the theoretical models or FE models of links are needed. Moreover, a reduced model of the link, which only contains the connection nodes, can be used to reduce the computation time.

2. Experimental work on an assembled structure: The receptance-based frequency assignment method for assembled structures is applied to a laboratory structure. The laboratory structure is a simplified model of a floating raft platform which is usually installed on the ship hull. It consists of two substructures and six simple links. A number of experiments were carried out to measure the required receptances, including the rotational receptances. The rotational receptances are measured with the help of an auxiliary structure and two angular accelerometers. The auxiliary structure used in this work is very simple and its flexibility is considered during the estimation. Moreover, the use of angular accelerometers makes it easier to estimate the rotational receptances when the excitation and response are not at the same connection points. One or two frequencies are successfully assigned on the assembled structure by optimizing the dimensions of the cross sections of links. A combination of the MATLAB codes and Abaqus scripts allows the optimization procedure to be finished efficiently.

3. Receptance-based partial eigenstructure assignment with hybrid control: A new receptance-based hybrid control method is proposed to solve partial eigenstructure assignment problem. For the existing receptance-based active control method, a desired eigenvector is assignable only if this eigenvector belongs to the allowable space which depends on the receptance of original system, or the projection of the desired eigenvector onto the allowable space is close enough to the desired eigenvector, quantifying by the angle between the desired eigenvector and its projection. However, this condition is usually not easy to satisfy for a general eigenvector. In contrast, the proposed hybrid control method is able to assign a general eigenvector with the help of passive modification. The required passive modification is determined through a rank minimization algorithm. Still, the hybrid control method is not guaranteed to assign exact desired eigenvectors but it can provide a better approximation than sole active control method. Only the receptance and some open-loop eigenvectors are needed in this hybrid method.

4. Receptance-based partial eigenstructure assignment by state feedback control: The existing receptance-based partial eigenvalue/eigenstructure assignment methods require either system matrices or open-loop eigenvectors. A new partial eigenstructure assignment method with state feedback control, which requires only receptance, is proposed in this thesis. In this new method, the force distribution matrix  $\mathbf{B}$  may not be fully predefined. Leaving some elements unknown in matrix  $\mathbf{B}$  allows an engineer to

have more freedom to achieve eigenstructure assignment. Although there is a disadvantage that multiple inputs are needed in the new method, it can still provide a solution which can avoid the measurement of open-loop eigenvectors, especially when only a small group of eigenvalues is supposed to be kept.

## **7.2 Future work**

This project has significantly improved the receptance method for structural modification and active control and explored its applications. Although significant contributions are made, there are some research problems that should be studied to improve the current methods and ease the applications in practical problems. Inspired by the research in this project and the published papers by other researchers, the following future work is considered worth studying:

1. Frequency assignment for assembled structure with nonlinear links can be very useful in real applications. For example, rubber isolators or air springs are widely used on a ship to reduce the vibrations transmitted to the ship hull from machines. Those isolators usually possess a moderate degree of nonlinearity. Therefore, the formulations in chapter 3 should be adapted into a new version to determine the required properties of the nonlinear links between the onboard machines and the ship hull.
2. Further improvements on the two proposed partial eigenstructure assignment method are expected. For example, for the proposed hybrid control method, it is still possible that a desired eigenvector is assignable in some cases, especially when only a few sensors and actuators are used in active control. For the state feedback control method, the requirement on the number of actuators may limit the application in real systems. The strategy that can reduce the number of actuators is worth exploring and is promising.
3. Experiments for partial eigenstructure assignment using the two proposed methods in this thesis may be carried out on laboratory structures and real systems, such as a pump installation system on a ship. Only limited locations can accommodate actuators or sensors and the measurement of open-loop eigenvectors will take great efforts. Also, some other problems in active control, like time-delay and robustness, should be considered when the methods are applied on a real system.



4. Applying the receptance method in vibration confinement is also of interest. Vibration confinement techniques have been widely used in flexible structures such as large space antennas. Those techniques can interrupt the propagation of vibration and confine the energy of vibration to the areas close to the source of vibration by scaling and reforming part or all of the system mode shapes. The existing techniques usually requires system matrices or first-order reformulations. Therefore, it will be useful to extend the receptance method to this topic.

## Appendix A

The simplification process from Eq. (3.29) to Eq. (3.30) is discussed here in details. Eq. (3.29) indicates that frequency assignment could be achieved if

$$\det(\tilde{\mathbf{I}} + \tilde{\mathbf{H}}\Delta\tilde{\mathbf{Z}}) = 0 \quad (\text{A1})$$

This equation could be expanded as

$$\det \left( \begin{array}{cccccccc} \mathbf{I}_a & \mathbf{0} & \mathbf{0} & \mathbf{0} & \mathbf{0} & \mathbf{0} & \mathbf{0} & \mathbf{0} \\ \mathbf{0} & \mathbf{I}_p & \mathbf{0} & \mathbf{0} & \mathbf{0} & \mathbf{0} & \mathbf{0} & \mathbf{0} \\ \mathbf{0} & \mathbf{0} & \mathbf{I}_i & \mathbf{0} & \mathbf{0} & \mathbf{0} & \mathbf{0} & \mathbf{0} \\ \mathbf{0} & \mathbf{0} & \mathbf{0} & \mathbf{0} & \mathbf{0} & \mathbf{0} & \mathbf{0} & \mathbf{0} \\ \mathbf{0} & \mathbf{0} & \mathbf{0} & \mathbf{0} & \mathbf{0} & \mathbf{0} & \mathbf{0} & \mathbf{0} \\ \mathbf{0} & \mathbf{0} & \mathbf{0} & \mathbf{0} & \mathbf{0} & \mathbf{I}_q & \mathbf{0} & \mathbf{0} \\ \mathbf{0} & \mathbf{0} & \mathbf{0} & \mathbf{0} & \mathbf{0} & \mathbf{0} & \mathbf{I}_j & \mathbf{0} \\ \mathbf{0} & \mathbf{0} & \mathbf{0} & \mathbf{0} & \mathbf{0} & \mathbf{0} & \mathbf{0} & \mathbf{I}_b \end{array} \right) + \left( \begin{array}{cccccccc} \mathbf{H}_{aa}^A & \mathbf{H}_{ap}^A & \mathbf{H}_{ai}^A & \mathbf{0} & \mathbf{0} & \mathbf{0} & \mathbf{0} & \mathbf{0} \\ \mathbf{H}_{pa}^A & \mathbf{H}_{pp}^A & \mathbf{H}_{pi}^A & \mathbf{0} & \mathbf{0} & \mathbf{0} & \mathbf{0} & \mathbf{0} \\ \mathbf{H}_{ia}^A & \mathbf{H}_{ip}^A & \mathbf{H}_{ii}^A & \mathbf{0} & \mathbf{0} & \mathbf{0} & \mathbf{0} & \mathbf{0} \\ \mathbf{0} & \mathbf{0} & \mathbf{0} & \mathbf{I}_c & \mathbf{0} & \mathbf{0} & \mathbf{0} & \mathbf{0} \\ \mathbf{0} & \mathbf{0} & \mathbf{0} & \mathbf{0} & \mathbf{I}_d & \mathbf{0} & \mathbf{0} & \mathbf{0} \\ \mathbf{0} & \mathbf{0} & \mathbf{0} & \mathbf{0} & \mathbf{0} & \mathbf{H}_{qq}^B & \mathbf{H}_{qj}^B & \mathbf{H}_{qb}^B \\ \mathbf{0} & \mathbf{0} & \mathbf{0} & \mathbf{0} & \mathbf{0} & \mathbf{H}_{jq}^B & \mathbf{H}_{jj}^B & \mathbf{H}_{jb}^B \\ \mathbf{0} & \mathbf{0} & \mathbf{0} & \mathbf{0} & \mathbf{0} & \mathbf{H}_{bq}^B & \mathbf{H}_{bj}^B & \mathbf{H}_{bb}^B \end{array} \right) \left( \begin{array}{cccccccc} \mathbf{0} & \mathbf{0} & \mathbf{0} & \mathbf{0} & \mathbf{0} & \mathbf{0} & \mathbf{0} & \mathbf{0} \\ \mathbf{0} & \mathbf{Z}_{pp}^C & \mathbf{0} & \mathbf{Z}_{pc}^C & \mathbf{0} & \mathbf{Z}_{pq}^C & \mathbf{0} & \mathbf{0} \\ \mathbf{0} & \mathbf{0} & \mathbf{Z}_{ii}^D & \mathbf{0} & \mathbf{Z}_{id}^D & \mathbf{0} & \mathbf{Z}_{ij}^D & \mathbf{0} \\ \mathbf{0} & \mathbf{Z}_{cp}^C & \mathbf{0} & \mathbf{Z}_{cc}^C & \mathbf{0} & \mathbf{Z}_{cq}^C & \mathbf{0} & \mathbf{0} \\ \mathbf{0} & \mathbf{0} & \mathbf{Z}_{di}^D & \mathbf{0} & \mathbf{Z}_{dd}^D & \mathbf{0} & \mathbf{Z}_{dj}^D & \mathbf{0} \\ \mathbf{0} & \mathbf{0} & \mathbf{0} & \mathbf{0} & \mathbf{0} & \mathbf{Z}_{qp}^C & \mathbf{0} & \mathbf{Z}_{qc}^C \\ \mathbf{0} & \mathbf{0} & \mathbf{0} & \mathbf{0} & \mathbf{0} & \mathbf{0} & \mathbf{Z}_{qj}^D & \mathbf{0} \\ \mathbf{0} & \mathbf{0} & \mathbf{0} & \mathbf{0} & \mathbf{0} & \mathbf{0} & \mathbf{0} & \mathbf{Z}_{jd}^D \\ \mathbf{0} & \mathbf{0} & \mathbf{0} & \mathbf{0} & \mathbf{0} & \mathbf{0} & \mathbf{0} & \mathbf{0} \end{array} \right) = 0 \quad (\text{A2})$$

It can also be rewritten as

$$\det \left( \begin{array}{cccccccc} \mathbf{I}_a & \mathbf{H}_{ap}^A \mathbf{Z}_{pp}^C & \mathbf{H}_{ai}^A \mathbf{Z}_{ii}^D & \mathbf{H}_{ap}^A \mathbf{Z}_{pc}^C & \mathbf{H}_{ai}^A \mathbf{Z}_{id}^D & \mathbf{H}_{ap}^A \mathbf{Z}_{pq}^C & \mathbf{H}_{ai}^A \mathbf{Z}_{ij}^D & \mathbf{0} \\ \mathbf{0} & \mathbf{I}_p + \mathbf{H}_{pp}^A \mathbf{Z}_{pp}^C & \mathbf{H}_{pi}^A \mathbf{Z}_{ii}^D & \mathbf{H}_{pp}^A \mathbf{Z}_{pc}^C & \mathbf{H}_{pi}^A \mathbf{Z}_{id}^D & \mathbf{H}_{pp}^A \mathbf{Z}_{pq}^C & \mathbf{H}_{pi}^A \mathbf{Z}_{ij}^D & \mathbf{0} \\ \mathbf{0} & \mathbf{H}_{ip}^A \mathbf{Z}_{pp}^C & \mathbf{I}_i + \mathbf{H}_{ii}^A \mathbf{Z}_{ii}^D & \mathbf{H}_{ip}^A \mathbf{Z}_{pc}^C & \mathbf{H}_{ii}^A \mathbf{Z}_{id}^D & \mathbf{H}_{ip}^A \mathbf{Z}_{pq}^C & \mathbf{H}_{ii}^A \mathbf{Z}_{ij}^D & \mathbf{0} \\ \mathbf{0} & \mathbf{Z}_{cp}^C & \mathbf{0} & \mathbf{Z}_{cc}^C & \mathbf{0} & \mathbf{Z}_{cq}^C & \mathbf{0} & \mathbf{0} \\ \mathbf{0} & \mathbf{0} & \mathbf{Z}_{di}^D & \mathbf{0} & \mathbf{Z}_{dd}^D & \mathbf{0} & \mathbf{Z}_{dj}^D & \mathbf{0} \\ \mathbf{0} & \mathbf{H}_{qq}^B \mathbf{Z}_{qp}^C & \mathbf{H}_{qj}^B \mathbf{Z}_{ji}^D & \mathbf{H}_{qq}^B \mathbf{Z}_{qc}^C & \mathbf{H}_{qj}^B \mathbf{Z}_{jd}^D & \mathbf{I}_q + \mathbf{H}_{qq}^B \mathbf{Z}_{qq}^C & \mathbf{H}_{qj}^B \mathbf{Z}_{jj}^D & \mathbf{0} \\ \mathbf{0} & \mathbf{H}_{jq}^B \mathbf{Z}_{qp}^C & \mathbf{H}_{jj}^B \mathbf{Z}_{ji}^D & \mathbf{H}_{jq}^B \mathbf{Z}_{qc}^C & \mathbf{H}_{jj}^B \mathbf{Z}_{jd}^D & \mathbf{H}_{jq}^B \mathbf{Z}_{qq}^C & \mathbf{I}_j + \mathbf{H}_{jj}^B \mathbf{Z}_{jj}^D & \mathbf{0} \\ \mathbf{0} & \mathbf{H}_{bq}^B \mathbf{Z}_{qp}^C & \mathbf{H}_{bj}^B \mathbf{Z}_{ji}^D & \mathbf{H}_{bq}^B \mathbf{Z}_{qc}^C & \mathbf{H}_{bj}^B \mathbf{Z}_{jd}^D & \mathbf{H}_{bq}^B \mathbf{Z}_{qq}^C & \mathbf{H}_{bj}^B \mathbf{Z}_{jj}^D & \mathbf{I}_b \end{array} \right) = 0 \quad (\text{A3})$$

According to Leibniz formula for determinants, this equation equals to

$$\det \left( \begin{array}{cccccc} \mathbf{I}_p + \mathbf{H}_{pp}^A \mathbf{Z}_{pp}^C & \mathbf{H}_{pi}^A \mathbf{Z}_{ii}^D & \mathbf{H}_{pp}^A \mathbf{Z}_{pc}^C & \mathbf{H}_{pi}^A \mathbf{Z}_{id}^D & \mathbf{H}_{pp}^A \mathbf{Z}_{pq}^C & \mathbf{H}_{pi}^A \mathbf{Z}_{ij}^D \\ \mathbf{H}_{ip}^A \mathbf{Z}_{pp}^C & \mathbf{I}_i + \mathbf{H}_{ii}^A \mathbf{Z}_{ii}^D & \mathbf{H}_{ip}^A \mathbf{Z}_{pc}^C & \mathbf{H}_{ii}^A \mathbf{Z}_{id}^D & \mathbf{H}_{ip}^A \mathbf{Z}_{pq}^C & \mathbf{H}_{ii}^A \mathbf{Z}_{ij}^D \\ \mathbf{Z}_{cp}^C & \mathbf{0} & \mathbf{Z}_{cc}^C & \mathbf{0} & \mathbf{Z}_{cq}^C & \mathbf{0} \\ \mathbf{0} & \mathbf{Z}_{di}^D & \mathbf{0} & \mathbf{Z}_{dd}^D & \mathbf{0} & \mathbf{Z}_{dj}^D \\ \mathbf{H}_{qq}^B \mathbf{Z}_{qp}^C & \mathbf{H}_{qj}^B \mathbf{Z}_{ji}^D & \mathbf{H}_{qq}^B \mathbf{Z}_{qc}^C & \mathbf{H}_{qj}^B \mathbf{Z}_{jd}^D & \mathbf{I}_q + \mathbf{H}_{qq}^B \mathbf{Z}_{qq}^C & \mathbf{H}_{qj}^B \mathbf{Z}_{jj}^D \\ \mathbf{H}_{jq}^B \mathbf{Z}_{qp}^C & \mathbf{H}_{jj}^B \mathbf{Z}_{ji}^D & \mathbf{H}_{jq}^B \mathbf{Z}_{qc}^C & \mathbf{H}_{jj}^B \mathbf{Z}_{jd}^D & \mathbf{H}_{jq}^B \mathbf{Z}_{qq}^C & \mathbf{I}_j + \mathbf{H}_{jj}^B \mathbf{Z}_{jj}^D \end{array} \right) = 0 \quad (\text{A4})$$

Since the matrix determinant would not change by swapping rows and columns, equation (A4) could be recast as

$$\det \begin{pmatrix} \mathbf{I}_p + \mathbf{H}_{pp}^A \mathbf{Z}_{pp}^C & \mathbf{H}_{pp}^A \mathbf{Z}_{pc}^C & \mathbf{H}_{pp}^A \mathbf{Z}_{pq}^C & \mathbf{H}_{pi}^A \mathbf{Z}_{ii}^D & \mathbf{H}_{pi}^A \mathbf{Z}_{id}^D & \mathbf{H}_{pi}^A \mathbf{Z}_{ij}^D \\ \mathbf{Z}_{cp}^C & \mathbf{Z}_{cc}^C & \mathbf{Z}_{cq}^C & \mathbf{0} & \mathbf{0} & \mathbf{0} \\ \mathbf{H}_{qq}^B \mathbf{Z}_{qp}^C & \mathbf{H}_{qq}^B \mathbf{Z}_{qc}^C & \mathbf{I}_q + \mathbf{H}_{qq}^B \mathbf{Z}_{qq}^C & \mathbf{H}_{qj}^B \mathbf{Z}_{ji}^D & \mathbf{H}_{qj}^B \mathbf{Z}_{jd}^D & \mathbf{H}_{qj}^B \mathbf{Z}_{jj}^D \\ \mathbf{0} & \mathbf{Z}_{di}^D & \mathbf{0} & \mathbf{Z}_{dd}^D & \mathbf{0} & \mathbf{Z}_{dj}^D \\ \mathbf{H}_{ip}^A \mathbf{Z}_{pp}^C & \mathbf{H}_{ip}^A \mathbf{Z}_{pc}^C & \mathbf{H}_{ip}^A \mathbf{Z}_{pq}^C & \mathbf{I}_i + \mathbf{H}_{ii}^A \mathbf{Z}_{ii}^D & \mathbf{H}_{ii}^A \mathbf{Z}_{id}^D & \mathbf{H}_{ii}^A \mathbf{Z}_{ij}^D \\ \mathbf{0} & \mathbf{0} & \mathbf{0} & \mathbf{Z}_{di}^D & \mathbf{Z}_{dd}^D & \mathbf{Z}_{dj}^D \\ \mathbf{H}_{jq}^B \mathbf{Z}_{qp}^C & \mathbf{H}_{jq}^B \mathbf{Z}_{qc}^C & \mathbf{H}_{jq}^B \mathbf{Z}_{qq}^C & \mathbf{H}_{jj}^B \mathbf{Z}_{ji}^D & \mathbf{H}_{jj}^B \mathbf{Z}_{jd}^D & \mathbf{I}_j + \mathbf{H}_{jj}^B \mathbf{Z}_{jj}^D \end{pmatrix} = 0 \quad (\text{A5})$$

Then it could be reformed as

$$\det \left( \begin{pmatrix} \mathbf{I}_p & \mathbf{0} & \mathbf{0} & \mathbf{0} & \mathbf{0} & \mathbf{0} \\ \mathbf{0} & \mathbf{0} & \mathbf{0} & \mathbf{0} & \mathbf{0} & \mathbf{0} \\ \mathbf{0} & \mathbf{0} & \mathbf{I}_q & \mathbf{0} & \mathbf{0} & \mathbf{0} \\ \mathbf{0} & \mathbf{0} & \mathbf{0} & \mathbf{I}_i & \mathbf{0} & \mathbf{0} \\ \mathbf{0} & \mathbf{0} & \mathbf{0} & \mathbf{0} & \mathbf{0} & \mathbf{0} \\ \mathbf{0} & \mathbf{0} & \mathbf{0} & \mathbf{0} & \mathbf{0} & \mathbf{I}_j \end{pmatrix} + \begin{pmatrix} \mathbf{H}_{pp}^A & \mathbf{0} & \mathbf{0} & \mathbf{H}_{pi}^A & \mathbf{0} & \mathbf{0} \\ \mathbf{0} & \mathbf{I}_c & \mathbf{0} & \mathbf{0} & \mathbf{0} & \mathbf{0} \\ \mathbf{0} & \mathbf{0} & \mathbf{H}_{qq}^B & \mathbf{0} & \mathbf{0} & \mathbf{H}_{qj}^B \\ \mathbf{H}_{ip}^A & \mathbf{0} & \mathbf{0} & \mathbf{H}_{ii}^A & \mathbf{0} & \mathbf{0} \\ \mathbf{0} & \mathbf{0} & \mathbf{0} & \mathbf{0} & \mathbf{I}_d & \mathbf{0} \\ \mathbf{0} & \mathbf{0} & \mathbf{H}_{jq}^B & \mathbf{0} & \mathbf{0} & \mathbf{H}_{jj}^B \end{pmatrix} \begin{pmatrix} \mathbf{Z}_{pp}^C & \mathbf{Z}_{pc}^C & \mathbf{Z}_{pq}^C & \mathbf{0} & \mathbf{0} & \mathbf{0} \\ \mathbf{Z}_{cp}^C & \mathbf{Z}_{cc}^C & \mathbf{Z}_{cq}^C & \mathbf{0} & \mathbf{0} & \mathbf{0} \\ \mathbf{Z}_{qp}^C & \mathbf{Z}_{qc}^C & \mathbf{Z}_{qq}^C & \mathbf{0} & \mathbf{0} & \mathbf{0} \\ \mathbf{0} & \mathbf{0} & \mathbf{0} & \mathbf{Z}_{ii}^D & \mathbf{Z}_{id}^D & \mathbf{Z}_{ij}^D \\ \mathbf{0} & \mathbf{0} & \mathbf{0} & \mathbf{Z}_{di}^D & \mathbf{Z}_{dd}^D & \mathbf{Z}_{dj}^D \\ \mathbf{0} & \mathbf{0} & \mathbf{0} & \mathbf{Z}_{ji}^D & \mathbf{Z}_{jd}^D & \mathbf{Z}_{jj}^D \end{pmatrix} \right) = 0 \quad (\text{A6})$$

In a compact form

$$\det \left( \begin{bmatrix} \tilde{\mathbf{I}}^C & \mathbf{0} \\ \mathbf{0} & \tilde{\mathbf{I}}^D \end{bmatrix} + \begin{bmatrix} \tilde{\mathbf{H}}_{CC} & \tilde{\mathbf{H}}_{CD} \\ \tilde{\mathbf{H}}_{DC} & \tilde{\mathbf{H}}_{DD} \end{bmatrix} \begin{bmatrix} \mathbf{Z}^C & \mathbf{0} \\ \mathbf{0} & \mathbf{Z}^D \end{bmatrix} \right) = 0 \quad (\text{A7})$$

So, the Eq. (3.30) in section 3.3 is derived.

## Appendix B

The knowledge of rotational-related receptance can be of extreme importance if one wishes to obtain reliable results when doing calculations of coupling, structural modification, model updating or joint identification. To help understand the effect of rotational receptance, a numerical example is given here.

Considering a beam as shown in Fig. B1, the properties of the beam are given in Fig. B1 (units are omitted here for simplicity).

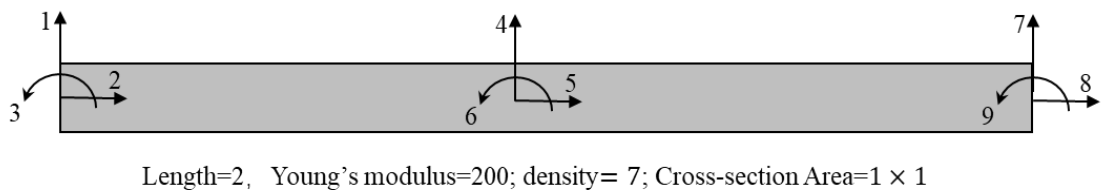


Fig. B1 A simple beam

If this beam is cut into two halves and the two short beams are coupled through 3 springs, including two translational springs ( $k_h, k_v$ ) and one rotational spring  $r_a$ , as shown in Fig. B2.

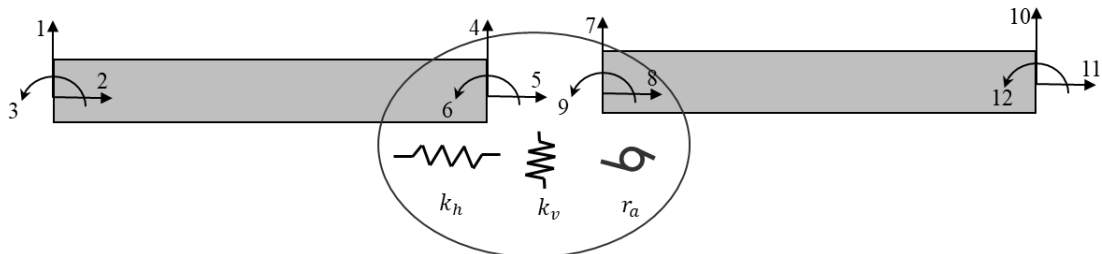


Fig. B2 two halves coupled through three springs

It is expected that the coupled beam can have the same dynamic behaviour with the original beam. Two cases are studied: the first one is the two beams are coupled through strong rotational springs and the second one is the two beams are coupled through weak rotational springs.

(1) if the stiffnesses of the three springs are very big, choosing  $k_h = k_v = r_a = 10^6$ , the receptances of the original beam and the coupled beam with strong rotational spring is shown in Fig. B3. It can be seen when the rotational spring is very strong, the coupled beam is as same as the original beam.

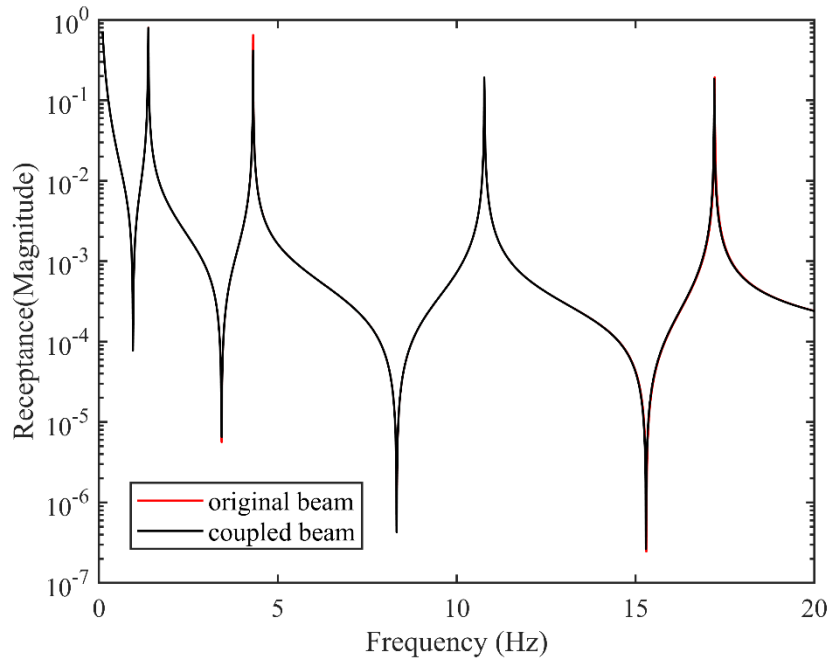


Fig. B3 Receptances  $h_{22}$  of the original beam and the coupled beam (with strong rotational spring)

(2) If the stiffnesses of the translational springs are big while the rotational spring is weak, choosing  $k_h = k_v = 10^6$  and  $r_a = 1$ . The comparison between the original beam and the coupled beam with weak rotational spring is presented in Fig. B4.

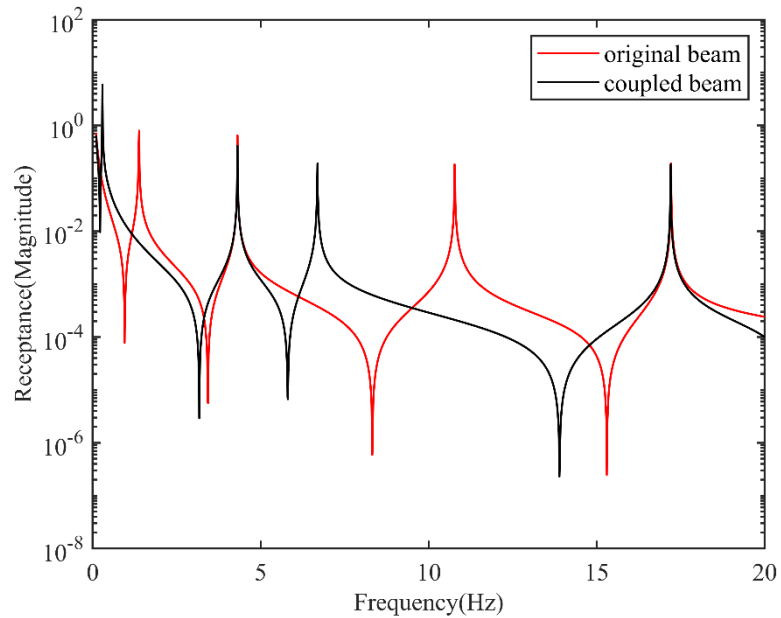


Fig. B4 Receptances  $h_{22}$  of the original beam and the coupled beam (with weak rotational spring)

Apparently, the coupled beam is different with original beam when the rotational spring is weak, even the translational springs are still very strong.

From the two simulations, it is known that without knowing the knowledge of rotational degrees of freedom, the coupled structure will not behave as expected. Therefore, it is critical to measure the rotational-related receptance when using the receptance method.

## References

- [1] J.E. Mottershead, Structural modification for the assignment of zeros using measured receptances, *J.Appl.Mech.*, 68 (2001) 791-798.
- [2] Y.M. Ram, J.E. Mottershead, Receptance method in active vibration control, *AIAA Journal*, 45 (2007) 562-567.
- [3] M. Ghandchi Tehrani, R.N.R. Elliott, J.E. Mottershead, Partial pole placement in structures by the method of receptances: Theory and experiments, *Journal of Sound and Vibration*, 329 (2010) 5017-5035.
- [4] J.E. Mottershead, M.G. Tehrani, S. James, Y.M. Ram, Active vibration suppression by pole-zero placement using measured receptances, *Journal of Sound and Vibration*, 311 (2008) 1391-1408.
- [5] N.D. Anh, N.Q. Hai, D.V. Hieu, The equivalent linearization method with a weighted averaging for analyzing of nonlinear vibrating systems, *Latin American Journal of Solids & Structures*, 17 (2017) 1723-1740.
- [6] D. Lisitano, S. Jiffri, E. Bonisoli, J.E. Mottershead, Experimental feedback linearisation of a vibrating system with a non-smooth nonlinearity, *Journal of Sound and Vibration*, 416 (2018) 192-212.
- [7] D.J. Ewins, *Modal Testing: Theory and Practice*, Research Studies Press, England, 1985.
- [8] A.J. McMillan, A.J. Keane, Shifting resonances from a frequency band by applying concentrated masses to a thin rectangular plate, *Journal of Sound and Vibration*, 192 (1996) 549-652.
- [9] Y.D. Song, L. Mitchell, Active damping control of vibrational systems, *IEEE Transactions on Aerospace and Electronic Systems*, 32 (1996) 569-577.
- [10] R. Schmid, A. Pandey, T. Nguyen, Robust pole placement with Moore's algorithm, *IEEE Transactions on Automatic Control*, 59 (2014) 500-505.
- [11] D.J. Inman, *Engineering vibrations*, Prentice-Hall, Englewood Cliffs, NJ, 1993.

- [12] J.Q. Sun, M. Jolly, M. Norris, Passive, adaptive and active tuned vibration absorbers—A Survey, *Journal of Mechanical Design*, 117 (1995).
- [13] J.E. Mottershead, G. Lallement, Vibration nodes, and the cancellation of poles and zeros by unit-rank modifications to structures, *Journal of Sound and Vibration*, 222 (1999) 833-851.
- [14] J. Calvo-Ramon, Eigenstructure assignment by output feedback and residue analysis, *IEEE Transactions on Automatic Control*, 31 (1986) 247-249.
- [15] D.W. Rew, J.L. Junkins, J.N. Juang, Robust eigenstructure assignment by a projection method - Applications using multiple optimization criteria, *Journal of Guidance, Control, and Dynamics*, 12 (1989) 396-403.
- [16] A.S. Yigit, S. Choura, Vibration confinement in flexible structures via alteration of mode shapes by using feedback, *Journal of Sound and Vibration*, 179 (1995) 553-567.
- [17] T.-Y. Wu, K.-W. Wang, Vibration isolator design via energy confinement through eigenvector assignment and piezoelectric networking, *Smart Structures and Materials 2004: Damping and Isolation*, International Society for Optics and Photonics, 11-26.
- [18] B.N. Datta, Partial eigenvalue assignment in linear systems: existence, uniqueness and numerical solution, *Proceedings of the Mathematical Theory of Networks and Systems (MTNS)*, Notre Dame, Citeseer.
- [19] D.R. Sarkissian, Theory and computations of partial eigenvalue and eigenstructure assignment problems in matrix second-order and distributed-parameter systems, Northern Illinois University, Ann Arbor, (2001) 127.
- [20] A. Sestieri, Structural dynamic modification, *Sadhana*, 25 (2000) 247-259.
- [21] K. Farahani, H. Bahai, An inverse strategy for relocation of eigenfrequencies in structural design. Part I: first order approximate solutions, *Journal of Sound and Vibration*, 274 (2004) 481-505.
- [22] W. Liangsheng Direct method of inverse eigenvalue problems for structure redesign\*, *Journal of Mechanical Design*, 125 (2004) 845-847.



- [23] D. Richiedei, A. Trevisani, G. Zanardo, A constrained convex approach to modal design optimization of vibrating systems, *Journal of Mechanical Design*, 133 (2011).
- [24] S.G. Braun, Y.M. Ram, Modal modification of vibrating systems: some problems and their solutions, *Mechanical Systems and Signal Processing*, 15 (2001) 101-119.
- [25] N.M.M. Maia, J.M.M. Silva, W.M. To, Theoretical and experimental modal analysis, Research Studies Press, John Wiley & Sons, 1997.
- [26] J.F. Baldwin, S.G. Hutton, Natural modes of modified structures, *AIAA Journal*, 23 (1985) 1737-1743.
- [27] S. Adhikari, Rates of change of eigenvalues and eigenvectors in damped dynamic system, *AIAA Journal*, 37 (1999) 1452-1458.
- [28] S. Garg, Derivatives of eigensolutions for a general matrix, *AIAA Journal*, 11 (1973) 1191-1194.
- [29] J.T. Weissenburger, Effect of local modifications on the vibration characteristics of linear systems, *Journal of Applied Mechanics*, 35 (1968) 327.
- [30] R.J. Pomazal, V.W. Snyder, Local modifications of damped linear systems, *AIAA Journal*, 9 (1971) 2216-2221.
- [31] J. Hallquist, V. Snyder, Synthesis of two discrete vibratory systems using eigenvalue modification, *AIAA Journal*, 11 (1973) 247-249.
- [32] K.M. Romstad, J.R. Hutchinson, K.H. Runge, Design parameter variation and structural response, *International Journal for Numerical Methods in Engineering*, 5 (1973) 337-349.
- [33] K. Elliott, L. Mitchell, The effect of modal truncation on modal modification, *International Modal Analysis Conference, London*, (1987)72-78.
- [34] Y.M. Ram, S.G. Braun, J. Blech, Structural modifications in truncated systems by the Rayleigh-Ritz method, *Journal of Sound and Vibration*, 125 (1988) 203-209.
- [35] Y.M. Ram, J.J. Blech, The dynamic behavior of a vibratory system after modification, *Journal of Sound and Vibration*, 150 (1991) 357-370.

- [36] Y.M. Ram, Dynamic structural modification, *The shock and Vibration Digest*, 32 (2000) 11-17.
- [37] J.A. Cafeo, M.W. Trethewey, H.J. Sommer, III, Beam element structural dynamics modification using experimental modal rotational data, *Journal of Vibration and Acoustics*, 117 (1995) 265-271.
- [38] H. Hang, K. Shankar, J.C.S. Lai, Prediction of the effects on dynamic response due to distributed structural modification with additional degrees of freedom, *Mechanical Systems and Signal Processing*, 22 (2008) 1809-1825.
- [39] R.R. Craig Jr, C.-J. Chang, *Substructure coupling for dynamic analysis and testing*, Washington USA: National Aeronautics and Space Administration, (1977).
- [40] W. Liu, D.J. Ewins, Substructure synthesis via elastic media part II: coupling analysis, *iic*, 200 (2000) 17.
- [41] T.L. Schmitz, R.R. Donalson, Predicting high-speed machining dynamics by substructure analysis, *Cirp Annals*, 49 (2000) 303-308.
- [42] M. Mehrpouya, E. Graham, S.S. Park, Identification of multiple joint dynamics using the inverse receptance coupling method, *Journal of Vibration and Control*, 21 (2015) 3431-3449.
- [43] M. Imregun, Structural modification and coupling dynamic analysis using measured FRF data, 5th International modal analysis conference, New York, USA: Union College, London, England, (1987) 1136.
- [44] R. Craig, M. Bampton, Coupling of substructures for dynamic analyses, *AIAA Journal*, 6 (1968) 1313-1319.
- [45] Y. Ren, C.F. Beards, On substructure synthesis with FRF data, *Journal of Sound and Vibration*, 185 (1995) 845-866.
- [46] D. de Klerk, D.J. Rixen, J. de Jong, The frequency based substructuring (FBS) method reformulated according to the dual domain decomposition method, In 24th International modal analysis conference, St. Louis, MO, Bethel, Connecticut, USA: Society for experimental Mechanics, 2006.

- [47] D.d. Klerk, D.J. Rixen, S.N. Voormeeren, General framework for dynamic substructuring: history, review and classification of techniques, *AIAA Journal*, 46 (2008) 1169-1181.
- [48] W. D'Ambrogio, A. Sestieri, A unified approach to substructuring and structural modification problems, *Shock and Vibration*, 11 (2004) 295-309.
- [49] W. Matthias, O. Özşahin, Y. Altintas, B. Denkena, Receptance coupling based algorithm for the identification of contact parameters at holder–tool interface, *CIRP Journal of Manufacturing Science and Technology*, 13 (2016) 37-45.
- [50] F. Latini, J. Brunetti, W. D'Ambrogio, A. Fregolent, Substructures' coupling with nonlinear connecting elements, *Nonlinear Dynamics*, 99 (2020) 1643-1658.
- [51] D.D. Sivan, Y.M. Ram, Optimal construction of a mass-spring system with prescribed modal and spectral data, *Journal of Sound and Vibration*, 201 (1997) 323-334.
- [52] I. Bucher, S. Braun, The structural modification inverse problem: an exact solution, *Mechanical Systems and Signal Processing*, 7 (1993) 217-238.
- [53] Y.M. Ram, S.G. Braun, An inverse problem associated with modification of incomplete dynamic systems, *Journal of Applied Mechanics*, 58 (1991) 233-237.
- [54] J. Mottershead, On the zeros of structural frequency response functions and their sensitivities, *Mechanical Systems and Signal Processing*, 12 (1998) 591-597.
- [55] T. Li, J. He, M. Sek, Local and global pole-zero cancellation on mass-spring systems, *Mechanical Systems and Signal Processing*, 15 (2001) 121-127.
- [56] H. Ouyang, J. Zhang, Passive modifications for partial assignment of natural frequencies of mass–spring systems, *Mechanical Systems and Signal Processing*, 50-51 (2015) 214-226.
- [57] R. Belotti, H. Ouyang, D. Richiedei, A new method of passive modifications for partial frequency assignment of general structures, *Mechanical Systems and Signal Processing*, 99 (2018) 586-599.

- [58] M.L. Wei, R.J. Allemang, D.L. Brown, Modal scaling considerations for structural modification application, *Proceedings of the 5th International Modal Analysis Conference*, London, 1987, pp. 1531-1537.
- [59] W.J. Duncan, The admittance method for obtaining the natural frequencies of systems, *The London, Edinburgh, and Dublin Philosophical Magazine and Journal of Science*, 32 (1941) 401-409.
- [60] A. Sestieri, W. D'Ambrogio, A modification method for vibration control of structures, (1989) 229-253.
- [61] Y.G. Tsuei, E.K.L. Yee, A method for modifying dynamic properties of undamped mechanical systems, *Journal of Dynamic Systems, Measurement, and Control*, 111 (1989) 403-408.
- [62] E.K.L. Yee, Y.G. Tsuei, Method for shifting natural frequencies of damped mechanical systems, *AIAA Journal*, 29 (1991) 1973-1977.
- [63] Y.-H. Park, Y.-S. Park, Structure optimization to enhance its natural frequencies based on measured frequency response functions, *Journal of Sound and Vibration*, 229 (2000) 1235-1255.
- [64] A. Kyprianou, J.E. Mottershead, H. Ouyang, Structural modification. Part 2: assignment of natural frequencies and antiresonances by an added beam, *Journal of Sound and Vibration*, 284 (2005) 267-281.
- [65] S.-H. Tsai, H. Ouyang, J.-Y. Chang, Inverse structural modifications of a geared rotor-bearing system for frequency assignment using measured receptances, *Mechanical Systems and Signal Processing*, 110 (2018) 59-72.
- [66] A. Kyprianou, J.E. Mottershead, H. Ouyang, Assignment of natural frequencies by an added mass and one or more springs, *Mechanical Systems and Signal Processing*, 18 (2004) 263-289.
- [67] J.E. Mottershead, A. Kyprianou, H. Ouyang, Structural modification. Part 1: rotational receptances, *Journal of Sound and Vibration*, 284 (2005) 249-265.

- [68] J.E. Mottershead, M. Ghandchi Tehrani, D. Stancioiu, S. James, H. Shahverdi, Structural modification of a helicopter tailcone, *Journal of Sound and Vibration*, 298 (2006) 366-384.
- [69] H. Ouyang, D. Richiedei, A. Trevisani, G. Zanardo, Eigenstructure assignment in undamped vibrating systems: A convex-constrained modification method based on receptances, *Mechanical Systems and Signal Processing*, 27 (2012) 397-409.
- [70] Z. Liu, W. Li, H. Ouyang, D. Wang, Eigenstructure assignment in vibrating systems based on receptances, *Archive of Applied Mechanics*, 85 (2015) 713-724.
- [71] O. Zarraga, I. Ulacia, J.M. Abete, H. Ouyang, Receptance based structural modification in a simple brake-clutch model for squeal noise suppression, *Mechanical Systems and Signal Processing*, 90 (2017) 222-233.
- [72] H. Liu, H. Gao, Y. Ma, Receptance-based assignment of dynamic characteristics: A summary and an extension, *Mechanical Systems and Signal Processing*, 145 (2020) 1-15.
- [73] O. Çakar, Mass and stiffness modifications without changing any specified natural frequency of a structure, *Journal of Vibration and Control*, 17 (2011) 769-776.
- [74] D.J. Inman, *Vibration with control*, Wiley, New York, 2006.
- [75] H. Ouyang, W. Nack, Y. Yuan, F. Chen, Numerical analysis of automotive disc brake squeal: A review, *International Journal of Vehicle Noise and Vibration*, 1 (2005) 207-230.
- [76] H. Ouyang, Prediction and assignment of latent roots of damped asymmetric systems by structural modifications, *Mechanical Systems and Signal Processing*, 23 (2009) 1920-1930.
- [77] J.E. Mottershead, Y.M. Ram, Inverse eigenvalue problems in vibration absorption: passive modification and active control, *Mechanical Systems and Signal Processing*, 20 (2006) 5-44.
- [78] G.S. Miminis, C.C. Paige, An algorithm for pole assignment of time invariant multi-input linear systems, 21st IEEE Conference on Decision and Control, (1982) 62-67.

- [79] G. Miminis, Deflation in eigenvalue assignment of descriptor systems using state feedback, *IEEE Transactions on Automatic Control*, 38 (1993) 1322-1336.
- [80] J. Kautsky, N. Nichols, Robust pole assignment in linear state feedback, *International Journal of Control*, 41 (1985) 1129-1155.
- [81] L. Carotenuto, G. Franzè, A general formula for eigenvalue assignment by static output feedback with application to robust design, *Systems & Control Letters*, 49 (2003) 175-190.
- [82] E.K. Chu, B.N. Datta, Numerically robust pole assignment for second-order systems, *International Journal of Control*, 64 (1996) 1113-1127.
- [83] B.N. Datta, F. Rincón, Feedback stabilization of a second-order system: a nonmodal approach, *Linear Algebra and its Applications*, 188-189 (1993) 135-161.
- [84] T. Abdelaziz, M. Valasek, Direct algorithm for pole placement by state-derivative feedback for multi-input linear systems-Nonsingular case, *Acta Polytechnica*, 41 (2005) 637-660.
- [85] H. Ouyang, Pole assignment of friction-induced vibration for stabilisation through state-feedback control, *Journal of Sound and Vibration*, 329 (2010) 1985-1991.
- [86] H. Ouyang, A hybrid control approach for pole assignment to second-order asymmetric systems, *Mechanical Systems and Signal Processing*, 25 (2011) 123-132.
- [87] K.V. Singh, H. Ouyang, Pole assignment using state feedback with time delay in friction-induced vibration problems, *Acta Mechanica*, 224 (2013) 645-656.
- [88] Y. Liang, H. Yamaura, H. Ouyang, Active assignment of eigenvalues and eigen-sensitivities for robust stabilization of friction-induced vibration, *Mechanical Systems and Signal Processing*, 90 (2017) 254-267.
- [89] M. Ghandchi Tehrani, J.E. Mottershead, A.T. Shenton, Y.M. Ram, Robust pole placement in structures by the method of receptances, *Mechanical Systems and Signal Processing*, 25 (2011) 112-122.

- [90] M. Ghandchi Tehrani, L. Wilmshurst, S.J. Elliott, Receptance method for active vibration control of a nonlinear system, *Journal of Sound and Vibration*, 332 (2013) 4440-4449.
- [91] B. Mokrani, A. Batou, S. Fichera, L. Adamson, D. Alaluf, J.E. Mottershead, The minimum norm multi-input multi-output receptance method for partial pole placement, *Mechanical Systems and Signal Processing*, 129 (2019) 437-448.
- [92] L.J. Adamson, S. Fichera, J.E. Mottershead, Receptance-based robust eigenstructure assignment, *Mechanical Systems and Signal Processing*, 140 (2020) 1-16.
- [93] D. Richiedei, I. Tamellin, A. Trevisani, Simultaneous assignment of resonances and antiresonances in vibrating systems through inverse dynamic structural modification, *Journal of Sound and Vibration*, 485 (2020) 1-22.
- [94] D. Richiedei, I. Tamellin, Active control of linear vibrating systems for antiresonance assignment with regional pole placement, *Journal of Sound and Vibration*, 494 (2021) 1-18.
- [95] D. Richiedei, I. Tamellin, A. Trevisani, Unit-rank output feedback control for antiresonance assignment in lightweight systems, *Mechanical Systems and Signal Processing*, 164 (2022) 1-20.
- [96] B. Moore, On the flexibility offered by state feedback in multivariable systems beyond closed loop eigenvalue assignment, *IEEE Transactions on Automatic Control*, 21 (1976) 689-692.
- [97] C. Minas, D.J. Inman, Matching finite element models to modal data, *Journal of Vibration and Acoustics*, 112 (1990) 84-92.
- [98] D.C. Zimmerman, M. Widengren, Correcting finite element models using a symmetric eigenstructure assignment technique, *AIAA Journal*, 28 (1990) 1670-1676.
- [99] Y. Kim, H.-S. Kim, J.L. Junkins, Eigenstructure assignment algorithm for mechanical second-order systems, *Journal of Guidance, Control, and Dynamics*, 22 (1999) 729.

- [100] B.N. Datta, Finite-element model updating, eigenstructure assignment and eigenvalue embedding techniques for vibrating systems,, *Mechanical Systems and Signal Processing*, 16 (2002) 83-96.
- [101] G.-R. Duan, G.-P. Liu, Complete parametric approach for eigenstructure assignment in a class of second-order linear systems, *Automatica*, 38 (2002) 725-729.
- [102] M. Rastgaar, M. Ahmadian, S. Southward, A Review on Eigenstructure Assignment Methods and Orthogonal Eigenstructure Control of Structural Vibrations, *Shock and Vibration*, 16 (2009) 706-731.
- [103] D.J. Laporte, V. Lopes, D.D. Bueno, An approach to reduce vibration and avoid shimmy on landing gears based on an adapted eigenstructure assignment theory, *Meccanica*, 55 (2020) 7-17.
- [104] R. Belotti, D. Richiedei, Dynamic structural modification of vibrating systems oriented to eigenstructure assignment through active control: A concurrent approach, *Journal of Sound and Vibration*, 422 (2018) 358-372.
- [105] R. Belotti, D. Richiedei, A. Trevisani, Multi-domain optimization of the eigenstructure of controlled underactuated vibrating systems, *Structural and Multidisciplinary Optimization*, 63 (2021) 1-16.
- [106] B.N. Datta, S. Elhay, Y.M. Ram, Orthogonality and partial pole assignment for the symmetric definite quadratic pencil, *Linear Algebra and its Applications*, 257 (1997) 29-48.
- [107] B.N. Datta, D.R. Sarkissian, Multi-input partial eigenvalue assignment for the symmetric quadratic pencil, *Proceedings of the 1999 American Control Conference (Cat. No. 99CH36251)*, 1999, pp. 2244-2247
- [108] Y.M. Ram, S. Elhay, Pole assignment in vibratory systems by multi-input control, *Journal of Sound and Vibration*, 230 (2000) 309-321.
- [109] J. Qian, S. Xu, Robust partial eigenvalue assignment problem for the second-order system, *Journal of Sound and Vibration*, 282 (2005) 937-948.



- [110] S. Xu, J. Qian, Orthogonal basis selection method for robust partial eigenvalue assignment problem in second-order control systems, *Journal of Sound and Vibration*, 317 (2008) 1-19.
- [111] Y.-F. Cai, J. Qian, S.-F. Xu, The formulation and numerical method for partial quadratic eigenvalue assignment problems, *Numerical Linear Algebra with applications*, 18 (2011) 637-652.
- [112] Y.M. Ram, J.E. Mottershead, M.G. Tehrani, Partial pole placement with time delay in structures using the receptance and the system matrices, 434 (2011) 1689-1696.
- [113] Z.-J. Bai, M.-X. Chen, J.-K. Yang, A multi-step hybrid method for multi-input partial quadratic eigenvalue assignment with time delay, *Linear Algebra and Its Applications*, 437 (2012) 1658-1669.
- [114] Z.-J. Bai, J.-K. Yang, B.N. Datta, Robust partial quadratic eigenvalue assignment with time delay using the receptance and the system matrices, *Journal of Sound and Vibration*, 384 (2016) 1-14.
- [115] M.G. Tehrani, R.N. Elliott, J.E. Mottershead, Partial pole placement in structures by the method of receptances: theory and experiments, *Journal of Sound and Vibration*, 329 (2010) 5017-5035.
- [116] Y. Ram, J.E. Mottershead, Multiple-input active vibration control by partial pole placement using the method of receptances, *Mechanical Systems and Signal Processing*, 40 (2013) 727-735.
- [117] X. Wei, J.E. Mottershead, Y.M. Ram, Partial pole placement by feedback control with inaccessible degrees of freedom, *Mechanical Systems and Signal Processing*, 70-71 (2016) 334-344.
- [118] M.G. Tehrani, H. Ouyang, Receptance-Based Partial Pole Assignment for Asymmetric Systems Using State-Feedback, *Shock and Vibration*, 19 (2012) 40-61.
- [119] J. Zhang, J. Ye, H. Ouyang, X. Yin, An explicit formula of perturbing stiffness matrix for partial natural frequency assignment using static output feedback, *Journal of Low Frequency Noise, Vibration and Active Control*, 37 (2018) 1045-1052.

- [120] A. Brauer, Limits for the characteristic roots of a matrix. IV: Applications to stochastic matrices, *Duke Mathematical Journal*, 19 (1952) 75-91.
- [121] J.M. Araújo, T. Santos, A multiplicative eigenvalues perturbation and its application to natural frequency assignment in undamped second-order systems, *Proceedings of the Institution of Mechanical Engineers, Part I: Journal of Systems and Control Engineering*, 232 (2018) 963-970.
- [122] M.O. de Almeida, J.M. Araújo, Partial Eigenvalue Assignment for LTI Systems with D-Stability and LMI, *Journal of Control, Automation and Electrical Systems*, 30 (2019) 301-310.
- [123] N.J.B. Dantas, C.E.T. Dorea, J.M. Araujo, Partial pole assignment using rank-one control and receptance in second-order systems with time delay, *Meccanica*, 56 (2021) 287-302.
- [124] H. Xie, A receptance method for robust and minimum norm partial quadratic eigenvalue assignment, *Mechanical Systems and Signal Processing*, 160 (2021) 1018-1038.
- [125] J. Lu, H. Chiang, J.S. Thorp, Partial eigenstructure assignment and its application to large scale systems, *IEEE Transactions on Automatic Control*, 36 (1991) 340-347.
- [126] K. Hee-Seob, K. Youdan, Partial eigenstructure assignment algorithm in flight control system design, *IEEE Transactions on Aerospace and Electronic Systems*, 35 (1999) 1403-1409.
- [127] B.N. Datta, S. Elhay, Y.a. Ram, D.R. Sarkissian, Partial eigenstructure assignment for the quadratic pencil, *Journal of Sound and Vibration*, 230 (2000) 101-110.
- [128] A.T. Alexandridis, Entire and partial eigenstructure assignment by output feedback, 2001 European Control Conference (ECC), (2001) 3196-3200.
- [129] A. Baddou, H. Maarouf, A. Benzaouia, Partial eigenstructure assignment problem and its application to the constrained linear problem, *International Journal of Systems Science*, 44 (2013) 908 - 915.

- [130] A. Benzaouia, The resolution of equation  $XA+XBX=HX$  and the pole assignment problem, *IEEE Transactions on Automatic Control*, 39 (1994) 2091-2095.
- [131] J. Zhang, H. Ouyang, J. Yang, Partial eigenstructure assignment for undamped vibration systems using acceleration and displacement feedback, *Journal of Sound and Vibration*, 333 (2014) 1-12.
- [132] A.H. Bajodah, H. Mibar, Partial eigenstructure assignment on LQR control for continuous LTI systems, 2016 4th International Conference on Control Engineering & Information Technology (CEIT), (2016) 1-6.
- [133] P. Yu, Partial eigenstructure assignment problem for vibration system via feedback control, *Asian Journal of Control*, (2020).
- [134] K. Janssens, L. Britte, Comparison of torsional vibration measurement techniques, in: G. Dalpiaz, R. Rubini, G. D'Elia, M. Cocconcelli, F. Chaari, R. Zimroz, W. Bartelmus, M. Haddar (Eds.) *Advances in Condition Monitoring of Machinery in Non-Stationary Operations*, Springer Berlin Heidelberg, Berlin, Heidelberg, (2014) 453-463.
- [135] P. Giuliani, D. Di Maio, C.W. Schwingshackl, M. Martarelli, D.J. Ewins, Six degrees of freedom measurement with continuous scanning laser doppler vibrometer, *Mechanical Systems and Signal Processing*, 38 (2013) 367-383.
- [136] B. Jo, H. Takahashi, T. Takahata, I. Shimoyama, An angular accelerometer with high sensitivity and low crosstalk utilizing a piezoresistive cantilever and spiral liquid channels, *IEEE Sensors Journal*, 21 (2021) 2687-2692.
- [137] N. Johnson, K.J. Mohan, K.E. Janson, J. Jose, Optimization of incremental optical encoder pulse processing, 2013 International Mutli-Conference on Automation, Computing, Communication, Control and Compressed Sensing (iMac4s), (2013) 769-773.
- [138] D.J. Ewins, M.G. Sainsbury, Mobility measurements for the vibration analysis of connected structures, *Shock and Vibration Bulletin*, 42 (1972) 105-122.
- [139] D.J. Ewins, P.T. Gleeson, Experimental determination of multidirectional mobility data for beams, 45 (1974) 153-173.

- [140] L. Cheng, Y.C. Qu, Rotational compliance measurements of a flexible plane structure using an attached beam-like tip, Part 1: analysis and numerical simulation, *Journal of Vibration and Acoustics*, 119 (1997) 596.
- [141] Y.C. Qu, D. Rancourt, Rotational compliance measurements of a flexible plane structure using an attached beam-like tip, Part 2: experimental study, *Journal of Vibration and Acoustics*, 119 (1997).
- [142] S.S. Sattinger, A method for experimentally determining rotational mobilities of structures, *Shock and Vibration Bulletin*, 50 (1980).
- [143] N. Maia, J. Silva, A. Ribeiro, Some applications of coupling/uncoupling techniques in structural dynamics part 3: estimation of rotational frequency-response-functions using MUM, 15th International Modal Analysis Conference (IMAC XV), 1997.
- [144] J. Silva, N. Maia, A. Ribeiro, An indirect method for the estimation of frequency response functions involving rotational DoFs, 15th International Modal Analysis Conference (IMAC XV), 2000.
- [145] M.J. Ratcliffe, N.A.J. Lieven, Measuring rotational degrees of freedom using a laser doppler vibrometer, *Journal of Vibration and Acoustics*, 122 (1997) 12-20.
- [146] M.L.M. Duarte, D.J. Ewins, Rotational degrees of freedom for structural coupling analysis via finite-difference technique with residual compensation, *Mechanical Systems and Signal Processing*, 14 (2000) 205-227.
- [147] B. Lv, H. Ouyang, W. Li, Z. Shuai, G. Wang, An indirect torsional vibration receptance measurement method for shaft structures, *Journal of Sound and Vibration*, 372 (2016) 11-30.
- [148] S.-H. Tsai, H. Ouyang, J.-Y. Chang, Identification of torsional receptances, *Mechanical Systems and Signal Processing*, 126 (2019) 116-136.
- [149] A. Zanarini, Chasing the high-resolution mapping of rotational and strain FRFs as receptance processing from different full-field optical measuring technologies, *Mechanical Systems and Signal Processing*, 166 (2022) 1018-1028.

- [150] M. Richardson, D. Formenti, Parameter estimation from frequency response measurements using rational fraction polynomials, 1st IMAC Conference, Orlando, FL, 1982.
- [151] H. Vold, J. Kundrat, G.T. Rocklin, R. Russell, A multi-Input modal estimation algorithm for mini-computers, SAE International Congress and Exposition, SAE International, 1982.
- [152] B. Peeters, H. Van der Auweraer, P. Guillaume, J. Leuridan, The PolyMAX frequency-domain method: a new standard for modal parameter estimation?, *Shock and Vibration*, 11 (2004) 395-409.
- [153] M. Richardson, Global frequency & damping estimates from frequency response measurements, International Modal Analysis Conference, Los Angeles, CA, 1986.
- [154] N.M.M. Maia, J.M.M. Silva, Modal analysis identification techniques, *Philosophical Transactions of the Royal Society A: Mathematical, Physical and Engineering Sciences*, 359 (2001) 29-40.
- [155] N.M.M. Maia, Modal Identification Methods in the Frequency Domain, in: J.M.M. Silva, N.M.M. Maia (Eds.) *Modal Analysis and Testing*, Springer Netherlands, Dordrecht, 1999, pp. 251-264.
- [156] N.M.M. Maia, D.J. Ewins, A new approach for the modal identification of lightly damped structures, *Mechanical Systems and Signal Processing*, 3 (1989) 173-193.
- [157] S.A. Zaghlool, Single-station time-domain vibration testing technique: theory and application, *Journal of Sound and Vibration*, 72 (1980) 205-234.
- [158] C.G. Koh, B. Hong, C.-Y. Liaw, Parameter identification of large structural systems in time domain, *Journal for Structural Engineering*, 126 (2000) 957-963.
- [159] S. Sandesh, K. Shankar, Time domain identification of structural parameters and input time history using a substructural approach, *International Journal of Structural Stability and Dynamics*, 09 (2009) 243-265.
- [160] P. Guillaume, P. Verboven, S. Vanlanduit, H. Van der Auweraer, B. Peeters, A poly-reference implementation of the least-squares complex frequency-domain estimator, *Proceedings of IMAC*, 21 (2003).

- [161] J. He, Z.-F. Fu, 7 - Frequency response function measurement, in: J. He, Z.-F. Fu (Eds.) *Modal Analysis*, Butterworth-Heinemann, Oxford, (2001) 140-158.
- [162] S. Zhang, O. Huajiang, Receptance-based partial eigenstructure assignment using hybrid control, *27th International Congress on Sound and Vibration, ICSV 2021*, July 11, 2021 - July 16, 2021, Silesian University Press, Virtual, Online, 2021.
- [163] N. Birchfield, K.V. Singh, S. Singhal, Dynamical structural modification for rotordynamic application, *ASME 2013 International Design Engineering Technical Conferences and Computers and Information in Engineering Conference*, American Society of Mechanical Engineers, New York, USA, 2013.
- [164] S.-H. Tsai, H. Ouyang, J.-Y. Chang, A receptance-based method for frequency assignment via coupling of subsystems, *Archive of Applied Mechanics*, 90 (2020) 449-465.
- [165] M. Woodbury, Inverting modified matrices. Memorandum Report 42, Statistical Research Group, Institute for Advanced Study, Princeton, NJ, 1950.
- [166] L. Ren, Y. Li, X. Huang, H. Hua, Dynamic modeling and characteristic analysis of floating raft system with attached pipes, *Shock and Vibration*, 2017 (2017) 1-13.
- [167] Y. Li, D. Xu, Vibration attenuation of high dimensional quasi-zero stiffness floating raft system, *International Journal of Mechanical Sciences*, 126 (2017) 186-195.
- [168] Z. Wang, C.M. Mak, Optimization of geometrical parameters for periodical structures applied to floating raft systems by genetic algorithms, *Applied Acoustics*, 129 (2018) 108-115.
- [169] M. Dumont, N. Kinsley, Using accelerometers for measuring rotational degrees-of-freedom, 50 (2016) 11-13.
- [170] L.H. Ivarsson, M.A. Sanderson, MIMO technique for simultaneous measurement of translational and rotational mobilities, *Applied Acoustics*, 61 (2000) 345-370.

- [171] L. Ntogramatzidis, J. Tréguët, R. Schmid, A. Ferrante, Globally monotonic tracking control of multivariable systems, *IEEE Transactions on Automatic Control*, 61 (2016) 2559-2564.
- [172] A. Wahrburg, J. Adamy, Parametric design of robust fault isolation observers for linear non-square systems, *Systems & Control Letters*, 62 (2013) 420-429.
- [173] P. Saraf, K. Balasubramaniam, R. Hadidi, E. Makram, Design of a wide area damping controller based on partial right eigenstructure assignment, *Electric Power Systems Research*, 134 (2016) 134-144.
- [174] R. Belotti, D. Richiedei, A. Trevisani, Optimal design of vibrating systems through partial eigenstructure assignment, *Journal of Mechanical Design*, 138 (2016).
- [175] G.-R. Duan, Circulation algorithm for partial eigenstructure assignment via state feedback, *European Journal of Control*, 50 (2019) 107-116.
- [176] E.B. da Silva, J.M. Araujo, Damping power system oscillations in multi-machine system: A partial eigenstructure assignment plus state observer approach, *International Journal of Innovative Computing, Information and Control*, 16 (2020) 1559-1578.
- [177] A. Argha, S.W. Su, A. Savkin, B. Celler,  $H_2/H_\infty$  based sliding mode control: A partial eigenstructure assignment method, 2016 IEEE 55th Conference on Decision and Control (CDC), (2016) 5354-5359.
- [178] K. Kuttler, *Linear algebra: theory and applications*, The Saylor Foundation, 2012.
- [179] G. Matsaglia, G. P. H. Styan, Equalities and inequalities for ranks of matrices, *Linear and Multilinear Algebra*, 2 (1974) 269-292.
- [180] S. Zhang, H. Ouyang, Receptance-based partial eigenstructure assignment by state feedback control, *Mechanical Systems and Signal Processing*, 168 (2022) .
- [181] S. Brahma, B. Datta, An optimization approach for minimum norm and robust partial quadratic eigenvalue assignment problems for vibrating structures, *Journal of Sound and Vibration*, 324 (2009) 471-489.